

UNIVERSITY OF SOUTHERN QUEENSLAND

Decadal Scale Relationship Between Indices of Climate Variability and A u s t r a l i a n R a i n f a l l

A thesis submitted by:

Bernard Stilgoe

For the award of

Master of Science (Research)

2016

Abstract

Australia's climate is characterised by high intra and inter annual; decadal and longer term variability of such elements as temperature and rainfall. Various drivers are responsible for variability at these tempos, for example: the Madden Julian Oscillation, El Niño Southern Oscillation (ENSO) and Pacific Decadal Oscillation respectively. Rainfall variability dramatically impacts on the nation's economy and efforts to understand it can assist in drought mitigation and safeguard farming and infrastructure from its associated weather extrema.

1. A Pearson's "r" technique incorporating Lanczos filtering to track the correlation of 24 globally diverse, monthly climate indices with spatially resolved Australian summer rainfall (December, January and February) for the 11 decades from 1900 – 2008.
2. Relationship was scored (ranked) in terms of four criteria:
 - a. population variance was assessed as non-biased indicator,
 - b. interdecadal variance change,
 - c. the area of significant correlation
 - d. and the temporal stability of a significant correlation pattern.
3. Finally each index was ranked by its overall score.

The highest scoring index was the BEST index a combination of the Southern Oscillation Index (SOI) and the Niño3.4 Index.

A novel aspect of this study is the use of Simple Ocean Data Analysis (SODA) datasets where necessary to overcome poor availability of ocean climate data prior to the satellite age. High correlations were from some of the oceanic warm pool (WP) indices that captured the size/volume of the WP regions adjacent to the Australian continent, either in terms of ocean heat content, or a Sea Surface Temperature metric. A WP index based on the Pacific Warm Pool (PWP) region achieved a much higher variance than the Southern Oscillation Index (SOI) and the Warm Water Volume West (WWV_W) index achieved equal second rank in score. There are no pre-existent studies that correlate WP indices with Australian decadal rainfall.

A large variety of climate indices were also correlated against South East Queensland rainfall where an unexplained reduction in summer rainfall had been observed since 1980. The de facto El Niño index, Niño3.4 and SOI fared worse than they do for other regions of Australia.

A WP index based on the Warm Water Volume East (WWV_E) was by far the highest scoring index. Derived ENSO indices also scored well.

The thesis expands on the existing literature and a subsequent paper will highlight the significance of WP indices and further investigations and applications.

Declaration:

I certify that the ideas, experimental work, results, analyses and conclusions reported in this dissertation are entirely my own effort, except where otherwise acknowledged. I also certify that the work is original and has not been previously submitted for any other award, except where otherwise acknowledged.

.....

Date:

Signature of Candidate

Bernard Stilgoe

ENDORSEMENT

.....

Date:

Signature of Supervisor

Associate Professor Joachim Ribbe

ENDORSEMENT

.....

Date:

Signature of Associate Supervisor

Doctor Harry Butler

Acknowledgements:

To Professor Roger Stone who rekindled the inspiration for study.

To the University of Southern Queensland who allowed me the privilege of studying there.

To Associate Professor Joachim Ribbe who helped develop what ability I have.

To my wife Susan, who has faith in my ability?

Table of Contents

Abstract.....	i
Declaration:.....	iii
Acknowledgements:.....	iv
Table of Contents.....	v
List of Figures:.....	x
List of Tables:.....	xviii
List of Abbreviations:.....	xx
Chapter 1 Introduction.....	1
1.1 Motivation for the Study.....	1
1.2 Towards Longer Range Rainfall Prediction.....	2
1.3 Brief Historical Background.....	2
1.4 Rationale of the study.....	3
1.5 Aims of the Study.....	7
Chapter 2 Literature Review.....	9
2.1 Introduction to Climate Indices and Rainfall.....	9
2.2 Historic Availability of Climate Data.....	13
2.3 Brief Description of a Climate Index.....	16
2.4 El Niño Southern Oscillation.....	16
2.5 Southern Oscillation Index Contemporary Usage.....	22
2.6 Development of the El Niño Southern Oscillation.....	24
2.7 Worldwide Climate Indices.....	30
2.7.1 Meridional Indices.....	32
2.7.2 Northern Hemisphere and Latitudinal Indices.....	32
2.7.3 The Warm Pools.....	33
2.8 Decadal and Multidecadal Scale Climate Variability.....	38
2.9 Australian and South East Queensland Decadal and Regional Climate.....	45
2.10 Investigations indicated by a summary of the literature.....	53
Chapter 3 Data and Methods.....	56
3.1 Data.....	56
3.1.1 Rainfall Data.....	56
3.1.2 Climate Indices.....	56
3.1.3 Reanalysis Data.....	68

3.2	Method	70
3.2.1	<i>A priori</i> Investigation.....	70
3.2.2	Basic Method	75
3.2.3	Correlation	75
3.2.3.1	Detrending/Windowing	76
3.2.3.2	Skewed Data	78
3.2.4	Data Analysis	79
3.3	Comparing SOI and Niño3.4.....	82
3.3.1	Cross Correlation	83
3.3.2	Wavelet Transforms.....	84
3.4	Summary	89
Chapter 4	Results.....	91
4.1	Introduction	91
4.2	Initial Analysis	94
4.2.1	Southern Oscillation Index Types.....	94
4.2.1.1	Southern Oscillation Index (SOI).....	94
4.2.1.2	BEST index.....	95
4.2.1.3	Cold Tongue Index (CTI).....	99
4.2.1.4	Equatorial Southern Oscillation Index (EQSOI).....	99
4.2.1.5	The Indian Ocean Dipole (IOD).....	99
4.2.1.6	El Niño Modoki (EMI).....	103
4.2.1.7	Multivariate El Niño Index (MEI).....	103
4.2.1.8	FIVEVAR.....	103
4.2.1.9	Trans Niño Index (TNI).....	103
4.2.1.10	Tropical Pacific Empirical Orthogonal Function (TPEOF)	108
4.2.1.11	Pacific Warm Pool (PWP).....	108
4.2.2	Summary of SOI Spectral Type Results	111
4.2.3	Niño Types.....	111
4.2.3.1	Niño3.4	111

4.2.3.2	North Atlantic Oscillation (NAO)	112
4.2.3.3	Western Hemisphere Warm Pool (WHWP).....	117
4.2.3.4	Warm Water Volume (WWV)	117
4.2.3.5	Warm Water Volume East (WWV_E).....	117
4.2.3.6	Warm Water Volume West (WWV_W)	122
4.2.4	Summary of Niño Spectral Type Results.....	124
4.2.5	Mixture Types	125
4.2.5.1	Pacific Decadal Oscillation (PDO).....	125
4.2.5.2	Inter Decadal Pacific Oscillation (IPO).....	125
4.2.6	Summary of Mixture Spectral Types	125
4.2.7	Meridional Types	128
4.2.7.1	Northern Oscillation Index (NOI)	128
4.2.7.2	Southern Annular Mode (SAM).....	129
4.2.7.3	Arctic Oscillation Index (AOI).....	129
4.2.7.4	Indo Pacific Warm Pool (IPWP)	129
4.2.8	Summary of Meridional Spectral Type Results.....	134
4.2.9	Unique Type.....	134
4.2.9.1	Quasi Biennial Oscillation (QBO).....	134
4.3	Summary of Australia-wide Results	136
4.4	South East Queensland Correlations of Significance.....	138
4.4.1	Southern Oscillation Index (SOI)	139
4.4.2	Niño3.4.....	141
4.4.3	Inter Decadal Pacific Oscillation (IPO).....	144
4.4.4	Pacific Warm Pool (PWP)	146
4.4.5	Warm Water Volume (WWV).....	148
4.4.6	Warm Water Volume West (WWV_W).....	150
4.4.7	Warm Water Volume East (WWV_E)	151
4.4.8	Indo Pacific Warm Pool (IPWP).....	153
4.4.9	The BEST index.....	155
4.4.10	The Cold Tongue Index (CTI)	156

4.4.11	El Niño Modoki (EMI) index	157
4.4.12	Equatorial SOI (EQSOI)	158
4.4.13	FIVEVAR index	159
4.4.14	Multivariate El Niño Index (MEI)	160
4.4.15	Northern Oscillation Index (NOI).....	162
4.4.16	Tropical Pacific Empirical Orthogonal Function (TPEOF).....	163
4.4.17	The Western Hemisphere Warm Pool (WHWP).....	164
4.5	Summary of South East Queensland Results	165
Chapter 5	Discussion, Conclusions and Future Directions	167
5.1	Overview	167
5.2	Australia-wide Index Performance.....	167
5.3	South East Queensland Index Performance	171
5.4	Atmospheric-Ocean effects on Decadal Correlation.....	173
5.4.1	Meridional Overturning Circulation	174
5.4.2	Sea Surface Temperature Increase	174
5.4.3	Change in Southern Oscillation Index	175
5.4.4	Change in Rainfall	177
5.4.5	Short Summary of Phenomena Effecting Decadal Correlation	178
5.5	Factors Affecting the Study Metrics	178
5.5.1	The Observational Framework	178
5.5.2	Statistical Significance	183
5.5.3	Spectral Significance	185
5.5.4	Performance Criteria.....	186
5.6	Concluding Remarks	187
5.6.1	Possible Future Work.....	188
Appendix I	190
References:	196

List of Figures:

Figure 1.1: Australian trend in annual total rainfall ($\text{mm}\cdot 10\text{yr}^{-1}$) during 1970 – 2012 (BoM 2013a) 1

Figure 1.2: Strategic Australian sites for preliminary study 6

Figure 2.1: Australian annual total average annual rainfall ($\text{mm}\cdot\text{yr}^{-1}$) 1900 – 2008 over land areas (Jones, Wang and Fawcett (2009) 9

Figure 2.2: Australian climatic regions based on the Köppen classification after BoM (2005). 10

Figure 2.3: Hovmöller diagrams showing 1982 – 1993 SST reconstructed anomalies. a) with b) OI and c) GISST data for between $\pm 5^\circ$ latitude. Contours are at 1°C with an inclusion of $\pm 0.5^\circ\text{C}$ and shading applied to anomaly greater than 2°C (Smith et al. 1996). 14

Figure 2.4: Simplified schematic of the Equatorial Pacific Ocean and Walker Circulation showing convection above the WPWP which is shown in red (PMEL 2008). 18

Figure 2.5: El Niño conditions where Walker Circulation has collapsed, convective area moves east as has the WPWP which has cooled somewhat but advected heat eastwards towards the central and E Pacific (PMEL 2008). 19

Figure 2.6: La Niña conditions showing enhanced Walker Circulation with vigorous convection over an anomalously warm WPWP (PMEL 2008). 20

Figure 2.7: Regions 7, 14, 15 and 16 represent SST; regions 1, 10, 11, 12 and 13 pressure; regions 2,3 and 6 zonal wind; regions 4, 5, 8 and 9 rainfall, from Wright et al. (1988). 21

Figure 2.8: Rainfall forecast probability values for Queensland for September - November 2011 (Stone, Hammer and Marcussen (1996)). 23

Figure 2.9: Comparison of EQSOI and SOI (IRI 2011). 24

Figure 2.10: The basic Niño regions (Climate Prediction Centre 2005a) 25

Figure 2.11: a) Correlation coefficients between May – June SOI and July Indian South Western Monsoon anomaly. b) Correlation coefficients between May – June MEI and July Indian South Western Monsoon anomaly 27

Figure 2.12: Comparison of statistical forecasting, actual data and climate model output for Australia; modified from Yang and DelSole (2011) (a – c) refers to DJF precipitation whilst

(d – f) refers to JAS. Across from left to right with canonical correlation is (a and d) observational results, (b and e) ECM model output and (c and f) MET output.....29

Figure 2.13: Relationship of near oceanic warm pool regions to Australia. In black the WWV region consisting of WWV_West ($\pm 5^\circ$ latitude, $120^\circ\text{E} - 155^\circ\text{W}$ longitude) and WWV_E ($\pm 5^\circ$ latitude, $155^\circ\text{W} - 80^\circ\text{W}$ longitude); as defined by McPhaden (2003) and TAO Project Office, NOAA/PMEL. In ochre the Pacific Warm Pool (PWP) region ($\pm 15^\circ$ latitude, $60^\circ\text{E} - 170^\circ\text{E}$ longitude) as defined by Hoerling (2009). In blue the Indo Pacific Warm Pool (IPWP) ($\pm 20^\circ$ latitude, $90^\circ\text{E} - 180^\circ\text{E}$ longitude) as defined by Wang and Mehta (2008). The Western Hemisphere Warm Pool (WHWP) (Wang & Enfield 2001) ($7^\circ - 27^\circ\text{N}$ latitude, $110^\circ\text{W} - 50^\circ\text{W}$ longitude) a more remote warm pool is also included.33

Figure 2.14: Comparison of: b) above, the WHWP SST anomaly and d) below, the Niño3 anomaly (from Wang & Enfield (2001)).35

Figure 2.15: Lagged correlation of ISMR with Niño3 SST with lag shown on abscissae (from Rajeevan and McPhaden (2004))......38

Figure 2.16: Lagged correlation of ISMR with WWV with lag shown on the abscissae (from Rajeevan and McPhaden (2004))......38

Figure 2.17: The six possible phase states corresponding to three consecutive points in a time series where the relative vertical position indicates the values; after (Tsonis, Swanson & Kravtsov 2007)......41

Figure 2.18: (a) shows network distance of the four climate modes as a time function, (b) coupling strength between modes, (c) global surface temperature record and (d) global ENSO index (from Tsonis, Swanson and Kravtsov (2007)).42

Figure 2.19: Timeline of articles examining late 20th century Pacific climate shift.43

Figure 2.20: Convergence of late 20th century changes to the tropical Pacific Climate system as discussed in the literature over time.44

Figure 2.21: HadSLP2r 1900-2008 linear trend patterns, in units of hPa/100 years. (A) Unfiltered. (B) ENSO-residual with the SLP-only optimal perturbation filter. (C) Unfiltered minus ENSO-residual. Stippling indicates trends are significant beyond the 95% confidence level (Solomon & Newman 2012).45

Figure 2.22: Cerberus; the three headed dog of ENSO, IOD and SAM, Cai (2011)......46

Figure 2.23: Relationship between; above IOD and below SE Australian rainfall from (Ummerhofer et al. 2009).....47

Figure 2.24: Time series of the SEQ rainfall-ENSO teleconnection calculated as correlations (black curve), using a 13 year sliding window of SEQ DJF rainfall with the DJF SOI over the period 1900–2011 (statistically significant correlation at the 95% confidence level is 0.55, indicated by a solid grey line). A PDO index is overlaid in green [Mantua et al., 1997] (uncertainty values are shown as a thinner curve). The correlation between the rainfall-ENSO teleconnection and the PDO is -0.41 . Time series of normalised OLR (blue), averaged over the equatorial Western Pacific ($\pm 5^\circ\text{N}$ and S, $137 - 175^\circ\text{E}$), has a correlation of -0.47 with the evolution of rainfall-ENSO teleconnection (statistically significant above the 95% confidence level); (Cai & van Rensch 2012).51

Figure 2.25: Correlation of significant climate indices with Australian Summer (DJF) rainfall using as a comparison the classical Bayes factor (from Schepen, Wang and Robertson (2011)). Indices A – F are the indices as labeled; G is average SST anomaly over $90 - 110^\circ\text{E}$ and $08^\circ\text{N} - 10^\circ\text{S}$; J is average SST anomaly over $120 - 130^\circ\text{E}$ and $08^\circ\text{N} - 10^\circ\text{S}$ and K is average SST anomaly over $150 - 160^\circ\text{E}$ and $30 - 40^\circ\text{S}$; (only indices with any real significance are identified).....53

Figure 3.1: Scatter plots of SODA data regressed against TOA data (1980–2008): a) WWV 70

Figure 3.2: Typical SOI and El Niño pattern fast Fourier transforms (FFT's). a) the SOI and b) Niño34 for the time domain greater than 2.2 months (0.185 yr)..... 72

Figure 3.3: Fast Fourier transforms (FFT's). a) The IPO a typical mixture type pattern containing both SOI and Niño characteristics and b) the AOI (NAM) a typical cluttered Meridional type pattern for the time domain greater than 2.2 months (0.185 yr). 72

Figure 3.4: FFT periodograms of SODA data for: WWV types: a) WWV, b) WWV_E and c) WWV_W. 73

Figure 3.5: Schematic flow diagram of data processing 75

Figure 3.6: a) Comparison of raw SOI data 1965 – 2005 (black line) and linearly detrended (red line). b) Scatterplot of raw SOI data with the trend line overlaid in red. 77

Figure 3.7: Effect of filter span width on ringing. 78

Figure 3.8: Histogram of SOI variance for 11 decades.....81

Figure 3.9: Cross-correlation of SOI and Niño3.4 showing high correlation at one month lag	83
Figure 3.10: Basis of time frequency decomposition; Kumar and Foufoula-Georgiou (1997)	85
Figure 3.11: Two types of Wavelet function, at a; the Morlet and b; its transform and c; the Dog and d; its transform, modified from Torrence and Compo (1998) Figure 2.	86
Figure 3.12: Wavelet decomposition of: bold blue and green colour is Niño3.4 and pastel shades the SOI time series 1900 – 2010 (conducted in MATLAB). Top row shows; a3 the third residual.	88
Figure 4.1: Summer (DJF) decadal Australian rainfall anomaly 1900 – 2008 ($\text{mm}\cdot\text{day}^{-1}$). ...	93
Figure 4.2: Standardised Australian area averaged summer (DJF) decadal rainfall anomaly (1900 – 2008).	94
Figure 4.3: Correlation of rainfall with SOI.	96
Figure 4.4: Correlation of DJF rainfall and SOI.	97
Figure 4.5: Correlation of DJF monthly rainfall and the BEST index.	98
Figure 4.6: Correlation of DJF monthly rainfall and the CTI.	100
Figure 4.7: Correlation of DJF monthly rainfall and the EQSOI.	101
Figure 4.8: Correlation of DJF rainfall and the IOD.	102
Figure 4.9: Correlation of DJF monthly rainfall and the EMI.	104
Figure 4.10: Correlation of DJF monthly rainfall and the MEI.	105
Figure 4.11: Correlation of DJF monthly rainfall and the FIVEVAR index.	106
Figure 4.12: Correlation of (DJF) monthly rainfall and the TNI.	107
Figure 4.13: Correlation of DJF monthly rainfall and the TPEOF index.	109
Figure 4.14: Correlation of DJF monthly rainfall and the PWP index.	110
Figure 4.15: Correlation of DJF monthly rainfall with the Niño3.4 index.	113
Figure 4.16: Correlation of rainfall with the Niño3.4 index.	114
Figure 4.17: Correlation of DJF rainfall with NAO index.	115

Figure 4.18: Correlation of DJF rainfall with WHWP index.....	116
Figure 4.19: Correlation of rainfall and the WWV index.....	118
Figure 4.20: Correlation of DJF rainfall and the WWV index.....	119
Figure 4.21: Correlation of rainfall and the WWV_E index.....	120
Figure 4.22: Correlation of DJF rainfall and the WWV_E index.....	121
Figure 4.23: Correlation of rainfall and the WWV_W index.....	123
Figure 4.24: Correlation of Australian summer (DJF) rainfall and the WWV_W index 1900 – 2008.....	124
Figure 4.25: Correlation of DJF rainfall and the PDO index.....	127
Figure 4.26: Correlation of DJF rainfall and the IPO index.....	128
Figure 4.27: Correlation of DJF rainfall and the NOI.....	130
Figure 4.28: Correlation of DJF rainfall and the SAM index.....	131
Figure 4.29: Correlation of DJF rainfall and the AOI.....	132
Figure 4.30: Correlation of DJF rainfall and the IPWP index.....	133
Figure 4.31: Correlation of DJF rainfall and the QBO index.....	135
Figure 4.32: Pictorial summary of Australian results. Abscissae shows the number of indices in each of the score bins and ordinate shows the index name.....	136
Figure 4.33: Standardised area averaged South East Queensland rainfall anomalies 1900 – 2008 by decade.a) annual rainfall and b) summer (DJF) rainfall.....	139
Figure 4.34: Decadal correlation of SEQ DJF rainfall and SOI.....	140
Figure 4.35: Decadal mean summer (DJF) SOI.....	141
Figure 4.36: Decadal area averaged correlation of SEQ rainfall and SOI.....	141
Figure 4.37: Decadal correlation of SEQ DJF rainfall and Niño3.4 index.....	142
Figure 4.38: Decadal mean summer (DJF) Niño3.4 index 1900 – 2008.....	143
Figure 4.39: Decadal area averaged correlation of SEQ rainfall and Niño3.4 index.....	143
Figure 4.40: Decadal correlation of SEQ DJF rainfall and IPO.....	144
Figure 4.41: Decadal mean DJF IPO index.....	145

Figure 4.42: Decadal correlation of SEQ DJF rainfall and PWP.....	146
Figure 4.43: Decadal area averaged correlation of SEQ DJF rainfall and PWP.	147
Figure 4.44: Decadal mean DJF PWP index.....	147
Figure 4.45: Decadal correlation of SEQ DJF rainfall and WWV index.	148
Figure 4.46: Decadal mean DJF WWV index.	149
Figure 4.47: Decadal area averaged correlation of SEQ rainfall and WWV index.	149
Figure 4.48: Decadal correlation of SEQ DJF rainfall and WWV_W index.....	150
Figure 4.49: Decadal mean DJF WWV_W index.....	151
Figure 4.50: Decadal area averaged correlation of SEQ rainfall and WWV_ West index...	151
Figure 4.51: Decadal correlation of SEQ DJF rainfall and WWV_E index.....	152
Figure 4.52: Decadal area averaged correlation of SEQ rainfall and WWV_ East index. ..	153
Figure 4.53: Decadal mean DJF WWV_E index.....	153
Figure 4.54: SEQ decadal correlation of DJF rainfall and IPWP index.	154
Figure 4.55: Decadal mean DJF IPWP index.	155
Figure 4.56: SEQ decadal correlation of DJF rainfall and BEST index.	156
Figure 4.57: SEQ decadal correlation of DJF rainfall and CTI index.	157
Figure 4.58: SEQ decadal correlation of DJF rainfall and EMI index.	158
Figure 4.59: SEQ decadal correlation of DJF rainfall and EQSOI index.	159
Figure 4.60: SEQ decadal correlation of DJF rainfall and FIVEVAR index.	160
Figure 4.61: SEQ decadal correlation of DJF rainfall and MEI index.	161
Figure 4.62: SEQ decadal correlation of DJF rainfall and NOI.....	162
Figure 4.63: SEQ decadal correlation of DJF rainfall and TPEOF Index.	163
Figure 4.64: SEQ decadal correlation of DJF rainfall and WHWP Index.....	164
Figure 4.65: Pictorial representation of top SEQ indices.....	165
Figure 5.1: Typical SEQ decadal rainfall anomaly 2000 – 2010) in mm.day ⁻¹ emphasising the east–west rainfall gradient. The dashed red outline approximates the region of Cai and van Rensch (2012) and the dashed black rectangle to that of Murphy and Ribbe (2004).....	172

Figure 5.2: Correlation of SOI with Australian decadal rainfall 1969 – 2008. a) Basic bandpassed SOI data. b) Fully detrended, bandpassed (both SOI and rainfall matrix) data for the period discussed by Trenberth and Hoar (1996)..... 176

Figure 5.3: Ten year linear trends of Indonesian and east tropical Pacific Ocean MSLP using ten sets of independent reanalysis data; L’Heureux, Lee and Lyon (2013)..... 177

Figure 5.4: Variance of Australian area averaged decadal rainfall anomaly 1900 – 2008... 179

Figure 5.5: Effect on SOI of a natural reference frame as opposed to a human one. a) 1905 – 1914 containing a more natural ENSO cycle. b) 1909 – 1918 artificial reference frame capturing La Niña dominance..... 181

Figure 5.6: Current Australia relief map (terrain altitude m) using the latitude and longitude register produced from the Australian weather and rainfall data set (**Jones, D. A., Wang, W. & Fawcett, R. 2009**). 181

Figure 5.7: The region of South East Queensland; after Cai and van Rensch (2012). 182

Figure 5.8: Region of Western Australia 182

Figure 5.9: Blue line shows distribution of Pearson’s r for each decade using an aggregate of 10^6 data sets each 120 years long. Red line shows the fit distribution of Pearson’s r for filtered data and in red dashes the equivalent of 2σ for a pseudo-Gaussian fit of the correlations..... 184

Figure 5.10: Blue line shows the distribution of the average correlation of the simulated and filtered decadal data over a continuous 120 year period and in red the fit of the distribution using a Gaussian function. Overlaid (red dashes) is a demarcation at 2σ of the Gaussian fit. 185

Figure 5.11: 55 month smoothed time series of SOI (black) and inverted IPO (red). 186

List of Tables:

Table 1.1: List of climate indices used in this study and their authorship4

Table 2.1: Correlation matrix of the indices depicted in Figure 2.4 in the Equatorial belt based on averages from July – November for each of the 30 years 1950 – 1979 and are arranged from west to east (Wright et al. 1988).21

Table 2.2: Grid point variance ratios for La Niña and El Niño phase for winter Pacific North Western regional temperatures in the US; after Smith and Sardeshmukh (2000).26

Table 2.3: Significance and correlation for six continents constructed from Yang and DelSole, (2011) for Boreal Winter; DJF and summer; JAS for precipitation and temperature at 2 m elevation.30

Table 2.4: Correlation of Niño4 (N4), Niño3 (N3), SOI, EOF2 Pacific Ocean SST and EOF2 Indian Ocean SST with SEQ rainfall, (Murphy & Ribbe 2004).49

Table 2.5: Past 110 year ranked La Niña events compared to 2010 – 2011 from Baird et al. (2011). Shown are five month averaged August-December values of the indices.50

Table 3.1: Climate Indices used in this study with their acronyms and source reference to the data series.58

Table 3.2: Indices separated into their generic types as indicated by FFT periodograms. SOI types have low frequency spectral peaks and are generally noisy. Niño types lack noise but have an annual peak. Mixture types have both characteristics of SOI and Niño. Meridional types have their pole meridionally disposed and with enhanced background noise throughout the spectrum. QBO signal is unique with just a single biennial peak.74

Table 3.3: Wavelet functions shown in Figure 3.11 (reproduced from Torrence and Compo (1998)).....86

Table 4.1: Performance (correlation) results of SOI type indices. The last four columns show the ranking of the index in terms of; strength, area coverage, consistency and overall performance of their major attribute (positive or negative) between decades. 111

Table 4.2: Performance (correlation) results of Niño type indices for the whole period. The last four columns show the ranking of the index in terms of; strength, area coverage, temporal stability and overall performance of their major attribute between decades. 125

Table 4.3: Performance (correlation) results of mixture type indices. The last four columns show the ranking of the index in terms of; strength, area coverage, temporal stability and overall performance of their major attribute between decades.	126
Table 4.4: Performance (correlation) results of mixture type indices. The last four columns show the ranking of the index in terms of; strength, area coverage, temporal stability and overall performance of their major attribute between decades.	134
Table 4.5: Performance (correlation) results of the QBO.	134
Table 4.6: Summary of Index Performance with DJF rainfall.	137
Table 4.7: South East Queensland decadal correlation results of climate indices and summer monthly rainfall.	166
Table 5.1: Summary of the performance of 24 climate indices and their correlation with DJF Australian rainfall in respect to: population variance, decadal stability of variance, total area coverage of significant correlation, temporal stability, total score and overall ranking. Table is a précis of the summary in Chapter 4.	169
Table 5.2: Summer (DJF) index performance for South East Queensland (land area within 20.5 –30.5°S, 150.5 –154.5°E after Cai and van Rensch (2012), the red dashed rectangle in Figure 5.1) with respect to: population variance, decadal stability of variance, total area coverage of significant correlation, temporal stability, total score and overall ranking. Table is a précis of the material in Chapter 4.	173
Table 5.3: A comparison of two decades of ENSO observations grouped by colour. Green cells group a decade according to ENSO prominence, yellow cells represent an arbitrary defined decade using indices obtained from Table 1 in Giese and Ray (2011). The blank cells represent absence of data.	180

List of Abbreviations:

Abbrev.	Full name.
AO	Arctic Oscillation
AOI	Arctic Oscillation Index aka Northern Annular Mode
AWAP	Australian Water Availability Project
COADS	Comprehensive Ocean-Atmosphere Data Set
CPC	Climate Prediction Centre
CTI	Cold Tongue Index
BEST	Combined Niño 3.4 and Southern Oscillation Index
DJF	Boreal winter/Austral summer months December, January, February
DPI	Darwin Pressure Index
EMI	El Niño Modoki Index
ENSO	El Niño Southern Oscillation
EQSOI	Equatorial SOI
FIVEVAR	Five Variable Niño Index
GCM	General Circulation ocean climate Model
IOD	Indian Ocean Dipole
IPWP	Indo Pacific Warm Pool
IPO	Inter Decadal Pacific Oscillation
JAS	Boreal summer/Austral winter months July, August, September
MEI	Multi-variant Niño Index

NAO	North Atlantic Oscillation
NOAA	National Ocean and Atmospheric Administration
NOI	Northern Oscillation Index
ONI	Oceanic Niño Index
POAMA-2	Pacific Ocean Atmosphere Model for Australia
PDO	Pacific Decadal Oscillation
PWP	Pacific Warm Pool
QBO	Quasi Biennial Oscillation
Niño34	Sea Surface Temperature Anomaly in Niño 3.4 region
NCEP	National Centre for Environmental Predictions
SAM	Southern Annular Mode
SEQ	South East Queensland
SODA	Simple Ocean Data Analysis
SOI	Southern Oscillation Index
SST	Sea Surface Temperature
SSTA	Sea Surface Temperature Anomaly
TNI	Trans Pacific Niño Index
TPEOF	Tropical Pacific Ocean Empirical Orthogonal Function
WWV	Warm Water Volume
WWV_E	Warm Water Volume East
WWV_W	Warm Water Volume West

WHWP	Western Hemisphere Warm Pool
------	------------------------------

Chapter 1 Introduction

1.1 Motivation for the Study

The inhabitants of the east coast of Australia, particularly in South East Queensland (SEQ), were left reeling in the wake of a series of extreme rainfall events in the latter months of 2010 and early 2011. This caused extensive flooding and loss of life (Hansard 2011). The episodes ended a decline in SEQ rainfall since 1980 (Cai et al. 2010) and a ten year period of drought in some areas, marking the establishment of a major global climate mode known as La Niña. It was the biggest such positive rainfall anomaly that had occurred in more than a hundred years. Yet this rainfall has made little difference on the long term decline. Other regions of Australia for example SW Western Australia continued to suffer from long term rainfall deficiencies in a changing climate (Figure 1.1) (BoM 2011; Hope, Timbal & Fawcett 2010).

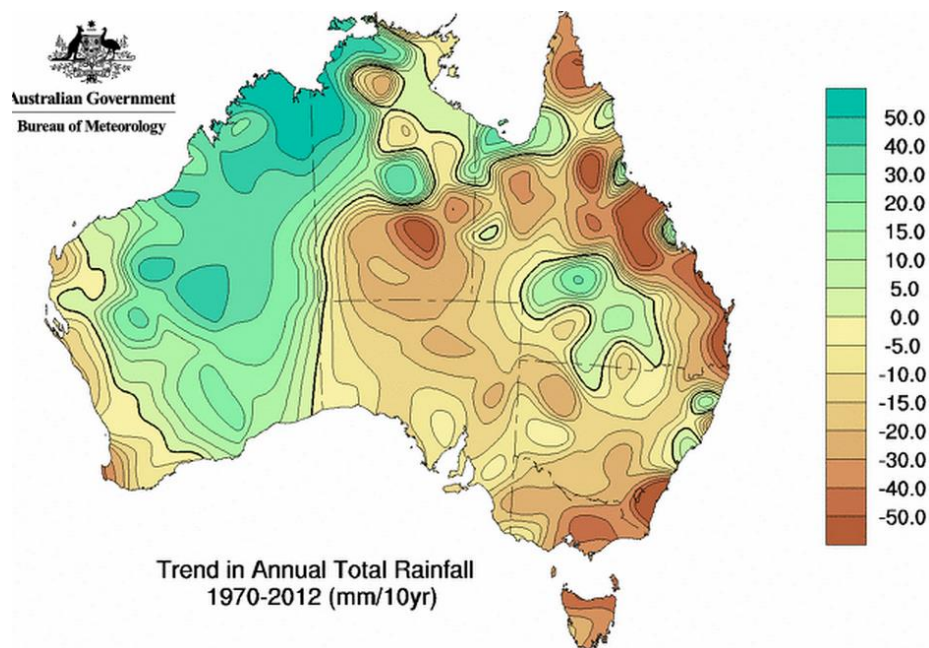


Figure 1.1: Australian trend in annual total rainfall ($\text{mm} \cdot 10\text{yr}^{-1}$) during 1970 – 2012 (BoM 2013a)

While it is true that until recently Australia has been regarded as a country of “droughts and flooding rains” (Mackellar 1908) these climate extremes should be viewed in the light of Australia’s vulnerability to climate change (Palutikof 2010). Such extrema are expected to get worse (Cleugh et al. 2011). This can often mask the simultaneous effect of reduced water

supply (Connor et al. 2009) and more subtle modes of climate variability (Cai et al. 2011), hence begging the question; how will Australian society adapt to the challenge of climate change (Wolter & Timlin 2011)?

It is in the nation's best interest to predict rainfall and climate as far ahead as possible. This would be of great benefit to the people of SEQ and Australian society in general. Farmers would be better able to forward manage their type, variety and mix of crop. Timely intervention in terms of resource allocation, physical planning and organisational infrastructure changes would be a great boon to policy makers.

1.2 Towards Longer Range Rainfall Prediction

Australia's climate varies on many different levels from the intraannual to geological time scales. Human knowledge becomes less in comparison as the scale increases possibly implying a limit to climate prediction (Dessai et al. 2009). One of the most important climate element for Australia is rainfall. A worthwhile goal would be to strive to predict rainfall variability in Australia out to as far into the future as possible and predictive ability out to the decadal scale might just become possible in the not too distant future. Advances in human understanding of climate processes driving decadal climate variability, plus building on predictive statistical and physical modelling capability and improvements in computer technology would play a role. Previous attempts at such prediction have met with little success (Power et al. 2006) and currently for conditions over land are limited to a few years (Meehl et al. 2014). This work does not seek to provide a methodology for decadal prediction, but signpost the way forward via review using many climate indices from all over the world in their correlation with decadal Australian rainfall.

1.3 Brief Historical Background

From 1904, the new director of the Indian Meteorological Office, Sir Gilbert Walker, initiated research into the causal factors of the Indian Monsoon using empiric, mathematical, but mainly statistical methods (Walker 1997) and went on to introduced the Southern Oscillation Index (SOI) (Walker & Bliss 1937) as a measure of the Southern Oscillation (SO). SOI is the statistical difference of mean sea level pressure between Tahiti and Darwin

and is an indicator of the strength of a global scale equatorial zonal atmospheric and ocean system referred to as the Walker Circulation.

Stone, Hammer and Marcussen (1996) linked global precipitation to the SOI using a combination of principal component analysis and a non-parametric statistical technique known as k-means (iterative partitioning) cluster analysis to turn the SOI into an important widely used predictor of Australian rainfall first used by (Stone & Auliciems 1992). Here the SOI enabled future rainfall patterns to be predicted three months ahead both in Australia and on other continents. This practical and reliable method is popular with both farmers and decision makers alike.

A different approach is numerical modelling where mathematics and physics are used to construct a virtual climate system from which rainfall predictions can be made. For example the Pacific Ocean Atmosphere Model for Australia (POAMA-2) has recently demonstrated a full seasonal forecasting ability (Wang et al. 2011).

Regression methods are a third methodology harking back to Walker's initial work; more specifically a Pearson's correlation coefficient test which is more suited to contemporary high resolution gridded data (Cai, Whetton & Pittock 2001). Cai, Whetton and Pittock (2001) used the SOI correlated decadal to the most accurate gridded rainfall data (1889 to 1998) available to them at that time (Nicholls & Lavery 1992).

This current study uses the latter method.

1.4 Rationale of the study

This study does not deal with the way climate indices affect Australian rainfall in a predictive sense in terms of interannual and intraannual variability, but compares relationships on a decadal time scale. The Literature review (Chapter 2) shows that previously very few climate indices have been used in correlation with Australian rainfall. Correlation analysis of rainfall and for the more familiar climate indices are however quite prolific and this study essentially used that adopted by (Cai, Whetton & Pittock 2001). In view of the fact that all indices of climate correlate with each other to a greater or lesser degree (de Viron, O., Dickey, J. O. & Ghil, M. 2013) two questions must be asked:

Why have a wide variety of climate indices not been previously investigated in their correlation with Australian rainfall?

Are there indices of climate that can outperform those currently in use for the prediction of Australian precipitation?”

The hypothesis for this thesis is therefore is that of the many extant climate indices irrespective of their source region some may exist which can outperform indices currently in use as predictors of Australian and SEQ precipitation, but hitherto have never been used for this purpose. Climate indices used in this thesis are shown in Table 1.1 giving; their name and alias if appropriate, their descriptive acronym and a reference to the authorship of their introductory paper. A very similar table is shown in Chapter 3 but differs in showing the origin of the data series used for analysis.

Table 1.1: List of climate indices used in this study and their authorship

Climate Index	Acronym	Author(s)
Arctic Oscillation Index aka Northern Annular Mode	AOI	(Baldwin, Cheng & Dunkerton 1994)
Cold Tongue Index	CTI	(Mitchell 1999)
Combined Niño 34 and Southern Oscillation Index	BEST	(Bamston, Chelliah & Goldenberg 1997)
El Niño Modoki Index	EMI	(Ashok et al. 2007)
Equatorial SOI	EQSOI	(Kistler et al. 2001)
Five Variable Niño Index	FIVEVAR	(Kuleshov et al. 2008)
Indian Ocean Dipole	IOD	(Saji et al. 1999)
Indo Pacific Warm Pool	IPWP	(Wang & Mehta 2008)
Inter Decadal Pacific Oscillation	IPO	(Folland et al. 1999)
Multi-variant Niño Index	MEI	(Volter 2009)
North Atlantic Oscillation	NAO	(Hurrell 1995)

Northern Oscillation Index	NOI	(Schwing, Murphree & Green 2002)
Pacific Decadal Oscillation	PDO	(Mantua et al. 1997)
Pacific Warm Pool	PWP	(Hoerling 2009)
Quasi Biennial Oscillation	QBO	(Baldwin, M. P. et al. 2001)
Sea Surface Temperature Anomaly in Niño 3.4 region	Niño34	(Bamston, Chelliah & Goldenberg 1997)
Southern Annular Mode	SAM	(Marshall 2003)
Southern Oscillation Index	SOI	(Walker & Bliss 1937)
Trans Pacific Niño Index	TNI	(Trenberth & Stepaniak 2001)
Tropical Pacific Ocean Empirical Orthogonal Function	TPEOF	(Weare, Navato & Newell 1976)
Warm Water Volume	WWV	(Meinen & McPhaden 2000)
Warm Water Volume East	WWV_E	"
Warm Water Volume West	WWV_W	"
Western Hemisphere Warm Pool	WHWP	(Wang & Enfield 2001)

In this context a preliminary investigation was conducted which led to this more detailed investigation whose results are shown in Chapter 4. The preliminary study correlated 13 climate indices to rainfall in ten strategically placed Australian towns (Figure 1.2) over a 32 year (1978 – 2010) time period (BoM 2010c). The preliminary analysis showed superficial agreement with previous work (Baird et al. 2011) as to how different indices perform (Table 1.1).

It is intriguing that the oldest but elegantly, simple index the SOI (Walker & Bliss 1937), whose apparatus consists of just two barometers and a link so that the pressures might be

compared, is able to outperform some of these other sophisticated modern indices. A probable reason why the SOI competes so well is because unlike many other indices which rely on near Equatorial Pacific climate elements the SOI uses as one of its elements the mean sea level pressure in Darwin (12°24'S 130°52'E) immediate to our location.

Table 1.2 makes an obvious but critical point that different indices do better in different regions of our continent supporting the work of previous authors (Cai, Whetton & Pittock 2001; Schepen, Wang & Robertson 2011) and that forecasting for a particular region should use the most appropriate highest correlation index. This study will therefore try to also identify the better performing indices in terms of SEQ rainfall correlation.

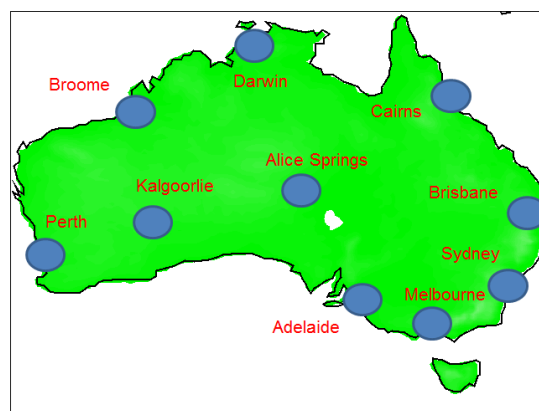


Figure 1.2: Strategic Australian sites for preliminary study

Table 1.2: Investigation showing statistically significant correlation (# indicates $p < 0.05$) of 13 monthly climate indices to rainfall in ten strategically placed Australian towns (1978 – 2010).

	Adelaide	Alice Springs	Brisbane	Broome	Cairns	Darwin	Kalgoorlie	Melbourne	Perth	Sydney
SOI		#		#	#		#			
TNI			#		#	#				
ONI				#	#			#		
EMI		#	#							#
EI					#					
LI		#			#	#				
ESPI					#					
MEI				#	#					
FIVEVAR			#	#	#	#		#		
BEST			#	#	#	#				
WHWP				#	#	#			#	
TPEOF					#			#		
EQSOI				#	#					

1.5 Aims of the Study

The aim of this study is to investigate how 24 indices of climate taken from all over the world compare in their correlation with Australian monthly rainfall for the 11 decades from 1900 to 2008. The end of each decadal period was set as the eighth year to enable results from this study to be compared with previous work, for example see Cai, Whetton and Pittock (2001). Initially the whole year period was used but this was later refined to Australian summer, December, January and February (DJF) when it was realised that different indices could fare

marked differently under the two regimes. This procedure results in a “Road Test” of differing climate indices and how they compare with Australian rainfall at a decadal resolution for the summer months. Key to the study is the fact that climate everywhere on the Earth’s surface is related to climate elsewhere (Walker 1928) so no one index should be favoured or discarded when being compared to another.

Chapter 2 Literature Review

2.1 Introduction to Climate Indices and Rainfall

Australia is an extremely dry continent (Figure 2.1) where approximately 60% of the land area has less than 400 mm·yr⁻¹ of rainfall. A more detailed decadal rainfall anomaly graphic is shown later (Figure 4.1).

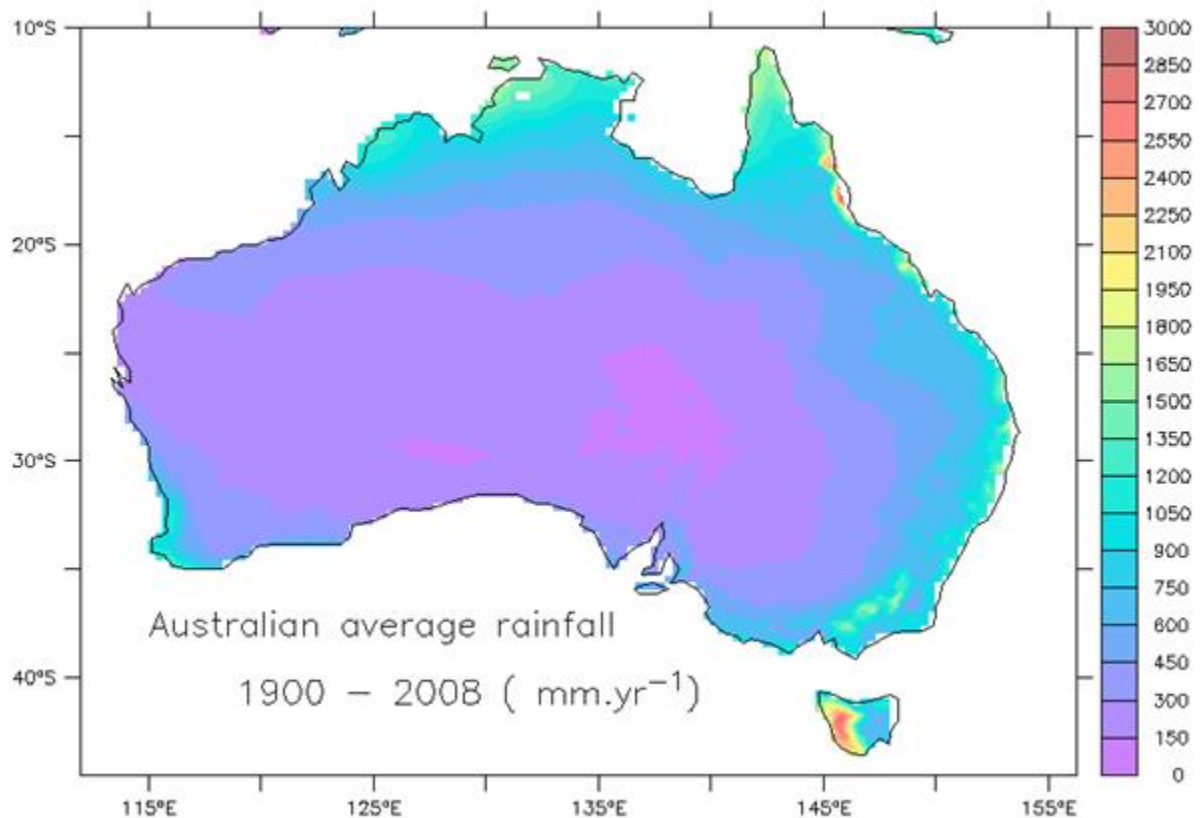


Figure 2.1: Australian annual total average annual rainfall (mm·yr⁻¹) 1900 – 2008 over land areas (Jones, Wang and Fawcett (2009))

Without discussing the basic climatology of Australia too deeply, details of which are widely available; for example in Sturman and Tapper (1996), the similarity of the rainfall contours shown in a map of Australian rainfall between 1900 – 2008 (Figure 2.1) matches quite closely the Köppen climatic regions of Australia BoM (2005) (Figure 2.2). The summer months allude to Monsoonal rainfall conditions in the tropical regions and weak rainfall conditions in the South's temperate climate. In winter the temperate regions are associated

with enhanced rainfall due to Northward progress of the sub-tropical ridge allowing westerly storm tracks to impinge on to the mainland (BoM 2010b) .

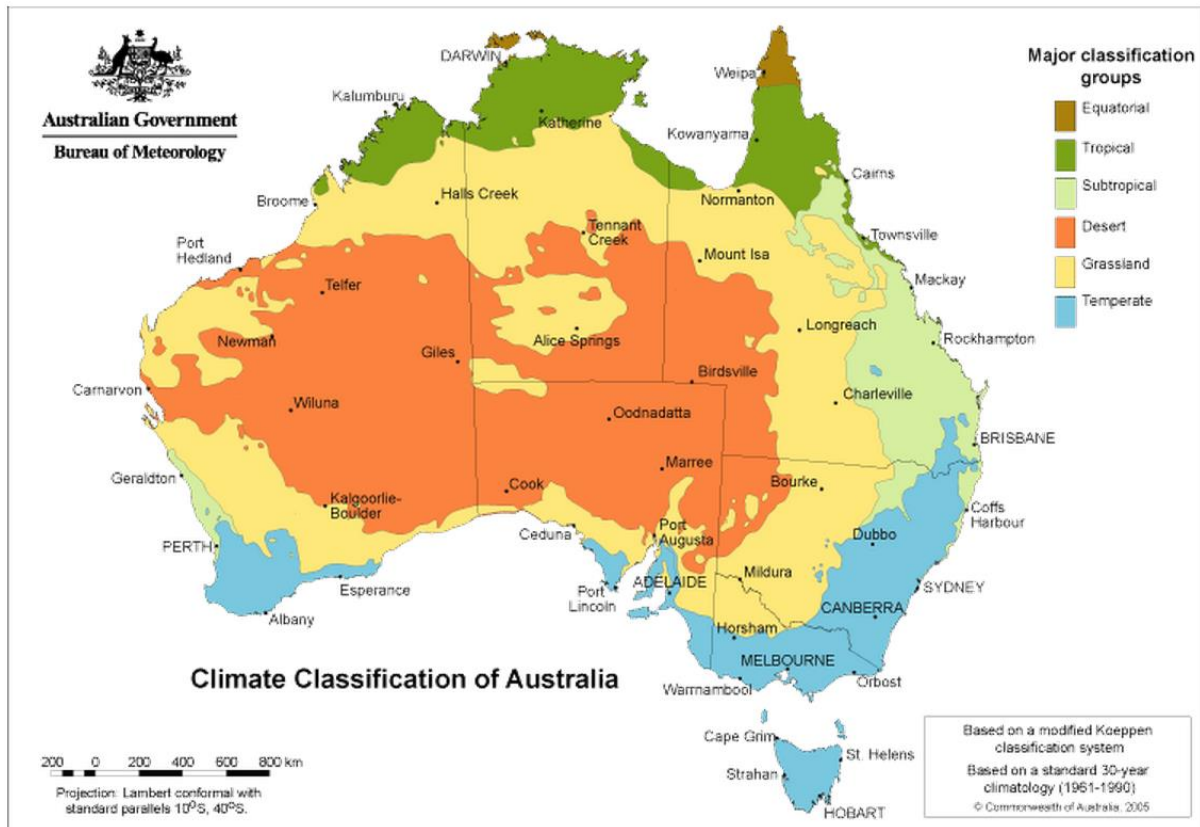


Figure 2.2: Australian climatic regions based on the Köppen classification after BoM (2005).

Rainfall in Australia is extremely variable (Nicholls, Drosowsky & Lavery 1997) and affected by various climate modes from the intra-annual, for example the Madden Julian Oscillation (MJO) (Madden & Julian 1972) that provides an underlying 30 – 60 day influence and up to and beyond the Inter Decadal Pacific Oscillation (IPO) (Folland et al. 1999; Power. et al. 1999) and can cause variability over a period greater than 30 years. It should be noted however that nothing stops these climate modes in working interactively with each other (Risbey et al. 2009). With the exception of intraannual variability these climate modes are discussed more fully in section 2.9.

With respect to South East Queensland (SEQ) the region itself is sub-tropical; precipitation is influenced by the position of the sub-tropical ridge in summer that provides a moist onshore flow. In many summers the presence of the East Coast Trough enhances this rainfall and

provides steering for La Niña ex-tropical cyclones that have their genesis in the warm waters of the Coral Sea SE of New Guinea (BoM 2010b; Klingaman, Woolnough & Syktus 2013). The region is sufficiently south to have significant winter rainfall.

The Southern Oscillation Index (SOI) via extended statistical analysis is a very important tool, if not the most important one for Australian seasonal climate forecasting (Hammer, Holzworth & Stone 1996). Many sectors of our society and economy, for example; farming, policy making/ planning, emergency services, finance and insurance are severely affected by climate extremes due to variability at the intra and inter annual scale (Nelson et al. 2010). Such climate extrema might also mask the initial effects of climate change affecting society at a longer temporal scale. It is therefore self-evident that any increase in the predictive ability of forecasting to identify the probability of climate extrema and climate trends would have great benefits for Australian society.

One potential avenue for improvement in forecasting is to investigate how indices other than the SOI perform as predictors of Australian climate. There have been a great number of studies of the correlation between individual indices and rainfall, Cai, Whetton and Pittock (2001) investigated the correlation between the SOI and Australian rainfall between 1899 and 1998. However, only one significant study was found in the literature that has used a multiplicity of indices for this purpose (Schepen, Wang & Robertson 2011) and then not to any great scope over a 28 year period.

This literature review is focused on the potential of a diversity of indices of climate that have not been previously used in Australia and irrespective of their source region. Northern hemisphere indices as discussed in Section 2.7.2 which independently show a strong teleconnection to Australian climate (Cai, Whetton & Pittock 2001; Sun et al. 2014). Oceanic heat content indices, for example the Warm Water Volume (WWV) (Meinen & McPhaden 2000) are also considered. Potential for using thermal energy contained within the near Australia warm pools are also considered, an example being the Indo Pacific Warm Pool (IPWP) (Wang & Mehta 2008).

Literatures reflecting how different climate indices, that are driven by or have a teleconnection with various climate modes, have been used to gain insight into the evolution of the climate system from the intra-annual to multidecadal scale are therefore discussed in this chapter. This was done as part of the attempt to identify if there are as yet unidentified

climate indices which can potentially outperform those currently in use for prediction of Australian climate.

The review also focusses in on the fact that regions close to Australia which have immense effects on World climate (Chen et al. 2004), but have not been used for the prediction of Australian rainfall. The recurrent observation made by many authors for example Tsonis, Swanson and Kravtsov (2007) that climate does not evolve in a smooth manner but is subject to aperiodic shifts in regime is discussed. This review also amplifies observations that climate indices do not have to be geographically adjacent to the area of interest (Cai, Whetton & Pittock 2001), that different regions are best depicted by different indices (Murphy & Ribbe 2004) and that some regions are devoid of any usable correlation with any index (Schepen, Wang & Robertson 2011).

Statistical climate prediction methods are not the only methods available. In passing it is noted that an alternative is numerical modelling, where mathematics is used to construct a virtual climate system from which rainfall predictions can be made. For example the Pacific Ocean Atmosphere Model for Australia (POAMA) (Wang et al. 2004) run by the Bureau of Meteorology (BoM 2010a) in Australia used a virtual Earth divided up into a latitude longitude grid of 0.7° (≈ 80 km) side with 50 levels in the atmosphere. A complex system of partial differential equations known as Navier Stokes Equations has to be solved at each grid point to provide a weather forecast up to ten days ahead. For medium term forecasting such model scenarios have to be continually updated with observational data of seven atmospheric variables. In such a complex system without such seeding over time the model predictions gradually diverge from reality (Lorenz 1963). Such evolution is also affected at the sub grid level by perhaps meso scale convection and stochastic processes potentially involving huge amounts of computing power for the solution of the resultant large dynamic systems of differential equations (Hirsch, Smale & Devaney 2012) unless parametric techniques are used (Stephens 1984). Progress is however being made and recently a full seasonal forecasting ability has been demonstrated with the updated POAMA-2 system (Wang et al. 2011) which has become the operational seasonal forecasting tool for the Australian Bureau of Meteorology.

It should be noted however that models, be they mathematical or statistical are at best an analogy not a theory, as a model is something like the system but is *not* the system (Derman 2011).

Climate indices are ubiquitous, inhabiting all parts of the World and for and all of them have a correlation with each other (de Viron, O., Dickey, J. O. & Ghil, M. 2013). The inference to be drawn from this is that all climate indices have a correlation with Australian climate to a greater or lesser degree. There might well be climate indices as yet unused that give better correlations with climate in particular regions of Australia than those currently in use.

The structure of this literature review tries to adhere to chronology wherever possible but with such a diverse subject matter this is not always possible. Inherent in the chronology is the development and relevant importance of indices of El Niño Southern Oscillation (ENSO) for not just Australian but World climate as they underpin the development of climate prediction methods. The review therefore covers historical development and discussion of these indices before moving on to indices from further afield.

Climate indices used in this thesis are shown in Table 1.1 giving; their name and alias if appropriate, their descriptive acronym and a reference to the authorship of their introductory paper. A very similar table is shown in Chapter 3 but differs in showing the origin of the data series used for analysis. This literature review uses as its base key drivers of climate; the Southern Oscillation (SO) and El Niño Southern Oscillation (ENSO) because historically they are also the drivers of all the major developments that have occurred in climate prediction methods.

2.2 Historic Availability of Climate Data

The current plethora of climate data springs from the era of space exploration. Consider that prior to this era only sparse SST data were available from ship's logs and more recently by instruments carried by ships of opportunity (Goni et al. 2010). The famous "Blue Marble" photograph of the Earth taken from space by the Apollo 17 crew (Przborski 1972) helped change the situation, inspired a whole generation to care more for our environment and heralded a paradigm shift from reductionism towards the holistic study of Earth System Science. In this new enlightened era there was a commensurate increase in remote sensing applications with an explosion in the availability of accurate data (Sarewitz & Pielke Jr 1999) with such programs as the Tropical Ocean Global Atmosphere (TOGA, 1985-1994) project (McPhaden et al. 1998). Even then there were problems because at least 80 years of data were required to obtain the required degrees of freedom for statistical analysis (McPhaden et al.

2006) resulting in over fitting concerns (Kug et al. 2010). These articles stress the importance of the time scale of the data series used.

Running parallel to the increased availability of data better use of previously more sparse data was achieved in 1995 by the use of Empirical Orthogonal Functions (EOFs) derived by a mathematical method known as Principal Component Analysis. Such methods enabling the climate record to be extended back into the past to produce Pacific Ocean SST anomaly data from 1950 – 1992 (Smith et al. 1996).

EOFs consist of a matrix system of eigenvalues that enable the highest variance data to be identified (Bjornsson 1997). The Smith et al. (1996) data came from the Comprehensive Ocean Atmosphere Data Set (COADS) (Woodruff et al. 1987), the UK Met Office Global Sea Ice and Sea Surface Temperature (GISST) (Parker et al. 1994) and optimally interpreted data from ships, buoys and satellites (Reynolds & Smith 1994). Initially the Optimum Interpretation (OI) method (Gandin 1960) was used to which a least squares smoothing technique was applied to get an accurate 1982 – 1993 climate analysis.

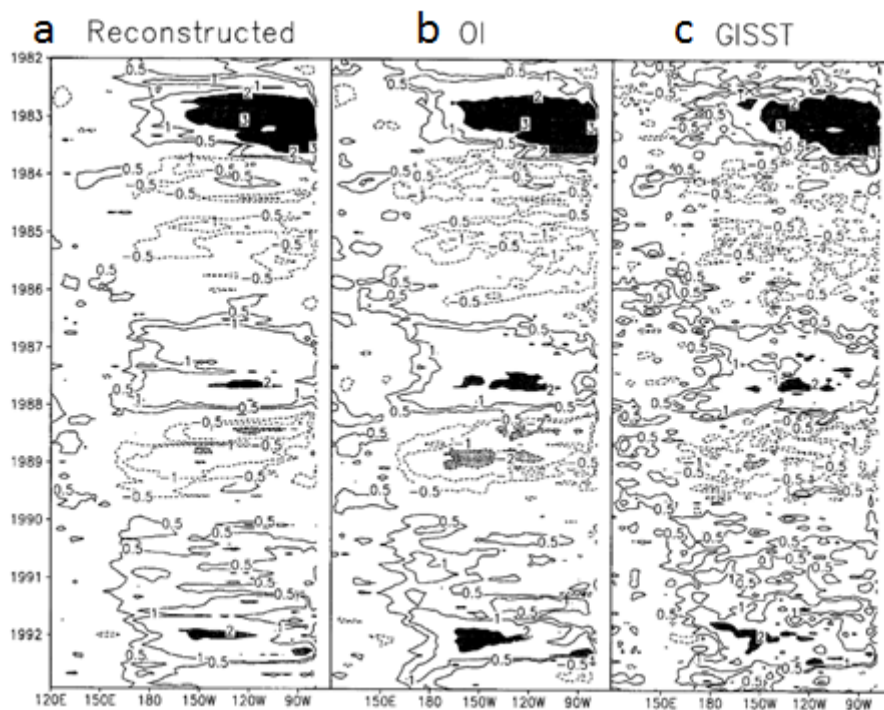


Figure 2.3: Hovmöller diagrams showing 1982 – 1993 SST reconstructed anomalies. a) with b) OI and c) GISST data for between $\pm 5^\circ$ latitude. Contours are at 1°C with an inclusion of $\pm 0.5^\circ\text{C}$ and shading applied to anomaly greater than 2°C (Smith et al. 1996).

All data values were then converted to anomalies by the removal of their monthly climatologies. EOF data were then regressed by least squares fit to the other series (OI and GISST). Finally a complete SST field was reconstructed from the spatial and temporal modes. Figure 2.3(a) shows that the reconstructed data are smoother than the (b) GISST alluding to a greater coherence but the size of the anomaly is bigger in the (c) OI. Smith et al. (1996) therefore assert that although the product is a marked improvement on previous material it cannot make up for lack of satellite data. The OI for its part is subject to larger errors as are the GISST data. The reconstructed data therefore is more accurate overall but are less so in regions of intense sampling.

An extension of the method followed using climate models incorporating those past, sparse records of “ships of opportunity” SST data from commercial vessels, plus satellite data to weave them into more reliable long term merged data series some of which reach back as far as 1856 (Rayner et al. 2003; Reynolds & Smith 1994).

A further improvement ensued with the introduction of a recursive, retrospective method to obtain a very accurate time series of ocean related variables including SST, salinity and later ocean heat content from the Simple Ocean Data analysis (SODA) (Carton et al. 2000) based on a general circulation ocean climate model (GCM). The model uses data contained in the World Ocean Atlas 1994 (WOA – 94) (Levitus & Boyer 1994) with additional SST data (Reynolds & Smith 1994), Geosat, ERS-1 and TOPEX/Poseidon between latitudes 62° North and South to provide a record of ocean variables between 1950 – 1996. Later on this method was used to extend the ocean data in the period 1871 – 2008 (Giese & Ray 2011).

Starting out with observational data subject to the OI method Carton et al. (2000) used the GCM to obtain a first guess of mass and momentum at each junction of the model matrix whilst statistical errors were computed a priori. Then the observed data were used to calculate error in the first guess and the effect of model bias so that the SODA algorithm could then apply continuous error updating to maintain results close to geostrophic equilibrium for the product.

An exciting recent development is Linear Inverse Modelling (LIM) (Solomon & Newman 2012) based on Principal Oscillation Pattern (POP) analysis (von Storch et al. 1995), where disparities in the output of climate models of the Indo Pacific Ocean temperature trends from the past 111 years (1900 – 2010) can be reconciled. EOFs are used where a linear (truncated) transform time series at time t is used as an index to see how it evolves at time $t +$

τ where τ is the lag period. Checking is then done by sampling the data at a 10 year interval and computing the resultant variables for the next interval in rather a similar fashion to the SODA method. Solomon and Newman (2012) have been able to verify that the Had1SST (Rayner et al. 2003) and KAPLAN SST data series (Kaplan et al. 1998) have negligible residual errors for the whole period.

An Australian precipitation and temperature record in the form of the Australian Water Availability Project (AWAP) whose records span between 1900 – 2008 on a 0.25° latitude longitude grid (Jones, Wang & Fawcett 2009) are applied in this research and described in section 3.1.

2.3 Brief Description of a Climate Index

A climate index is a diagnostic tool used to describe the state and changes of a climate system (University Hamburg 2012). Climate indices are most often represented with a time series, each point in time corresponds to one index value. An index can be constructed to describe almost any geophysical event, from summer monsoon rainfall in India, to pressure differences at two locations in the Pacific Ocean, or spatially-averaged sea surface temperatures (Emanuel 2009). Each index is created for a specific purpose: to monitor some aspect of climate.

2.4 El Niño Southern Oscillation

The El Niño Southern Oscillation (ENSO) is an approximately eight year cycle of alternating warming and cooling events of the Equatorial Pacific Ocean (Giese & Ray 2011) accompanied by commensurate atmospheric changes. The oceanic warming and cooling are termed El Niño and La Niña events respectively whilst the atmospheric change is called the Southern Oscillation (SO). This coupled atmosphere/ocean phenomenon is the most dominant year-to-year climate signal on Earth (McPhaden, Zebiak & Glantz 2006) affecting every region of the globe but is more evident in the Equatorial region.

The Southern Oscillation

“He decided that since he saw no prospect of treating the weather as a subject to which mathematical reasoning from well-established

premises could be applied (at the time), he would collect all the relevant information which had been recorded and treat it statistically without attempting to trace physical connections between cause and effect”,

thus said G. L. Taylor (1962) of Sir Gilbert Walker. Taylor (1962) was referring to the appointment of Sir Gilbert as Director of the Indian Meteorological Office in 1904 and his research into the causal factors of the Indian Monsoon. Walker's reasoning was sound because it took until the late 1930's for the components of the general circulation of the atmosphere to be understood (Crutzen & Ramanathan 2000). Walker (1928) found that climate conditions everywhere were related, how rainfall in Australia was associated both with the Indian Monsoon and dry conditions in Canada whilst identifying three significant global scale circulations; the Southern Oscillation (SO), the North Atlantic Oscillation and the North Pacific Oscillation. Interest in the SO languished for nearly three decades during which Walker's work attracted criticism for lacking a physical mechanism to explain its existence whilst other researchers cast about trying to distil causal linkages Allen (2006).

The thermodynamic and physical nature of the SO were eventually discovered (Bjerknes 1969) and a much simplified diagram of the ocean atmosphere system it represents is shown in Figure 2.4 where the normal (ENSO neutral) condition is depicted. Atmospheric convective activity above the Western Pacific Ocean associated with low surface barometric pressure leads to divergence at the tropopause where the Westerly component aloft is constrained by the Equatorial Wave guide effect (Matsuno 1966). At the longitude of the Eastern Pacific Gyres upper convergence takes place under the influence of the high barometric surface pressure (Sturman & Tapper 1996). The circulation is then completed by the Easterly trade winds which entrain and advect cold water from the abyss produced by Ekman Pumping adjacent to the West coast of the Americas (Thorade 1909). During this 16,000km advection the water is warmed by insolation to contribute to the West Pacific Warm Pool (WPWP).

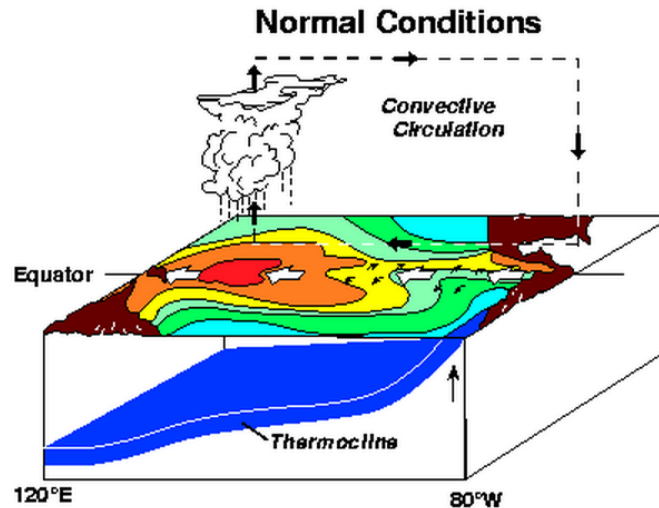


Figure 2.4: Simplified schematic of the Equatorial Pacific Ocean and Walker Circulation showing convection above the WPWP which is shown in red (PMEL 2008).

By way of a tribute to Sir Gilbert Walker, Bjerknes (1969) referred to the atmospheric part of system as the Walker Circulation; a term that has entered common usage.

El Niño and La Niña

The Walker Circulation via the SO led eventually to the understanding of ENSO and its components; El Niño and La Niña (Bjerknes 1961, 1966, 1969; Wyrtki 1975). Bjerknes (1961) first associated the SO to the anomalous warming and cooling of the East Pacific Ocean which occurred on average every 4.5 years (Giese & Ray 2011). He showed that anomalous sea surface temperature (SST) increase in the central and East Pacific was related to the destruction of the trade winds a component of the Walker Circulation (Figure 2.5). This SST variation led to the understanding of the El Niño (Christ Child) which occurs near Christmas time, an ironic colloquialism invented by the poor fishermen of Chile and Peru who suffer food shortages when their sardine fishing industry collapse (Pontecorvo 2001) and devastating floods (Wells 1990). In Australia, El Niño is often associated with drought, although this is not always the case as often other causal factors come into play (BoM 2013b; Risbey et al. 2009).

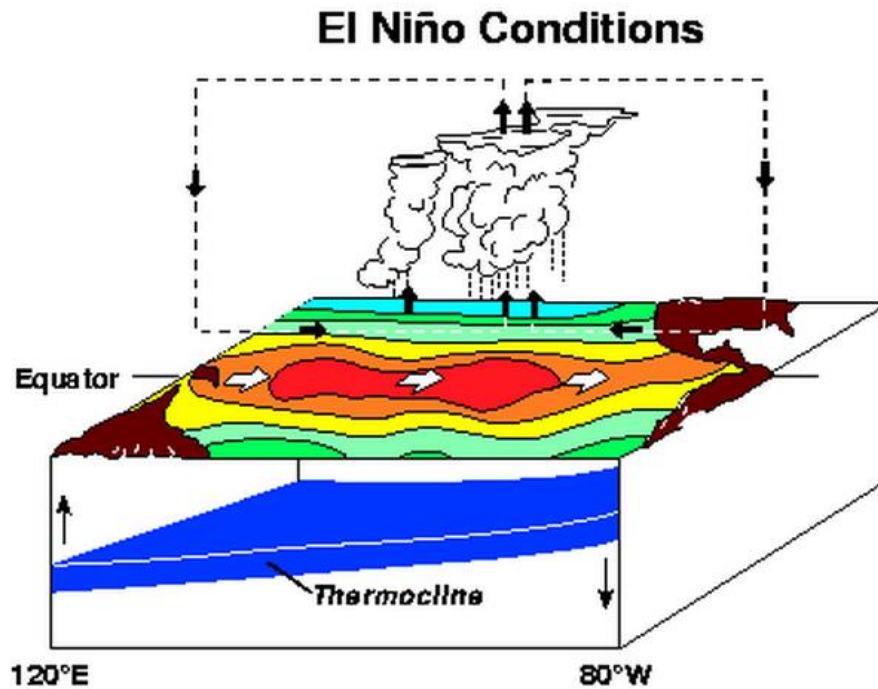


Figure 2.5: El Niño conditions where Walker Circulation has collapsed, convective area moves east as has the WPWP which has cooled somewhat but advected heat eastwards towards the central and E Pacific (PMEL 2008).

La Niña (The Girl) (Figure 2.6), a more benign regime for the fishermen (Pagès et al. 2001), is also normally associated with above average rainfall in eastern and northern Australia. It is difficult to conjecture which of the two extreme phases La Niña or El Niño impacts more adversely on society for both conditions can impact adversely on society dependent on the region of the globe considered (Glantz 2000). Though other factors besides La Niña or El Niño also influence drought (Risbey et al. 2009).

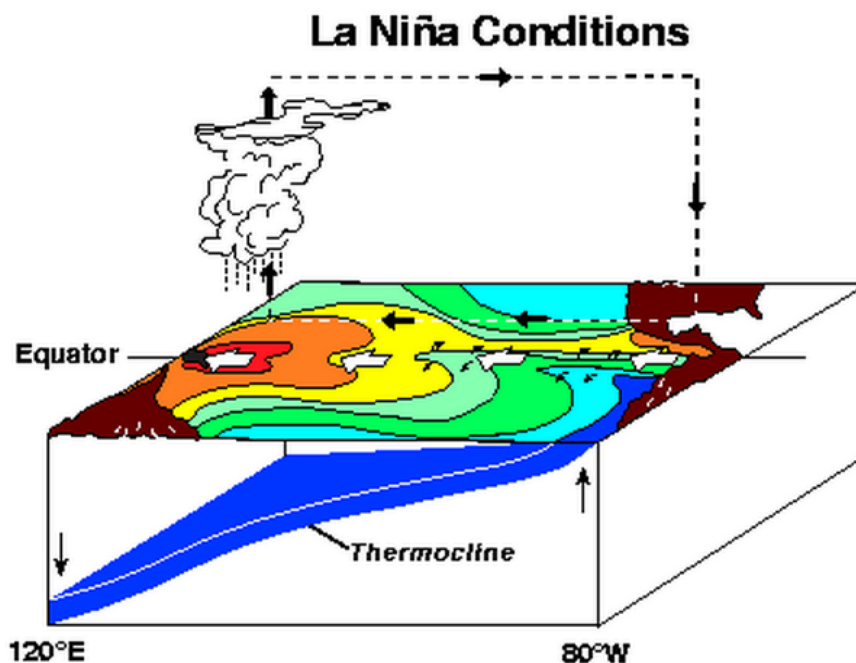


Figure 2.6: La Niña conditions showing enhanced Walker Circulation with vigorous convection over an anomalously warm WPWP (PMEL 2008).

Southern Oscillation Index

The Southern Oscillation Index (SOI) (Walker & Bliss 1937) followed as a natural development of the SO concept, being its descriptive index that reflects the state of the Walker Circulation and trade wind strength. SOI is based on Mean Sea Level Pressure (MSLP) difference anomaly between Tahiti ($\approx 17^\circ\text{S}$, 149°W) and Darwin ($\approx 12.5^\circ\text{S}$, 131°E) which enjoy the same MSLP to give normal conditions (Figure 2.4).

In Australian usage this result is multiplied by 10 to produce the "Troup SOI" (Troup 1965) which provides a non-decimal output.

With respect to Australia ENSO neutral conditions ($\text{SOI} = 0$) is normally associated with average rainfall. $\text{SOI} < 0$ can be indicative of what is known as an El Niño or ENSO warm event (Rasmusson & Wallace 1983). A converse situation known as a La Niña or ENSO cold event (pressure anomalously greater in Tahiti than Darwin and $\text{SOI} > 0$) tends to produce greater than average probability in Australia (Glantz 2000).

Southern Oscillation Index history

It has been widely accepted that there is a robust association between SOI and the Equatorial Sea Surface Temperature (SST) field (Rasmusson & Carpenter 1982). Wright et al. (1988) confirmed a correlation between pressure and SST in one of the first works to establish the

concept of a distinct predictive Equatorial region of SST (Figure 2.7) where regions 14 and 15 approximate to regions known as the Niño's 1 and 2 regions. Niño regions are discussed in Section 2.6.

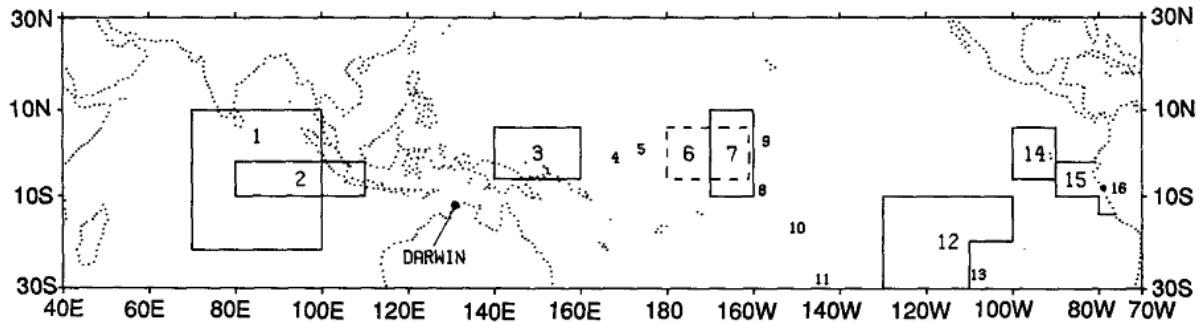


Figure 2.7: Regions 7, 14, 15 and 16 represent SST; regions 1, 10, 11, 12 and 13 pressure; regions 2,3 and 6 zonal wind; regions 4, 5, 8 and 9 rainfall, from Wright et al. (1988).

Wright et al. (1988) used the Comprehensive Ocean-Atmosphere Data Set (COADS) (Woodruff et al. 1987) a climate record based on data from ships of opportunity to obtain regression fields across the tropical Indian and Pacific oceans to produce climate indices based on SST, zonal wind, rainfall and MSLP. A Darwin Pressure Index (DPI) was chosen rather than the SOI although the SO signature was apparent in COADS. Reflecting the paucity of data the DPI was compared with non-parametric (ranked) seasonal rainfall data for the whole tropical Indo-Pacific region to produce correlations maps. The results are reproduced in Table 2.2 and probably represent one of the earliest examples of a multiple index study and show quite remarkable correlation of 0.78 between the DPI and rainfall at Line Island some 3500 km distant from Darwin. With respect to East Pacific Ocean MSLP measured at 6600 km distance from Darwin the correlation was -0.75 but improved to 0.82 for rainfall at Line Island when a type of index akin to the SOI based on DPI minus the E Pacific MSLP was used (Wright et al. 1988). The most significant outcome is the correlation of DPI and central Pacific SST of 0.88 which alludes to the interchangeability of pressure and SST indices as first asserted in (Berlage 1966) as cited in Rasmusson and Carpenter (1982).

Table 2.1: Correlation matrix of the indices depicted in Figure 2.4 in the Equatorial belt based on averages from July – November for each of the 30 years 1950 – 1979 and are arranged from west to east (Wright et al. 1988).

	1	2	3	4	5	6	7	8
	Indian Ocean zonal wind (110–80°E)	Darwin SLP (131°E)	West Pacific zonal wind (160–140°E)	Line Island rainfall index (160°W)	Central Pacific SST (170–160°W)	East Pacific SLP (110–90°W)	Darwin minus E. Equatorial Pacific SLP	Puerto Chicama SST
(1)	1.00	-.84	-.86	-.64	-.77	.61	-.79	-.61
(2)	-.84	1.00	.88	.78	.88	-.76	.95	.80
(3)	-.86	.88	1.00	.84	.84	-.80	.90	.82
(4)	-.64	.78	.84	1.00	.75	-.75	.82	.90
(5)	-.77	.88	.84	.75	1.00	-.78	.90	.80
(6)	.61	-.76	-.80	-.75	-.78	1.00	-.92	-.86
(7)	-.79	.95	.90	.82	.90	.92	1.00	.88
(8)	-.61	.80	.82	.90	.80	-.86	.88	1.00

It took until 1987 for a robust SOI time series to be obtained (Ropelewski & Jones 1987). Ropelewski and Jones (1987) utilised new pre 1935 Tahiti data as it had been found that prior to 1935 the existing Tahiti MSLP time series data were unsuitable for accurate use suffering as they did from missing values and a datum error of one hPa. Trenberth and Hoar (1996) cast doubt as to the veracity of the pre 1935 Tahiti data. However, as it was shown that the correlation of Tahiti to Darwin MSLP anomalies was only -0.19 prior to 1935 but improved to -0.35 for post 1935 (Trenberth & Hoar 1996). It should be noted however that the SOI underwent a marked amplitude change during the 1920s and 1930s (Wang & Wang 1996).

2.5 Southern Oscillation Index Contemporary Usage

In 1996 SOI pressure relationship was utilised as a predictor for global, but more specifically to this study, Australian seasonal rainfall (Stone, Hammer & Marcussen 1996). Stone, Hammer and Marcussen (1996) reasoned that a good predictive model of global rainfall would lead to better management of world agricultural production. Stone, Hammer and Marcussen (1996) went on to describe a system based on the phase of the SOI with respect to ENSO able to predict the lagged probability of rainfall variation from three to six months in advance. Such a system would minimise risks to farmers in years subject to inadequate rainfall, so that they might change their planting requirements in advance and maximise profits for them in years where rainfall amount is suitable for their requirements.

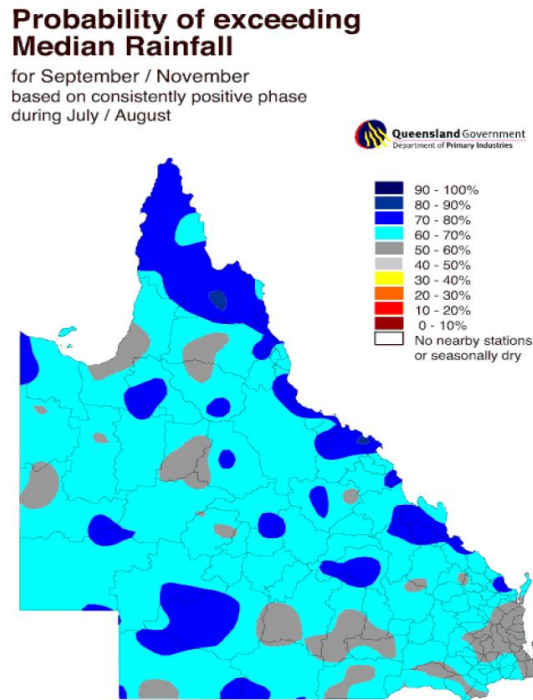


Figure 2.8: Rainfall forecast probability values for Queensland for September - November 2011 (Stone, Hammer and Marcussen (1996)).

For their data Stone, Hammer and Marcussen (1996) used a 120 year rainfall record and the Troup SOI. SOI data were subject to Principle Component Analysis (PCA) to provide PCA scores which were then subject to *k*-means Cluster Analysis. Cluster Analysis, a non-parametric procedure that puts things or events into different taxonomic groups, of the data which enabled five distinct phases of the SOI (Stone & Auliciems 1992) to be categorised: consistently negative, consistently positive, rapidly increasing, rapidly decreasing and consistently near zero. The historical Australian monthly rainfall records were then incorporated into an atlas of these SOI regimes to produce a rainfall probability forecast for various regions. A typical forecast for Queensland for September – November 2011 is shown in Figure 2.8.

Applications of the SOI have been used for cereal crop yield prediction (Potgieter, Hammer & Butler 2002) and risk management for farmers (Stone, Best & Sosenko 2008).

There is no barrier to this method being used for other indices should they prove to have greater predictive ability than the SOI. SOI has been found to have less fidelity in prediction of some of the more important ENSO warm events prompting the Climate Prediction Centre (CPC) at the National Oceanic and Atmospheric Administration (NOAA) to produce the

Equatorial SOI (EQSOI) based on Eastern Equatorial Pacific and near Indonesia barometric pressure difference (Kistler et al. 2001). One would imagine that due to the regions remoteness to Darwin that this index would be less sensitive to Australian precipitation but this is not necessarily the case as Figure 2.9 shows, where on the whole EQSOI appears to respond more assertively to wetter than average conditions than does SOI. This is a most interesting and unusual point extending the predictive reference frame eastwards to 90°E (almost to the Mascarene High) within the Pacific Warm Pool (PWP).

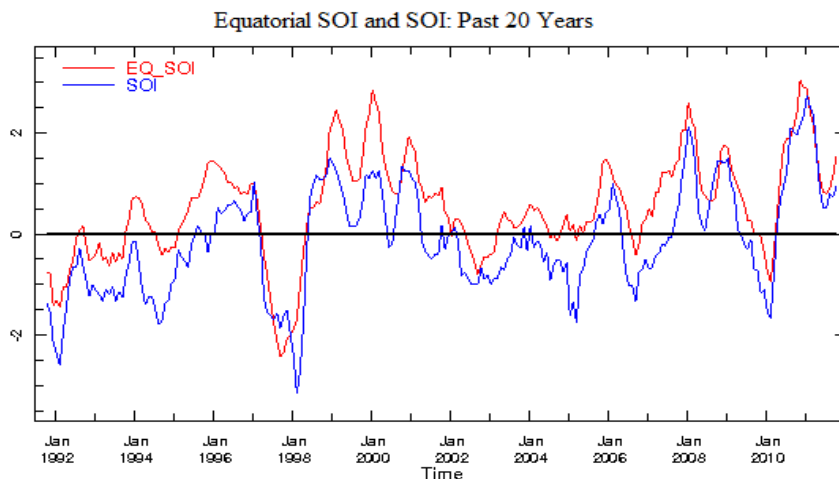


Figure 2.9: Comparison of EQSOI and SOI (IRI 2011).

2.6 Development of the El Niño Southern Oscillation

ENSO is recognised as the most important year to year climate fluctuation on Earth (McPhaden 2004) which possibly explains why there are at least ten actual ENSO indices in existence based on eight different combinations of the five Niño regions (Figure 2.10).

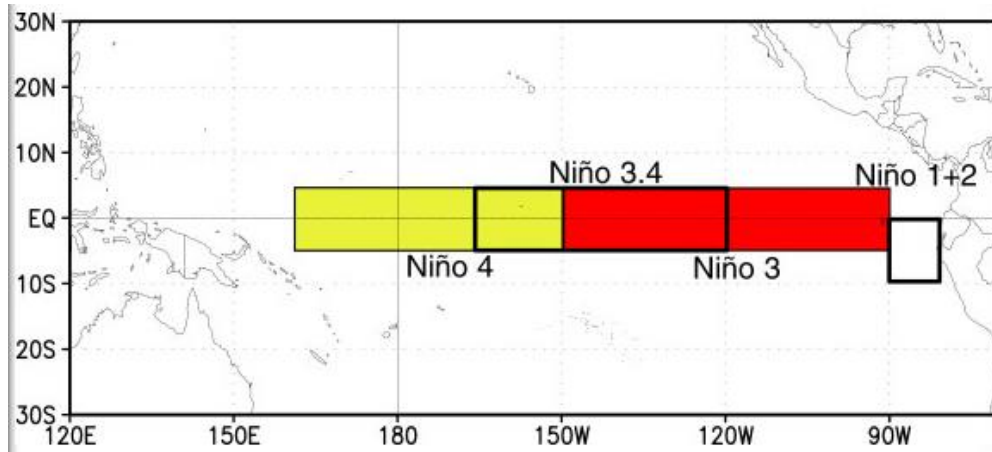


Figure 2.10: The basic Niño regions (Climate Prediction Centre 2005a)

The Niño34 Index (Bamston, Chelliah & Goldenberg 1997) is the five month running mean of SST anomaly in the Niño3.4 region of $\pm 5^\circ\text{N}$ and S latitude and $120 - 170^\circ\text{W}$ longitude (Figure 2.11) became accepted as the standard ENSO index (Trenberth 1997). For predictive and definition purposes the National Oceanic and Atmospheric Administration (NOAA) an arm of the US government may also define this index as a three month running mean known as the Oceanic Niño Index (ONI) (Kaplan et al. 1998; Reynolds & Smith 1994). The ONI defines El Niño as five consecutive three month periods of greater than $+0.5^\circ\text{C}$ SST anomaly and La Niña as five consecutive three month periods of less than -0.5°C SST anomaly. In Australia the Troup SOI is used to define ENSO phases where values greater than 8 are associated with La Niña conditions whilst values below -8 are associated with El Niño conditions(BoM 2013b).

It was found that climate descriptions based on a single index did not do justice to the complexity of climate variability over the Equatorial Pacific during the Tropical Ocean Global Analysis (TOGA) decade (Wallace et al. 1998). Further complications arose with the so called, May, June and July “spring barrier” (Torrence & Webster 1998) which causes a lack of forecasting skill for Boreal Summer possibly due to a combination of the ENSO phase locking to the annual cycle of Pacific SST variability which involves the March-May movement of tropical convection moving northwest from the WPWP and the Boreal winter peak of ENSO warm events (Rasmusson & Carpenter 1982) varying interdecadally.

Attempts followed to increase the predictive ability of ENSO indices; A multivariate El Niño Index (MEI) followed (Wolter & Timlin 1998) which utilised the six most important prognostic variables of ENSO in an attempt to most accurately depict El Niño; it included the

first principal components of surface pressure, surface air temperature (SAT), **u** and **v** wind, SST and total cloudiness fraction of the sky. Subsequently the cloudiness fraction has now been superseded by the use of outgoing long wave radiation (OLR) (Wolter 2009). The MEI is regarded as a more complete and flexible descriptor of the El Niño than any single index (Wolter & Timlin 2011).

MEI was also found to better able reflect Monsoon rainfall in India on an overall basis than the SOI (Singh 2001) Correlation of the univariate SOI was found to vary substantially over different parts of the sub-continent whereas the MEI correlation coefficients achieved consistently higher values. Digressing somewhat it is worth noting that Monsoon prediction currently uses a multivariate technique using a variety of GCM products (Singh et al. 2012). Significantly, (Singh 2001) also postulated that different indices of climate might be used for rainfall correlation in different parts of the country. This example shows how the MEI might be utilised to successfully predict Indian Monsoon Rainfall (IMR)India (Figure 2.11).

Table 2.2: Grid point variance ratios for La Niña and El Niño phase for winter Pacific North Western regional temperatures in the US; after Smith and Sardeshmukh (2000).

Grid point location	Index			
	Best	SOI	Niño34	MEI
37.5°N 105°W	1.8	1.33	1.64	1.54
25°N 65°W	0.58	0.53	0.57	0.55

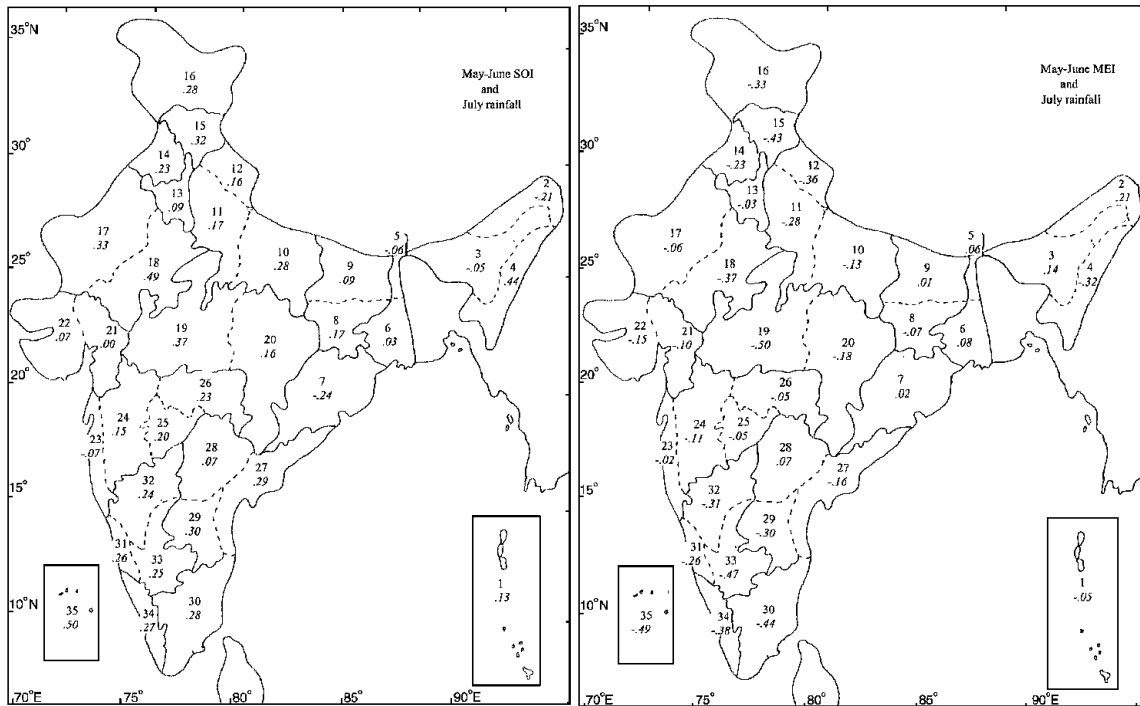


Figure 2.11: a) Correlation coefficients between May – June SOI and July Indian South Western Monsoon anomaly. b) Correlation coefficients between May – June MEI and July Indian South Western Monsoon anomaly

Irrespective of their ability to track Pacific SST variation a wide variety of ENSO indices were developed for quite different purposes, for example a bivariate index was introduced in 1998 as a predictor of United States mainland climate (Smith & Sardeshmukh 2000) known as the BEST index consisting of a combination of the SOI and the Niño34 index. Smith and Sardeshmukh (2000) developed the BEST index because it was thought that having both an atmospheric (MSLP) and an oceanic (SST) component the index would be more robust than a univariate index that just used either an atmospheric or an oceanic component. The index was used to investigate the relationship between ENSO and the boreal (DJF) winter-time temperature of the Pacific Mid-West of the United States (US). The results, some of which are shown in Table 2.3, shows the variance ratios at two grid points between La Niña and El Niño temperatures were of great interest to the energy and heating industries for energy demand applications in that region.

The FIVEVAR index was developed to be better able to predict tropical cyclone activity in the South Pacific and South Indian oceans. (Kuleshov et al. 2008). FIVEVAR is also a multivariate index consisting of the first principle components of: Darwin Mean Sea Level Pressure (MSLP), Tahiti MSLP, Niño3, Niño3.4 and Niño4 SST anomalies. Kuleshov et al.

(2008) were able to show that both FIVEVAR and MEI achieved equal ranking in the identification of ENSO warm and cold events but assert that FIVEVAR is preferential because it can consistently be extended further back in time.

As will be discussed later in Section 2.9 FIVEVAR has also been shown to be an excellent predictor of Australian rainfall (Baird et al. 2011).

All El Niño events are not the same, sometimes the SST anomaly occurs in the eastern Pacific and sometimes in both the eastern and central Pacific simultaneously. In 2001 it was mooted that at least two indices of ENSO were necessary to depict these “two flavours of El Niño” (Trenberth & Stepaniak 2001) and the Trans Niño Index (TNI) was introduced. The TNI uses the SST anomaly for the Niño 1 and 2 regions compared to the Niño 4 region (Figure 2.11). (Trenberth & Stepaniak 2001) expressed an opinion that the TNI was clearly involved with the low frequency behaviour of ENSO the combined index seeming to point more readily to Torrence and Webster’s (1998) inter-decadal variation of ENSO with Monsoon variance. The central Pacific El Niño concept was pursued further when it was realised that effect on precipitation in many parts of the World was different to those of an ordinary El Niño event and it was named El Niño Modoki (Ashok et al. 2007) an index based on the 2nd EOF of Sea Surface Temperature Anomaly (SSTA) in the Central Pacific Ocean. Ashok and Yamagata (2009) also found, as an interesting aside, that this El Niño Modoki Index (EMI) was highly correlated to the TNI (coefficient of 0.8). Effect of EMI on Australian rainfall as opposed to the more conventional El Niño was found to delay the Australian Monsoon so that precipitation peaked a month later (March) in an El Niño Modoki (Taschetto et al. 2010) although time of termination was not affected.

A recent innovation is the introduction of hybrid prediction systems for climate. A technique of comparing statistical climate predictions with both observational and climate model outcomes has been used (Yang & DelSole 2011). In this work the Niño3.4 index was correlated to the National Centre for Environmental Predictions (NCEP) data for the air temperature at 2m above land and land area precipitation both on a 2.5° grid between 1948 and 2010. These actual data were then in turn compared with the integration of a five climate model hindcast known as ENSEMBLES (Weisheimer et al. 2009). ENSEMBLES are 1960 – 2005 predictions from the European Centre for Medium-Range Weather Forecasts (ECMWF) which were integrated with a seven climate model reconstruction known as DEMETER (Palmer et al. 2004) between 1958 – 2001. Four ensembles were chosen; two from the ECMWF coupled model (ECM) and two from the Météo Francaise coupled model (MET).

Yang and DelSole (2011) show that correlation between the Niño3.4 index and global land precipitation could be described as robust, moderate, weak or insignificant (Table 2.4) and only two of the six continents analysed are shown not to have statistically significant teleconnections; Europe for both variables in DJF and JJA and North America for both variables in JJA. For the Australian continent it was found that the correlation with precipitation was robust at the 5% significance level for both models. For the 2m above land elevation temperature correlation was also robust at the same confidence level with ECM hindcast, but correlation was only moderate using the MET model. The results of the correlations Yang and DelSole (2011) found are shown in Figure 2.12 (refer to the key for details) including canonical correlation, ρ^2 , values. Results for the other continent are also included in Table 2.4 for comparison.

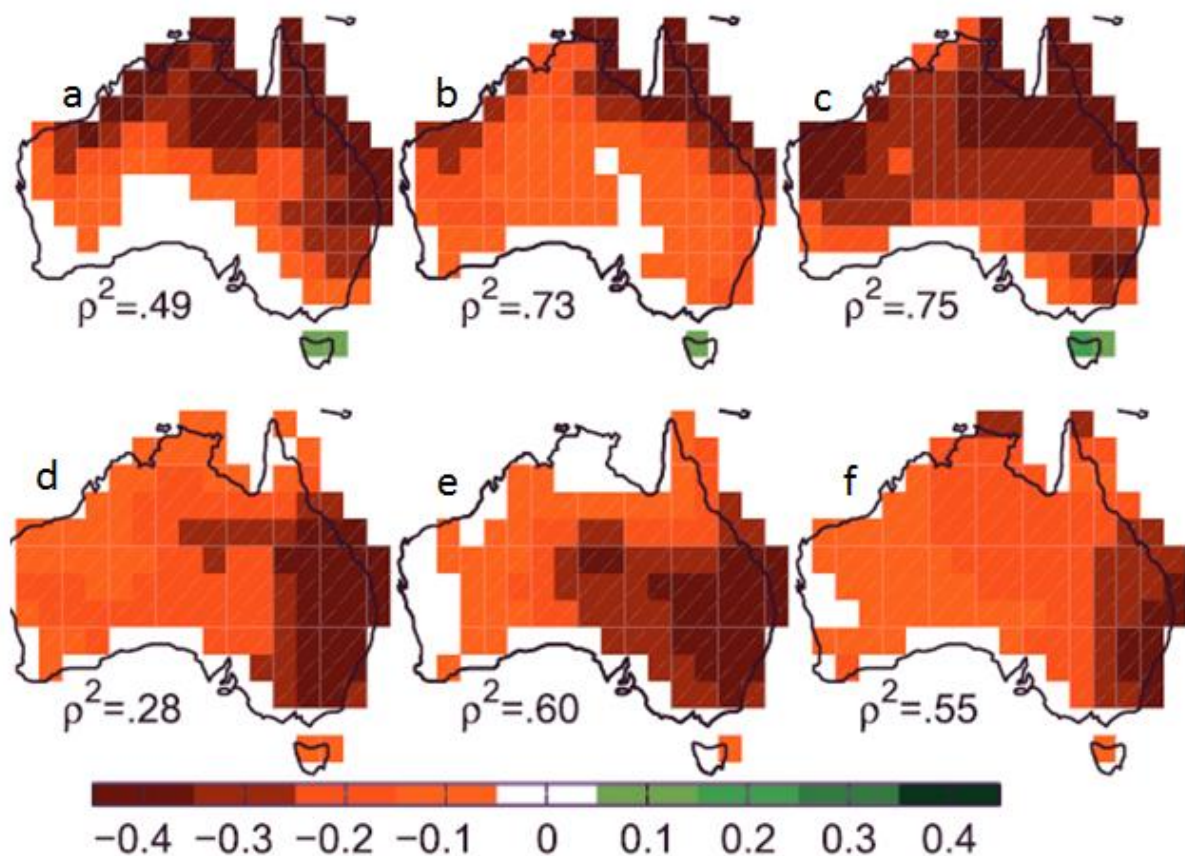


Figure 2.12: Comparison of statistical forecasting, actual data and climate model output for Australia; modified from Yang and DelSole (2011) (a – c) refers to DJF precipitation whilst

(d – f) refers to JAS. Across from left to right with canonical correlation is (a and d) observational results, (b and e) ECM model output and (c and f) MET output.

Not only does the El Niño Southern Oscillation (ENSO) cause climate anomalies throughout the World (Kumar et al. 2006) but also affects the health and wellbeing of the World’s population (Kovats et al. 2003). Kovats et al. (2003) were able to show apart from the flood/drought impact of ENSO epidemiologically the SOI became a significant index of cholera and malarial type diseases throughout the World.

Indices of ENSO are not a panacea for accurate climate prediction and other indices can outperform them (Steinbach et al. 2006). I were able to show by the use of cluster analysis that hitherto unused oceanic climate indices could be defined that outperformed the normal ENSO climate indices and SOI over certain regions of the globe.

This section reviewed the status quo of our understanding of ENSO, the use of the SOI and current research activities. Particular focus was on this, since ENSO is the most significant of the global climate drivers (McPhaden 2004) and has been successfully used in managing societal activities (Stone, Hammer & Marcussen 1996). In the following section other climate processes and their indices are reviewed.

Table 2.3: Significance and correlation for six continents constructed from Yang and DelSole, (2011) for Boreal Winter; DJF and summer; JAS for precipitation and temperature at 2 m elevation.

	Precipitation			T2m		
	Observed	ECM	MET	Observed	ECM	MET
Continent	Significance	DJF	JAS	Significance	DJF	JAS
Africa	5%	Low	Low	5%	Moderate	Moderate
Asia	5%	Mod	Low	5%	Mod	Low
Australia	5%	Robust	Robust	5%	Robust	Moderate
Europe	insignificant	insignificant	insignificant	insignificant	insignificant	insignificant
S America	5%	Low	Moderate	5%	Robust	Low
N America	5% DJF	Not stated	insignificant	5% DJF	Not stated	insignificant

2.7 Worldwide Climate Indices

In this section the focus moves out from the ENSO phenomenon; climate indices and other processes are reviewed that drive climate/rainfall in Australia and other parts of the world. The indices which monitor these climate processes are discussed including; Northern Hemisphere, other meridional and latitudinal indices and most importantly indices connected with the near Australia oceanic Warm Pools (WPs).

de Viron, O., Dickey, J. O. and Ghil, M. (2013) revisits and extends Walker's (1928) hypothesis of a completely coupled global climate system, since some of the climate modes discussed by de Viron, O., Dickey, J. O. and Ghil, M. (2013) were not fully described or known by Walker (1928). Large scale phenomena for example; ENSO, the Asian Monsoon, North Atlantic Oscillation (NAO) and MJO being oscillatory in character at greatly different temporal scales, were shown by de Viron, O., Dickey, J. O. and Ghil, M. (2013) to be inter-related and can be monitored by a number of climate indices. Some 25 globally diverse climate indices associated with different climate fields were used and irrespective of location when any two of these indices were compared they were shown to correlate with each other at the interannual level. For example, a teleconnection between the NAO and Australian rainfall might well exist based on the strong coherence between the SOI and mid latitude northern hemisphere mean sea level pressure variability (Cai, Whetton & Pittock 2001) . The SOI can be used to predict global rainfall probability values (Stone, Hammer & Marcussen 1996). MJO, a 30 to 60 day tropical, Equatorial variability, apart from its well-known local effects of modulating Monsoon rainfall variability, controls rainfall in the western, high northern latitude United States via the "Pineapple Express" (Gottschalck et al. 2010) where it appears to reposition the jet stream (Weickmann & Sardeshmukh 1994) and modulate mid latitude pressure fields. Weickmann and Sardeshmukh (1994) also note that MJO forces global angular momentum affecting day length. Other effects are mostly confined to the northern hemisphere where it forces a persistent high pressure anomaly in the lee of the Himalayas and a modulation of the circumpolar vortex. These studies and summaries indicate that the entirety of global climate and weather is linked. It is logical to assume given the extensive linkages between the different mechanisms governing Earth's climate that indices tracking the changes in these phenomena will correlate. If correlations between these indices are robust then regardless of the mechanism they represent they might be able to be used to predict climate and weather at a time and place (Walker 1928). Further research into the

causality behind these indices is essential for the future development of: models of Earth's weather and climate, and new or improved climate indices.

2.7.1 Meridional Indices

The phases of Quasi Biennial Oscillation (QBO) which is an approximately two year reversal of the tropical stratospheric zonal wind (Baldwin, M. et al. 2001) and ENSO were found to coincide (Van Loon & Labitzke 1987). Additionally, the QBO was found to have a signal in the 11 year solar cycle in boreal winter (Mason & Lindesay 1993; Naito & Hirota 1997; Williams & Stone 2009). It is worth noting that the relationship of decadal climate variability and the 11 year solar cycle has at times been an intense area of debate as it was found that the solar cycle effects winds and temperature in the upper stratosphere (Baldwin, M. et al. 2001). In addition Labitzke (2004) also noted QBOs relationship with SAM which has an affect on south-eastern NSW rainfall.

2.7.2 Northern Hemisphere and Latitudinal Indices

Mitchell and Wallace (2004) suggested that Australian rainfall might be able to be linked to an index based on the Arctic Oscillation (AO). This supposition was never confirmed, but Cattiaux and Cassou (2013) however did find that in addition to a relationship between AO and Arctic Ocean sea ice fluctuation that there was a completely unexpected strong teleconnection between warming of the West Pacific Warm Pool (WPWP) region and AO in Austral summer. Cai, Whetton and Pittock (2001) noted that ENSO exerts a strong effect on mid to high latitude atmospheric circulation in the Northern Hemisphere. Lau (1997) showed that as well as the tropical effect of ENSO that there is also an extra-tropical driver, also that ENSO related SST anomalies in the tropical Pacific are well correlated with changes elsewhere in the world's oceans. It was found that the effects of the NAO were statistically indistinguishable from that of the AOI (Feldstein & Franzke 2006) and Sun et al. (2014) found a decadal scale teleconnection whereby the NAO led eastern Australian rainfall by 15 years.

The Northern Oscillation Index (NOI) (Schwing, Murphree & Green 2002) based on the MSLP difference between the North Pacific High ($\approx 35 - 45^\circ\text{N}$, 150°W) and Darwin

represents climate extremes that are not well represented by the tropical SOI and undergoes an approximate 14 year cycle. NOI represents the climatic forcing in the North East Pacific Ocean.

2.7.3 The Warm Pools

With respect to the near Australia oceanic Warm Pools (WPs) I will now discuss some that have been demonstrated to have relationship with temperature and rainfall elsewhere, but have not been used for Australia to date.

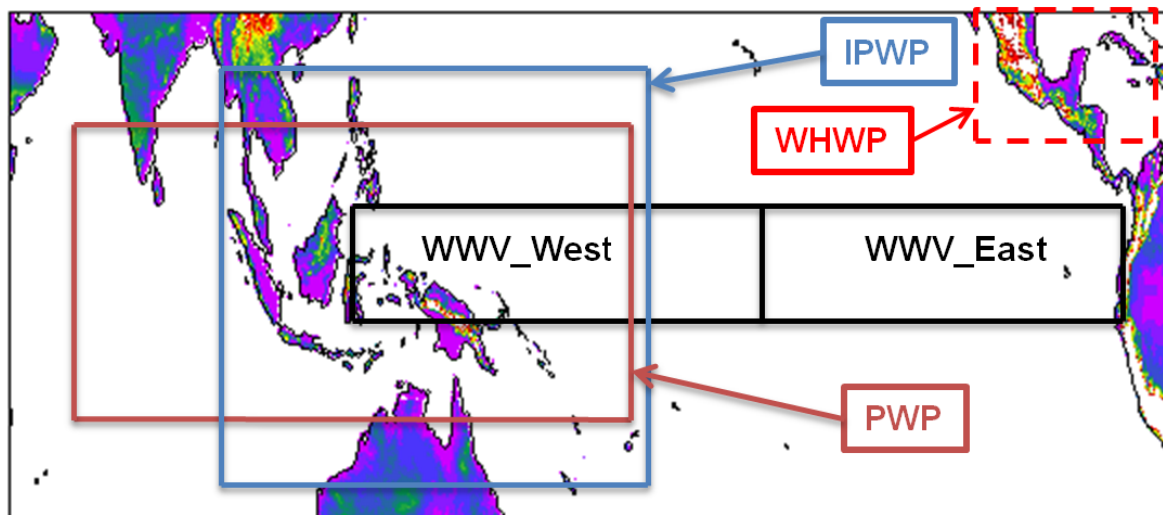


Figure 2.13: Relationship of near oceanic warm pool regions to Australia. In black the WWV region consisting of WWV_West ($\pm 5^\circ$ latitude, $120^\circ\text{E} - 155^\circ\text{W}$ longitude) and WWV_E ($\pm 5^\circ$ latitude, $155^\circ\text{W} - 80^\circ\text{W}$ longitude); as defined by McPhaden (2003) and TAO Project Office, NOAA/PMEL. In ochre the Pacific Warm Pool (PWP) region ($\pm 15^\circ$ latitude, $60^\circ\text{E} - 170^\circ\text{E}$ longitude) as defined by Hoerling (2009). In blue the Indo Pacific Warm Pool (IPWP) ($\pm 20^\circ$ latitude, $90^\circ\text{E} - 180^\circ\text{E}$ longitude) as defined by Wang and Mehta (2008). The Western Hemisphere Warm Pool (WHWP) (Wang & Enfield 2001) ($7^\circ - 27^\circ\text{N}$ latitude, $110^\circ\text{W} - 50^\circ\text{W}$ longitude) a more remote warm pool is also included.

These indices will be subsequently applied to the Australia Climate data. The strongest source areas for continental precipitation are located adjacent to the continents in question (van der Ent & Savenije 2013). van der Ent and Savenije (2013) found that in Australia, both local SST and the Niño 3.4 region appear to have a big influence on precipitation. They also noted that ENSO related SST variations also played a role. The effect of the local ocean on Australian climate was noted by (Taschetto et al. 2011). For correlation to precipitation; in addition to purely oceanic properties atmospheric oceanic coupling also plays a role (Kumar, Chen & Wang 2013). Kumar, Chen and Wang (2013) found that in some regions where atmospheric phenomena drive the oceanic coupling strongly the SST correlation with precipitation became weaker tending towards being weakly negative. On the other hand, with a slowly changing oceanic driver, correlation was more reliable being robustly positive an indication of the primary role of SST. Li, Yu and Li (2013) showed that increased SST in the tropical west Pacific accounts for 50% of the rainfall increase in North Australia over the past 33 years. The work done by these authors' points to an examination of correlations between indices from regions near to Australian rainfall, examples of these regions are shown in Figure 2.13. It must be stated that a contra view does exist however that in general regional SST has only a weak relationship with Australian rainfall (Watterson 2001, 2010).

WHWP furthest away of the WPs, laying on the most Eastern fringe of the Niño regions and in terms of surface area (though variable) is the second largest oceanic warm pool on Earth (Wang & Enfield 2001). Contained within the WHWP is a region of global density driven circulation that experiences very large freshwater fluxes into the atmosphere (Rahmstorf 2006). WHWP undergoes the largest annual cycle and interannual departures in area and intensity and causes large fluctuations in the Hadley and Walker Circulation hence effecting global climate (Wang & Enfield 2001). Wang and Enfield (2001) also state that WHWP variation is associated with large changes in; tropospheric heat, moisture and stability over the Tropical Americas, perhaps driven by feedback from Outgoing Longwave Radiation (OLR) and variation in cloud cover. Unlike the West Pacific Warm Pool (WPWP) (Cravatte et al. 2009) it is not associated with large zonal flux changes or Kelvin Wave propagation and is entirely N of the Equator. Having stated this, Figure 2.14 shows that there is a similarity between the SST anomalies of the WHWP time series and that of the Niño3 region. Extending from the Eastern North Pacific to the Gulf of Mexico and the Caribbean the WHWP is characterised by SST greater than 28.5°C (Wang & Enfield 2001) and despite the incursion of the tropical American mainland responds as a monolithic whole. There is a

marked correlation of the WHWP and precipitation from Northern South America to the Southern US. An index based on the WHWP could potentially be used for rainfall prediction in the Eastern Pacific and Atlantic. If such potential is realised it could lead to improvements in both seasonal climate forecasting and hurricane forecasting in both the Pacific and Atlantic regions of the Americas. This is beyond the scope of this thesis but could be an very important area of future research.

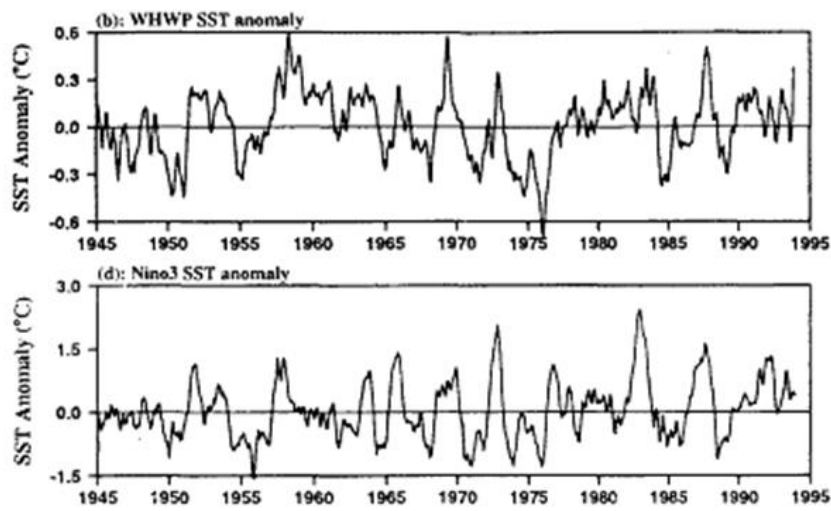


Figure 2.14: Comparison of: b) above, the WHWP SST anomaly and d) below, the Niño3 anomaly (from Wang & Enfield (2001)).

WHWP has the potential to perform quite well as a predictor of Australian rainfall when the WHWP intensity index (WHWPPI) is used (this current study, using the WHWP area index as described in Section 3.1.2). The WHWPPI is defined as the average SST over the region: 7°N – 27°N latitude and 50°W – 110°W longitude (Wang & Enfield 2003).

Drosowsky and Chambers (2001) used sea surface temperature anomaly (SSTA) patterns over the Indian and Pacific Oceans to forecast lagged rainfall anomalies in Australia. The region and methodology more nearly mimics that for the Tropical Empirical Orthogonal Function (TPEOF) a concept which follows on from much earlier work (Weare, Navato & Newell 1976); here the region of interest was from $\pm 30^\circ$ N and S by 120°E to 60°W and uses the first principle component of SST anomaly enabling 40% of its variance to be explained (Hoerling, Kumar & Xu 2001). The thrust of this research was to gauge the robustness of the climate system response to ENSO extreme phases. With respect to North American winter

climate; strong correlation between the TPEOF and rainfall was apparent but there was lesser correlation with temperature. The geopotential height of the 500 hPa level was also found to be predictable for warm and cold phases of ENSO alluding to a weather forecasting potential (Hoerling, Kumar & Xu 2001).

The Pacific Warm Pool (PWP) (Figure 2.13) has a coincident Rain Pool (RP). PWP and RP are portrayed as being situated at the heart of the global climate system and described as its ventricle and atrium respectively (Chen et al. 2004). A PWP index is available from the NOAA climate indices web page (ERSL 2011) (Hoerling 2009) using the first EOF of SST from $\pm 15^{\circ}\text{N}$ and S and $60 - 170^{\circ}\text{E}$.

The Indo Pacific Warm Pool (IPWP; Figure 2.13) encompasses the oceans of tropical Australasia (De Deckker, Tapper & Van Der Kaars 2003). IPWP contains some of the warmest water on Earth stretching from $\pm 20^{\circ}\text{N}$ and S and $90 - 180^{\circ}\text{E}$, it includes all water above the temperature of 28°C (Yan et al. 1992), the threshold for atmospheric deep convection. The IPWP can vary in extent by: 25%, 22% and 11% at the; seasonal, interannual and decadal time scale respectively. Energy contained within the IPWP drives significant atmospheric ocean variability; the Madden Julian Oscillation (MJO), ENSO and the Asian Monsoon at interannual, annual and importantly interdecadal scales (Wang & Mehta 2008). Increase in SST in the IPWP is shown to actually cool the planet through an intensely complicated causal linkage that has its origins in increasing the depth of deep atmospheric convection (Fu 2013; Garfinkel et al. 2013). The IPWP index is based on satellite derived data which first became available circa 1983 is the area contained within the 28.5°C isotherm and used for American climate prediction (Wang & Mehta 2008) where it was attributed with forcing rainfall anomalies from Florida, through Texas, Arizona and the West Coast in Boreal winter. In Boreal summer these anomalies were maintained in the Midwest and Southeast. Another study shows how the IPWP affected the East Asian Monsoon over the last two millennia (Tierney et al. 2010). The IPWP straddles Australia and this index should attract a high priority for use in prediction of Australian climate. A word of caution is appropriate because there is a tendency to confuse between the PWP and the IPWP. In view of the potential importance of the IPWP for Australian rainfall prediction a IPWP index from 1900 – 2008 is constructed for this study using Simplified Ocean Data Assimilation analysis technique (SODA) (Carton & Giese 2008).

As discussed in Section 2.9 an ocean heat content index bearing a relationship to Warm Water Volume (WWV, Figure 2.13) using the Central Pacific 20°C isotherm anomaly was

tentatively used for Australian rainfall prediction, but not pursued in any great detail, as the record extended from only 1980 onwards (Schepen, Wang & Robertson 2011). However WWV has been successfully used as an indicator of Indian Summer Monsoon Rainfall (ISMR) activity onset (Rajeevan & McPhaden 2004) where it compared favourably to the Niño3 index.

WWV is the volume of warm water contained between the ocean surface and the 20⁰C isotherm used as a proxy for the thermocline between $\pm 5^{\circ}$ N and S latitude and 120^oE and 80^oW longitudes. Rajeevan and McPhaden (2004) used a 1980 – 2004 time series of this data augmented by SODA (Carton et al. 2000) to extend the time series further back in time to 1950. The results using WWV data were a dramatic improvement compared to the Niño3 index with respect to correlation with ISMR activity (Figures: 2.15 – 2.16).

Figure 2.16 shows that the WWV predicts ISMR onset at a greater correlation and lead (>99% level and five months) than does the Niño3 index (<95% and five months) (Figure 2.15) whose results are too weak to be used in forecast models. As an indicator WWV might show great promise for rainfall prediction. The WWV region is also divided into two portions; the Eastern arm, 155 – 80^oW termed WWV_E and the Western arm 120 – 155^oE (Meinen & McPhaden 2001) WWV_W the latter of which suggests itself for climate prediction purposes in Australia.

In comparison PWP has never been used for Australian climate prediction except at the micro-scale (Catto, Jakob & Nicholls 2012; Smith & Timbal 2012).

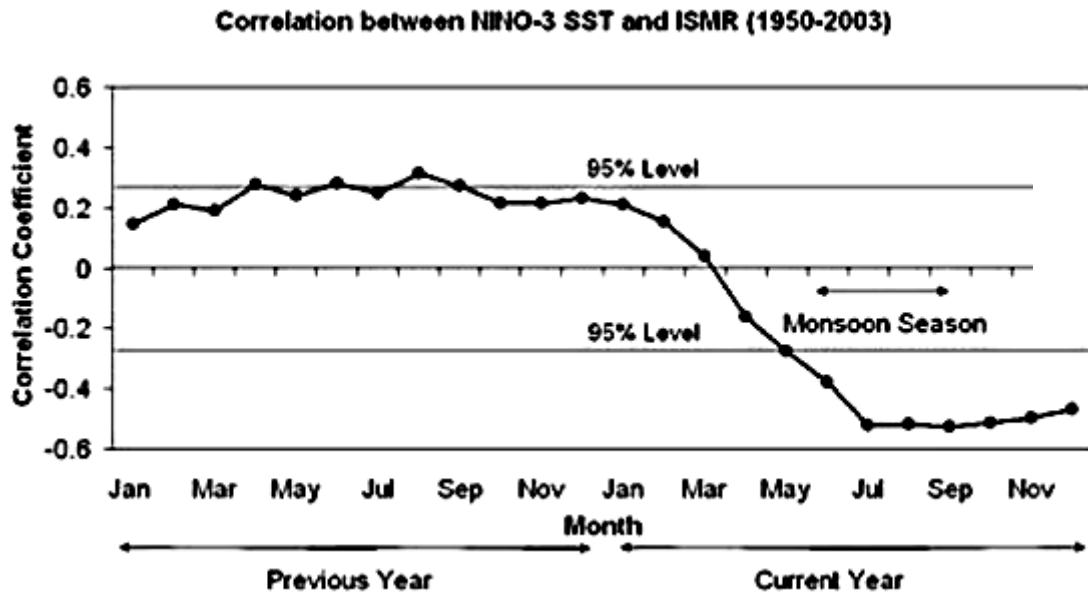


Figure 2.15: Lagged correlation of ISMR with Niño3 SST with lag shown on abscissae (from Rajeevan and McPhaden (2004)).

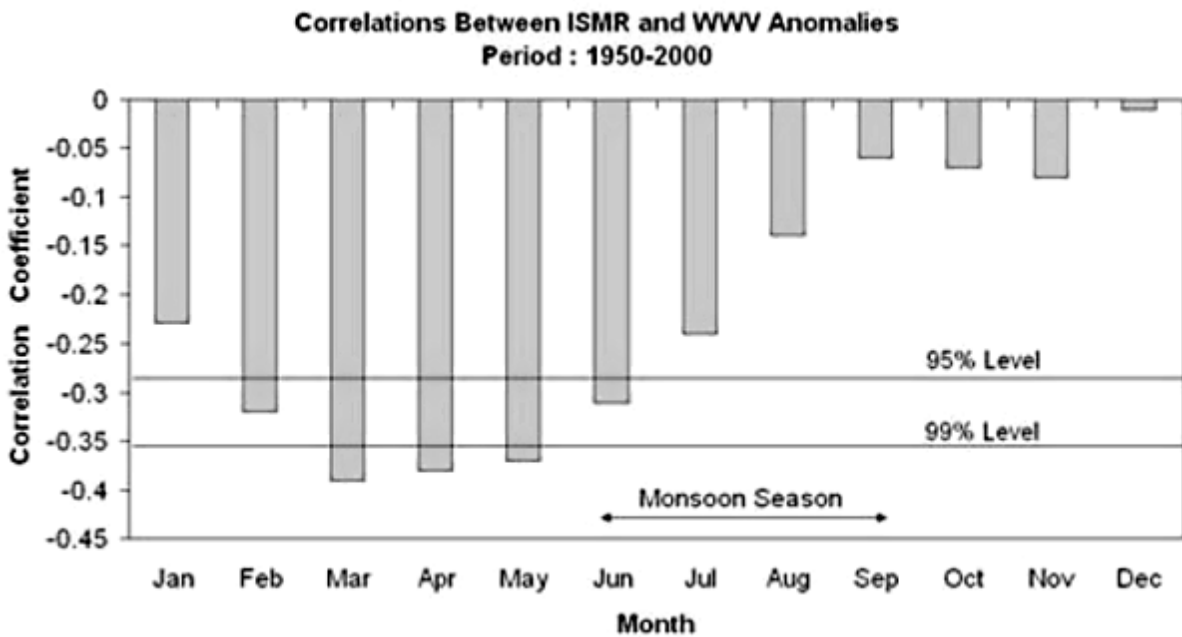


Figure 2.16: Lagged correlation of ISMR with WWV with lag shown on the abscissae (from Rajeevan and McPhaden (2004)).

There would appear to be a strong incentive to investigate correlation of these Major WP indices with Australian climate.

2.8 Decadal and Multidecadal Scale Climate Variability

Intra-annual and interannual climate modes have the ability to affect climate at far greater temporal scales. Interannual Very Low Frequency (VLF) modes of the shallow water equations exist as part of the coupled recharge oscillator theory for ENSO (Jin 2001). Jin (2001) was able to demonstrate greater than decadal length VLF modes were produced by extremely low velocity off Equatorial Rossby Waves, extending the interannual realm of ENSO like phenomena, allowing periods of between four and fourteen years to exist. Importantly such off Equatorial region solutions are independent of wind stress forcing, so not subject to the normal ENSO control mechanism allowing the tropical Pacific to be subject to feedback mechanisms outside the remit of the recharge/discharge theatre. It might therefore be seen that this region might be under the influence of phenomena from the MJO level of 30 to 60 days to the PDO level of 30 years and beyond.

Decadal capability of predicting Australian climate variability was found to be virtually non-existent Power et al.(1999)and that it was doubtful if any success would ever be achieved in this endeavour. Nonetheless, Power et al. (1999) examined high quality Australian temperature and rainfall records 1910 – 1993 to quantify relative importance of decadal variability to see if there was any relationship with SST (Mehta & Dubey 1995) over the adjacent oceans in the same period. By use of an eight year low pass filter it was found that area averaged Australian rainfall over east Australia (Lavery, Joung & Nicholls 1997) were shown to have an association with Indian Ocean SST south of 40°S.

Ansell et al. (2000) found that a quasi-decadal variability of Australian JJA rainfall from many regions (Hennessy, Suppiah & Page 1999; Jones & Beard 1998; Lavery, Joung & Nicholls 1997) including southwest Western Australia (SW WA), parts of South Australia (SA) and Tasmania were found to correlate with MSLP variation (Basnett & Parker 1997).

Meinke et al. (2005) although pointing out the importance of ENSO in relation to rainfall variability document a large numbers of authors who have described a relationship between global lower frequency phenomena and rainfall. Here bandpass filtering was used to isolate MSLP and SST data into five distinct temporal regions; 2.5 – 8 yr, 9 –13 yr, 13 – 18 yr and 18 – 39 yr. Interaction between ENSO at the quasi-biennial, classic interannual and decadal level was evident in the 9 – 13 yr band. The delayed oscillator mechanism of ENSO seemed to operate up to the decadal level (Battisti & Hirst 1989).

The work of Wang and Mehta (2008) later discussed in Section 2.7.3 in respect of the near Australian Warm Pool (WP) regions is mentioned here in respect of decadal correlation of a long term SST time series reconstructed using Simple Ocean Data Analysis (SODA).

Temperatures greater than 28°C, in the Indo Pacific Warm Pool (IPWP) region (Carton & Giese 2008) force rainfall anomalies in the United States (Higgins et al. 2000) southern states in Boreal winter when subjected to a seven year low-pass filter.

Risbey et al. (2009) were able to show that Australian rainfall (Lavery, Joung & Nicholls 1997) at a specific location varied decadal when subjected to many different climate drivers based on SST (Rayner et al. 2003). These climate drivers were shown not to be independent of each other especially the relationship between ENSO and IOD. It was therefore difficult to separate the effect of each individual mode on rainfall.

The fact that such climate modes tend to evolve at a different rate was used to provide a possible explanation for the climate shift of the 1970s where SST cooling occurred in the central Pacific Ocean and warming off the coast of Western North America (Tsonis, Swanson & Kravtsov 2007). This climate shift, of which the causes are unknown, has been observed by many (Graham 1994; McPhaden & Zhang 2004; Meehl, Hu & Santer 2009). Tsonis, Swanson and Kravtsov (2007) used monthly indices of North Atlantic Oscillation (NAO), North Pacific Oscillation (NPO), PDO and ENSO constructed using data mostly obtained from the Joint Institute for the Atmosphere and Oceans (JISAO). Additionally the NPO was used from the University Corporation for Atmospheric Research (UCAR) and all data were treated as non-linear sub components of the climate system. The four climate modes were then modelled into an $N \times N$ distance matrix ($N, 1: 4$) and treated as a network of four intersecting nodes whose topology is subjected to a sliding window technique where the behaviour of the nodes represented the dynamics of the system. The absolute distance between nodes may be thought of as the averaged correlation between all possible pairs of nodes as a measure of their synchronisation. The outcome is six phase states which by a “nearest is two neighbours” technique (Figure 2.17). The points in each triplet represent three consecutive points in a time series and their relative vertical position to each other indicates their respective values. (Tsonis, Swanson & Kravtsov 2007).

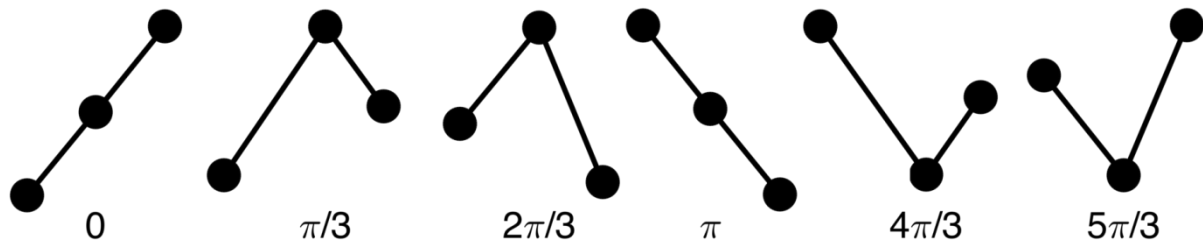


Figure 2.17: The six possible phase states corresponding to three consecutive points in a time series where the relative vertical position indicates the values; after (Tsonis, Swanson & Kravtsov 2007).

A graphic of Tsonis, Swanson and Kravtsov (2007) results are shown in Figure 2.18 where the vertical lines represent where the indices are synchronised at a 95% confidence interval to a null hypothesis of red noise. The network is synchronised in 1910 where at the time coupling strength increased but came out of the synchronous state as shown by the vertical line in 1912. This coincided with a sharp global temperature rise and the tendency for stronger, more frequent ENSO warm events. A new synchronous state occurred in the early 1920s but this was not followed by an increase in coupling strength so no major climate shifts occurred. In the early 1940s an extant synchronous state was subjected to an increase in coupling strength which soon destroyed it (vertical line) causing a new shift resulting in cooling global temperatures and less prevalent El Niños. In the 1950s synchronicity occurs once more but was followed by a decrease in coupling strength so no major climate swing occurred. In the 1970s however synchronicity is followed by an increase in coupling with a change in climate.

Checking of these results was achieved by bootstrapping to two climate models that interestingly also showed similar climate variation to occur in the 21st century, the first of which occurs in 2017 so will soon be verifiable. Tsonis, Swanson and Kravtsov (2007) were also able to conject that the 1970s warming event may have been superimposed on a Global warming trend.

The significance of this work is the possible ability to explain how the temporal relationship between an index and climate evolves.

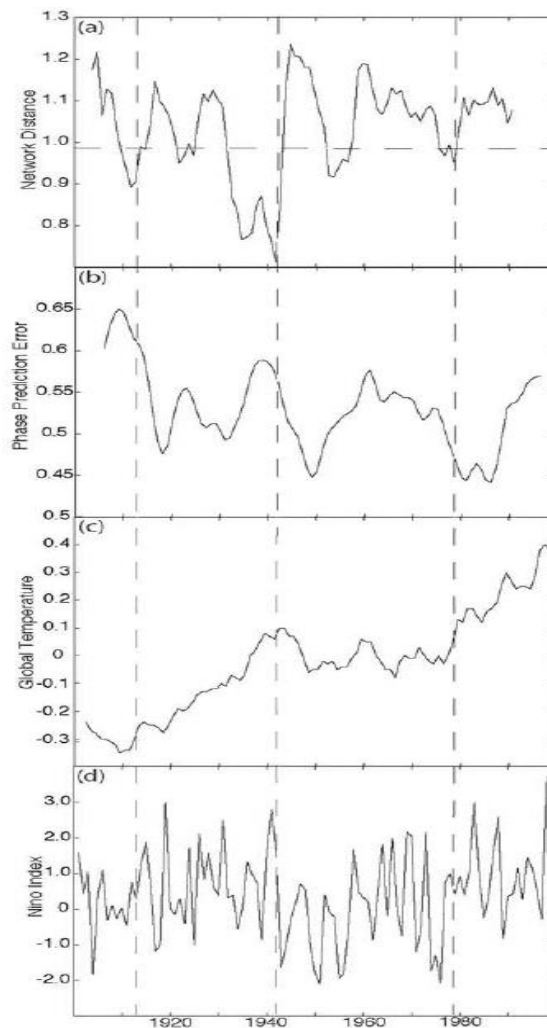


Figure 2.18: (a) shows network distance of the four climate modes as a time function, (b) coupling strength between modes, (c) global surface temperature record and (d) global ENSO index (from Tsonis, Swanson and Kravtsov (2007)).

Several articles shown in the timeline (Figure 2.19) document observed changes in the Pacific environment both tropical and extra tropical that could have an effect on Australian climate in the latter half of the 20th century and also provides a time line as to when the observed changes occurred. These changes are summarised symbolically in Figure 2.20. There is always a potential that it might be possible to follow the teleconnections between indices by studying variation of correlation of climate indices with Australian rainfall even at decadal resolution.

In terms of rainfall; Murphy and Ribbe (2004) noted that there had been a change in Australian rainfall conditions in 1946 and Shi et al. (2008) noted that Australian rainfall had decreased since 1951.

In terms of atmospheric pressure; Trenberth and Hoar (1996) detected a long term negative trend in the SOI from approximately 1976 whilst Nicholls (2008) seems to indicate that this trend was extant since the mid 50s by virtue of Darwin MSLP increasing. Latterly a decrease of the mean SOI was confirmed (Power & Smith 2007).

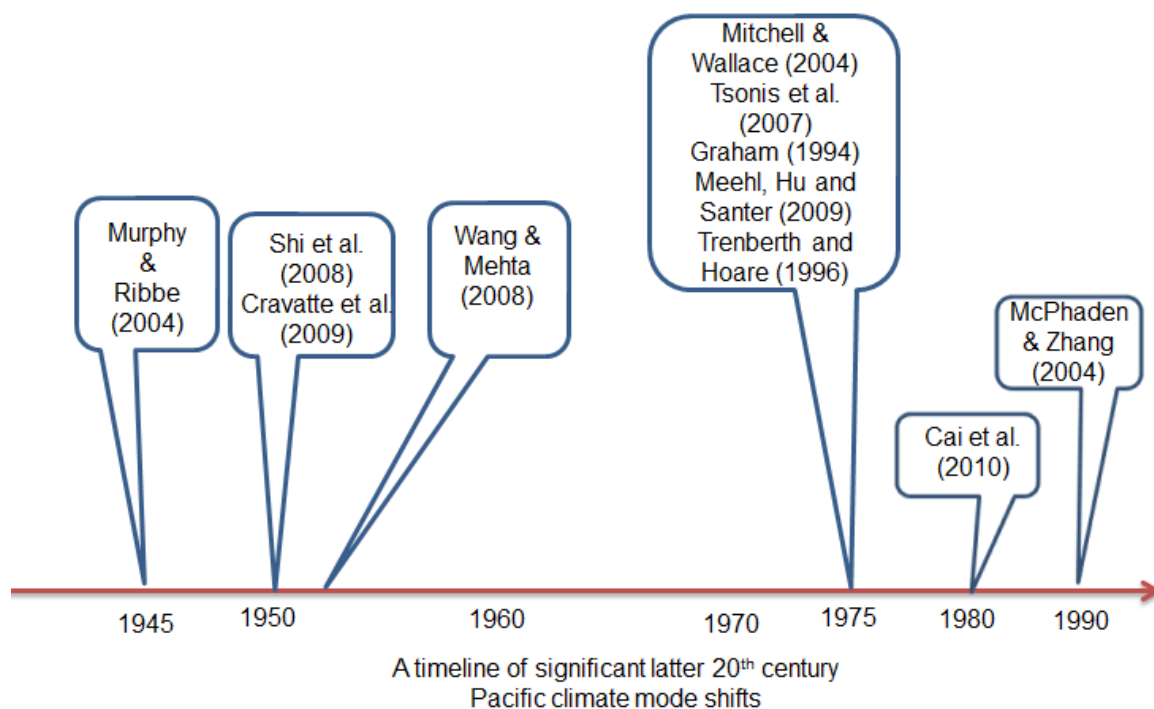


Figure 2.19: Timeline of articles examining late 20th century Pacific climate shift.

Many authors have remarked on changes with respect to Pacific SST including; Cravatte et al. (2009) who noted that the West Pacific Warm Pool (WPWP) had warmed since the mid-50s with a decrease in salinity and an increase in its Warm Water Volume (WWV). This latter change corroborated the results of Wang and Mehta (2008). Furthermore Meehl, Hu and Santer (2009) detected that the North Pacific Ocean SST had increased in the mid-70s. Cai et al. (2010) noted from the 1980s the IPO/PDO index had been in a positive phase but decreased to below zero by 2000. McPhaden and Zhang (2004) noted a drop in the PDO index from 0.84 in 1992 to -0.36 in 1998 and associated the decrease with a restoration of the

Pacific Meridional Overturning Circulation (MOC) since 1998 to levels experienced prior to 1975.

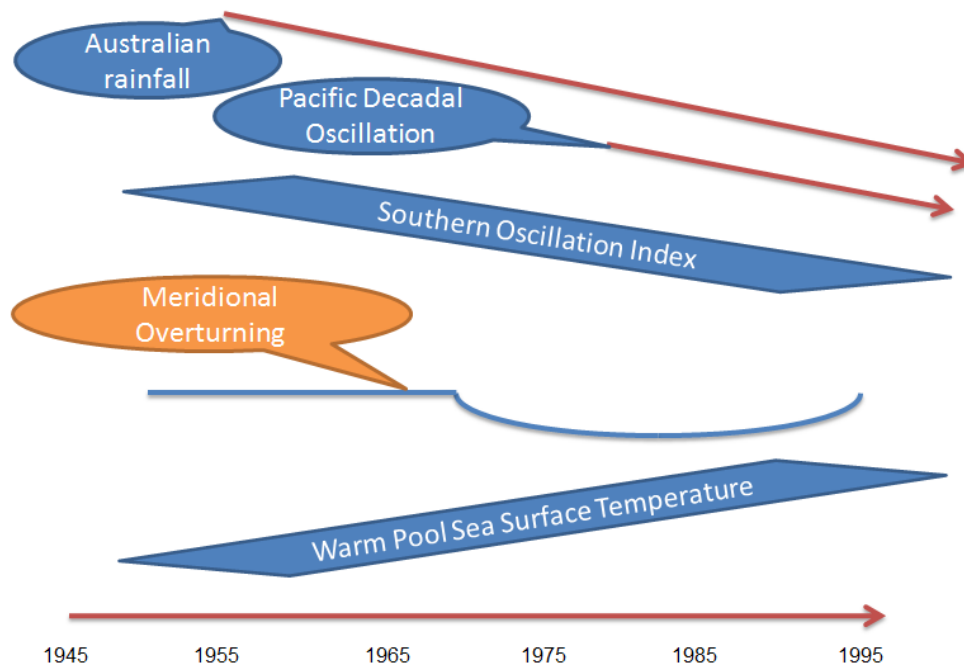


Figure 2.20: Convergence of late 20th century changes to the tropical Pacific Climate system as discussed in the literature over time.

A long term negative trend in the SOI was first noted in 1996 (Trenberth & Hoar 1996). Others observed that over a 68 year period Darwin MSLP had increased but that Tahiti MSLP had remained constant (Suppiah & Hennessy 1996). This situation was partially accounted for by the 1983 and 1997 ENSO warm episodes. Solomon and Newman (2012) partially support these arguments where it was found that in the 1900 – 2008 period there had been a slight decrease in the SO pressure gradient (Figure 2.21). Even with the unfiltered data (Figure 2.21a) by interpolation a representative change in SOI (MSLP [Tahiti – Darwin]) would be less than 0.5 hPa.

It is expected that these multi-decadal changes will be evident in this research, perhaps spreading more light on the mechanism(s) as to their cause.

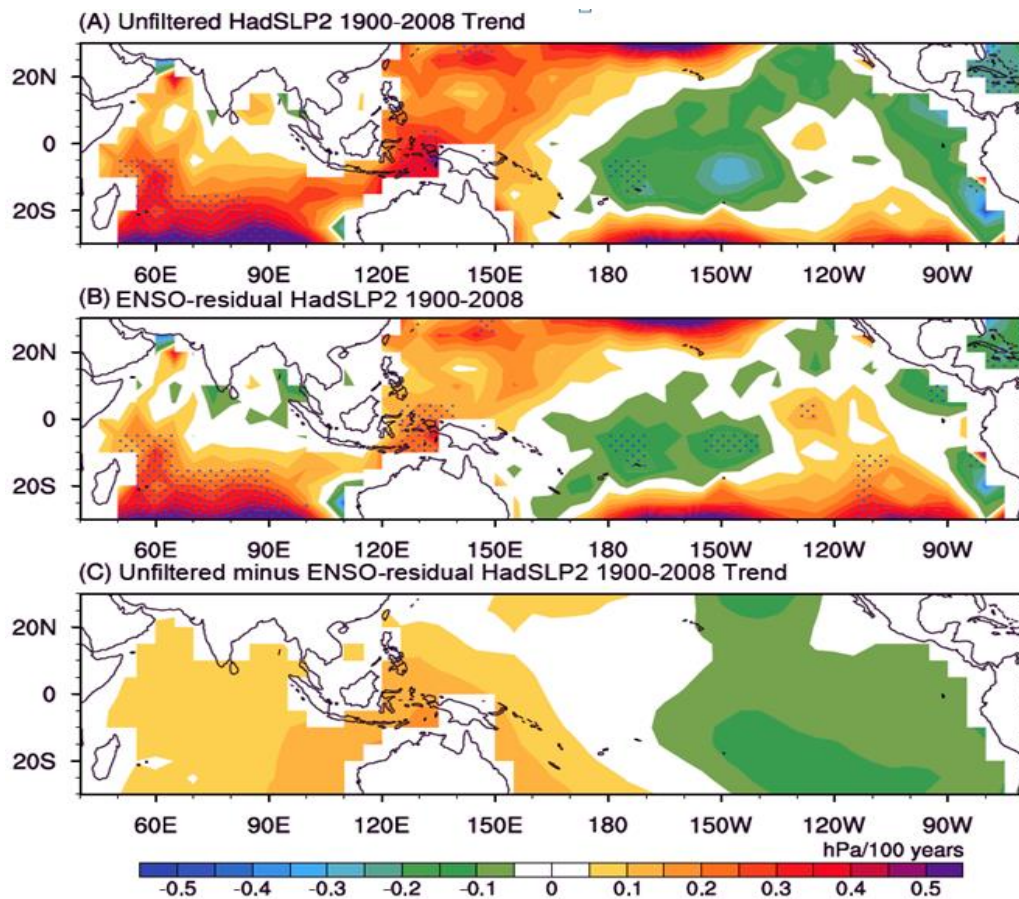


Figure 2.21: HadSLP2r 1900-2008 linear trend patterns, in units of hPa/100 years. (A) Unfiltered. (B) ENSO-residual with the SLP-only optimal perturbation filter. (C) Unfiltered minus ENSO-residual. Stippling indicates trends are significant beyond the 95% confidence level (Solomon & Newman 2012).

2.9 Australian and South East Queensland Decadal and Regional Climate

In this section climate drivers that have an effect on Australian and South East Queensland (SEQ) are reviewed. Until comparatively recently it was believed that of the climate modes that affect Australian precipitation three of the five most important ones; Indian Ocean Dipole (IOD) (Saji et al. 1999), the Southern Annular mode (SAM) (Limpasuvan & Hartmann 1999) and the El Niño Southern Oscillation (ENSO) (Bjerknes 1969) have such an impact that they have been likened to Cerberus the mythical three headed dog (Cai 2011) which barks in three different directions at once, but their interactions have been somewhat downplayed (Cai, Sullivan & Cowan 2010). Comparatively recently a paradigm shift has

occurred as Zhao and Nigam (2015) have analysed the mooted structure of IOD and can only find scant evidence for a basin wide zonal dipole structure in the Indian ocean inferring that the IOD does not exist. The situation as it was believed to exist prior to the Zhao and Nigam (2015) paper are shown in Figure 2.22 depicting the effect of these modes on Australian climate. ENSO affects Australia's climate all year round whilst the effect of SAM is in winter and the IOD makes its presence known in winter and spring (Cai 2011). Marshall (2003) asserts that SAM is the dominant mode of climate variability in the Southern Hemisphere. High SAM index polarity is associated with an increase in mid latitude baroclinic eddies especially in the Austral winter (Rao, do Carmo & Franchito 2003) thereby providing a seasonal effect to the climate of Southern Australia.

It was believed that the IOD was more ENSO-like in character (Risbey et al. 2009), but was independent of it (Cai, Sullivan & Cowan 2009) and based on the difference of SST between the Western Indian Ocean adjacent to Africa and the East adjacent to Indonesia (Saji et al. 1999). An ENSO-IOD connection was not currently discernible (Cai, Sullivan & Cowan 2009).

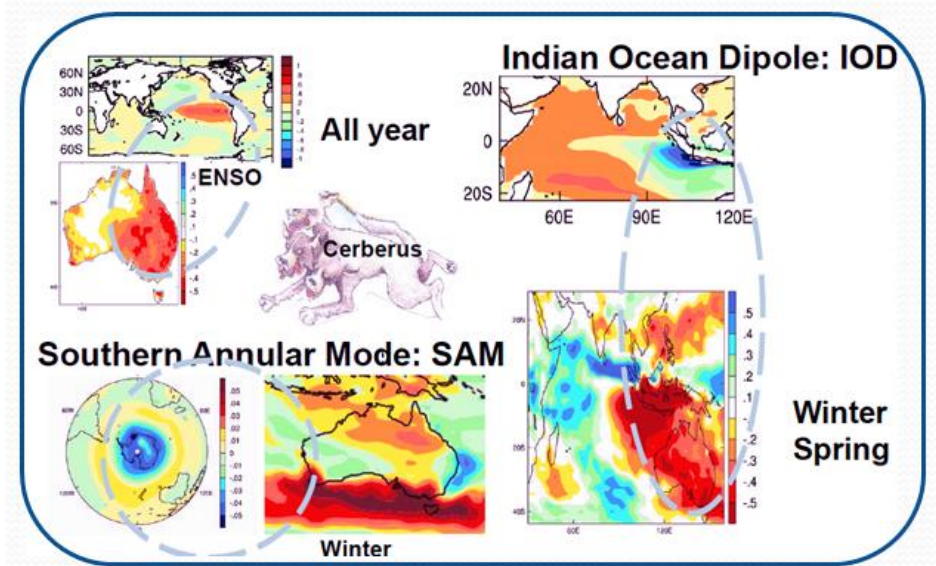


Figure 2.22: Cerberus; the three headed dog of ENSO, IOD and SAM, Cai (2011).

It was also postulated that variability in the Indian Ocean (absence of a negative IOD) results in poor rainfall in Australia and may be responsible for south east Australia's worst droughts (Ummenhofer et al. 2009) (Figure 2.23).

Furthermore, it has been suggested that the Inter Decadal Pacific Oscillation (IPO) and the Madden Julian Oscillation (MJO) should be included as drivers of Australian climate (Klingaman, Woolnough & Syktus 2012; Risbey et al. 2009).

Stone, Hammer and Marcussen (1996) using Principle Component Analysis and *k*-means cluster analysis determined five phases of the SOI and were able to predict the probability of world and Australian rainfall. This constitutes a powerful tool for Australian seasonal climate forecasting (Stone, Hammer & Marcussen 1996). Many sectors of our society and economy, for example; farming, policy making/ planning, emergency services, finance and insurance are severely affected by climate extremes due to variability at the intra and inter annual scale (Nelson et al. 2010). Such climate extrema might also mask the initial effects of climate change affecting society at a longer temporal scale.

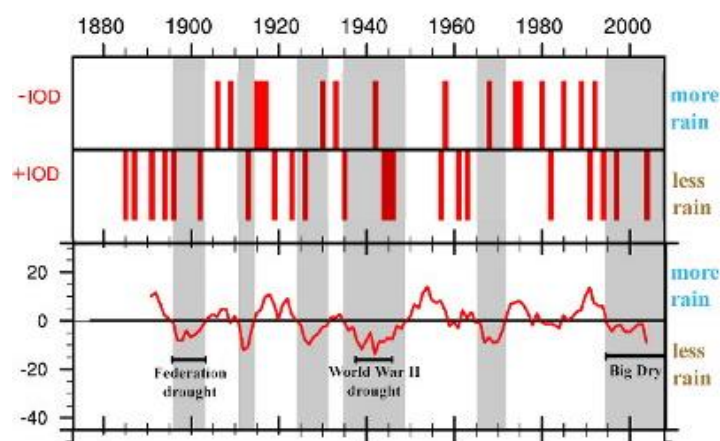


Figure 2.23: Relationship between; above IOD and below SE Australian rainfall from (Ummenhofer et al. 2009)

Although there have been many studies on seasonal and interannual variation of Australian climate this cannot be said for decadal variability. Statistically, the significance at the decadal resolution is far less than at the seasonal level but has a profound impact on agricultural production with great hardship for agricultural communities during drought (Power et al. 1999). This motivated Power et al. (1999) to attempt to move towards the very difficult goal of forecasting decadal climate variability to the same skill as seasonal variation so that better advantage could be taken of existing climate conditions for the benefit of society. Power et al. (1999) pointed out that at that time decadal scale climate predictive ability was practically non-existent and used area averaged data of the whole of Australia for rainfall and

temperature; (Lavery, Joung & Nicholls 1997; Torok & Nicholls 1996) and Pacific and Indian Ocean SST data (Mehta & Dubey 1995). The data were subject to an eight year low pass filter to remove sub decadal variability. Power et al. (1999) found that the first EOF of Interannual Pacific SST is associated with Australian rainfall and was out of phase with the SOI. At the decadal level variability of Indian Ocean SST south of 40°S was associated with rainfall over eastern Australia. An out of phase relationship between decadal rainfall and temperature was also apparent but below the 95% significance level. Phase relationships between the SOI and both interannual and decadal rainfall were also apparent but did not achieve the same significance.

The SOI was used to show that the relationship between ENSO and Australian rainfall fluctuated interdecadally (Cai, Whetton & Pittock 2001) which supported the work of Power et al. (1999) and also showed that this relationship tended to weaken when the globally detrended mean temperature was rising or particularly high. In North East (NE) Australia prior to any weakening an increased correlation to El Niño was noted in North Western (NW) Australia followed by an increase in Eastern and South East Australia before finally NE Australia. The ENSO rainfall relationship weakened before reversing followed by a rapid recovery during one period between 1931 and 1945. Cai, Whetton and Pittock (2001) also noted that a similar dynamic was observed during a time of global elevated temperature and that during the course of El Niño events the South Pacific Convergence zone moved eastwards as previously observed (Philander 1990). Cai, Whetton and Pittock (2001) also speculated that Australian rainfall correlated with the North Atlantic Oscillation (NAO) (Hurrell & Van Loon 1997) via an unexplained causal chain including the Pacific North American (PNA) pattern. A most significant observation was that there might not be a “one size fits all” solution which supports the earlier assertion in this text (Singh 2001). It is worth noting here that the Arctic oscillation (AO) (Climate Prediction Centre 2005) has also been shown to have a correlation to the ENSO (Zhou et al. 2001). In addition it was found that ENSO signals project strongly on to the SAM (Cai, Sullivan & Cowan 2010; Fogt, Bromwich & Hines 2011).

A changing relationship between Australian rainfall predictability and ENSO was also detected to occur in 1946. SEQ rainfall was most subject to breakdown in the correlation than elsewhere in Australia (Murphy & Ribbe 2004) whilst simultaneously SE Australian rainfall remained at the same degree of correlation. 1946 was identified by other authors (Cai, Whetton & Pittock 2001; Power. et al. 1999) as being when the Inter Decadal Pacific

Oscillation (IPO) changed from a positive phase to negative at the same time as ENSO impact on climate was weak. The period 2000 – 2002 was shown to be the lowest rainfall on record and Murphy and Ribbe (2004) set out to correct the lack of previous study on climate variability in SEQ. Murphy and Ribbe (2004) found that SEQ rainfall was best represented by the Niño4 index whereas the Niño3 and SOI indices produced successively weaker correlation. The SOI relationship was weak in the pre-1946 period but stronger later and both the other indices showed smaller change than the SOI. The Pacific Ocean second EOF of SST (PEOF2) and the Indian Ocean second EOF of SST (IEOF2) were used as indices. PEOF2 has a large percentage of the WPWP variance, and has recently been dubbed as “The Warm Pool Mode”, (Park, Yeh & Kug 2012). Table 2.5 shows a collation of Murphy and Ribbe’s (2004) results.

Table 2.4: Correlation of Niño4 (N4), Niño3 (N3), SOI, EOF2 Pacific Ocean SST and EOF2 Indian Ocean SST with SEQ rainfall, (Murphy & Ribbe 2004).

Index	SE Qld rainfall correlation coefficient		
	1891–2000	1891–1945	1946–2000
N4	–0.57	–0.59	–0.65
N3	–0.49	–0.48	–0.53
SOI	0.42	0.06	0.72
PEOF2	–0.33	–0.33	–0.33
IEOF2	–0.39	–0.39	–0.41

Variability between SEQ rainfall at multidecadal teleconnections to ENSO was also linked to an eastward shift in the SPCZ associated with the positive phase of the Interdecadal Pacific Oscillation (IPO) since 1980 (Cai et al. 2010). SEQ rainfall decreased in this same period with a commensurate breakdown of the ENSO rainfall relationship. The teleconnection was also subject to an asymmetry whereby the summer La Niña rainfall relationship was robust, but with El Niño it was weak (Cai et al. 2010). These latter observations agree in general terms with those of Wang and Hendon (2007) who put it quite succinctly that “Australian rainfall tends to linearly increase with the strength of La Niña, whereas the decline with El Niño is much less linear.” In other words, while La Niña conditions build there is

commensurate increase in positive rainfall anomaly, but with El Niño conditions building the magnitude of the associated rainfall reduction is not assured.

To examine the increasing trend in north western Australian rainfall (Shi et al. 2008) with a commensurate decrease in south eastern Australian rainfall the output of the CSIRO Mk 3a global coupled (atmosphere and ocean) climate model plus Empirical Orthogonal Functions (EOF)s of Australian rainfall was regressed against the Niño3.4 index. In the latter case, summer rain increased under the influence of the SAM whilst winter rain was still under the influence of SAM but decreased amounting to overall decline that fell under the influence of the IOD.

This review has pointed to the assertion of Wallace et al. (1998) that no one index can represent the complexities of tropical Pacific climate. This emphasised the significance of the work of Baird et al. (2011) who used four climate indices; the MEI, SOI, ONI and FIVEVAR in an attempt to rank the severe La Niña event of 2010 – 2011 in comparison with other similar occurrences that had affected Australia in the previous 110 years. This La Niña had the most profound effect on climate with the wettest end of the year in Australia’s recorded history (Baird et al. 2011). Perusal of Table 2.6 shows that not only do the rankings vary but different indices highlight entirely different events within their rankings. In the table according to the SOI the largest event in the previous 110 years was the La Niña of 1917 but none of the other three indices ranked this event at all and the ensemble aggregate points to both 1955 and 2010 having equal ranking for being the strongest event!

Table 2.5: Past 110 year ranked La Niña events compared to 2010 – 2011 from Baird et al. (2011). Shown are five month averaged August-December values of the indices.

MEI		SOI		ONI		5_VAR	
Year	Index	Year	Index	Year	Index	Year	Index
1955	-1.86	1917	+24.6	1955	-1.73	2010	-17.90
1975	-1.83	2010	+21.1	1973	-1.70	1988	-17.55
2010	-1.77	1975	+18.8	1975	-1.60	1975	-17.45
1973	-1.64	1973	+16.8	1988	-1.60	1955	-15.85

Remote sensing applications have played a role since 1974. Baird et al. (2011) showed that Outgoing Long Wave Radiation (OLR) anomalies used as a proxy for cloudiness between September and November 2010 indicated a very strong Walker Cell, La Niña situation. Baird et al. (2011) also showed a greater negative anomaly in east Australia in 2010 compared to 1975 commensurate with greater precipitation.

Increase in Australian summer rainfall during the 2011 La Niña has been linked to the PDO turning negative once more (Cai & van Rensch 2012) asserting that high SEQ rainfall and SOI values only occur in negative PDO phases. There have only been three such summers where SEQ rainfall anomaly exceeded + 300 mm in the past 111 years and none when the IPO was positive. The phalanx of SEQ summers prior to 1980 (Figure 2.24) were all associated with negative PDO. OLR anomaly shows development towards a condition typical of a negative PDO. The 2011 event re-establishes a 13 year ENSO rainfall relationship above the 95% confidence level that represents transition to a negative PDO phase.

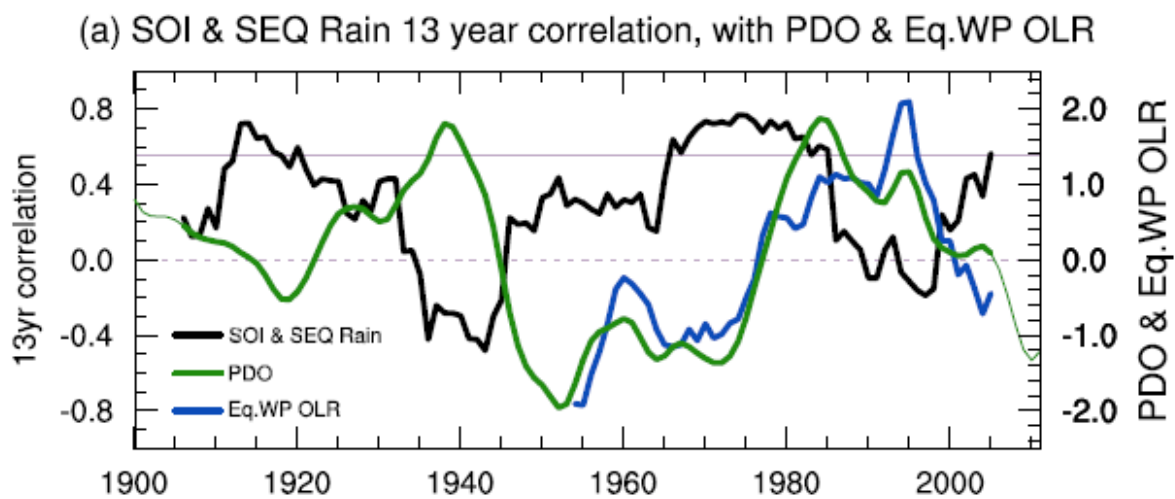


Figure 2.24: Time series of the SEQ rainfall-ENSO teleconnection calculated as correlations (black curve), using a 13 year sliding window of SEQ DJF rainfall with the DJF SOI over the period 1900–2011 (statistically significant correlation at the 95% confidence level is 0.55, indicated by a solid grey line). A PDO index is overlaid in green [Mantua et al., 1997] (uncertainty values are shown as a thinner curve). The correlation between the rainfall-ENSO teleconnection and the PDO is -0.41 . Time series of normalised OLR (blue), averaged over the equatorial Western Pacific ($\pm 5^\circ\text{N}$ and S, $137 - 175^\circ\text{E}$), has a correlation of -0.47 with the

evolution of rainfall-ENSO teleconnection (statistically significant above the 95% confidence level); (Cai & van Rensch 2012).

The results in Figure 2.24 show a PDO time series (Mantua et al. 1997) using a 13 year running average. The correlation through 2011 cannot be confirmed (Cai & van Rensch 2012) until 2017 (half scale of the windowing technique used), but it alludes to the important concept of evolution of climate modes at different rates as discussed in Section 2.8 (Tsonis, Swanson & Kravtsov 2007)

It was recognised that more than just a few climate indices might have a significant relationship to seasonal Australian climate and rainfall (Schepen, Wang & Robertson 2011). Schepen, Wang and Robertson (2011) hypothesised that seasonally, Pacific SST might have a better relationship to Australian climate than the Indian Ocean region and that some regions of the continent were poorly served for practical climate prediction. Five existent and eight constructed climate indices of: Pacific and Indian Ocean SST, zonal wind and one ocean heat content index similar to Warm Water Volume (WWV) (Meinen & McPhaden 2000) were correlated against Australian seasonal climate using a Bayesian cross validation technique to see how they compared. The indices shown in Figure 2.25 are their significant results for Summer DJF rainfall. As can be seen great areas of the Australian continent seem not to have any significance with any of the selected indices. Unfortunately perhaps through taking a very cautious approach the authors did not utilise their ocean heat content index due lack of data so they discounted those particular results.

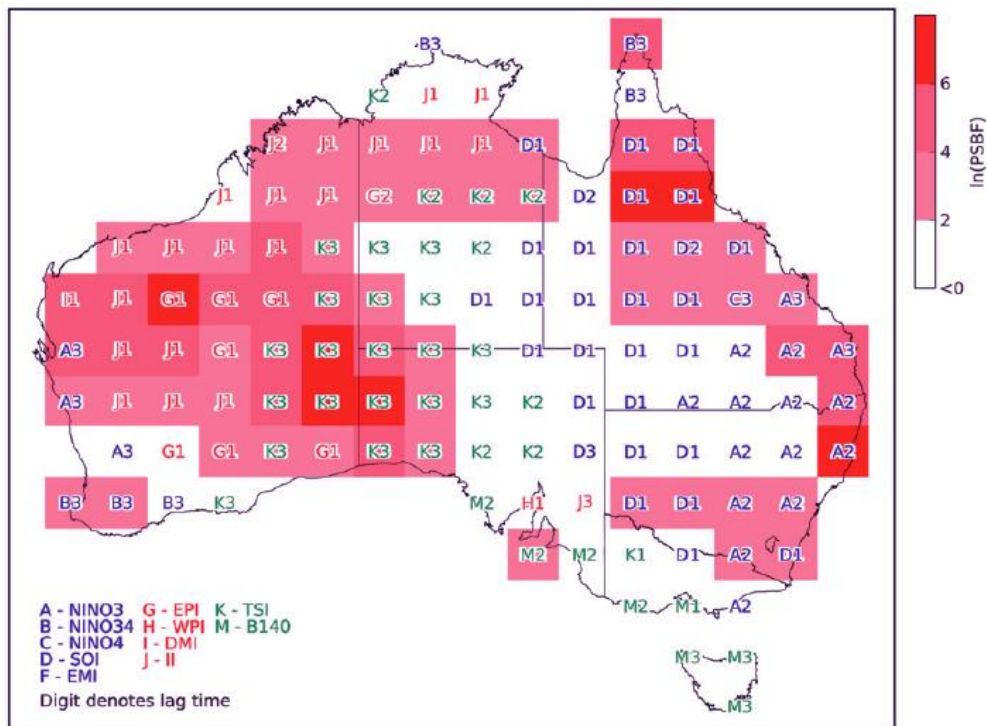


Figure 2.25: Correlation of significant climate indices with Australian Summer (DJF) rainfall using as a comparison the classical Bayes factor (from Schepen, Wang and Robertson (2011)). Indices A – F are the indices as labeled; G is average SST anomaly over 90 –110°E and 08°N –10° S ; J is average SST anomaly over 120 – 130°E and 08°N – 10°S and K is average SST anomaly over 150 –160°E and 30 – 40° S; (only indices with any real significance are identified).

Schepen, Wang and Robertson (2011) might be regarded as the most comprehensive study yet, having gone some way to relating different indices in correlation with Australian climate. It remains for a study with a true multiplicity of climate indices to be produced. This aspect in conjunction with close scrutiny of the pointers in the rich field of literature provided the motivation for this current study.

2.10 Investigations indicated by a summary of the literature

In view of the wide ranging number of climate indices visited in this study the scope of this chapter is necessarily large. An attempt has been made in this chapter to link climate modes from all over the world to Australian climate. However, in many cases the literature does not have an Australian focus so this is not always possible and so the term teleconnection has to suffice highlighting the deficiency of current knowledge.

This chapter briefly reviews the climate of Australia before discussing the major climate modes affecting the continent.

A large fraction of the literature reviewed in this chapter covers the development of statistical climatology for Australian climate prediction and a brief introduction of numerical climate models. A combination of both methodologies has been used in a variety of recursive techniques to extend the climate record back before the satellite age to make long term data sets available. The climate index is loosely defined.

The chapter describes the El Niño Southern Oscillation (ENSO) phenomenon: its relationship to World and Australian climate through the Walker Circulation and historical development of the Southern Oscillation Index. Due to its importance; the spin off from ENSO in terms of the climate indices produced is reviewed.

Other worldwide climate indices are then discussed including those from the large oceanic warm pools adjacent to Australia. These warm pools have been subjected to intense study due to their intimate connection with global climate, but have never been seriously used for Australia wide climate prediction.

Multidecadal variability of major climate modes affects Australian climate and this is discussed. The chapter ends with a review of studies of Australian and South East Queensland climate noting that there is still much scope for using a multiplicity of indices for Australian rainfall correlation.

The extant literature has indicated the following points:

- Climate is globally linked
- Correlations between indices vary with time and space. Robust correlations can imply the existence of deeper climatic mechanisms.

The literature reviewed has indicated methods and background which will allow the following interrelated points to be investigated and amplified within this thesis:

- Using the literature to pinpoint indices previously unused for correlation with Australian rainfall.
- Postulating how climate indices have a correlation with Australian rainfall.
- Using bandpass filtering in recognition of the nonlinear evolution of climate modes to find correlations.

- Identifying, if possible, the longer term effect of variation of climate modes on correlations.
- Using the results obtained to broadcast the suitability of these indices as pointers for other research.

Chapter 3 Data and Methods

3.1 Data

3.1.1 Rainfall Data

The rainfall data used in this study consist of Australian precipitation depicted in $\text{mm}\cdot\text{day}^{-1}$, on a 0.25° geographic, Cartesian graticule for the contiguous Australian continental land mass, at monthly intervals from 1900 – 2008, (Jones, Wang & Fawcett 2009) as part of the Australian Water Availability Project (AWAP) (Raupach et al. 2009). A typical representation of the data series is shown in Figure 2.1 (mean rainfall over the period of interest). Some authors, for example Ummenhofer et al. (2011) and Gallant et al. (2013) point out that the AWAP data tend to be unreliable in certain remote regions (approximately 122°E – 132°E and 30°S – 20°S) prior to the 1950s where rain gauges were sparsely situated so that seasonal rainfall climatologies and their anomalies had to be used. This current study deals with decadal resolution material so reliance on temporal averaging as used in Jones, Wang & Fawcett (2009) has less of an effect, where for example the daily rainfall is actually derived from the monthly rainfall. It should also be noted that Figure 2.1 shows that less than 27 mm of rain have fallen in these regions per decade for the 111 years of the study so the veracity of correlation results for this region prior to the introduction of remote sensing methods should be treated with some caution. It should be noted however that Cai et al. (2014) used the AWAP data for their study of Australian rainfall trends without any such restriction.

3.1.2 Climate Indices

Attention is drawn to Table 3.1 which lists the various climate indices used, their acronyms and a reference to their source. This should not be confused with Table 1.1 which refers to the authorship of the indices therefore please consult Table 1.1 for authorship details.

Unless otherwise stated the source for the climate indices are:

US Department of Commerce, National Oceanic and Atmospheric Administration, Earth
System Research Laboratory, Physical Science Division
<http://www.esrl.noaa.gov/psd/data/climateindices/list/>

For these indices the reference is omitted from the table.

Following Table 3.1, brief descriptions of the indices and figures of their standardised raw (unfiltered and undetrended) time series are included. In the results section, the indices used are at decadal resolution and have been appropriately treated to bandpass filtering. Their generic derivation shown in section 3.2 and the correlation results of the method may be viewed in Chapter 4 Results.

Table 3.1: Climate Indices used in this study with their acronyms and source reference to the data series.

Index	Acronym	Data source
Arctic Oscillation Index	AOI	
Combined Niño 3.4 and Southern Oscillation Index	BEST	
Cold Tongue Index	CTI	<i>(Mitchell 1999)</i>
El Niño Modoki Index	EMI	<i>(Ashok 2013)</i>
Equatorial SOI	EQSOI	
Five Variable Niño Index	FIVEVAR	(Fawcett 2014)
Indian Ocean Dipole	IOD	<i>(Yu 2013)</i>
Inter Decadal Pacific Oscillation	IPO	(Folland et al. 1999) Met Office, Hadley Centre
Indo Pacific Warm Pool	IPWP	(APDRC 2014)
Multi-variant Niño Index	MEI	
North Atlantic Oscillation	NAO	
SST Anomaly in Niño 3.4 region	Niño3.4/ONI	
Northern Oscillation Index	NOI	
Pacific Decadal Oscillation	PDO	<i>(Mitchell 2012)</i>
Pacific Warm Pool	PWP	
Quasi Biennial Oscillation	QBO	
Southern Annular Mode	SAM	
Southern Oscillation Index	SOI	<i>(Jones & Salmon 2010)</i>
Trans Pacific Niño Index	TNI	
Tropical Pacific Ocean Empirical Orthogonal Function	TPEOF	
Western Hemisphere Warm Pool	WHWP	
Warm Water Volume	WWV	(APDRC 2014)
Warm Water Volume East	WWV_E	“
Warm Water Volume West	WWV_W	“

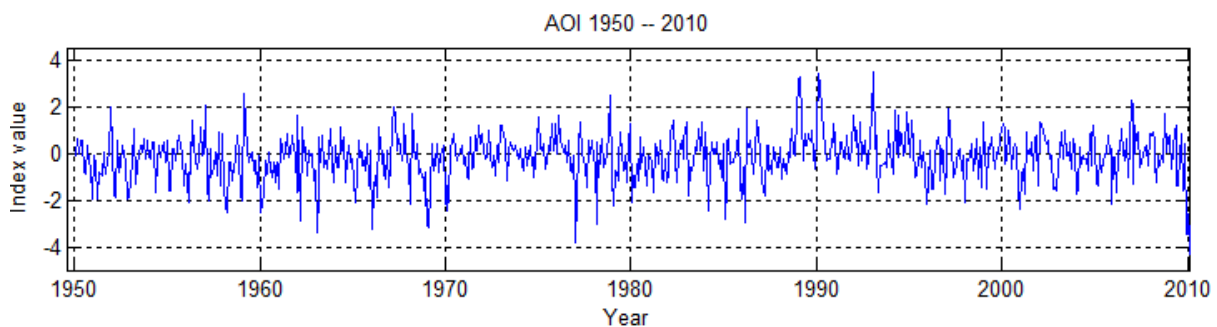
It is customary for such climate data to be processed using a computational recipe (CR) as laid out in von Storch and Zwiers (2001) and Box, Jenkins & Reinsel (2013) amongst many. For this study this procedure was dispensed with as it was found to be superfluous as the filtering method guarantees stationarity of the data series (see Appendix 1) analogous to using a long term running mean. It was observed that the majority of climate indices selected for the study had been standardised so all indices were dealt with in this fashion. An index value was transposed into a Z score:

$$Z = \frac{y - \bar{y}}{\sigma_y},$$

where Z the transformed variable of the original series, y, with mean, $\bar{Z} = 0$, and standard deviation, $\sigma_y = 1$. This method has the advantage of potentially providing better conditioned matrices in any subsequent correlation calculations, see Kreyszig (2006), p 855.

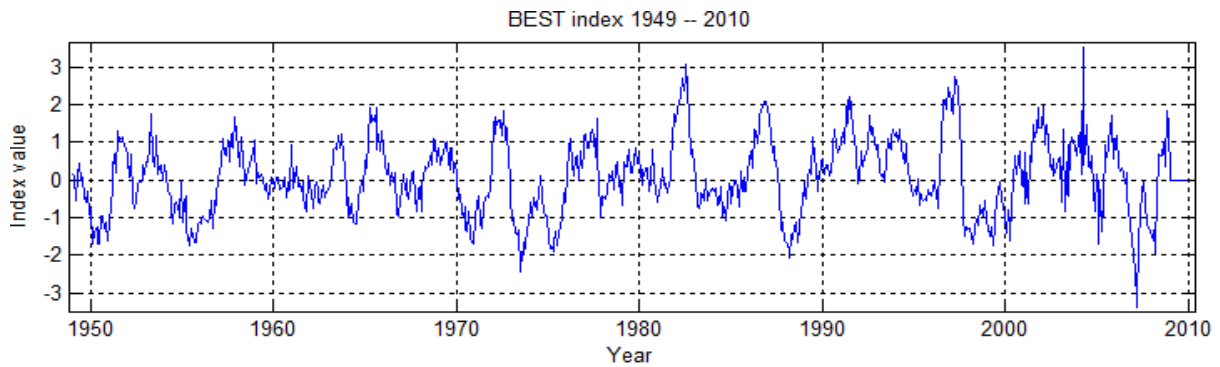
AOI

The AOI is the daily 1000hPa height anomaly polewards of 20°N projected on to its loading pattern (1st EOF pattern) which is the leading mode of the Empirical Orthogonal Function (EOF) of monthly mean height of the 1000hPa of the 1979 – 2000 base period. This index does not adhere to the conventional computational recipe methods (Box, Jenkins & Reinsel 2013) using instead normalised values for both variables.



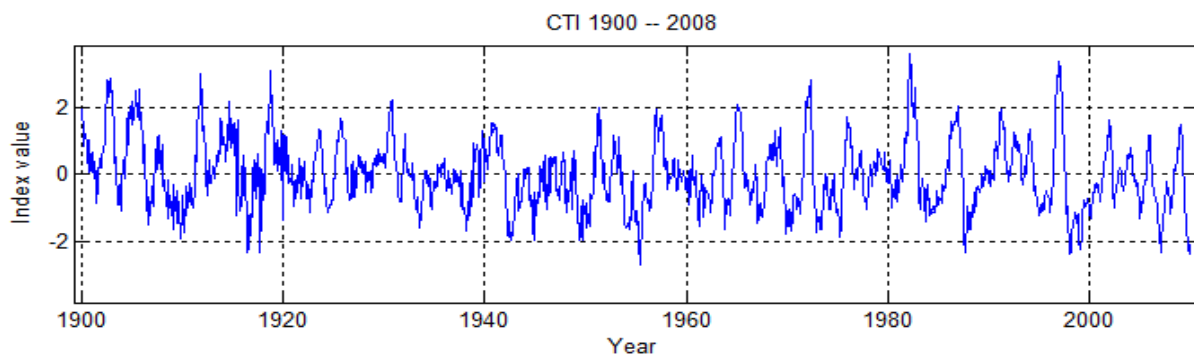
BEST index

The BEST index is a bivariate mixture of normalised SOI and Niño3.4 indices and as in the case of the AOI does not adhere to CR, (see SOI and Niño3.4 indices for details)(Smith & Sardeshmukh 2000).



CTI

The CTI is the average Sea Surface Temperature (SST) anomaly over $\pm 6^\circ\text{N}$ and S, $180^\circ - 90^\circ\text{W}$ region minus the global mean SST between 1840 and 2011. This relates to the region of cold water upwelling as part of the Walker Circulation (Mitchell 1999).



EMI

The term Modoki in EMI means; “similar but different” and refers to EMI tracking a central Pacific El Niño phenomenon rather than an Eastern Pacific one and is based on equatorial Pacific sea surface temperature anomalies (SSTAs) (Ashok et al. 2007). It follows that:

$$EMI = [SSTA]_A - 0.5 * [SSTA]_B - 0.5 * [SSTA]_C$$

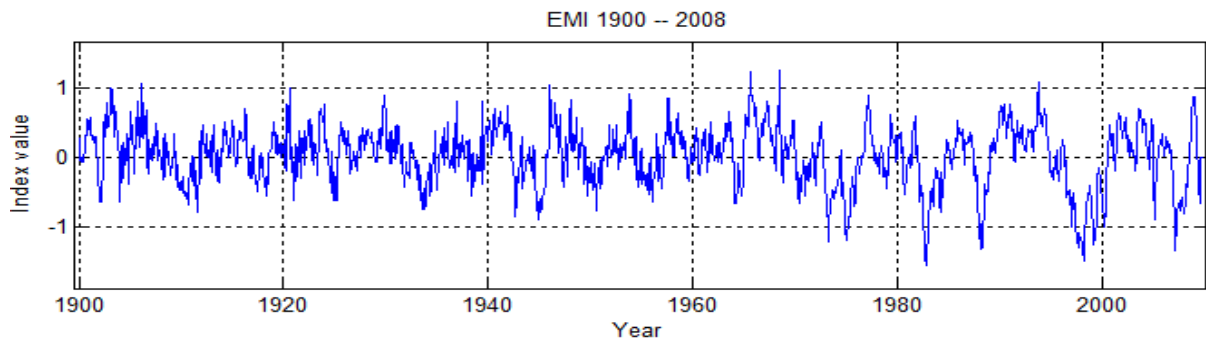
Within the bracket are the area averaged SSTA for:

$$A = (\pm 10^\circ \text{ lat and } 165^\circ\text{E} - 140^\circ\text{W}),$$

$$B = (15^\circ\text{S} - 5^\circ\text{N and } 110^\circ\text{W} - 70^\circ\text{W})$$

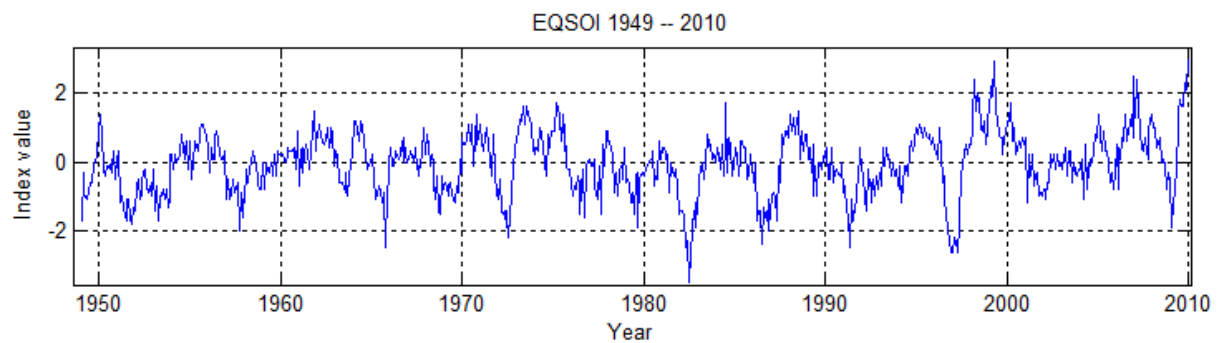
$$C = (10^\circ\text{S} - 20^\circ\text{N and } 125^\circ - 145^\circ\text{E}).$$

(Ashok 2013).



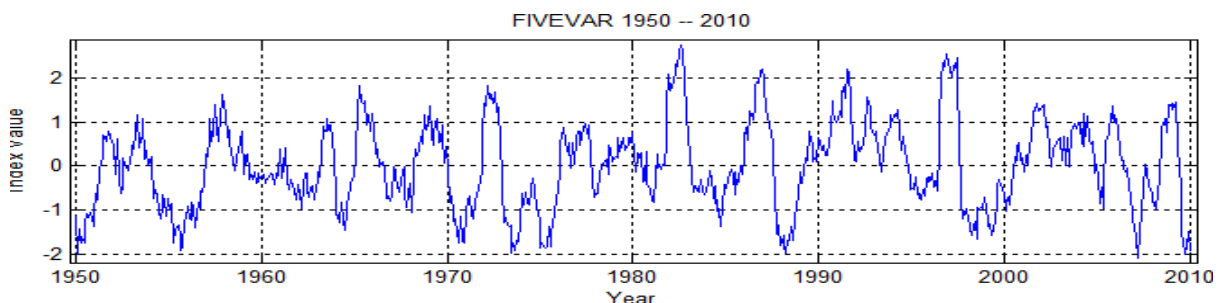
EQSOI

The EQSOI consist of the difference in monthly mean sea level pressure (MSLP) standardised anomalies between the Eastern Pacific (EPAC) region ($\pm 5^{\circ}\text{N}$ and S $150 - 90^{\circ}\text{W}$) and Indonesia (INDO) region ($\pm 5^{\circ}\text{N}$ and S $80 - 130^{\circ}\text{E}$).



FIVEVAR or 5_VAR

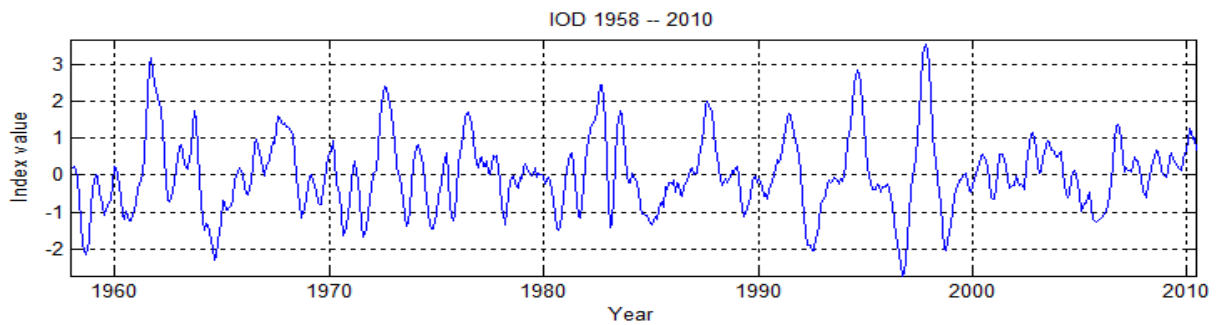
The FIVEVAR index was introduced to investigate tropical cyclone frequency in the southern Hemisphere, Indian and Pacific Ocean regions between 30°E to 120°W . A multivariate ENSO index FIVEVAR is based on the first principal component of monthly Darwin mean sea level pressure (MSLP), Tahiti MSLP, and the NINO3, NINO3.4 and NINO4 SST indices (Fawcett 2014).



IOD

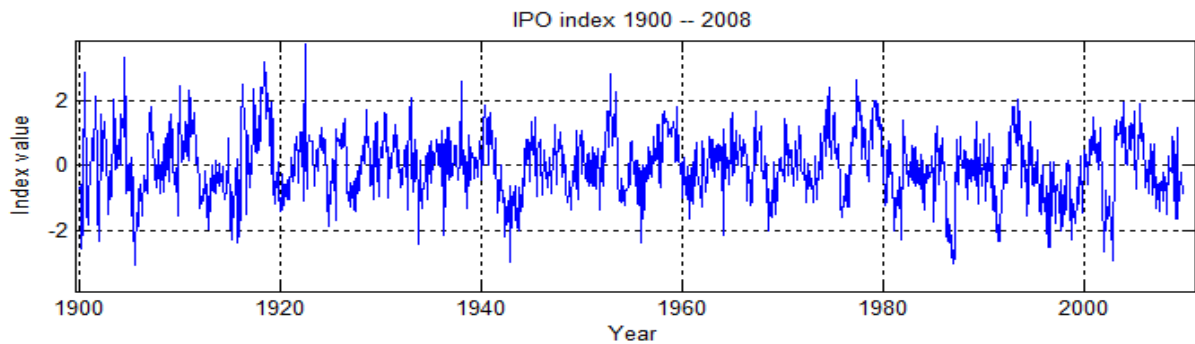
The Indian Ocean Dipole (IOD) is defined by the difference in SST between two areas (or poles, hence a dipole) – a western pole in the Arabian Sea (western Indian Ocean) and an

eastern pole in the eastern Indian Ocean south of Indonesia. The poles are (SST) anomalies in the western (50°E to 70°E and 10°S to 10°N) and eastern (90°E to 110°E and 10°S to 0°S) equatorial Indian Ocean (Yu 2013).



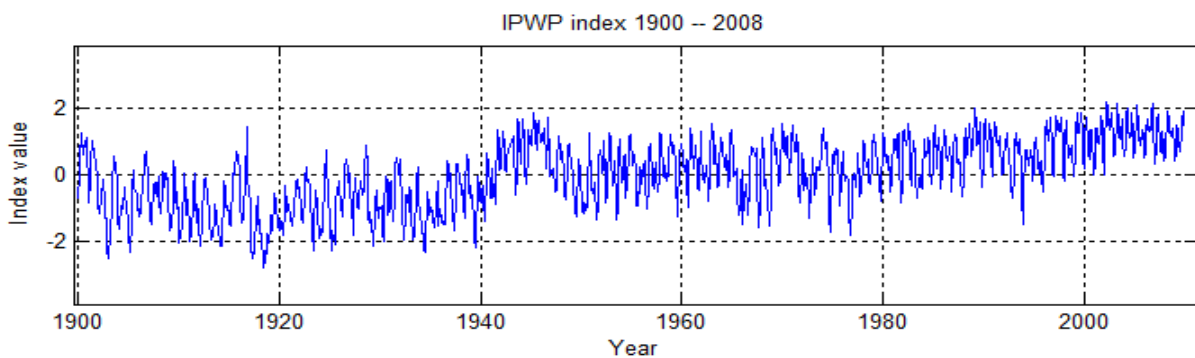
IPO

The IPO is the Pacific wide SST aspect of the PDO (see below) as given by the 3rd EOF of Global SST. IPO is symmetrical about the Equator providing variance up to 55°S although the east Pacific is shows less variance than the W Pacific (Folland et al. 1999).



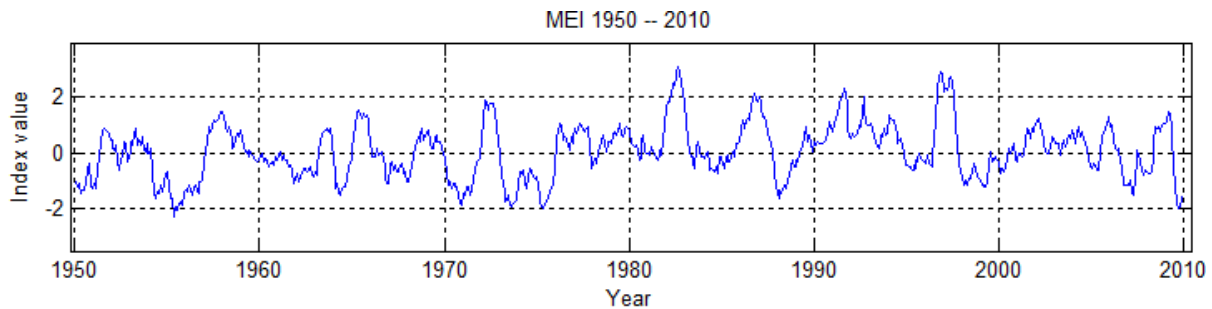
IPWP

The IPWP index is a derived index of the area of SST entirely within the 28.5°C isotherm in the region ±20° latitude and between 90°E – 180°E longitude in the Indian and Pacific Ocean (APDRC 2014).



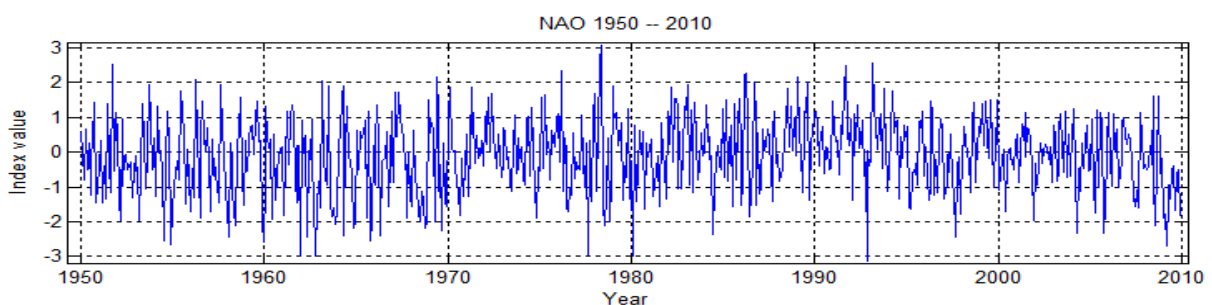
MEI

The MEI is a multivariate El Niño index which included the first principal components of Pacific: surface pressure, surface air temperature (SAT), **u** and **v** wind SST and total cloudiness fraction of the sky. Subsequently the cloudiness fraction has now been superseded by the use of outgoing long wave radiation (OLR).



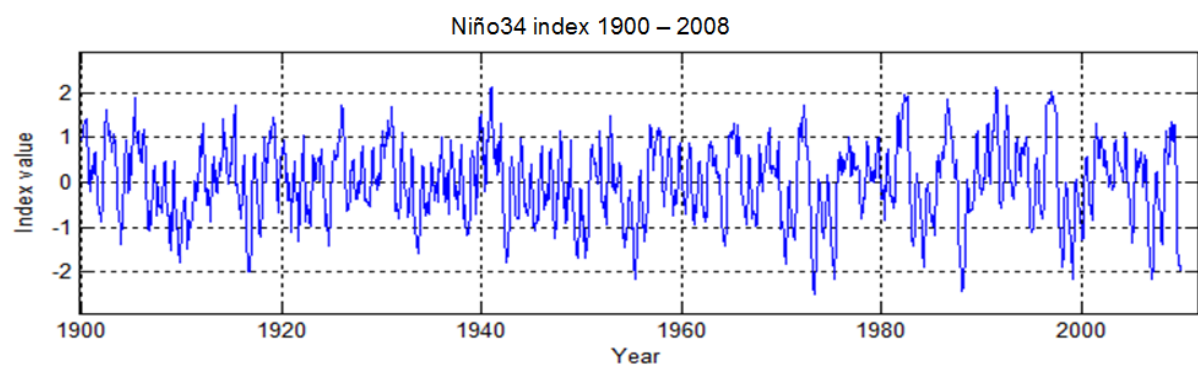
NAO

The NAO consists of a see-saw pattern in change of atmospheric mass between the Azores High and the Icelandic Low and is defined in this instance as the normalised MSLP difference between Reykjavik and Ponta Delgada.



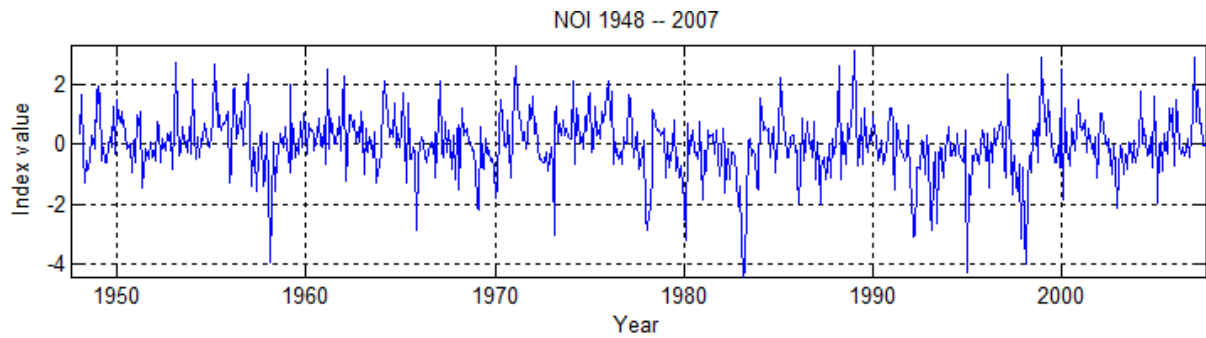
Niño3.4/ONI

Niño3.4/ONI are respectively; the five month and three month running mean of SST anomaly in the Niño3.4 region of $\pm 5^\circ\text{N}$ and S latitude and $170^\circ\text{W} - 120^\circ\text{W}$ (shown is Niño3.4). Niño indices are extensively described in the Literature Review Section 2.6.



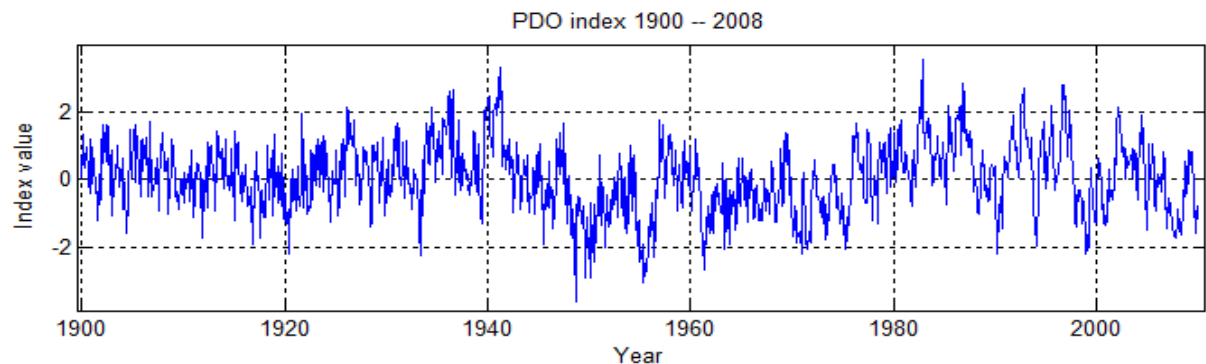
NOI

The NOI is based on the MSLP difference between the North Pacific High ($\approx 35 - 45^\circ\text{N}$, 150°W and Darwin).



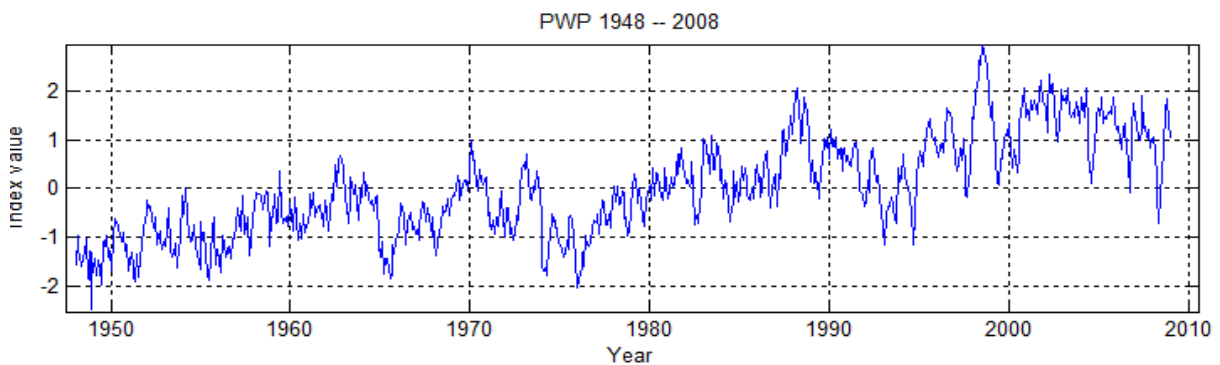
PDO

The PDO is derived as the leading Principal Component (PC) of monthly SST anomalies in the North Pacific Ocean, polewards of 20°N . The monthly mean global average SST anomalies are removed to separate this pattern of variability from any “global warming” signal that may be present in the data (Mitchell 2012).



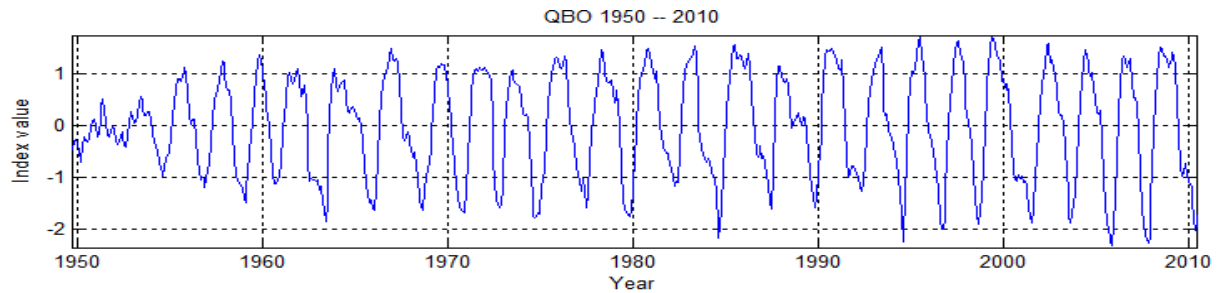
PWP

The PWP is the 1st EOF of ($\pm 15^\circ\text{N}$ and S, $60 - 170^\circ\text{E}$), SST.



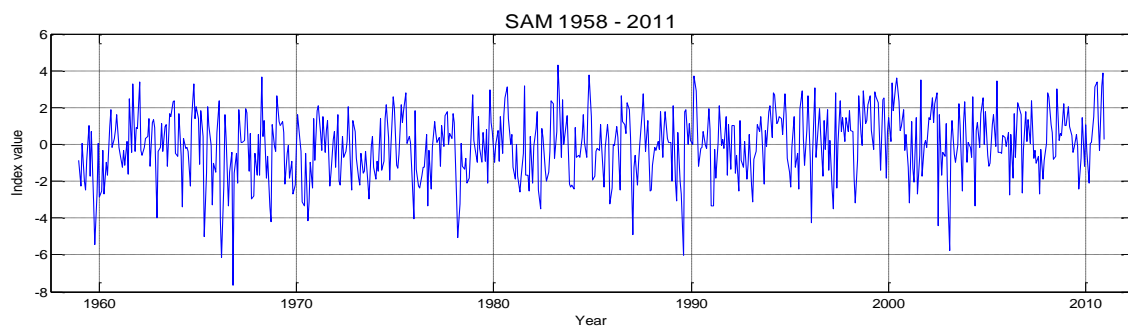
QBO

The QBO is based on an approximately 24 – 28 month cycle of the Equatorial stratospheric wind which occurs at approximately the 30 hPa level.



SAM

The SAM or AAO index tracks the north–south movement of the westerly wind belt that circles Antarctica, dominating the middle to higher latitudes of the southern hemisphere. The SAM is the daily 700 hPa height anomaly poleward of 20°S projected on to its loading pattern (1st EOF pattern) which is the leading mode of the Empirical Orthogonal Function (EOF) of monthly mean height of the 700 hPa during the 1979 – 2000 base period.



SOI

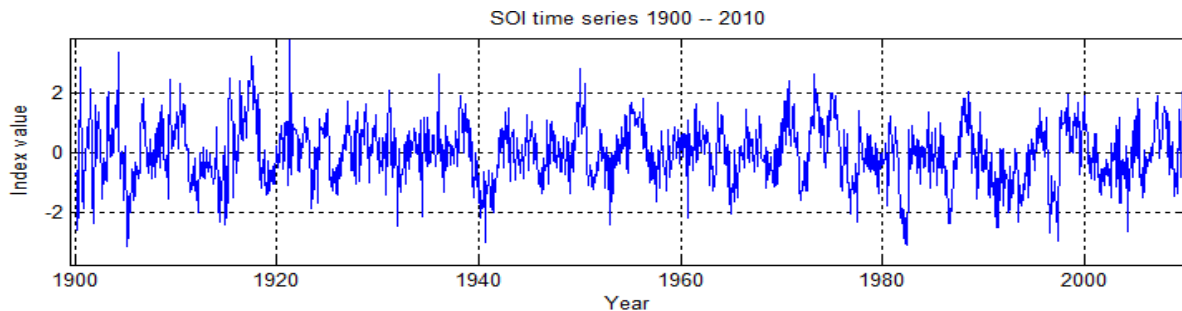
The Southern Oscillation Index (SOI) is a standardized index based on the observed sea level pressure differences between Tahiti and Darwin expressed as a five month running mean (Ropelewski & Jones 1987) and describes the strength of the Southern Oscillation and hence the state of the Walker Circulation trade wind strength. SOI can be based on Mean Sea Level Pressure (MSLP) difference between Tahiti ($\approx 17^\circ\text{S}$, 149°W) and Darwin ($\approx 12.5^\circ\text{S}$, 131°E) which nominally enjoy the same MSLP to give normal conditions (Figure 2.6). The SOI is formally defined as:

$$SOI = \frac{(\Delta P_0 - \Delta P_c)}{\sigma \Delta P_c} ,$$

where: ΔP_0 is the standardised mean sea level pressure of Tahiti and , ΔP_c is the standardised mean sea level pressure of Darwin and $\sigma \Delta P_c$ is the standard deviation of the 1951 – 1980

climatological pressure difference. This produces values of SOI between $\approx \pm 3.5$ with no units (Jones & Salmon 2010).

Normally in Australian usage this result is multiplied by 10 to produce the "Troup SOI" and is described comprehensively in the Literature Review Sections 2.4 and 2.5.

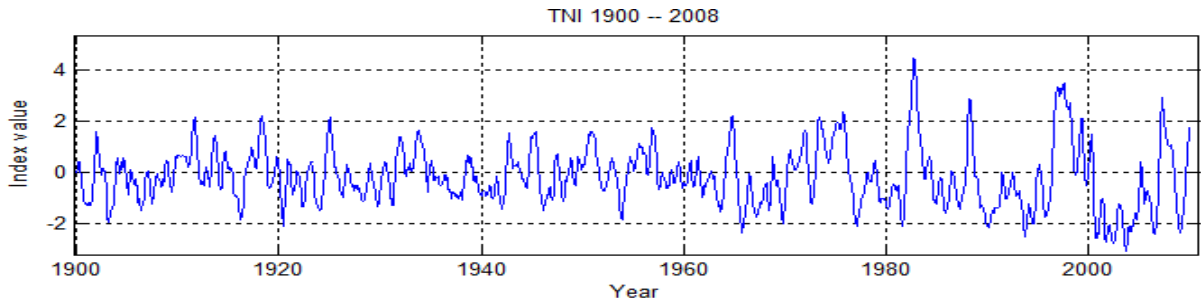


TNI

TNI uses difference in SST between the Niño1,2 region and Niño4 region using the normal CR:

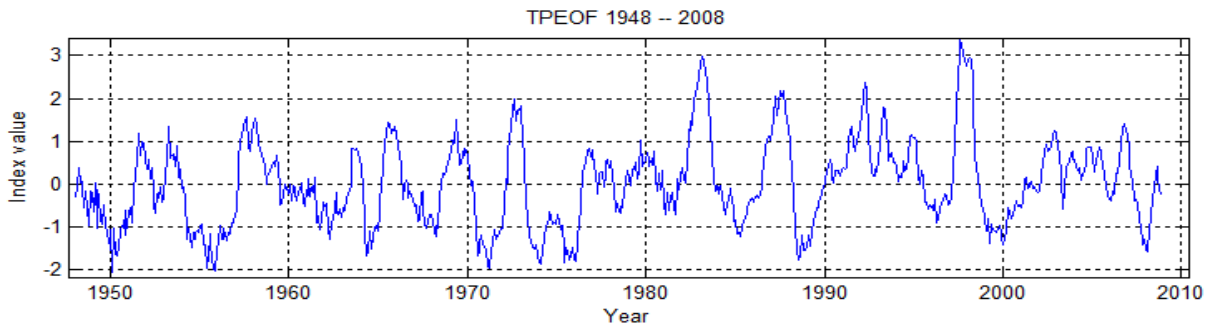
- Compute area averaged total SST from Niño 1+2 region.
- Compute area averaged total SST from Niño 4 region (Niño regions defined in Section 2.6).
- Compute monthly climatologies (1950-1979) for area averaged total SST from Niño 1+2 region, and Niño 4 region, and subtract climatologies from area averaged total SST time series to obtain anomalies.
- Normalize each time series of anomalies by their respective standard deviations over the climatological period 1950-1979.
- Define the raw *TNI* as Niño 1+2 normalized anomalies *minus* Niño 4 normalized anomalies.
- Smooth the raw *TNI* with a 5-month running mean.
- Normalize the smoothed *TNI* by its standard deviation over the climatological period 1950-1979. (The smoothed *TNI* has a standard deviation of 0.818 over the climatological period 1950-1979.)
- Thus, $TNI = (Niño\ 1+2_N - Niño\ 4_N)_{S,N}$ where N indicates normalized and S smoothed.

(Trenberth & Stepaniak 2001).



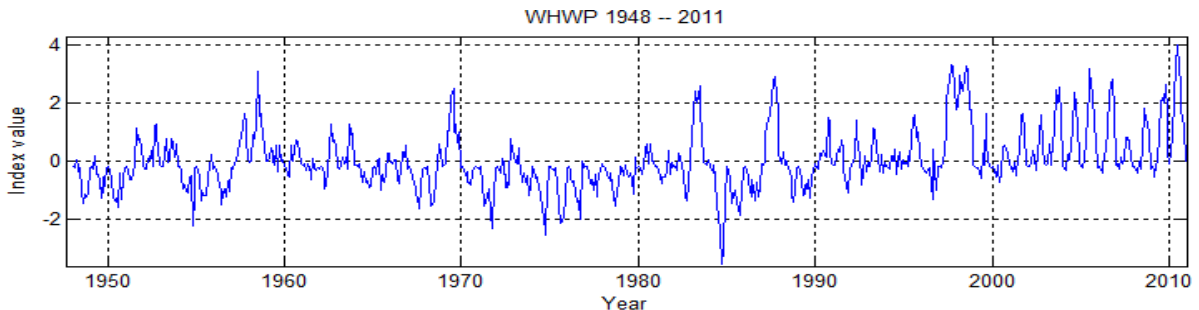
TPEOF

The TPEOF uses the 1st EOF of tropical Pacific SST (20°N-20°S, 120°E-60°W).



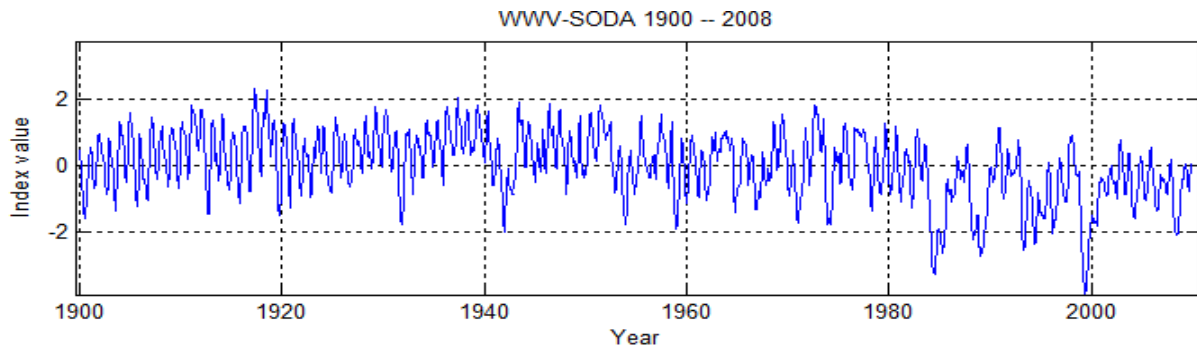
WHWP

The WHWP is the surface area of water contained above the 28.5 °C SST isotherm in the region; 7° – 27°N latitude, 110°W – 50°W longitude .



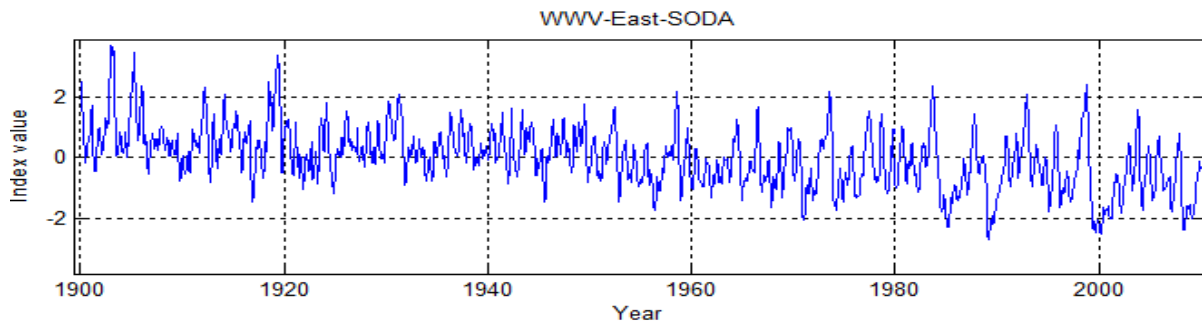
WWV

The WWV is a measure of upper ocean heat content analogous to the volume of water contained within the oceanic mixed layer in the region between; ± 5 °N-S, and 120°E to 80°W. Refer to the Literature Review Section 2.7.3 for fuller details of all WWV indices.



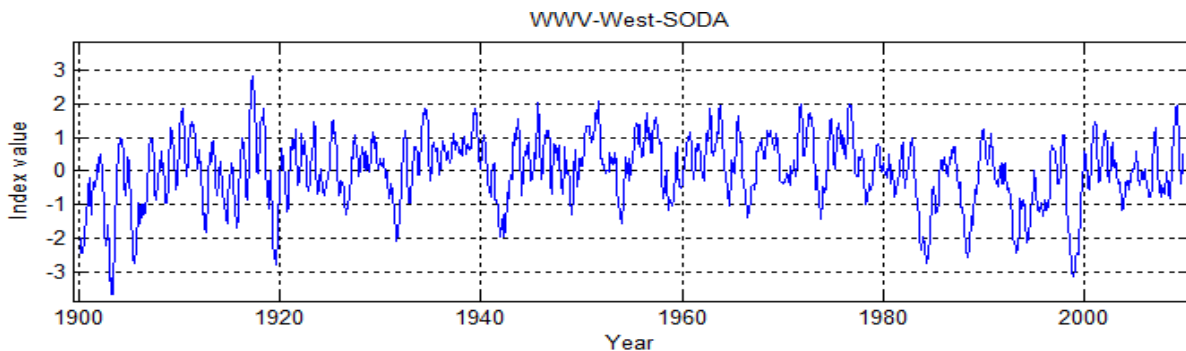
WWV_E

Similar to WWV but WWV_E region is contained within; $\pm 5^\circ\text{N-S}$, 155°W to 80°W .



WWV_West

Similar to WWV but the WWV_W region is contained to between $\pm 5^\circ\text{N-S}$, 120°E to



3.1.3 Reanalysis Data

Very many climate data series use reanalysis data as a matter of course these days, for example the TNI uses HadISST (Rayner et al. 2003). Two of the indices used and which figured prominently in this study; WWV and IPWP are constructed using Simple Ocean Data Analysis (SODA) (Carton & Giese 2008). This was discussed in Chapter 2. Some authors, including Schepen, Wang and Robertson (2011) thought that SODA data was not reliable enough to be used in their study of climate indices. Other authors (Giese & Ray 2011; Rajeevan & McPhaden 2004) have used SODA data with some success however. In fact for their decadal study of Pacific Subtropical Cell (STC) and its linkages with the PDO (Hong et

al. 2014) used SODA 2.2.4 the same as used in this current study and took the reanalysis back prior to 1880.

To investigate in a little more detail, data for WWV and its variants; WWV_E and WWV_W from the Tropical Atmosphere Ocean Project (TAO 2011) from 1980–2008 inclusive (Meinen & McPhaden 2000) were regressed with the same data as computed from SODA reanalysis (Figure 3.1). As can be seen very high ‘r’ values are obtained giving one a high confidence in the quality of the product. In respect of IPWP the SST (temperature at 5m depth) is part of the same data series so enjoys the same confidence.

SODA reanalysis data was correlated decadal with Australian rainfall for the first time to allow this research to expand significantly on previous studies.

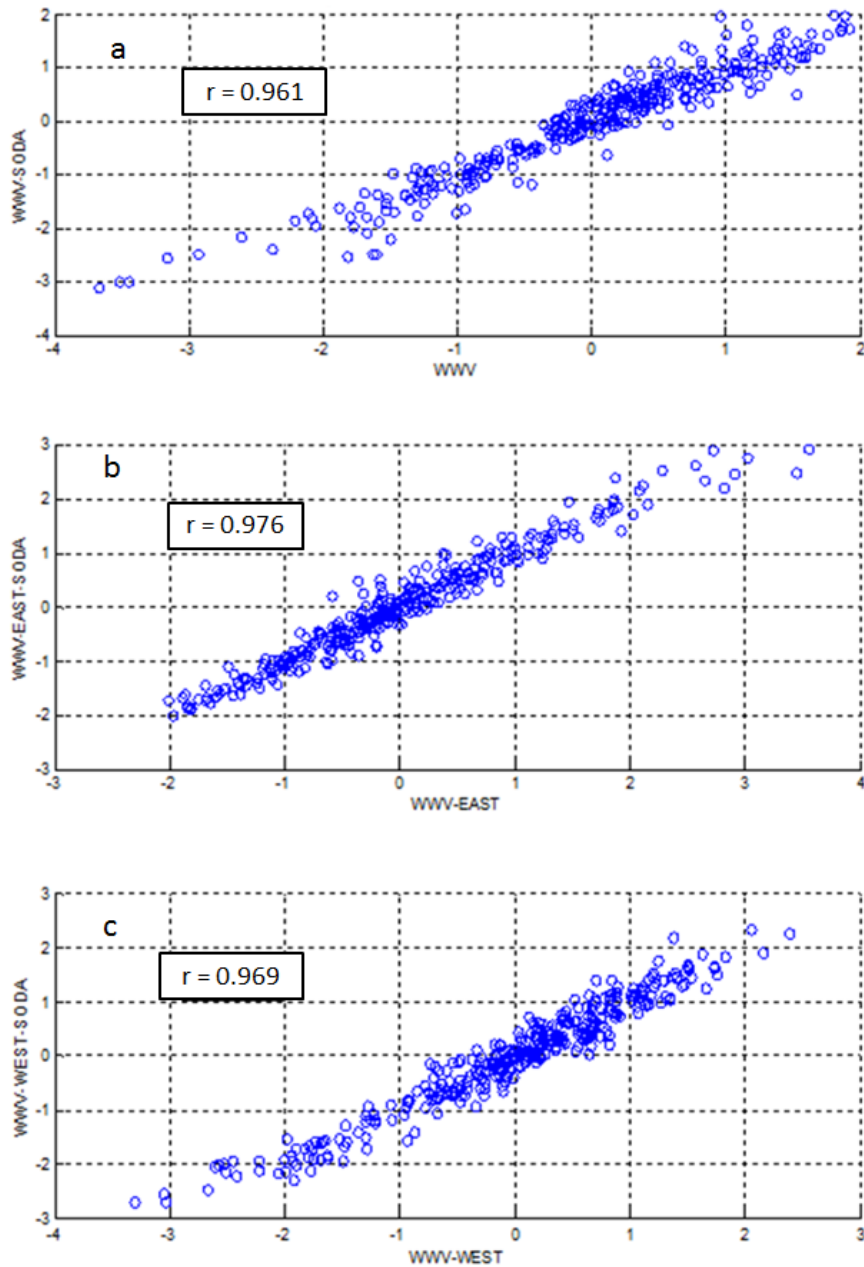


Figure 3.1: Scatter plots of SODA data regressed against TOA data (1980–2008): a) WWV
 b) WWV_E and c) WWV_W

3.2 Method

3.2.1 *A priori* Investigation

Initially the standardised climate indices time series were subjected to a Fast Fourier Transform (FFT) technique in MATLAB (MathWorks 2007) to examine their frequency domain spectral characteristics using the FFT function nested within the MATLAB Graphical

User Interface *tstool*. It was expected that this analysis might reveal fundamental differences in the characteristics of different climate indices. This procedure produced periodograms to separate the indices into distinct generic groupings dependent on spectral characteristics.

The MATLAB FFT function is included for completeness:

$$X^{(k)} = \sum_{j=1}^N x(j) \omega_N^{(j-1)(k-1)},$$

where $\omega_N = e^{(-2\pi i)/N}$ an *N*th root of unity.

The periodograms revealed two major generic types of results depicted in Figure 3.2a) showed an SOI pattern and b) showed an El Niño pattern. El Niño patterns are evident by their large amplitude annually recurrent signal and an otherwise overall lack of noise. In comparison SOI type signals have two or more low frequency spectral peaks; for example SOI has peaks at approximately 44 and 23.75 months as well as having a more uniform but enhanced background noise throughout the spectrum. Two other less dominant types of spectrum were also evident; one exhibited a mixture of the characteristics of the former two, having low frequency spectral peaks but with an annual signal. This has been termed the Mixture type as exemplified by the IPO (Figure 3.3a). Another more chaotic, type associated with indices whose poles were meridionally dispersed did not fit into any clear category due to a lack of low frequency dominance, but exhibited enhanced background noise throughout the spectrum is termed the Meridional type. An example of this Meridional type is the AOI (Figure 3.3b). A unique type also exists with the Quasi Biennial Oscillation as its sole member with a solitary spectral peak at 27.97 months (not shown).

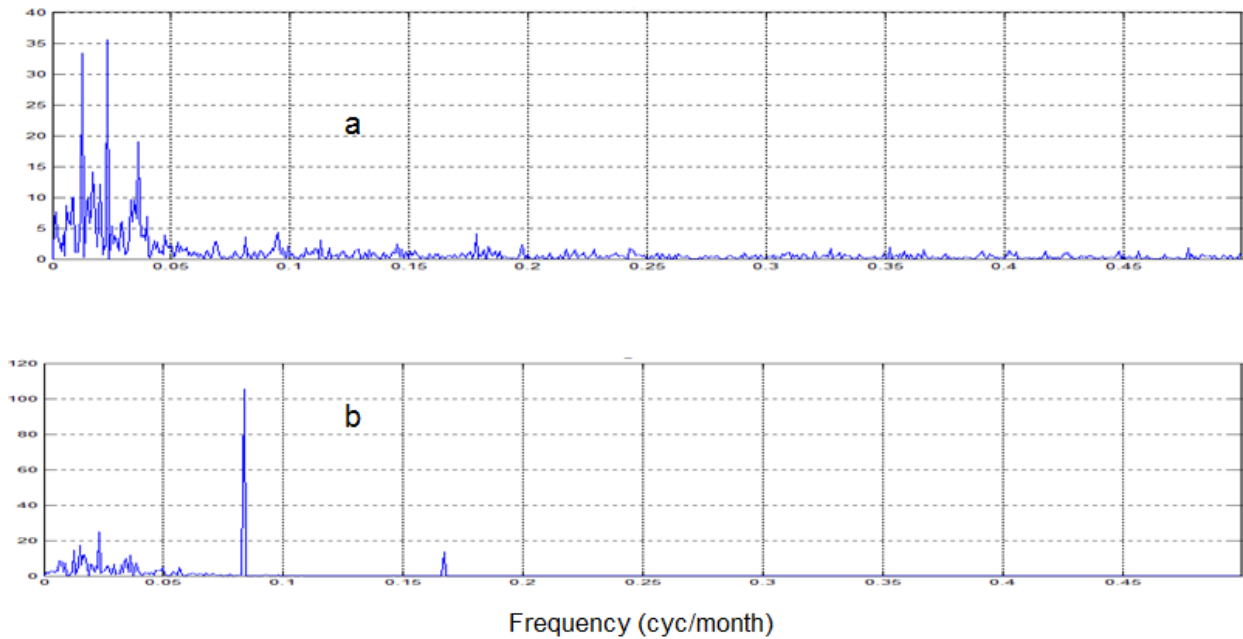


Figure 3.2: Typical SOI and El Niño pattern fast Fourier transforms (FFT's). a) the SOI and b) Niño34 for the time domain greater than 2.2 months (0.185 yr).

Inspection of the FFT periodograms for WWV type indices (Figure 3.4) shows how they have the same characteristics as Niño3.4. WWV and WWV_E (Figures 3.4a and b) are most similar whereas WWV_W (Figure 3.4c) captures some of the low frequency variability of the SOI power spectrum.

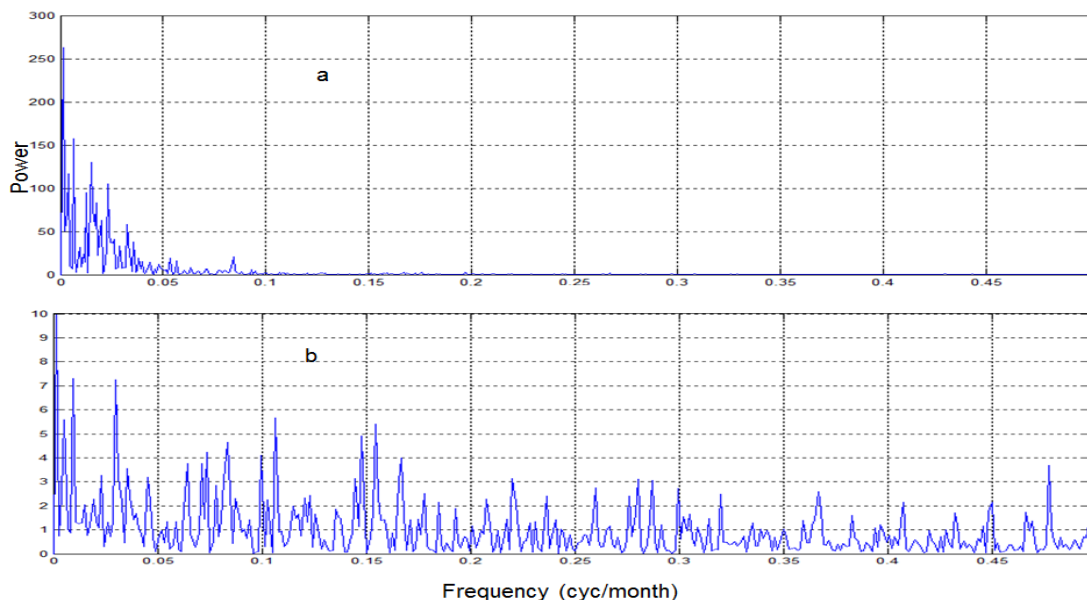


Figure 3.3: Fast Fourier transforms (FFT's). a) The IPO a typical mixture type pattern containing both SOI and Niño characteristics and b) the AOI (NAM) a typical cluttered Meridional type pattern for the time domain greater than 2.2 months (0.185 yr).

The climate indices are shown separated into their generic groups in Table 3.2. Most surprisingly certain indices did not fit with where they would normally be assumed to fit as perusal of column 1 in Table 4.1 shows. At first glance an informed observer would think that for example; Multivariate El Niño (MEI) and similar indices are members of the El Niño category, but their spectral signatures place them in the SOI generic group. The WWV indices although generically in the Niño group have very good consistent correlations with rainfall that warrants them being dealt with as a separate entity.

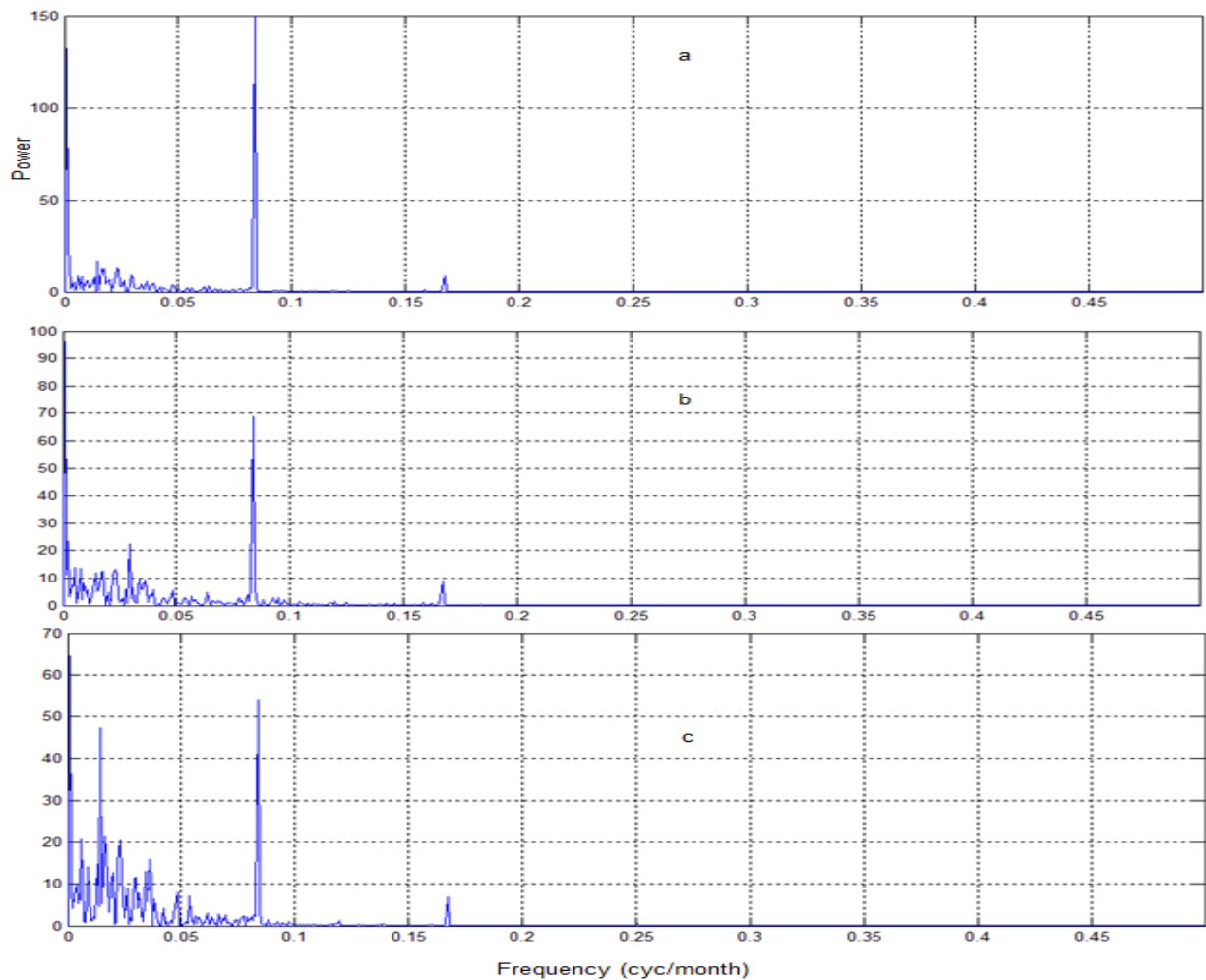


Figure 3.4: FFT periodograms of SODA data for: WWV types: a) WWV, b) WWV_E and c) WWV_W.

In terms of the correlation between index and rainfall many indices showed a marked change, for example changing from positive to negative in the last two decades of the 20th century

before reverting to the original configuration at the millennium, so this variation is noted as a matter of course in the analysis.

Table 3.2: Indices separated into their generic types as indicated by FFT periodograms. SOI types have low frequency spectral peaks and are generally noisy. Niño types lack noise but have an annual peak. Mixture types have both characteristics of SOI and Niño. Meridional types have their pole meridionally disposed and with enhanced background noise throughout the spectrum. QBO signal is unique with just a single biennial peak.

	SOI	Niño	Mixture	Meridional	Unique
1	SOI	Niño3.4	IPO	AOI (NAM)	QBO
2	BEST	NAO	PDO	NOI	
3	CTI	WHWP		SAM	
4	EQSOI	WWV		IPWP	
5	IOD	WWV_E			
6	MEI	WWV_W			
7	EMI				
8	FIVEVAR				
9	TNI				
10	TPEOF				
11	PWP				

3.2.2 Basic Method

In this section the fundamental operation of the method is introduced.

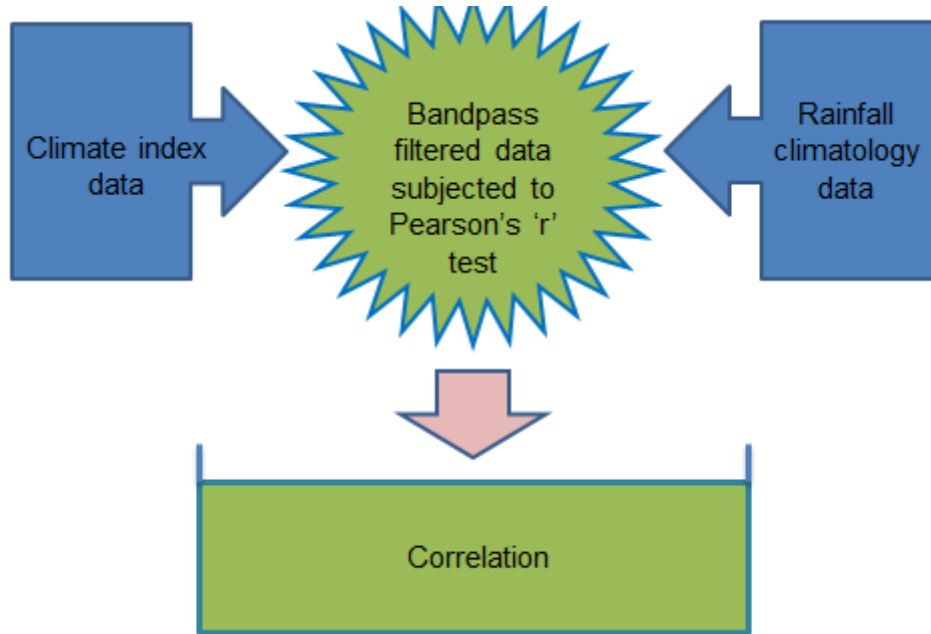


Figure 3.5: Schematic flow diagram of data processing

Figure 3.5 shows a schematic diagram of the fundamentals of the method used; the more involved technical aspects of which are amplified elsewhere in this chapter. Climate indices (Section 3.1.2) are subjected to Lanczos bandpass filtering (Section 3.2.3.1) and correlated (Section 3.2.3) with rainfall using Ferret (PMEL 2011) to produce gridded decadal correlation maps between the index and Australian rainfall. The correlation results of different indices are then compared with each other using non-parametric means (Section 3.2.4) to assess the relative potential of different indices for their suitability as possible predictors of Australian rainfall.

3.2.3 Correlation

The method used to process the indices and Australian monthly rainfall time series was the Pearson product moment correlation stated thus:

$$r = \frac{\frac{\sum(x-\bar{x})(y-\bar{y})}{(n-1)}}{\sqrt{\frac{\sum(x-\bar{x})^2}{n-1}} \sqrt{\frac{\sum(y-\bar{y})^2}{n-1}}}, \text{ (Walford 2011),}$$

where x and y might represent the sample index and rainfall covariance divided by the product of their standard deviations and n the number. For simplicity this expression may be written:

$$r = \frac{n \sum xy - (\sum x)(\sum y)}{\sqrt{(n \sum x^2) - (\sum x)^2} \sqrt{(n \sum y^2) - (\sum y)^2}}$$

For a significance test the t statistic may be used:

$$t = \frac{|r|(n-2)}{(1-r^2)} \text{ (Wackerly, Mendenhall & Scheaffer 2008).}$$

The actual climate data series are of 10 years duration or $n = 120$ months at $(n - 2)$ or 118 degrees of freedom (df). It is found that for a 95% confidence interval r is 0.1509 and t is 1.658 (calculated in R) (Ihaka & Gentleman 1996). Calculations were performed in “Ferret” (PMEL 2011) in the LINUX environment to produce a graphical output of correlation for the Australian continent where necessary. To make interpretation of significant data easier all r values of less than 0.15 have been made white in colour so that they may be disregarded by the viewer.

3.2.3.1 Detrending/Windowing

In this study a departure from the method of Cai, Whetton and Pittock (2001) is made as linear detrending does not faithfully reproduce real life situations (Wu et al. 2007). An example of this is given in the development of SEQ rainfall variability where Klingaman, Woolnough and Syktus (2013) found that the time series of rainfall is dominated by variability rather than a slowly evolving trend. The effects of detrending of the SOI are discussed further in Section 5.4.3 where it was found that the effects of a linear trend had no significant effect on correlation results. Some authors (Suppiah 2004; Trenberth & Hoar 1996) detected a 50 year change/decrease in the SOI. Figure 3.6 shows the small effect of detrending the SOI data. Figure 3.6a) compares raw 1965 – 2005 data (black) with linearly detrended data (red) which displays most of the same characteristics of the unmodified data. Figure 3.6b) shows a scatterplot of the data overlaid with the trend line representing a 0.8% decrease in SOI per decade. As can be seen the difference is extremely small.

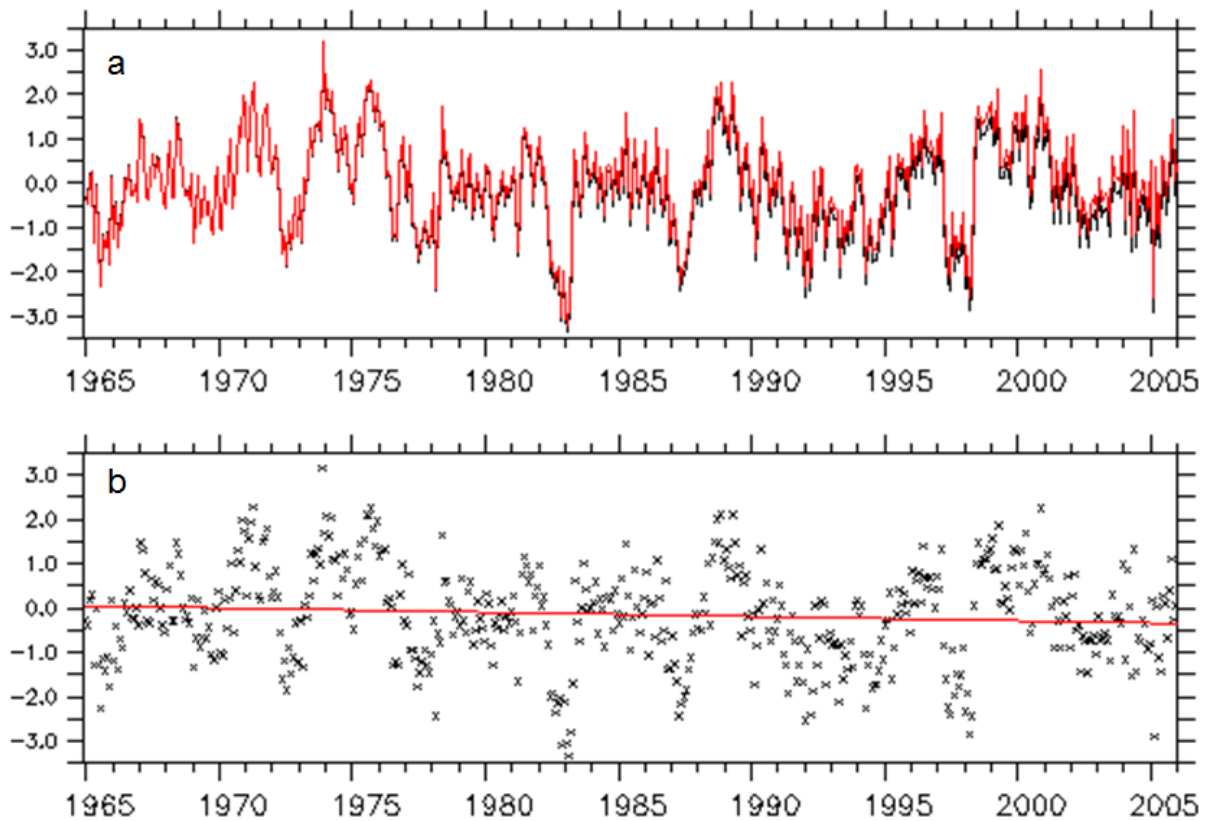


Figure 3.6: a) Comparison of raw SOI data 1965 – 2005 (black line) and linearly detrended (red line). b) Scatterplot of raw SOI data with the trend line overlaid in red.

When decadal apertures are used the difference is even less detectable (see Section 5.4.3).

Initially, for the whole year case both the precipitation time series and the climate index were both subject to band pass filtering using a moving Fourier windowing technique. The windowing technique used is inherent in the Ferret program and is known as a Lanczos filter as fully described in Duchon (1979). The Lanczos function parameters are as follows:

$$\text{Lanczos}(A, F1, F2, N)$$

where A is the data series in the x , y and z axis along the time vector, the cut off frequency ($F1$), high frequency cut off and number of weights (N). $F1$ was selected to remove sub decadal variability and approximates to an eight year period (95 months) or ≈ 0.0105 cycles \cdot month $^{-1}$ as used by Power et al. (1999). $F2$ was chosen at the high end of interannual variability (62) months or as or ≈ 0.016 cycles \cdot month $^{-1}$. Ideally the filter response is zero up to $F1$, unity between $F1$ and $F2$, the filter span and zero elsewhere. Filter span can be problematic as its width combined with the number of weights determines how much ringing

IE distortion to the Fourier transform by the Gibbs Phenomenon. Figure 3.7 shows the ideal lowpass filter (red line). Too wide a span gives a narrow frequency response band, but results in ringing occurring, whilst too narrow a span (solid black line), although reducing data loss results in a wider frequency transition width (data falling away too slowly above the cut off) (Cokelet 1999).

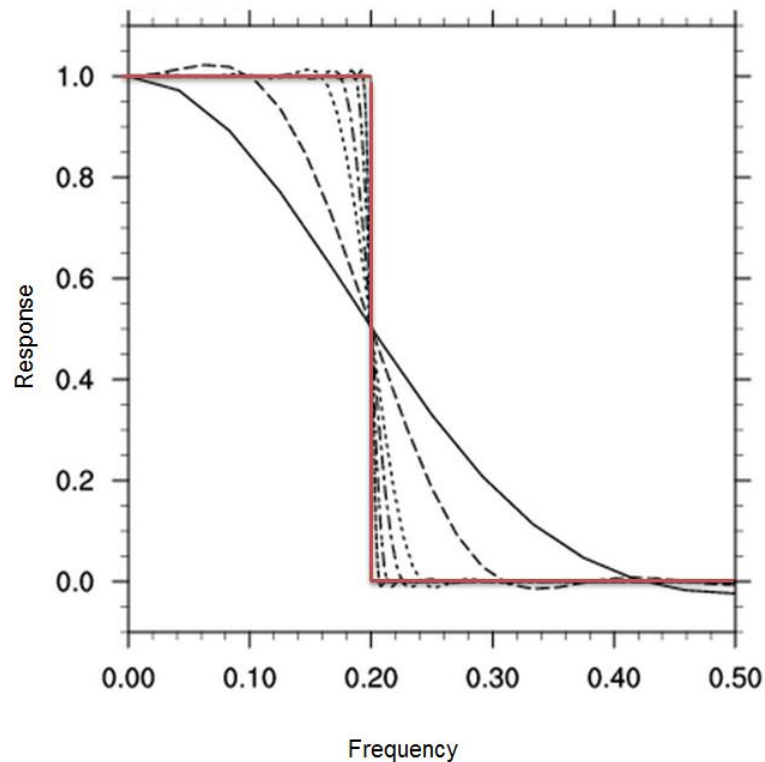


Figure 3.7: Effect of filter span width on ringing.

The number of weights (N) was selected as 19, which was a compromise between total variance for a high number of weights but loss of data or loss of variance and high data retention at the ends of the data series.

3.2.3.2 Skewed Data

One potential limitation of the method is possible skewness of the rainfall data (Schepen, Wang & Robertson 2011). To check for any untoward effects of this nature, logarithmic transforms both to base₁₀ and natural logarithms were tried but had little or no effect on the integrity of the resultant correlation coefficients.

3.2.4 Data Analysis

The basic method and windowing techniques as discussed earlier in this chapter produced a series of spatially defined correlation maps between climate indices and rainfall for the Australian continent. Just one procedure alone cannot easily describe all aspects of the relationship however, so as an aid to assist interpretation five further analyses were undertaken.

The large sample of correlations between a climate indices and Australian rainfall occupied a 110 year period and was divided into 11 samples each of one decade duration. Some data series were only available for sixty years so were divided into six decades. The DJF correlation data for both Australia and SEQ was assessed with respect to five different criteria which were deemed to be important:

1. Strength in respect of the range of correlation for the whole range of data expressed as sample variance.
2. Persistence, how the correlations (using the decadal sample variance) varied interdecadally.
3. Area of significant correlation.
4. Temporal stability, as to how the predominant pattern of correlation varied interdecadally.
5. The overall ranking of the indices.

Ranking as a method was chosen for its computational simplicity in its ability to express large amounts of data in a comparatively small data series (Legendre & Legendre 2012). In each category the range of data was divided into equally sized intervals so that a mark (rank) from 1 to 10 in increasing significance could be assigned for the performance of each index. These criteria are not always complimentary as they have been designed to emphasise different aspects of the relationship, each of which might be of value to other researchers. It should be noted in relation to the spread of data true population variance cannot be known, but Wackerly, Mendenhall and Scheaffer (2002) (page 424) show that sample variance may be used as an unbiased indicator of the spread of a population and is used here. Variance in this case refers to the square of correlation standard deviation over the entire area under consideration:

$$s^2 = \frac{\sum_{i=1}^N (y_i - \bar{y})^2}{N-1}, (\text{Wackerly, Mendenhall \& Scheaffer 2002}),$$

where s is the sample standard deviation, \bar{y} the sample mean, N the number of units in the sample and y_i the i -th unit in the sample.

A description of each of the criteria and rationale for their usage follows:

1. Strength is indicated by the sample variance of the correlation for the whole 11 decades. Australia occupies several different climate regions from the Equatorial to Mediterranean. An index with a large variance represents a large range of correlations and different climate regions will not all have the same correlation and sign. This implies strong anti-correlation in some regions and strong correlation in others, either way this index is strongly linked to rainfall or some other parameter if chosen.
2. Persistence, the interdecadal power of the variance, was analysed by constructing histograms of the sample variance of correlation (loosely analogous to heteroscedasticity) for all decades where it was found that variance had the potential to fall into five regions: 0.2 – 1.2 with intervals of 0.2 on the probability function. Persistence may then be expressed as:

$$\frac{\text{Number of decades}}{\text{Number of bins occupied}}$$

If there was no significant changing correlation ie if the variances generated were entirely random there would be equal likelihood of all variances being obtained (a uniform distribution). The expected value (mean) would not be suitable as a descriptor if the distribution was not normal. The mode (the value that appears most often in the distribution) might be a better descriptor but it only describes the position of a proportion of some values on the probability function and was regarded as lacking in sensitivity to adequately describe interdecadal power. A similar logic showed that skewness did little in describing power. An extremely stable correlation would show all the sample variances occupying only one bin. This could be likened to a leptokurtic distribution but without the disadvantages of kurtosis.

Kurtosis deals with the peakiness and the thickness of the tails of the distribution (DeCarlo 1997) and is given by the expression:

$$\gamma_2 = \frac{\mu_4}{\mu_2^2} - 3, (\text{Walck 2007}),$$

shown here for completeness, where γ_2 is the kurtosis, μ_4 and μ_2 are the fourth and second moment respectively. In this study the persistence method shown was preferred to kurtosis because kurtosis is normally associated with symmetrical distribution as a skewed distribution is always leptokurtic (Hopkins & Weeks 1990). Another disadvantage of kurtosis is that it becomes more unreliable with a small number of degrees of freedom (Snedecor & Cochran 1967).

A consistently performing index, even if it has low correlation, will yield a higher number indicating that correlation is less likely to change over time with the potential of making it a good predictor of interdecadal stability.

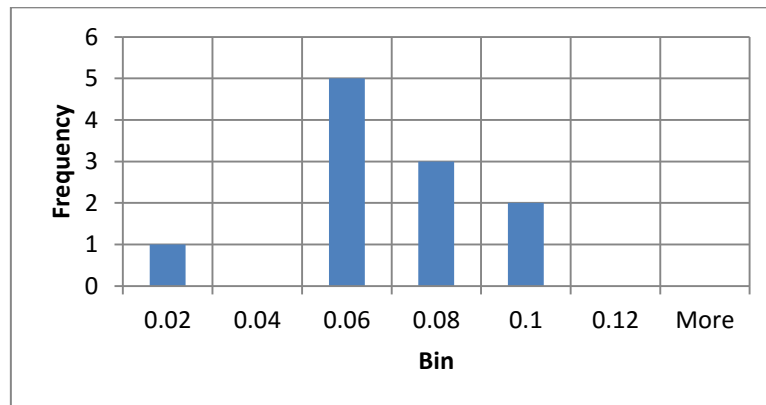


Figure 3.8: Histogram of SOI variance for 11 decades

Take the SOI as an example as shown in Figure 3.8, it can be seen that four bins were occupied so a measure of persistence was obtained by dividing the number of decades by the number of occupied bins to deliver:

$$11/4 = 2.75.$$

If this was compared to another higher performing index, say the TNI where it was found only three bins were occupied resulting in a score of:

$$11/3 \approx 3.67.$$

This method was deliberately chosen so as to penalise the shorter six decadal time series due to their relative lack of information. For example the Best Index sample variance also occupies the same number of bins as the SOI, but would give a value of $6/4 = 1.5$.

The area of significant correlations for Australia within the whole time period was obtained. The larger the area then the greater confidence one could have in any predictive outcome over a wide region. This was determined numerically from the Ferret application as the ratio of areas (pixels) containing a significant correlation to the total number of pixels expressed as a percentage:

$$\frac{\text{Number of occupied pixels}}{\text{Total number of pixels}} \times 100(\%)$$

Temporal stability relates to how correlation changed by decade. Ideally an index should have the same significant pattern for every decade in the whole time series. This was assessed by visual examination of the correlation maps thus:

$$\frac{\text{Number of decades with a specific significant pattern}}{\text{Total number of decades}} \times 100(\%).$$

Again consider the SOI, it was noted that the same significant pattern occurred in seven of the 11 map panels to give a score of $7/11 \times 100 \approx 64\%$. Of all the tests this is one most liable to subjectivity as it relied on visual assessment of the patterns on the correlation maps. To avoid subjectivity as much as possible four assessments were made each after altering the colour palate of the correlation maps. These included the normal colour palate, an inverse colour scheme, a black and white scheme and a negative black and white scheme. This result thus amplifies that obtained in criterion 2 in describing interdecadal stability.

Finally the scores for each criterion for each index were added together (von Helmholtz 1977) and an overall, unbounded ranking of each index obtained where 1 was highest ranking.

Taken together these criteria enable a comprehensive assessment as to the relative performance, both spatial and temporal of different climate indices with respect to Australian rainfall to enhance the information obtained from the correlation maps.

3.3 Comparing SOI and Niño3.4

Subsequent to the spectral analysis technique described in Section 3.2.1, which separates indices into different spectral classes, methods that compare indices from different spectral

groupings were also considered necessary. Such methods including Cross Correlation and Wavelet Analysis do not form part of the main thrust but are included for completeness.

3.3.1 Cross Correlation

If two indices are correlated together it enables them to be compared producing a range of correlation coefficients between them, at various lags over the whole spectral range in vector form. As an example of this is SOI and the Niño3.4 time series which are essentially part of the same phenomenon to analyse their fundamental differences and similarities:

$$\hat{R}_{xy}(m) = \begin{cases} \sum_{n=0}^{N-m-1} x_{n+m} Y_n^* & m \geq 0 \\ \hat{R}_{yx}^*(-m) & m < 0, \end{cases}$$

The output vector c has elements given by $c(m) = R_{xy(m-N),m=1,\dots,2N-1}$. (MathWorks 2007)

The vector may be plotted in MATLAB or using the MATLAB *tstool* Graphical User Interface (GUI).

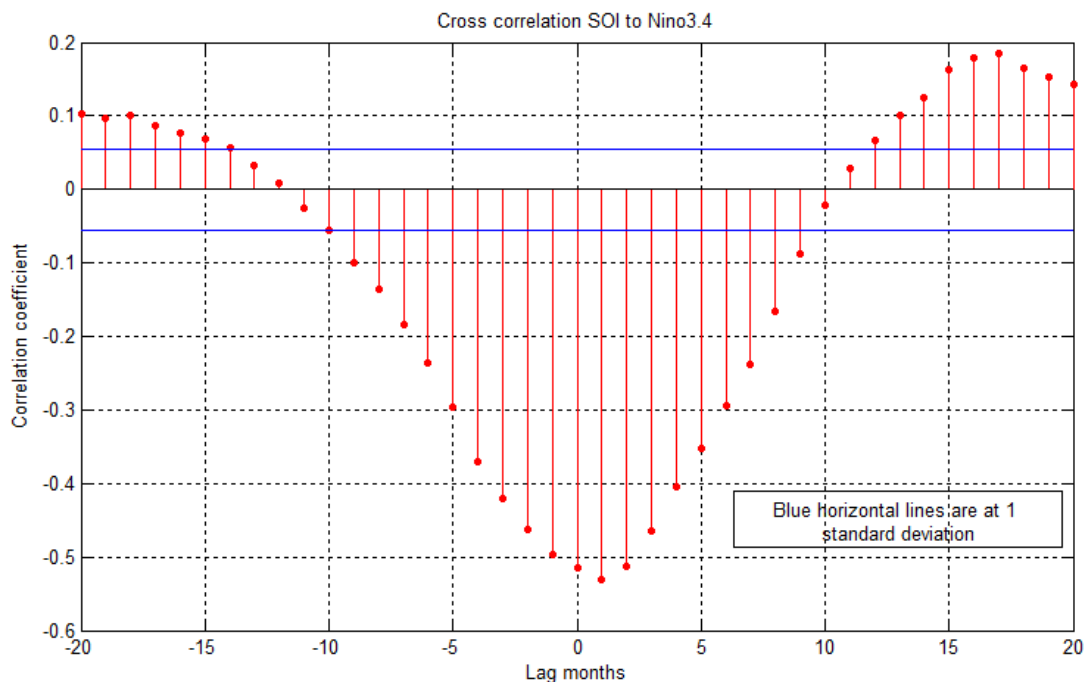


Figure 3.9: Cross-correlation of SOI and Niño3.4 showing high correlation at one month lag

Cross correlation (Figure 3.9) also found that SOI and Niño3.4 were highly correlated with each other with a lag of Niño3.4 to SOI of only one month. Evidence of this slight lag may also be observed in the Wavelet pattern (Figure 3.12).

3.3.2 Wavelet Transforms

Further spectral treatment to compare SOI and the Niño3.4 time can be performed using Wavelet decomposition.

At the heart of Wavelet Analysis is a *Wavelet Transform* which is a bandpass filter of uniform shape but of varying location and width (Torrence & Compo 1998) (Figure 3.10d). Note the difference to the Fourier window (Figure 3.10b) as used in the periodogram. It may also be described as a microscope whose magnification is $1/\lambda$ where λ is a scale factor and whose optics are the waveform (Kumar & Foufoula-Georgiou 1997). The Wavelet Transform is used to analyse time series x_n with equal time spacing δ_t ($n=0, 1, 2, \dots, N-1$) calculating the scalar (dot) product of the wavelet function and the series of interest. It also assumed that a Wavelet function $\Psi_0(\eta)$ depends on a nondimensional parameter η which must have zero mean and be local in time and frequency space.

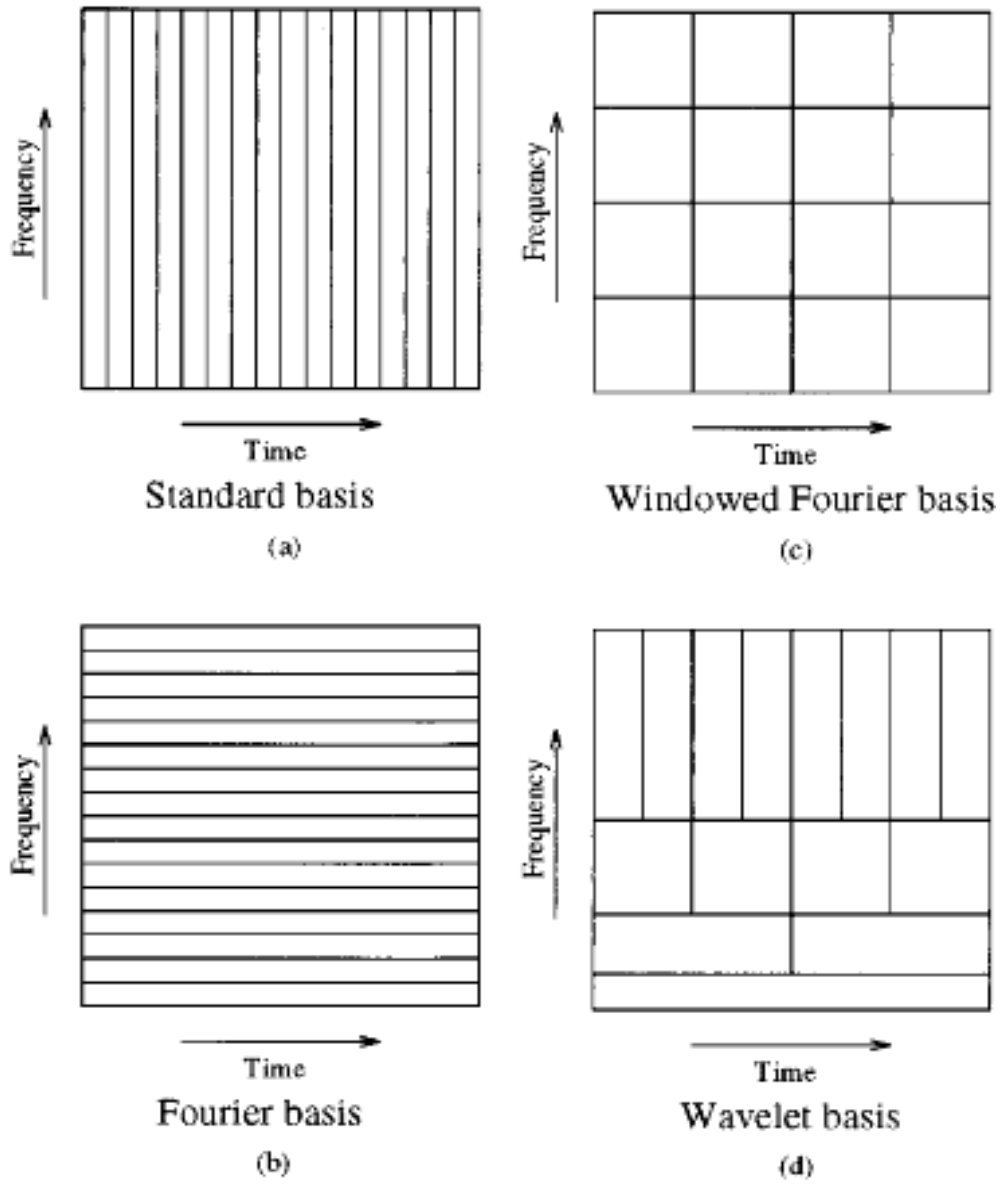


Figure 3.10: Basis of time frequency decomposition; Kumar and Foufoula-Georgiou (1997)

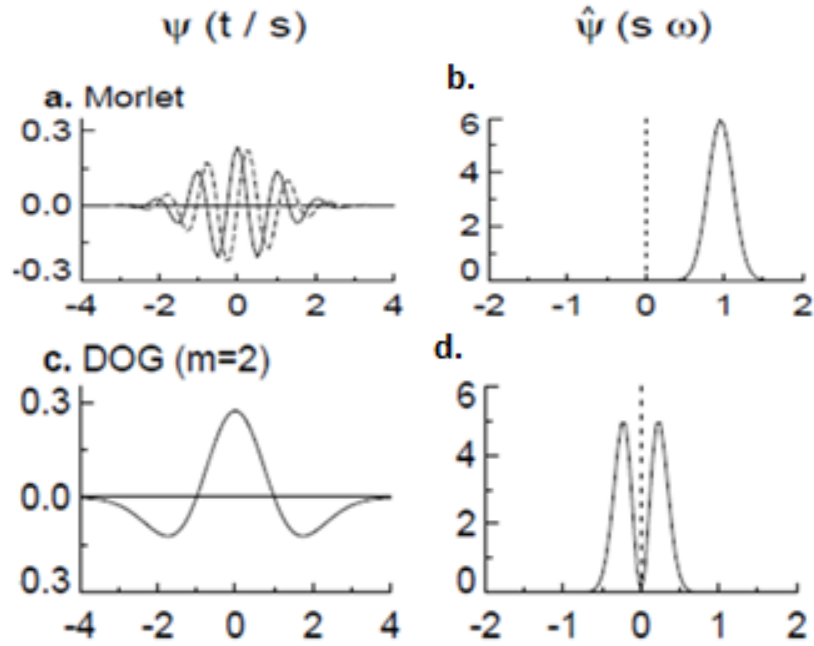


Figure 3.11: Two types of Wavelet function, at a; the Morlet and b; its transform and c; the Dog and d; its transform, modified from Torrence and Compo (1998) Figure 2.

Figure 3.11 shows two types of Wavelet Transform, on the left is the functional representation in the time domain and at right is their transform (hatted) in the frequency domain. The upper example (a) shows the Morlet Transform which has both a real part (solid line) and an imaginary part (shown dotted) it is this quality that enables phase related data to be represented. Below is shown an example of a derivative of a Gaussian (DOG) distribution known as the "Mexican Hat" for obvious reasons (Table 3.3). Wavelet function refers to all wavelet functions both continuous and discrete but the term *orthogonal* Wavelet function refers only to the discrete cases.

Table 3.3: Wavelet functions shown in Figure 3.11 (reproduced from Torrence and Compo (1998))

Name	$\psi_0(\eta)$	$\hat{\psi}_0(s\omega)$	<i>e</i> -folding time τ_s	Fourier wavelength λ
Morlet ($\omega_0 =$ frequency)	$\pi^{-1/4} e^{i\omega_0 \eta} e^{-\eta^2/2}$	$\pi^{-1/4} H(\omega) e^{-(s\omega - \omega_0)^2/2}$	$\sqrt{2}s$	$\frac{4\pi s}{\omega_0 + \sqrt{2 + \omega_0^2}}$
DOG ($m =$ derivative)	$\frac{(-1)^{m+1}}{\sqrt{\Gamma(m + \frac{1}{2})}} \frac{d^m}{d\eta^m}$	$\frac{i^m}{\sqrt{\Gamma(m + \frac{1}{2})}} (s\omega)^m e^{-(s\omega)^2/2}$	$\sqrt{2}s$	$\frac{2\pi s}{\sqrt{m + \frac{1}{2}}}$

Rainfall data in climate data series are usually discrete in nature and therefore the discrete or orthogonal Wavelet transform is used. Modern accurate climate data series are usually quite short so it is customary to pad the ends of the data series. This means to add a series of zeroes to each end of the series that are slightly wider than the window interval so that all of the data can be analysed.

The Wavelet decomposition for the Southern Oscillation Index (SOI) and Niño34 was conducted in the Matlab Wavelet Toolbox GUI (MathWorks 2007).

The two premier indices, the components of ENSO; SOI and Niño3.4 were also compared using a Wavelet decomposition technique (Torrence & Compo 1998) again in Matlab (figure 3.12). Initially it appeared as if the two signals were completely different, a point not borne out by closer examination. Apart from the smoothing; five months in the case of Niño34 and a statistical smoothing for the SOI, the two signals are almost the inverse of each other as the top line “a3” the third residual signal, shows by close scrutiny.

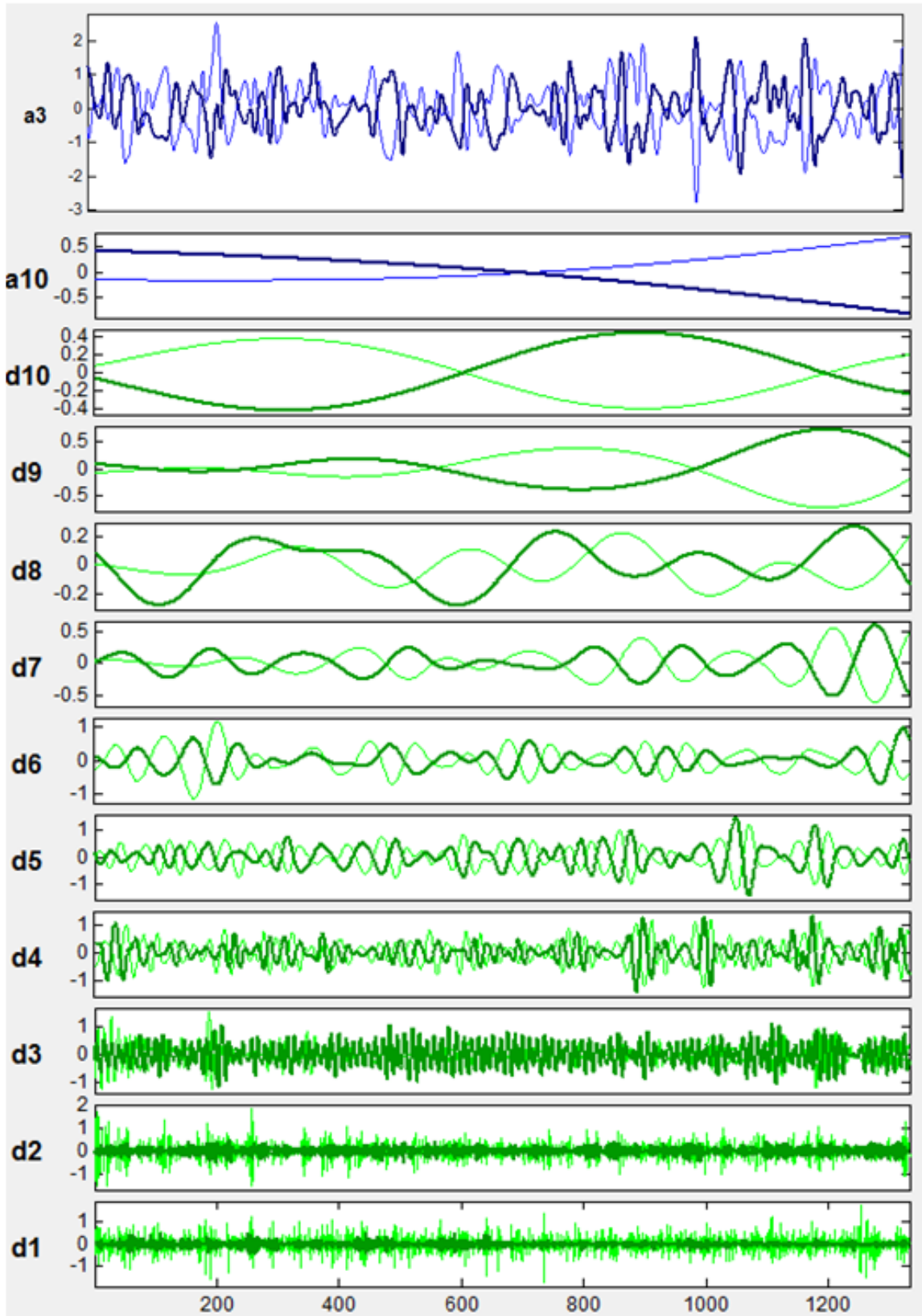


Figure 3.12: Wavelet decomposition of: bold blue and green colour is Niño3.4 and pastel shades the SOI time series 1900 – 2010 (conducted in MATLAB). Top row shows; a3 the third residual.

The final residual at a10 also show a distinct inverse relationship as does d10, the final noise exclusion. The reversal is less apparent, but still discernible at noise exclusions; d7, d6, d5 and d4. It is only at noise levels below four months as depicted at; d3, d2 and d1 that the relationship is not really apparent.

3.4 Summary

The best, most accurate and longest time series data were selected in a procedure that takes into account the non-linear evolution of rainfall time series. Initially correlations were conducted in groupings relating to spectral similarity. The method used a moving spectral windowing technique that removed sub decadal variability and intra-annual noise whilst preventing truncation of the data series at its beginning and end to make maximum use of the available data. Non-statistically significant results were masked by careful selection and design of the graphics key. The method attempted to remove subjectivity wherever possible.

Spectral cross correlation and Wavelet decomposition are tools that enable indices from the different spectral groupings to be compared. These techniques were used to analyse the differences between the Niño3.4 and SO indices which are both indicators of essentially the same phenomenon.

Chapter 4 Results

4.1 Introduction

This chapter is by necessity full of acronyms so it is suggested that the reader refers to the introductory glossary in Table 1.1 for assistance if necessary. Contained in this chapter are the results after correlating December, January and February (DJF) Australian summer rainfall with 24 monthly climate indices at decadal resolution 1900 – 2008. No previous study has been conducted with such a wide variety of indices. Schepen, Wang and Robertson (2011) came near to doing a comprehensive study, but conducted at a 29 year resolution and on just 13 indices and without pursuing the promising topic of ocean heat content indices in any great depth.

Decadal resolution was chosen as it has previously been shown that decadal variation in the Indian Ocean SST is associated with rainfall variability in parts of Australia (Power et al. 1999) and that it varies in symaltaneously with an interdecadal oscillation in the Pacific (Cai, Whetton & Pittock 2001). The relationship of decadal climate variability and the 11 year solar cycle has also at times been an intense area of debate (Baldwin, M. et al. 2001).

From a practical standpoint climate prediction using a decadal timespan if possible is highly desirable providing more certainty in all aspects of human endeavour by minimising socio economic impact especially for primary production (Keenlyside & Ba 2010). This chapter is structured by initially using the spectral signatures of climate indices divided into distinct spectral types as described in Chapter 3, Section 3.3.1 "*A Priori* Investigation", and later, Section 4.2 "Initial analysis".

A particular focus is on the analysis represented in section 4.4 and subsequent discussion in Chapter 5 of these results for South East Queensland (SEQ). Such a comparative analysis of all available climate indices and rainfall relationship is currently lacking for SEQ, although previous analysis by Murphy and Ribbe, (2004) noted that SEQ is more prone to periods of weaker correlation than any other region in Australia.

A most significant outcome was how well indices constructed using the near Australia Pacific warm pools (WPs) performed in comparison to the more traditionally used indices. Using the spectral signatures also revealed a surprising linkage between the SOI and the Interdecadal Pacific Oscillation as alluded to previously (Cai, Whetton & Pittock 2001; Cai & van Rensch 2012).

In short the analysis and presentation of results concentrate on:

- Expanding the work of Schepen, Wang and Robertson (2011), extending it to 24 different climate indices
- Decadal resolution
- Making SEQ an area analysed with a multiplicity of indices

The material presented in Section 2.1 links climate indices with Australian rainfall to a greater or lesser degree, a starting point for this research. Correlation between indices and rainfall will be performed as a basis for future investigation of links between pressure and temperature phenomena and Australian Climate. It is expected that a spread of correlations will be observed due to correlations between indices (de Viron, O., Dickey, J. & Ghil, M. 2013).

The Oceanic Niño Index (ONI) (Kaplan et al. 1998) was discarded as it was found that its correlation pattern using a three month running mean was indistinguishable from the five month running mean of the Niño3.4 index (Bamston, Chelliah & Goldenberg 1997).

Contextual descriptions of indices where appropriate are found in Chapter 3, Section 3.1.2. Correlations between climate indices and annual (January – December) rainfall are not included unless significant apart from WWV variants and the Niño3.4 and SOI indices; the latter two of which exhibit a poorer correlation at summer resolution than annual (January – December) resolution. Thus to prevent this document becoming too unwieldy, correlation maps for other indices for the (January – December) are contained in the attached library on compact disk. The inclusion of Warm Water Volume correlation with annual (January – December) rainfall is included because of the remarkable consistency of this product.

The rainfall graphic (Figure 2.1), although interesting is of limited application. Figures 4.1 and 4.2, summer (DJF) decadal rainfall anomaly maps, gridded actual anomaly and area averaged standardised anomaly respectively are included to help the reader make comparisons between rainfall and correlation when assessing the results. For accurate assessment it is suggested that Figure 4.1 might be used and for a more rudimentary, less accurate initial assessment Figure 4.2 is recommended. Australian rainfall in this period has varied about its mean by $\approx \pm 1 \text{ mm}\cdot\text{day}^{-1}$. In terms of standard deviation at decadal resolution, Australian rainfall anomalies for the period are varying only by $\approx \pm 0.3$ standard deviations on average.

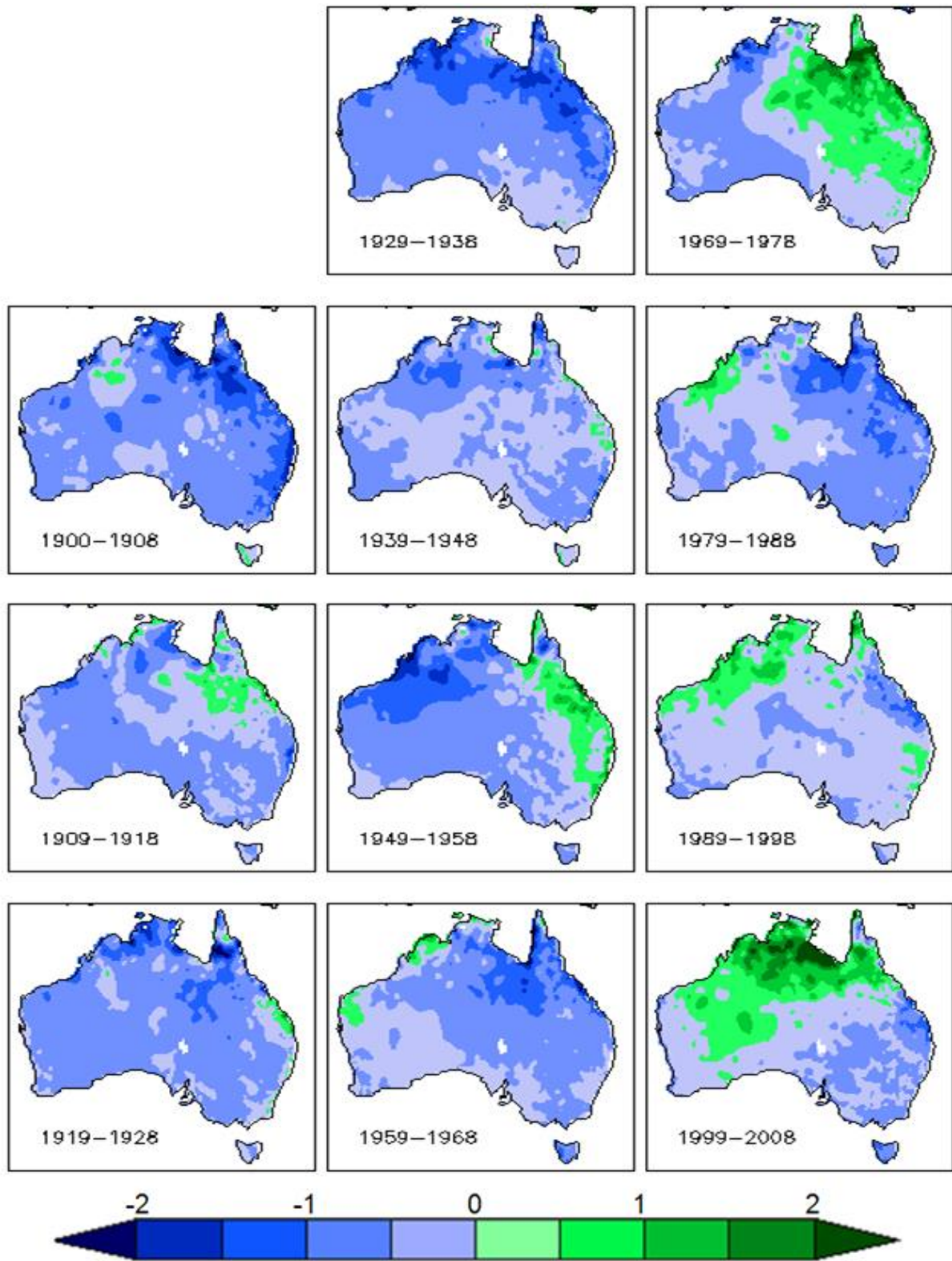


Figure 4.1: Summer (DJF) decadal Australian rainfall anomaly 1900 – 2008 (mm day^{-1}).

Significant changes in the relationship of climate indices and Australian rainfall over 11 decades are documented in this study which uniquely includes a 110 year subset of Simple Ocean Data Assimilation (SODA), a measure of tropical Pacific Ocean heat content. SODA

is used to investigate decadal rainfall variability and allow the extension of Warm Water Volume and Indo Pacific Warm Pool indices beyond the directly observed data.

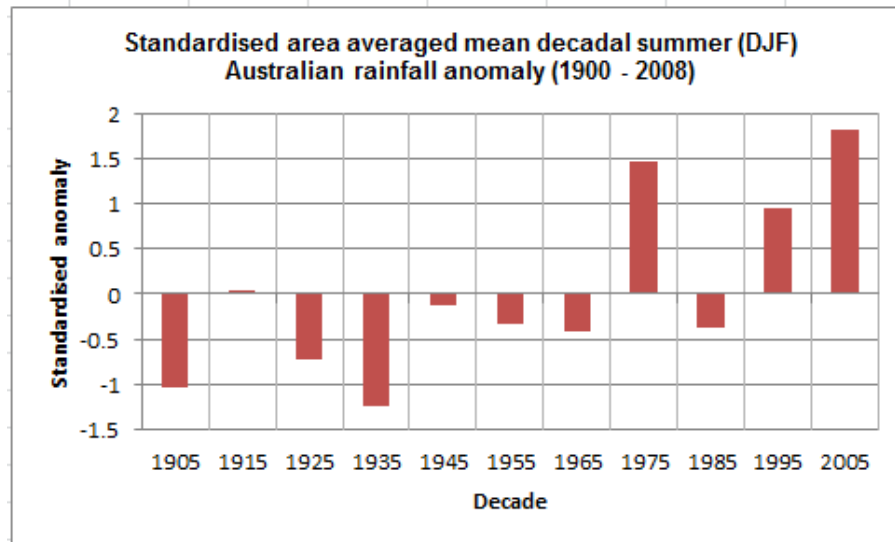


Figure 4.2: Standardised Australian area averaged summer (DJF) decadal rainfall anomaly (1900 – 2008).

4.2 Initial Analysis

An initial analysis was conducted on the indices using a fast Fourier transform (FFT) technique in Matlab to produce periodograms as described in Chapter 3 section 3.3.1; A *Priori* Investigation. Like Spectral signatures are grouped as shown in Table 3.2 and their correlations with rainfall are shown. The groupings (Spectral class) are: SOI type, Niño type, mixture type, meridional type and a unique type. Absence of a decadal correlation panel on a decadal correlation graphic reflects the unavailability of index data for that decade.

4.2.1 Southern Oscillation Index Types

4.2.1.1 Southern Oscillation Index (SOI)

The SOI is an index which has been comprehensively dealt with in the literature and overall, generally shows a positive correlation with DJF rainfall (population mean 0.256. The decade with the highest mean correlation was the 1970s at 0.49 (Figure 4.4). In the last two decades of the last century the correlation was of opposite sign than previously and markedly weaker

achieving 0.3 in the 1980s even though rainfall for the continent was near average. No distinct isoline of zero correlation apparent. Area coverage was also poor for seven of the 11 decades and in the 1980s and 1990s especially so where less than 30% of the land area achieved a correlation significant at the 95 % Confidence Interval (CI). SOI does show a weak positive correlation in SW Queensland and the adjacent Northern Territory.

A decadal graphic of the monthly SOI at an annual scale (Figure 4.3) show comparably greater significant correlation. The correlation tracks the index in a weak fashion in north-east (NE) Australia including Queensland, SEQ and north-west (NW) Australia. It is interesting to note that Power et al. (1999) SOI correlation results (their Figure 5 1910 – 1992) are very similar to panel 1 in Figure 4.3 which is based on 1900 – 2008.

4.2.1.2 BEST index

The BEST index (Figure 4.5), is only available from 1949 – 2008 and the missing panels in this and other graphics reflects on the unavailability of data for the relevant decades.

Overall pattern was the inverse of the SOI (positive correlation where SOI is negative and vice versa). The index exhibited a mean negative correlation with rainfall Area averaged correlation (not shown) was quite high at -0.5 in the 1970s. Variance altered significantly interdecadally, its histogram occupying four bins in six decades. Worst correlation range was in the 1980s. Within Australia this correlation tracks weakly to index except in Western Australia and enjoys quite a high area average of correlation of 37% for the whole period. Temporally the same approximate configuration of correlation pattern persists for five of the six decadal panels. For the whole year (not shown) correlation is similar with a much greater significant area.

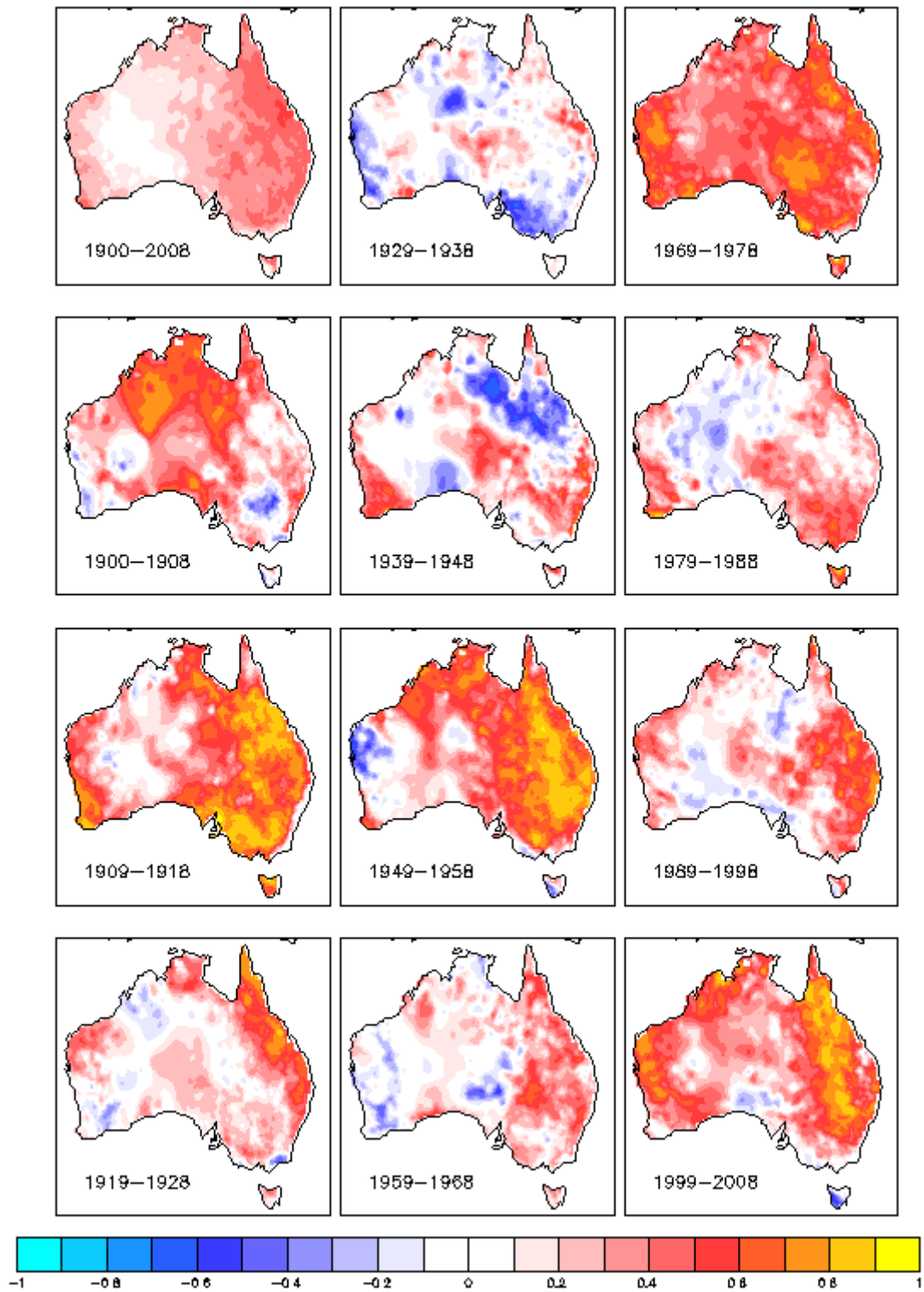


Figure 4.3: Correlation of rainfall with SOI.

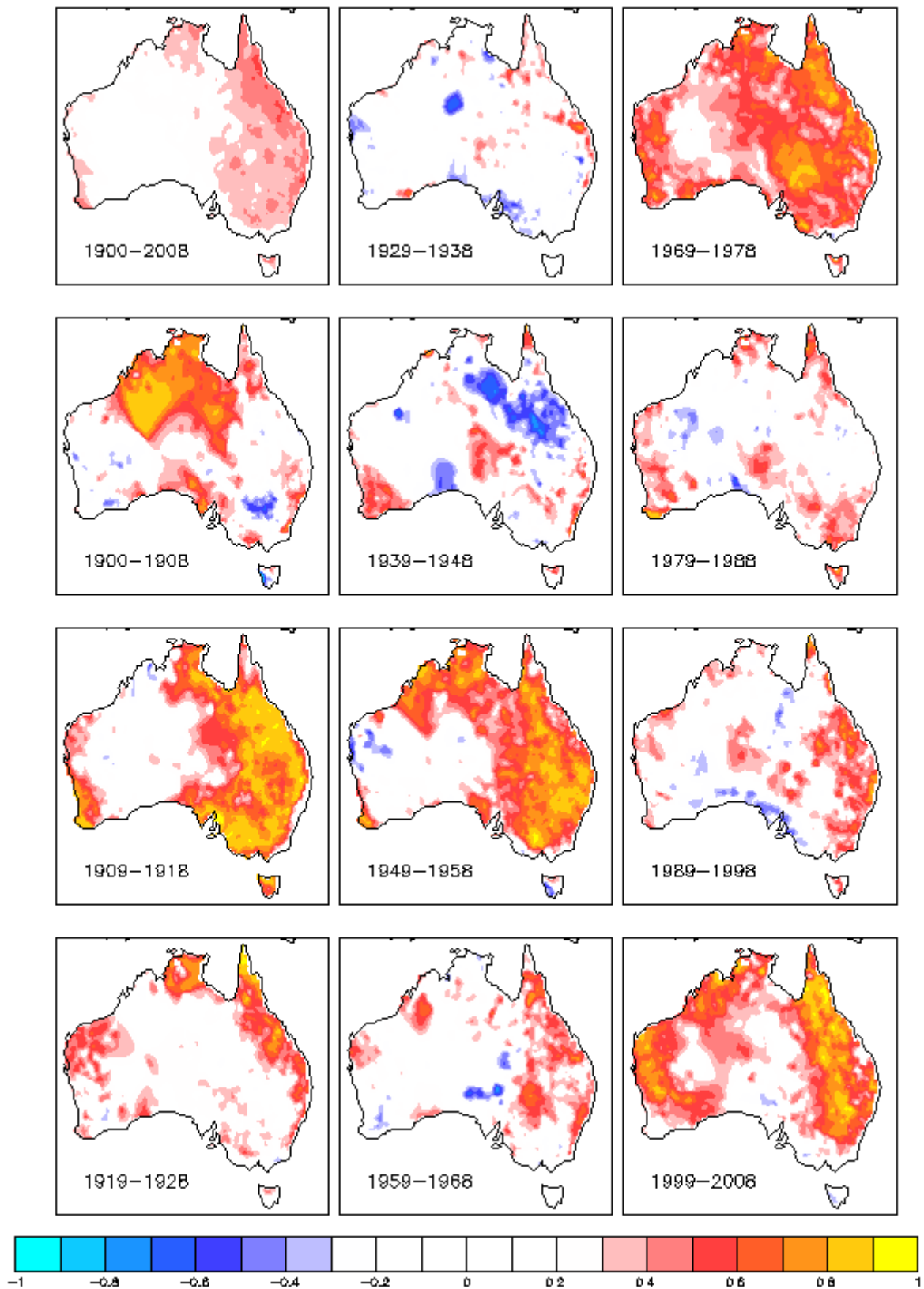


Figure 4.4: Correlation of DJF rainfall and SOI.

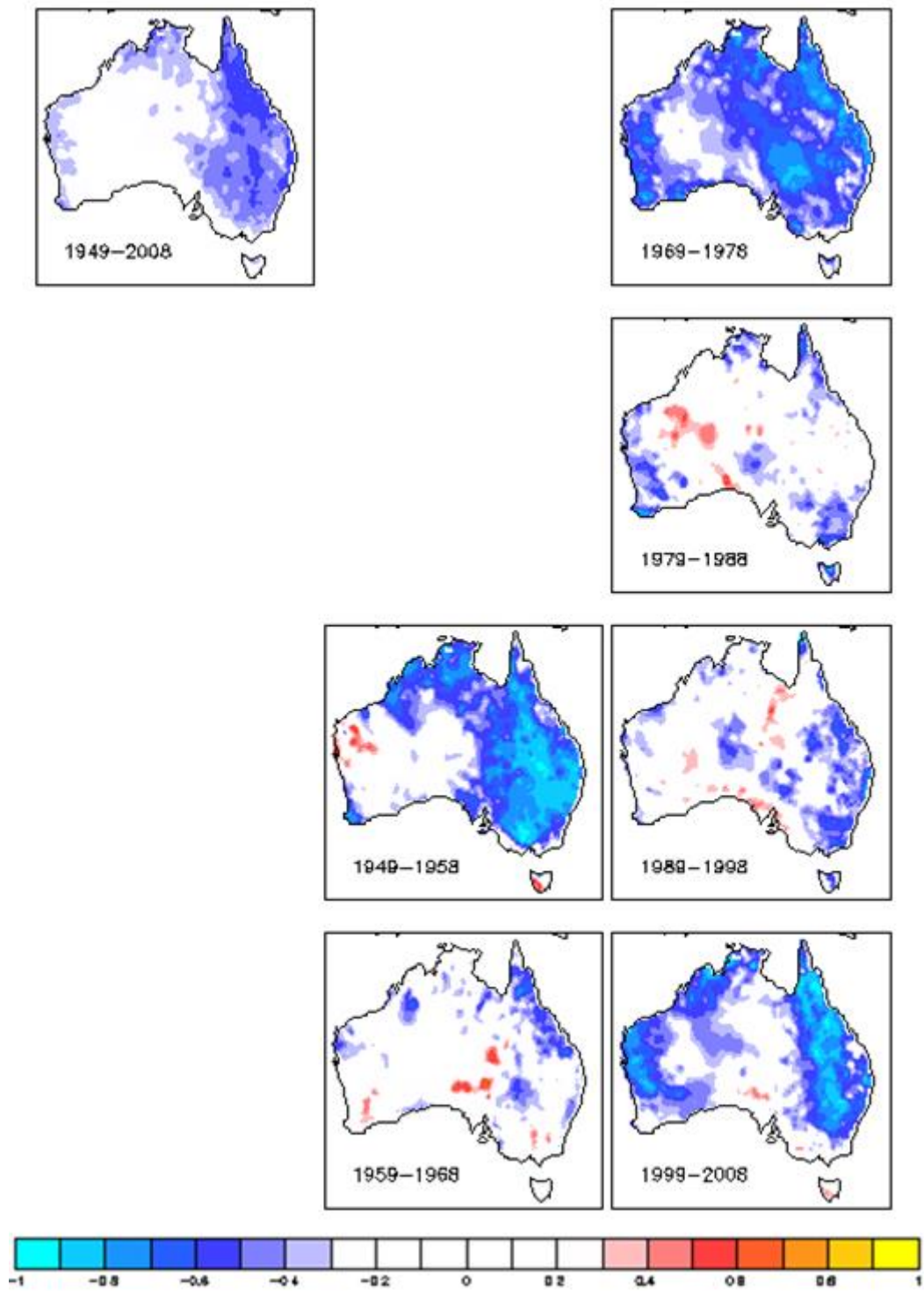


Figure 4.5: Correlation of DJF rainfall and the BEST index.

4.2.1.3 Cold Tongue Index (CTI)

The CTI exhibits an average negative correlation of -0.22 generally opposite to that of the SOI but differing markedly in the 1930s and 1940s where it swings positive. There is some evidence of a multidecadal oscillation and the pattern is more in keeping with the IPO (Figure 4.26). Population variance was low and showed poor decadal stability. Overall significant area coverage of correlation was 38% which was especially low in the 1980s and 1990s (approximately 15%). Temporally stability for a significant pattern is 73%. Compared to other indices correlation (Figure 4.6) does not track well to its index and whole year correlation (not shown) is slightly weaker.

4.2.1.4 Equatorial Southern Oscillation Index (EQSOI)

Figure 4.7 indicates that the EQSOI has a very similar correlation pattern to the SOI. In respect to its other attributes all were less robust apart from area coverage of 39%.

4.2.1.5 The Indian Ocean Dipole (IOD)

The IOD correlation maps (Figure 4.8) appeared unique in appearance not matching the pattern of any other index and all attributes fell mainly in the lower ranks especially the area of significant correlation at 13%. Population mean was very low at -0.013 and temporal variability ill-defined. Whole year correlation (not shown) was similar and showed a weakly-defined zero isoline of correlation running ESE – WNW dividing the continent in two.

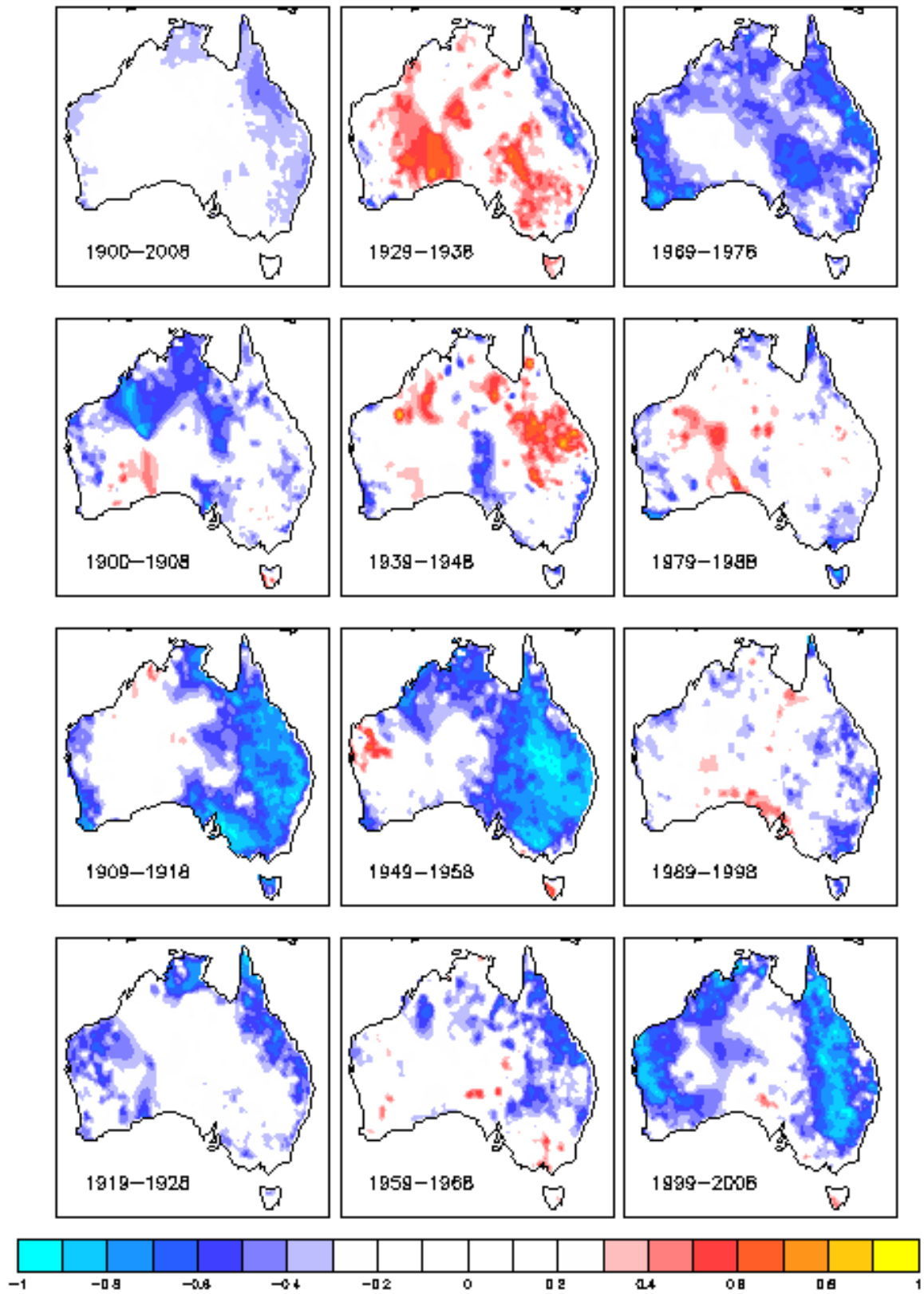


Figure 4.6: Correlation of DJF rainfall and the CTLI.

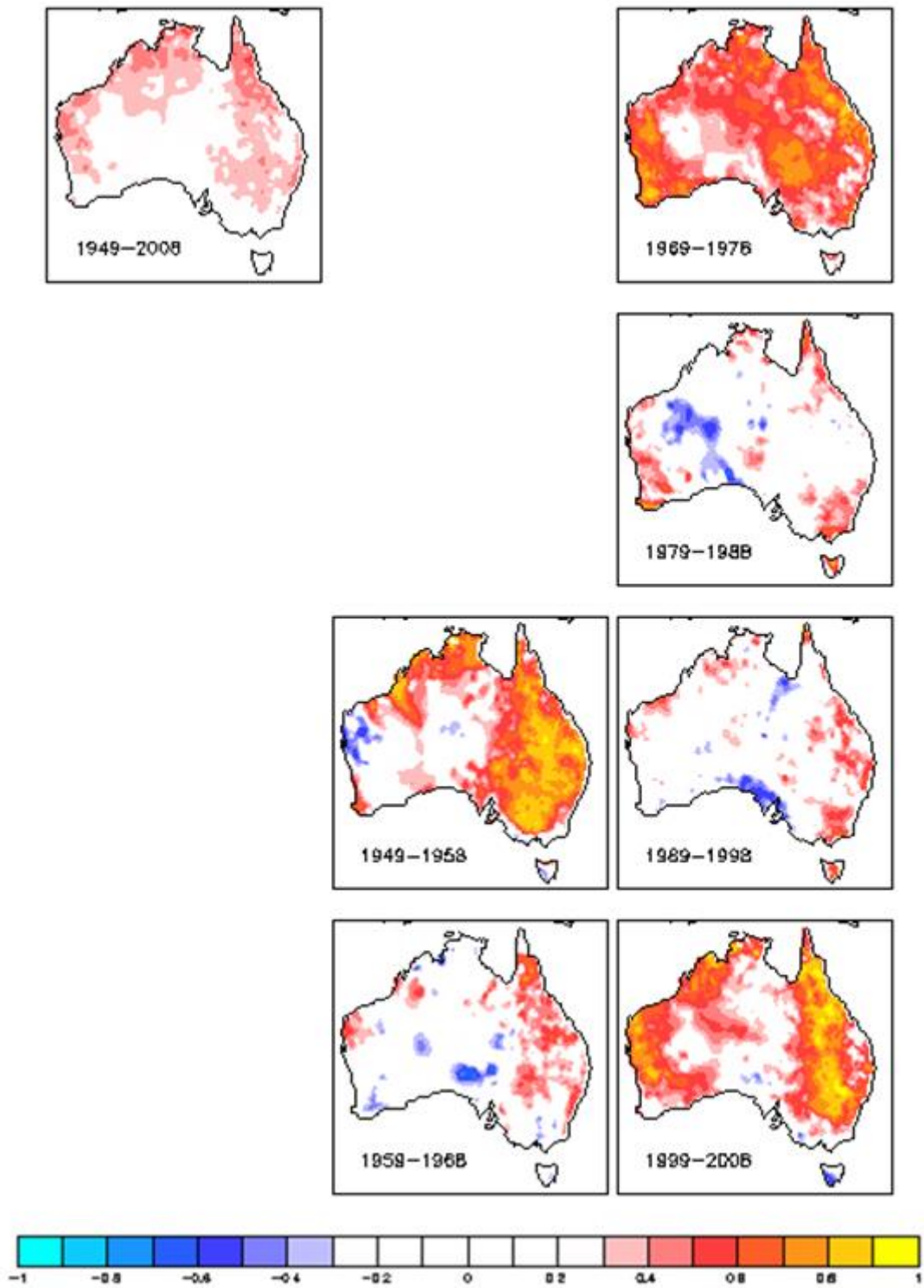


Figure 4.7: Correlation of DJF rainfall and the EQSOI.

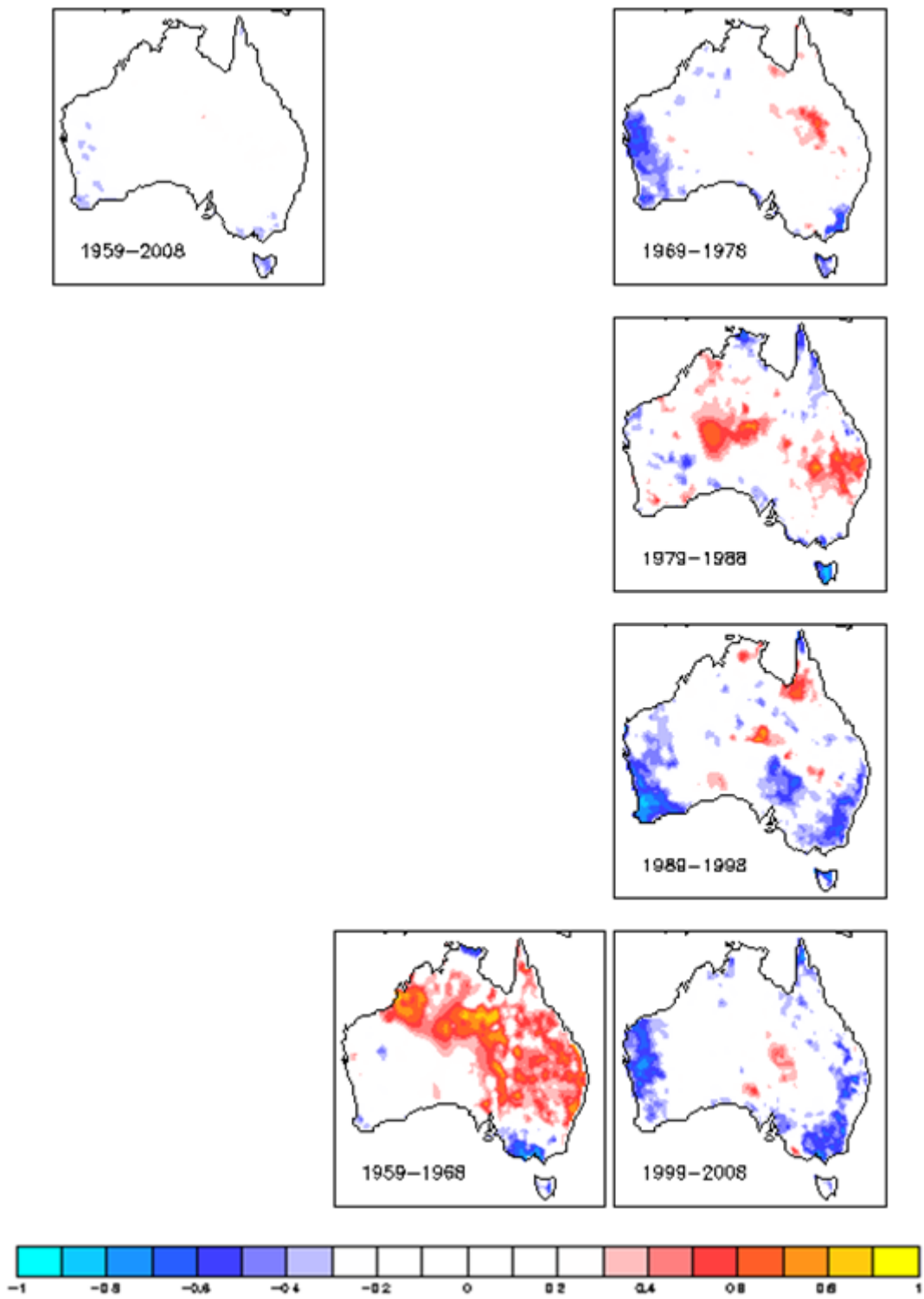


Figure 4.8: Correlation of DJF rainfall and the IOD.

4.2.1.6 El Niño Modoki (EMI)

Figure 4.9 shows the DJF correlation of the EMI and Australian rainfall with population mean correlation of -0.238. Average area coverage was 39% and temporal stability of the predominant pattern was 55%. At all year resolution (not shown) EMI correlation was broadly similar but positive correlation was weaker whilst negative correlation was stronger. The correlation tracks weakly to EMI and rainfall anomaly in Queensland. EMI correlation is similar to the EQSOI (opposite sign) after the millennium.

4.2.1.7 Multivariate El Niño Index (MEI)

Correlation for the MEI and Australian DJF rainfall is shown in Figure 4.10. Average correlation range for all decades was very similar to the Niño3.4 index which it marginally outperformed due to its higher population variance. The correlation pattern reverses in the 1980s and 1990s. For the whole year (not shown) correlation range was similar. MEI correlation is similar to BEST in the 1950s, the EMI in the 1970s and to the EQSOI in the 1960s and 1990s.

4.2.1.8 FIVEVAR

Correlation pattern for the FIVEVAR index (Figure 4.11) was generally similar to Niño3.4 having a mean value of -0.283 and achieving a maximum value in the first decade of this century. Mean area coverage was 37% whilst a significant correlation pattern existed for 50% of the time. Other indices having an overall correlation similar to FIVEVAR were the BEST, MEI and EQSOI. The EMI had a similar correlation from the 1970s onwards.

4.2.1.9 Trans Niño Index (TNI)

The TNI (Figure 4.12) as already alluded to in Chapter 2 as having a high correlation with the EMI (Ashok & Yamagata 2009) so that its pattern is almost its inverse (Figure 4.9). With respect to decadal consistency of variance TNI is the highest performer of any indices whose mean is ≈ 0.072 whilst average area coverage was 29%. Temporally the same significant pattern was achieved on 45% of the time. TNI correlation has an overall similar pattern to MEI and BEST in the 21st century.

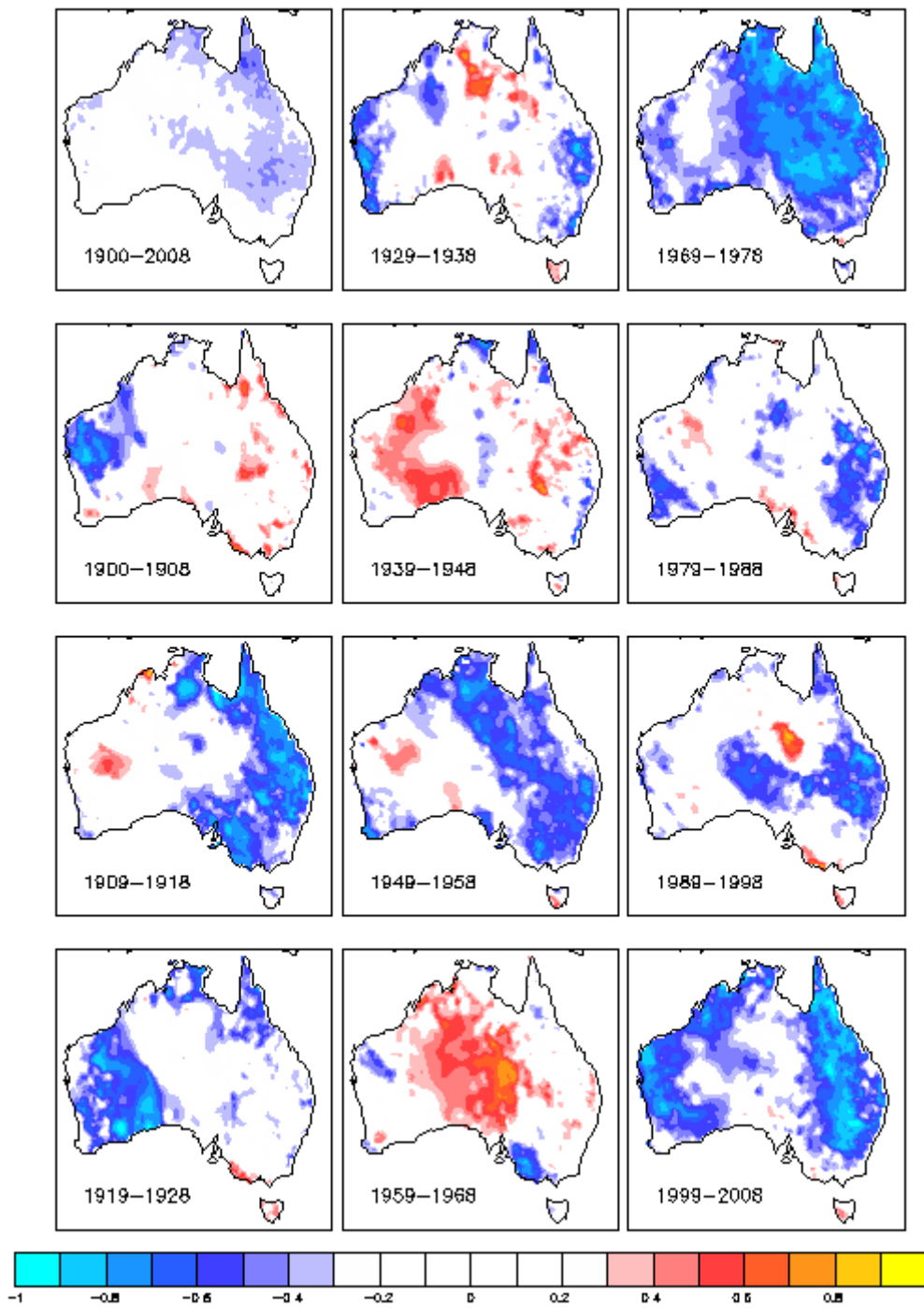


Figure 4.9: Correlation of DJF rainfall and the EMI.

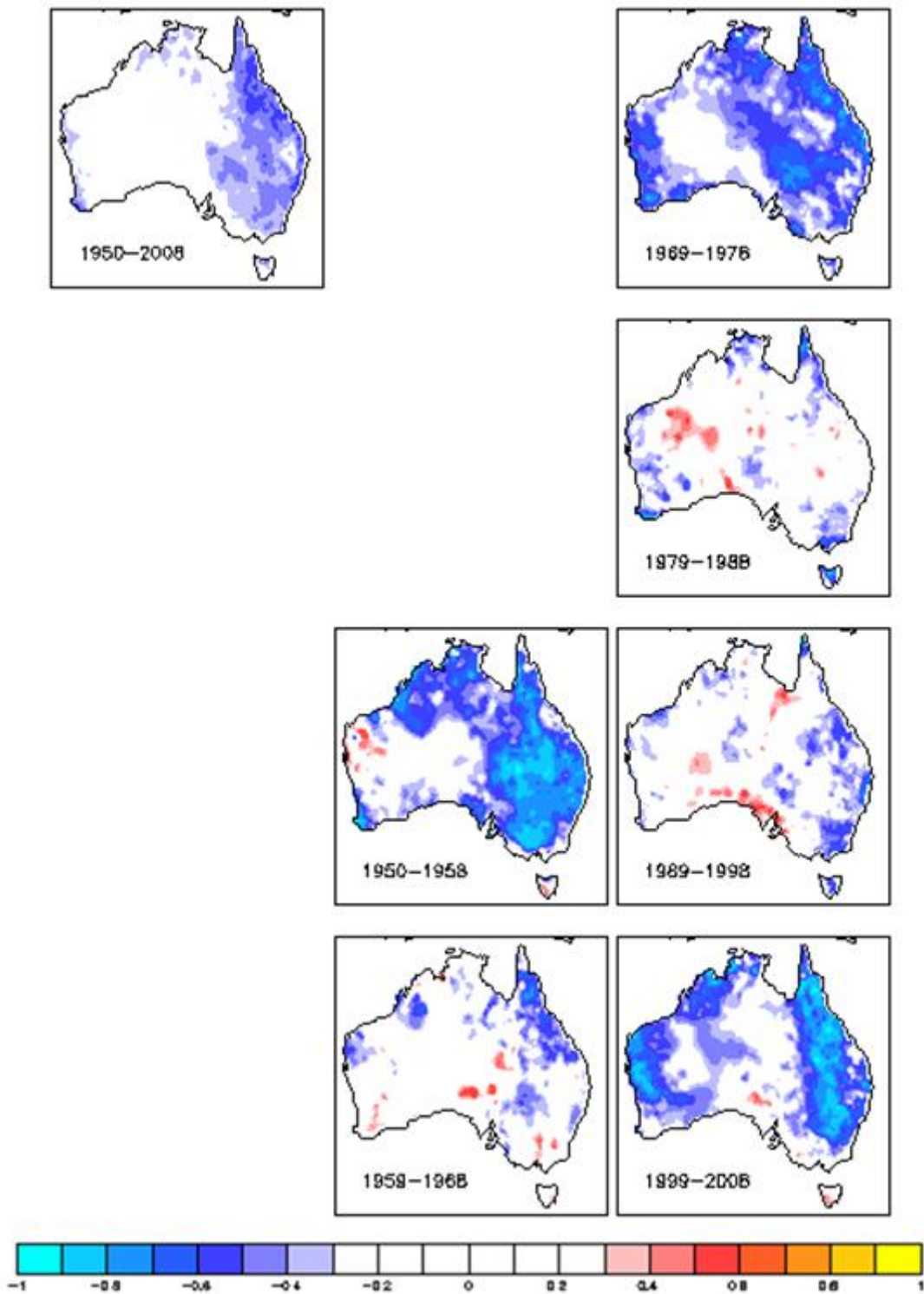


Figure 4.10: Correlation of DJF rainfall and the MEI.

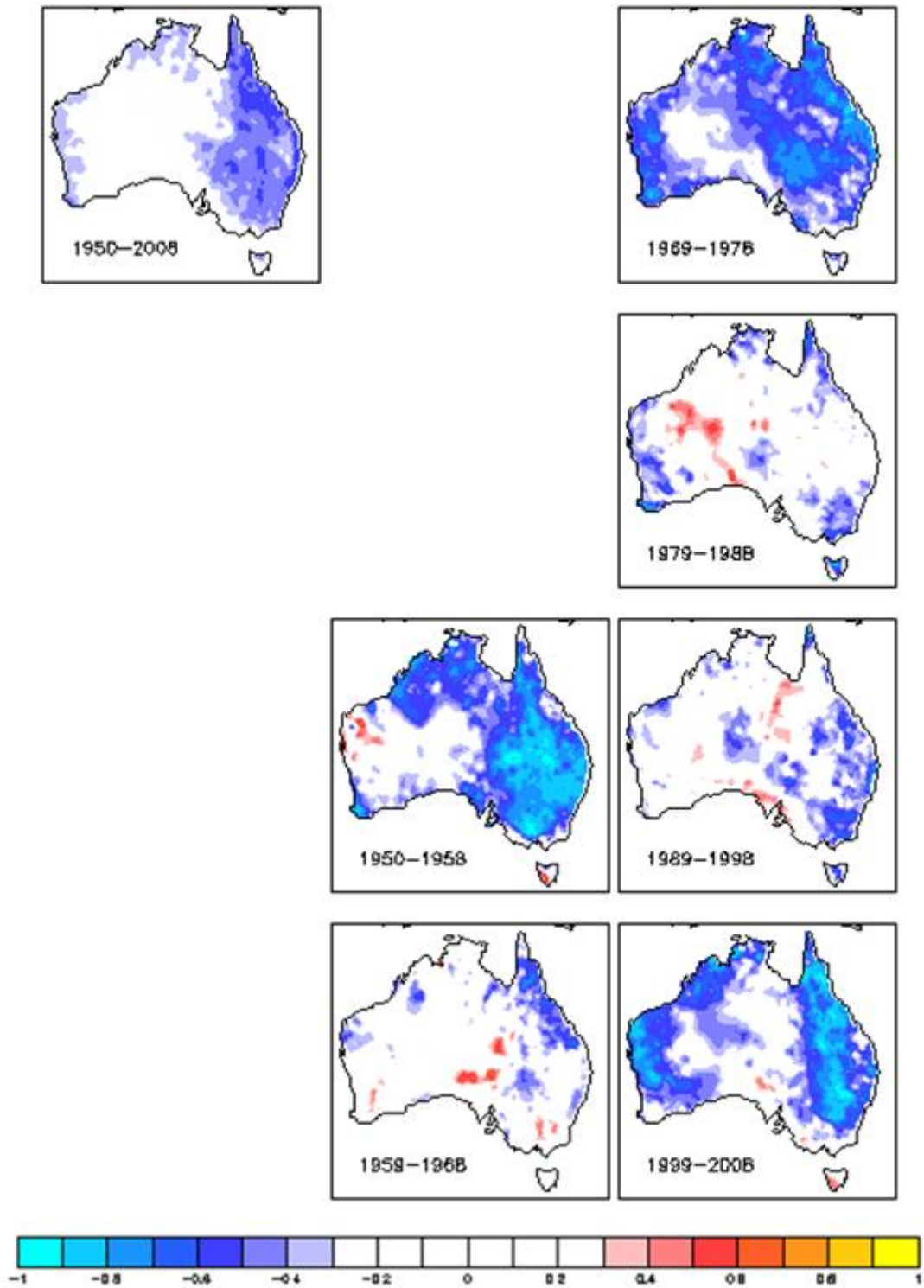


Figure 4.11: Correlation of DJF rainfall and the FIVEVAR index.

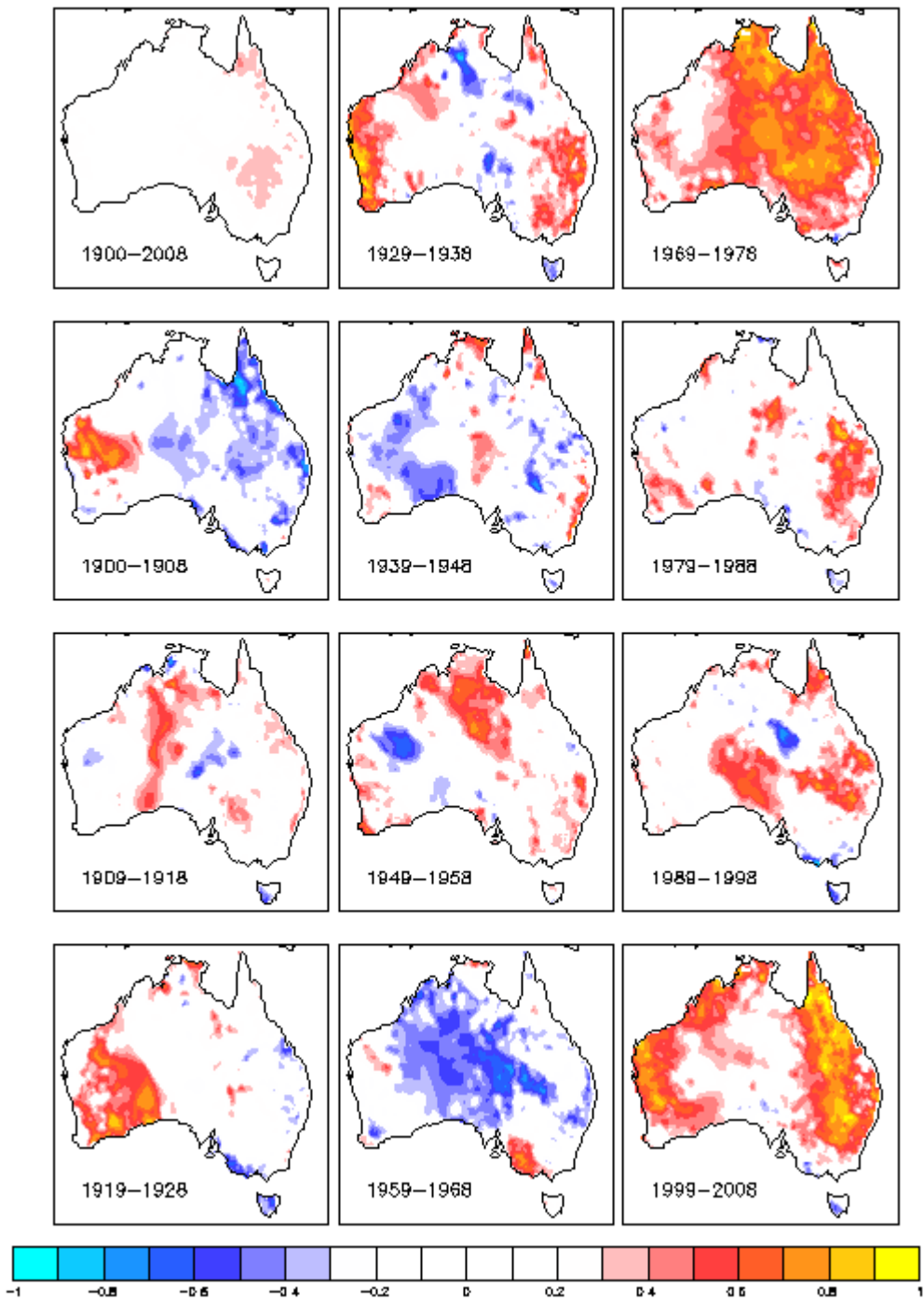


Figure 4.12: Correlation of (DJF) rainfall and the TNI.

4.2.1.10 Tropical Pacific Empirical Orthogonal Function (TPEOF)

For most decades the TPEOF correlation (Figure 4.13) moderately tracks the index (not shown) in SEQ and weakly for NE and NW Australia. Mean correlation was - 0.235 and significant area of correlation 31%. All year resolution (not shown) was of similar strength. TPEOF has an overall similar correlation pattern to the EQSOI, BEST, CTI, FIVEVAR and MEI.

4.2.1.11 Pacific Warm Pool (PWP)

PWP (Figure 4.14) had the highest population variance of any index as well as the highest mean decadal variance of 0.092. There is strong evidence of multidecadal variability and the correlation is similar to the IPO hence the low temporal variability (50%) and mean (-0.11). Mean significant area coverage of correlation was 28%. The correlation does not match the significant increase in SST that the region underwent during that period as indicated by its index (Figure 4.43). PWP has a mean correlation range of 1.6 increasing to 1.7 after the year 2000. The all year perspective (not shown) has a slightly weaker correlation and multidecadal variation.

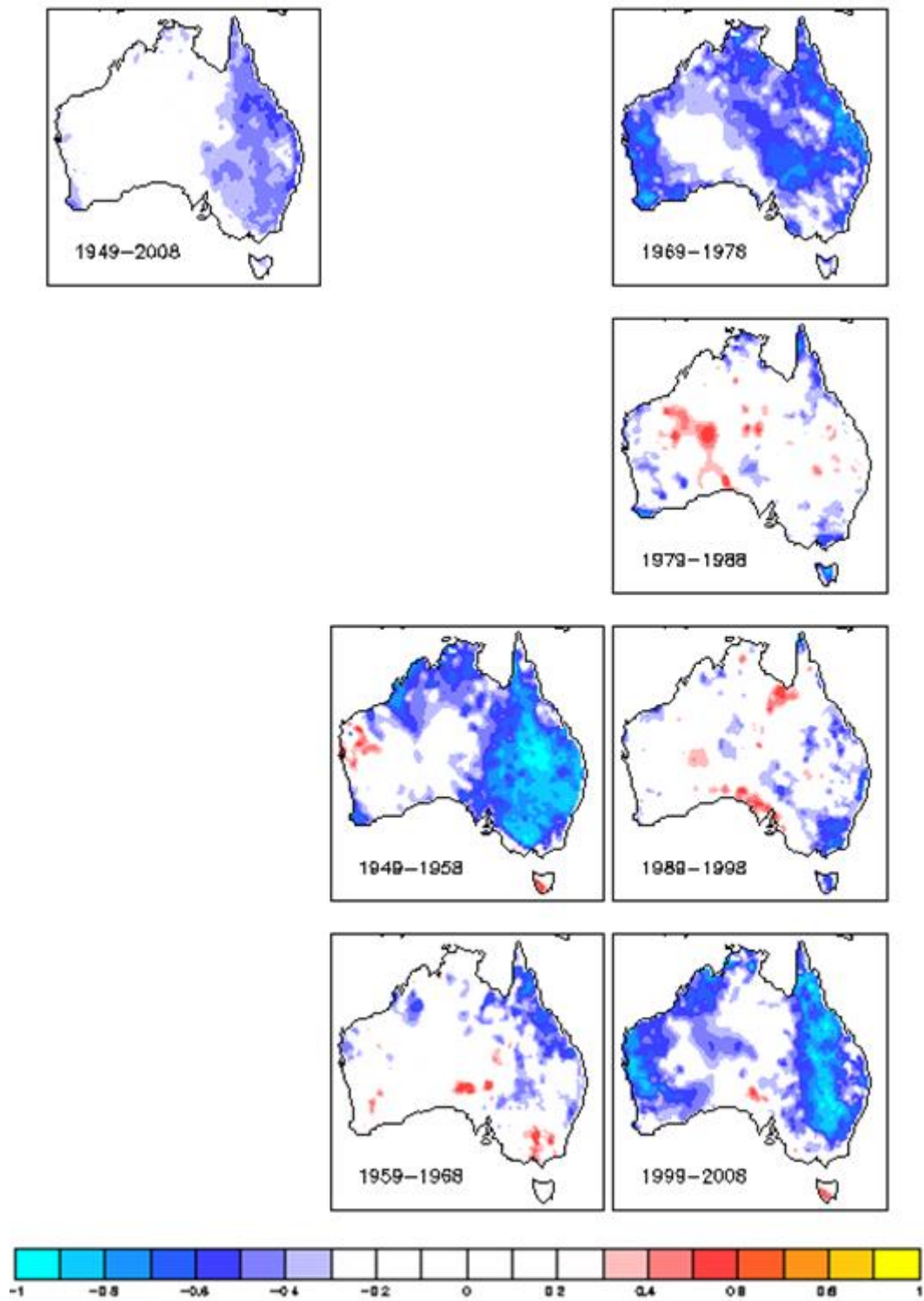


Figure 4.13: Correlation of DJF rainfall and the TPEOF index.

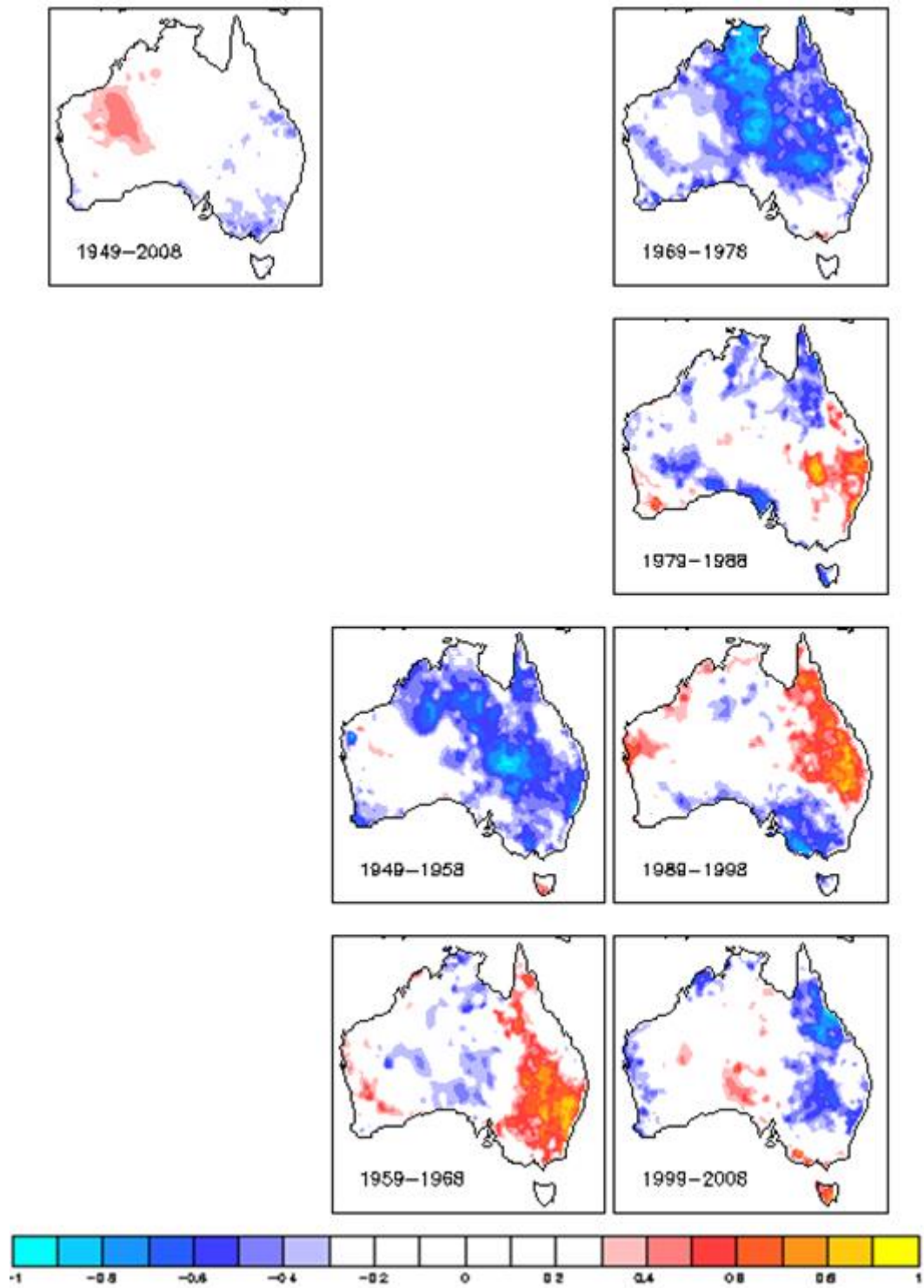


Figure 4.14: Correlation of DJF rainfall and the PWP index.

4.2.2 Summary of SOI Spectral Type Results

Results for indices with SOI spectral types as identified in Section 3.2.1 are shown in Table 4.1. Overall the BEST index achieved the highest ranking when all criteria were taken into consideration although there was very little to choose between the first five indices in this spectral group. PWP index (joint fourth rank) had extremely population variance and mean decadal variance.

Table 4.1: Performance (correlation) results of SOI type indices. The last four columns show the ranking of the index in terms of; strength, area coverage, consistency and overall performance of their major attribute (positive or negative) between decades.

Index	Population Variance		Decadal Variance		Correlation Area		Temporal Stability		Final Score	
	Global	Score	Global	Score	Global	Score	Global	Score	Total	Rank
BEST	0.0238	4	1.5	1	37	10	80	10	25	1
CTI	0.0132	1	2.2	4	38	10	73	8	23	3
EMI	0.0137	1	2.75	6	39	10	55	3	20	4
EQSOI	0.0151	2	2	3	39	10	50	2	17	9
FIVEVAR	0.0241	4	2	3	37	10	50	2	19	6
IOD	0.0196	3	1.67	1	13	2	60	5	11	11
MEI	0.0242	4	1.5	1	34	9	50	2	16	10
PWP	0.0517	10	1.5	1	28	7	50	2	20	4
SOI	0.0177	2	2.75	6	38	10	64	6	24	2
TNI	0.0112	1	3.67	10	29	7	45	1	19	6
TPEOF	0.0252	4	1.5	1	31	8	67	6	19	6

4.2.3 Niño Types

Here a reminder that white space on the correlation maps means that the correlation coefficient is less than approximately 0.36 so not significant at the 95% confidence level.

4.2.3.1 Niño3.4

Correlation results for the de facto El Niño index, the DJF Niño3.4 index (Figure 4.15) which is the five month running mean of SST anomaly in the Niño3.4 region are described here.

Oceanic Niño Index (ONI) is almost identical to Niño3.4 in every respect except that it is a three month running mean so is omitted from the analysis.

Average correlation range for Niño3.4 was found to be -0.247 and it achieved the best correlation of -0.48 in the 1970s. The lowest value of -0.01 was obtained in the 1940s and 1990s. Average area coverage was found to be 38% and the most significant temporal pattern existed for 45% of the time. Correlation is better on the east side of the continent for most decades.

For whole year resolution (Figure 4.16) the N – S correlation pattern is similar.

Niño3.4 correlations at decadal DJF resolution were slightly less than and approximately the obverse of the SOI except for the 1930s. Many other indices were also found to have a similar correlation pattern: BEST, CTI, EQSOI, FIVEVAR, MEI and TPEOF. The MEI showed similarities in the 1960s and 1970s whilst WWV_E and WWV_W were similar in the first half of the 20th century.

4.2.3.2 North Atlantic Oscillation (NAO)

NAO (Figure 4.17) data are available from 1950 and is the worst performing index in this category having an overall weakly positive correlation of 0.066 and had a maximum in the 21st century of 0.32. Mean area coverage was 12% and significant temporal pattern achieved on 50% of occasions. Annually NAO correlation (not shown) is similar to DJF but weaker.

In terms of an NAO/ENSO relationship there is slight evidence of NAO variability with respect to the 15 year lagged relationship with subtropical eastern Australian rainfall (SEAR) as postulated by Sun et al. (2014). NAO correlation (Figure 4.17) appears to lead SOI (Figure 4.4) correlation by 10 years for the 1950s, 1970s and 1980s. Similarly NAO leads Niño 3.4 (Figure 4.15) in the same decades if it is remembered that the signs are reversed. Currently such north Atlantic connections to southern hemisphere climate relationship are of great interest judging by the proliferation of such literature.

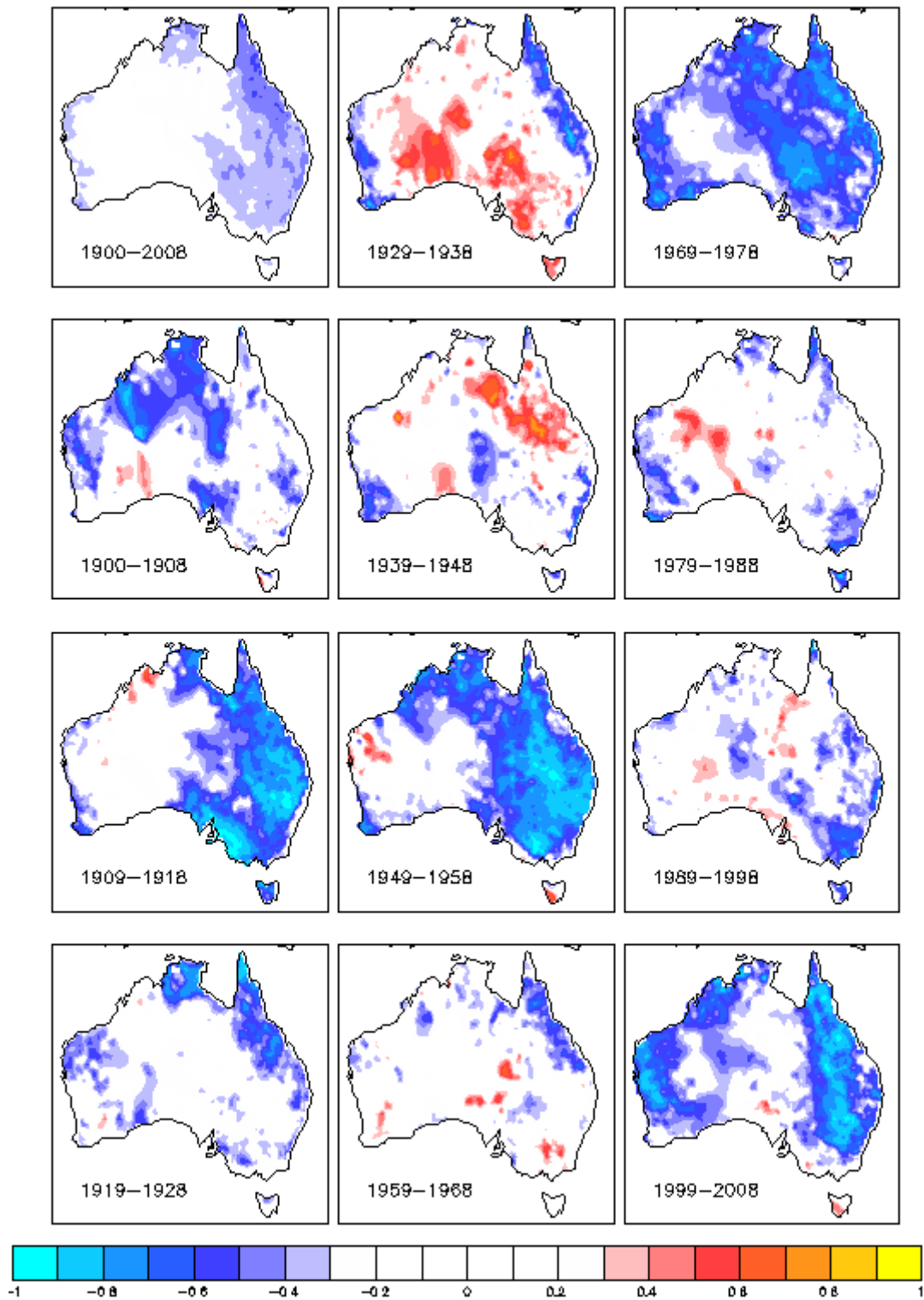


Figure 4.15: Correlation of DJF rainfall with the Niño3.4 index.

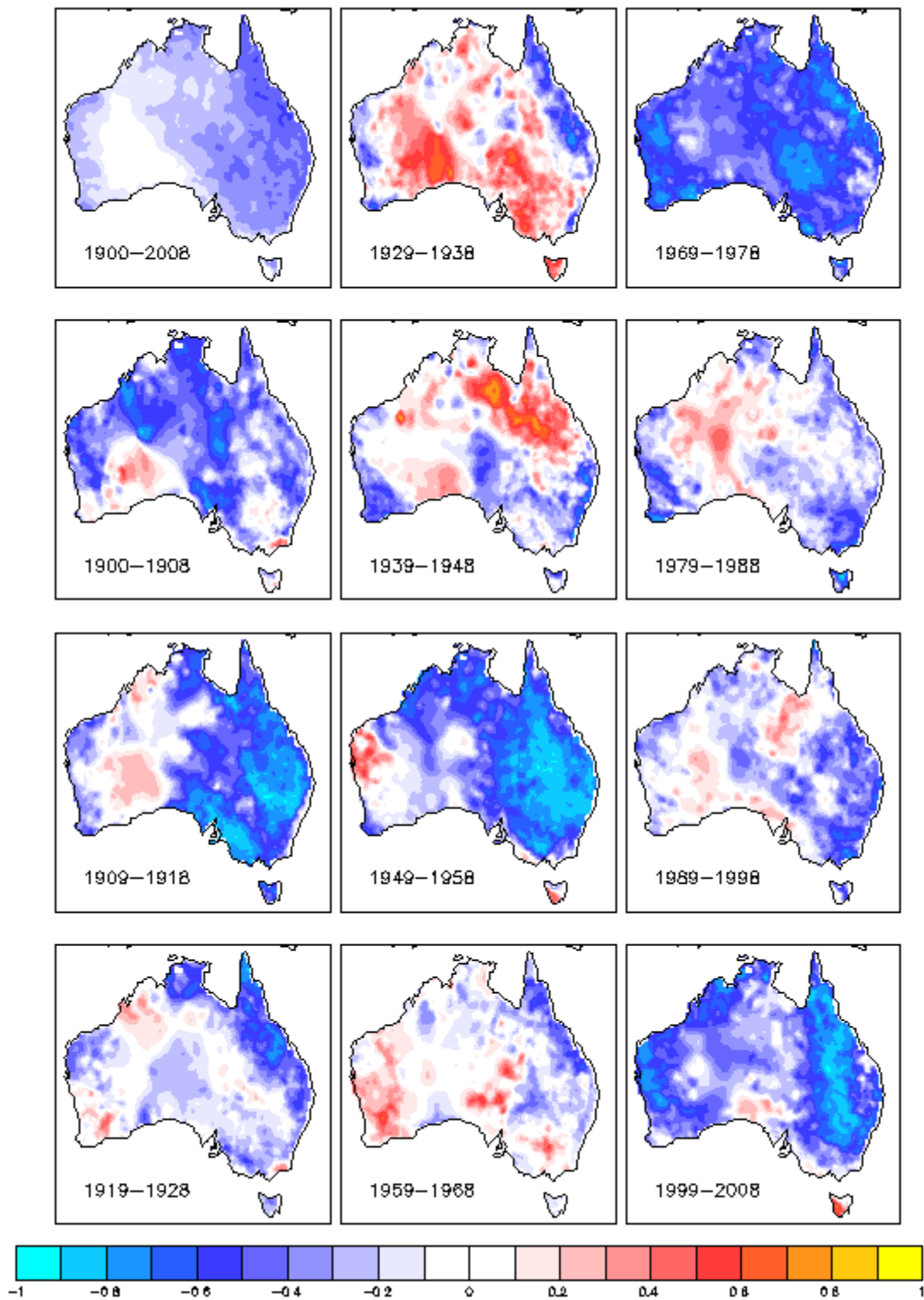


Figure 4.16: Correlation of rainfall with the Niño3.4 index.

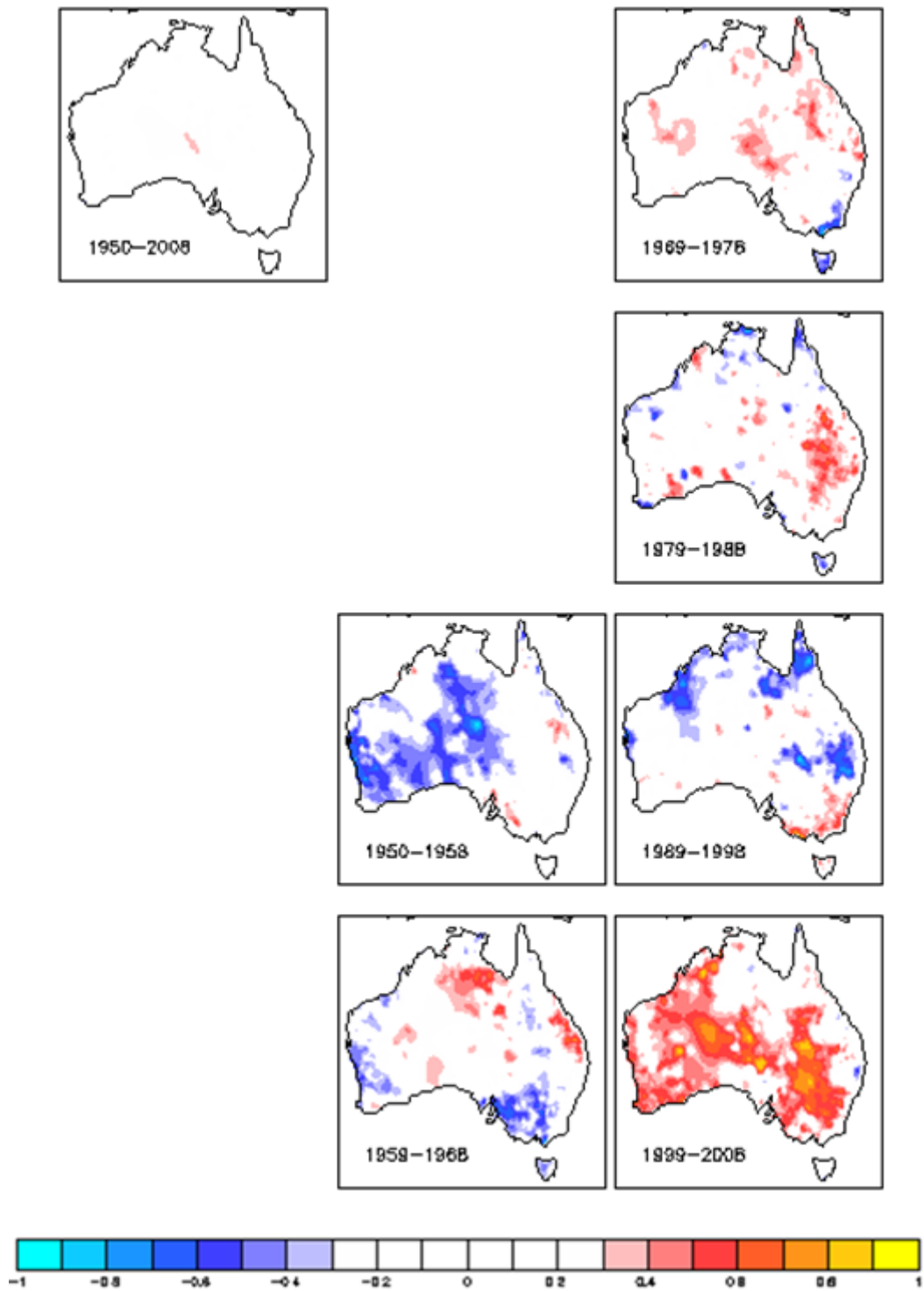


Figure 4.17: Correlation of DJF rainfall with NAO index.

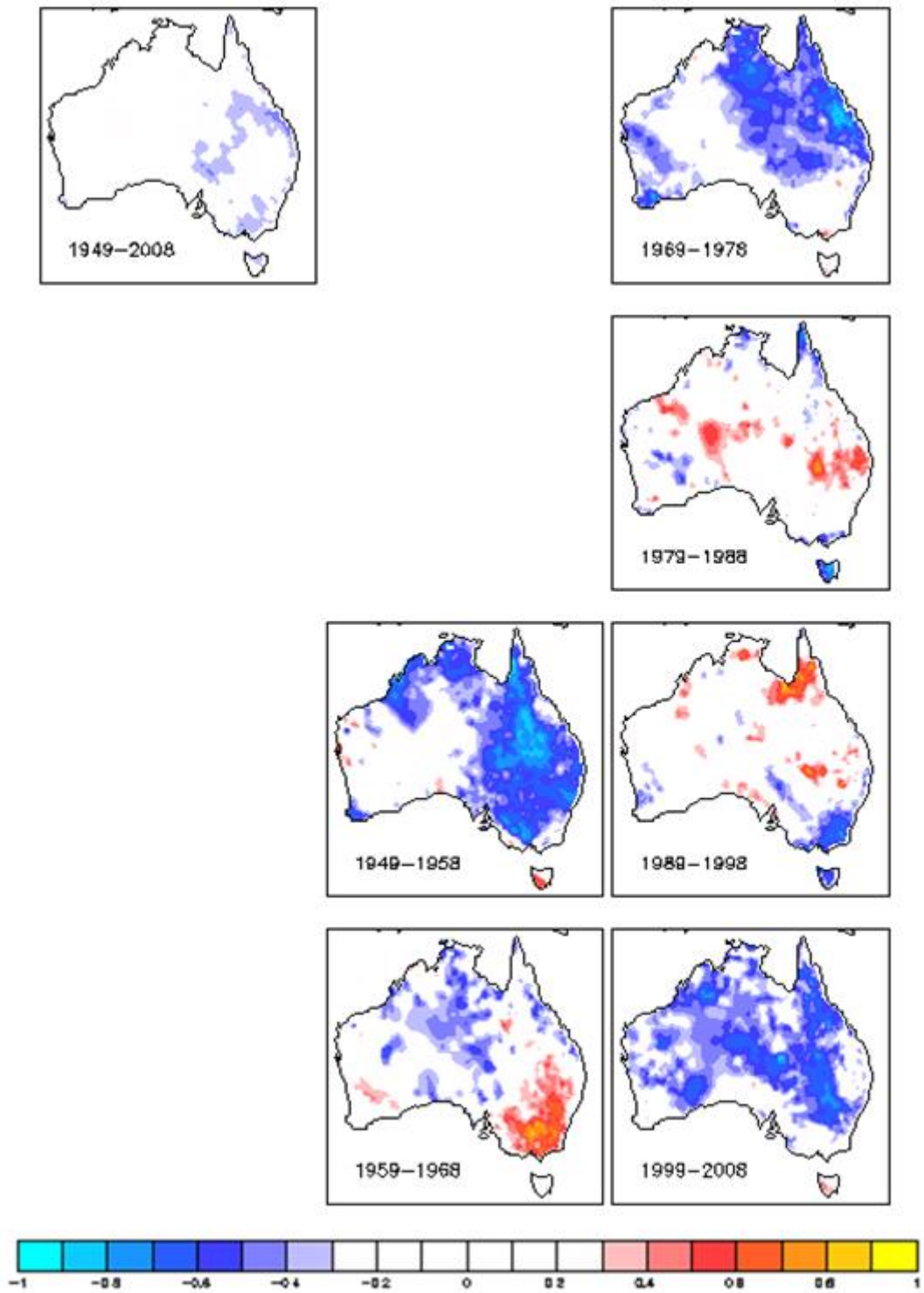


Figure 4.18: Correlation of DJF rainfall with WHWP index.

4.2.3.3 Western Hemisphere Warm Pool (WHWP)

WHWP (Figure 4.18) has a mean correlation of -0.121 and population variance of 0.0221. Mean area coverage is at 23% whilst temporal stability of the most significant pattern occurred on 50% of occasions and bears a similarity to the IPO, MEI, TPEOF and WWV_W. At the whole year resolution (not shown) correlation is similar but weaker.

4.2.3.4 Warm Water Volume (WWV)

Figure 4.20 show the decadal DJF correlation of Australian rainfall and the WWV index WWV had a poor population variance of 0.0214 and decadal variance of 0.024 but a high stability. The highest correlation mean value (0.35) occurred in the 1910s. Mean area coverage was 18% and the predominant correlation configuration occurred on 55% of occasions being subject to a multidecadal variability. At annual resolution (Figure 4.19) correlation was not as strong.

4.2.3.5 Warm Water Volume East (WWV_E)

Figure 4.22 shows the decadal DJF WWV_E correlation to Australian rainfall. Mean area coverage was 39% and temporal stability 64%. The WWV_E index has a low mean correlation of -0.223 and attained maximum value of -0.39 in the first decade of the 21st century. Annually WWV_E (Figure 4.21) exhibits a similar correlation pattern. The MEI had an overall similar pattern to WWV_E whilst FIVEVAR was similar except for the 1960s and 1970s.

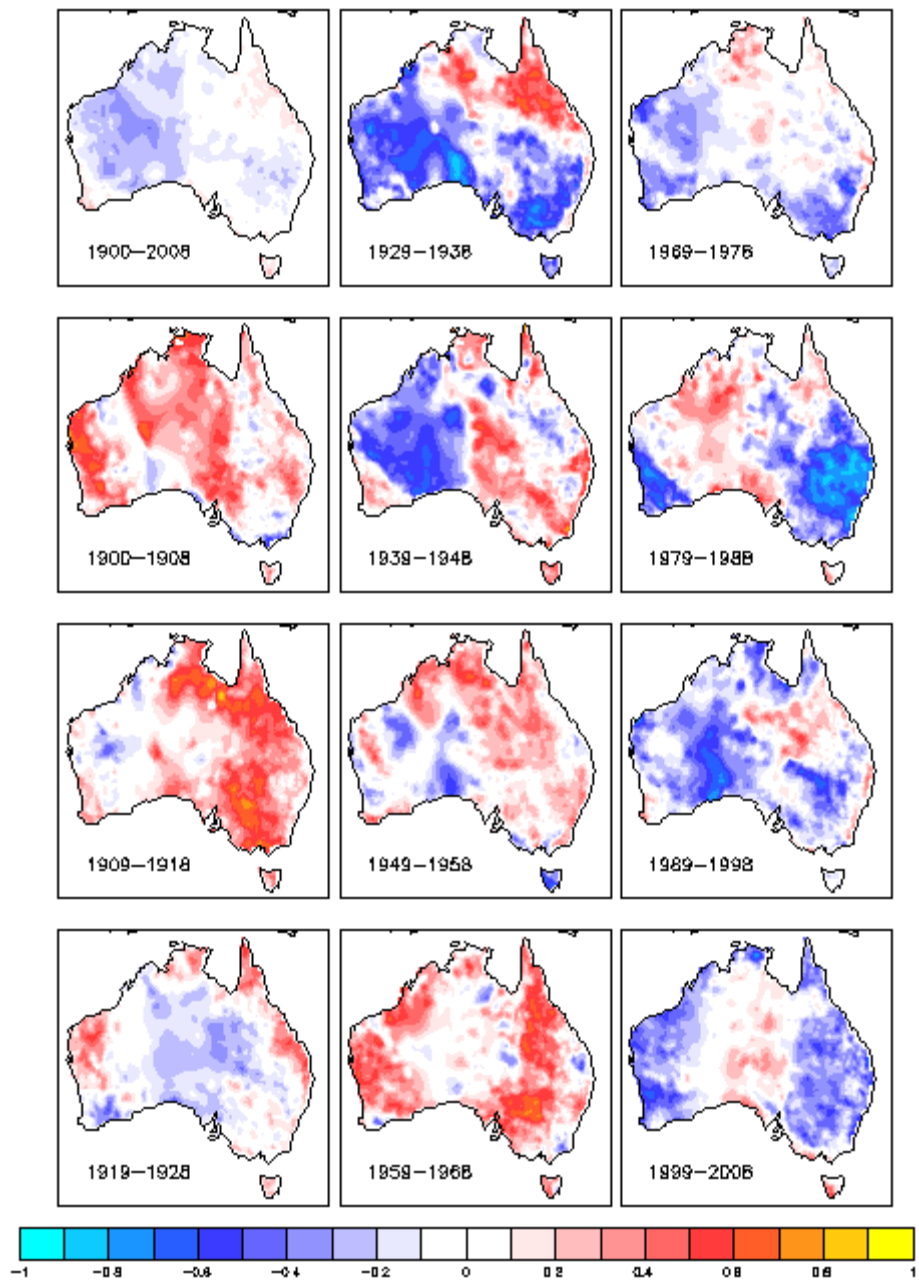


Figure 4.19: Correlation of rainfall and the WWV index.

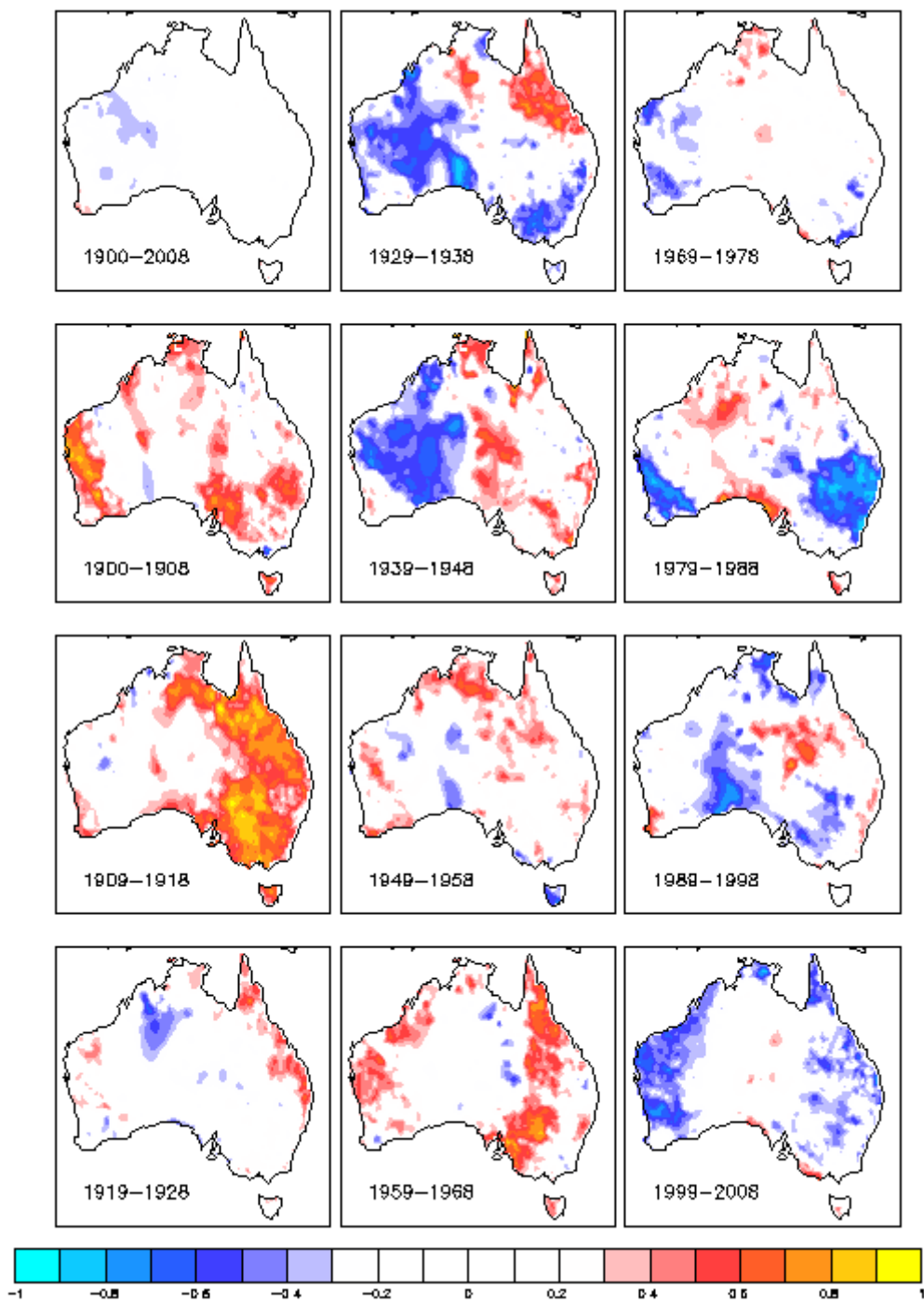


Figure 4.20: Correlation of DJF rainfall and the WWV index.

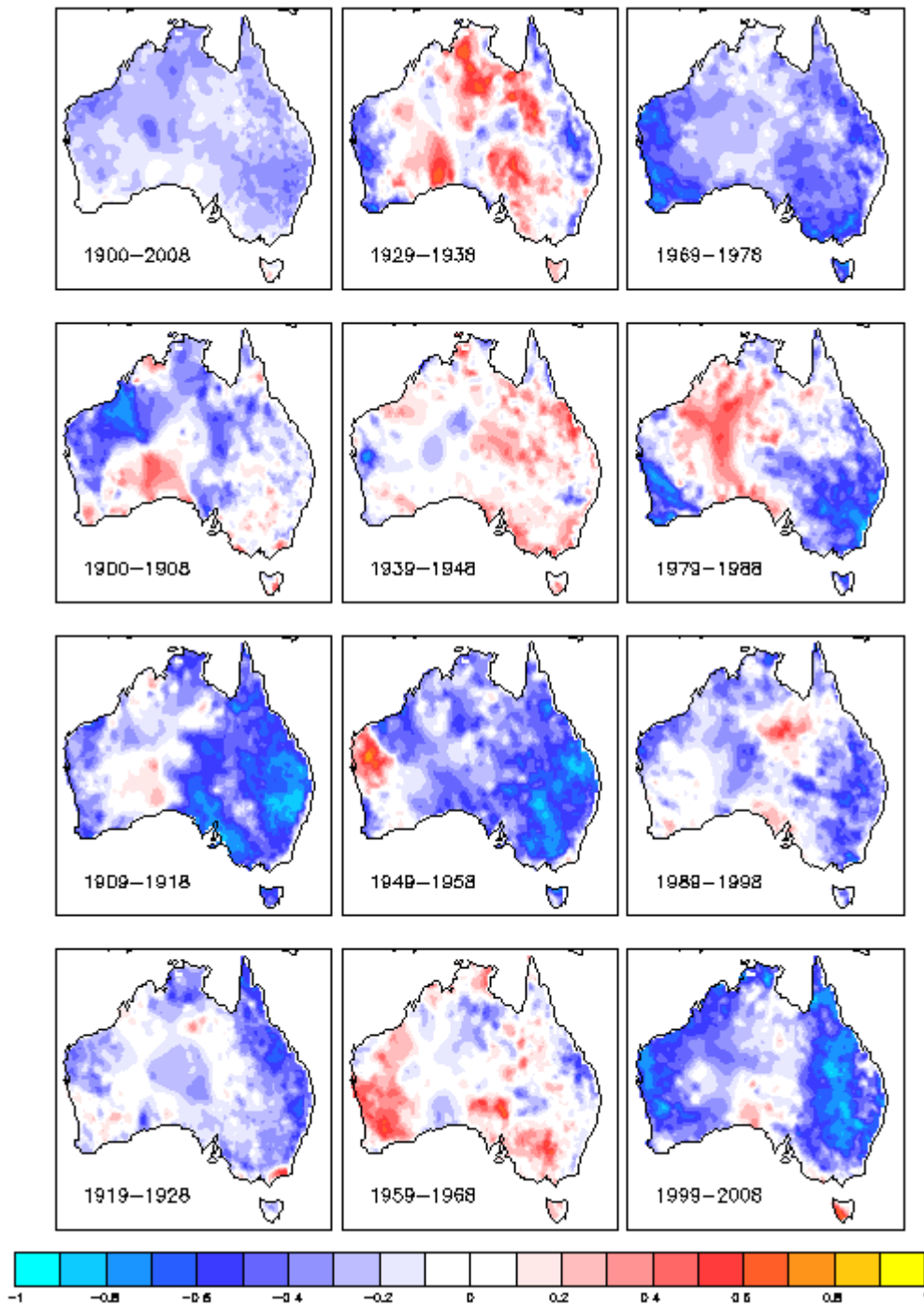


Figure 4.21: Correlation of rainfall and the WWV_E index.

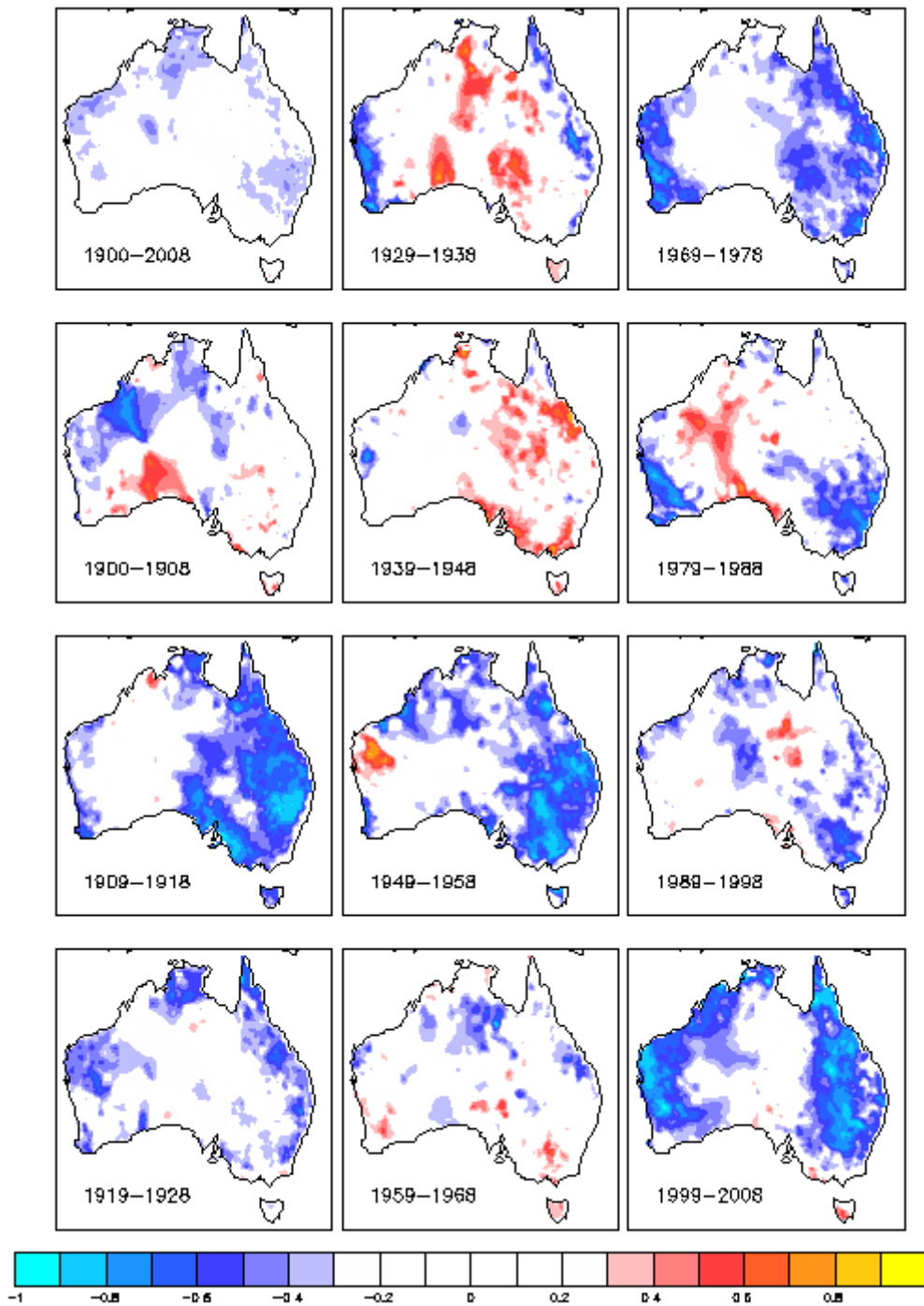


Figure 4.22: Correlation of DJF rainfall and the WWV_E index.

4.2.3.6 Warm Water Volume West (WWV_W)

Figure 4.24 show the DJF WWV_W index correlation to Australian rainfall. WWV_W has a mean correlation of 0.103. Area coverage was found to be 29% with a temporal stability at 82%. This configuration for east Australia was stable but reversed during the 1980s to recover by the next decade. As with the other two WWV indices WWV_W correlation (Figure 4.23) is more consistent at annual resolution but not quite as weakened as the former at only approximately minus 0.1. Correlation tracks the WWV_W index to a medium level in most regions of Australia, weaker in NE Australia and not at all in the S coastal region. The Niño3.4 was found to have an overall similar pattern for the first seven decades. IPO was similar for many decades and BEST had similar pattern in the 1960s and 1970s.

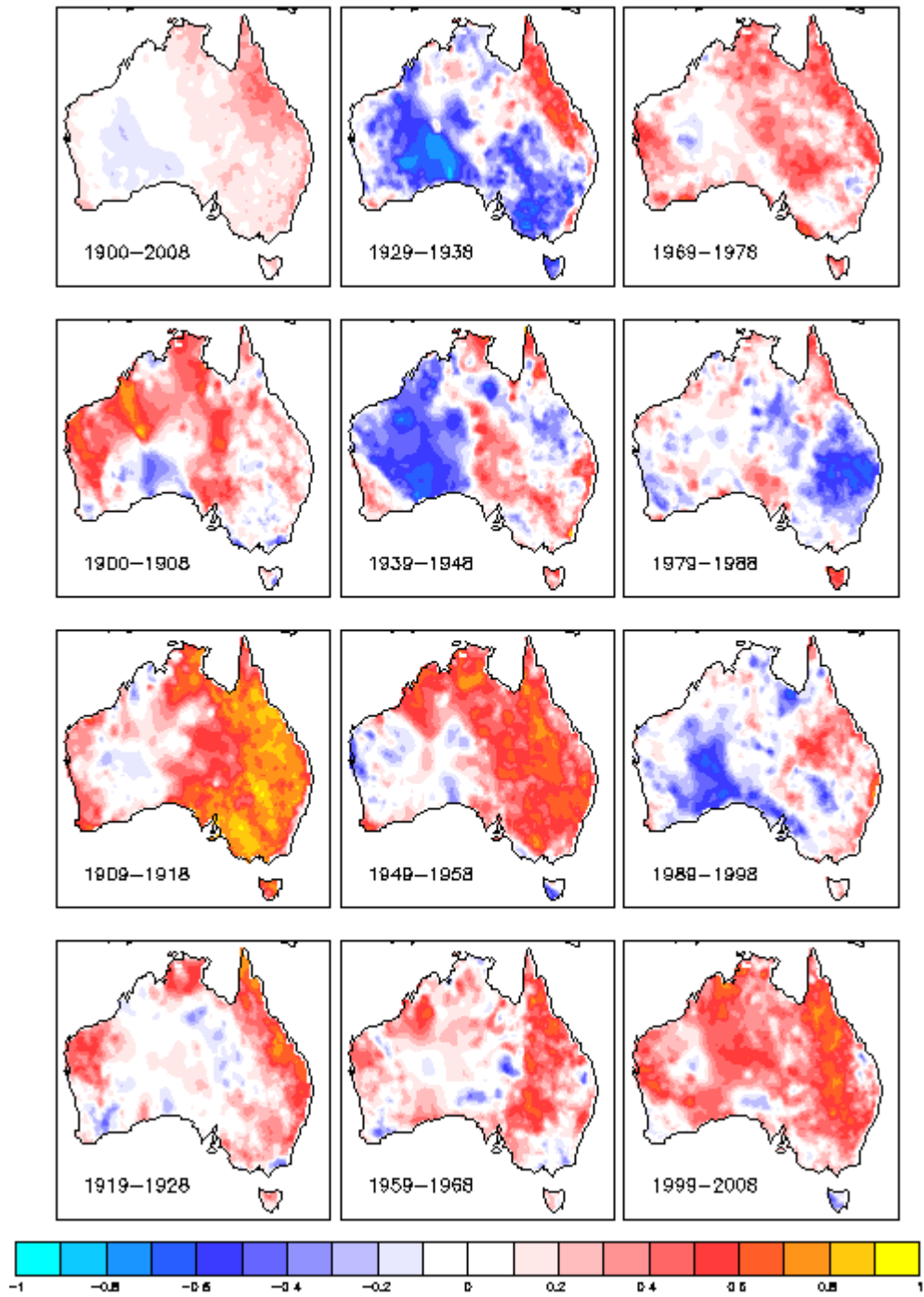


Figure 4.23: Correlation of rainfall and the WWV_W index.

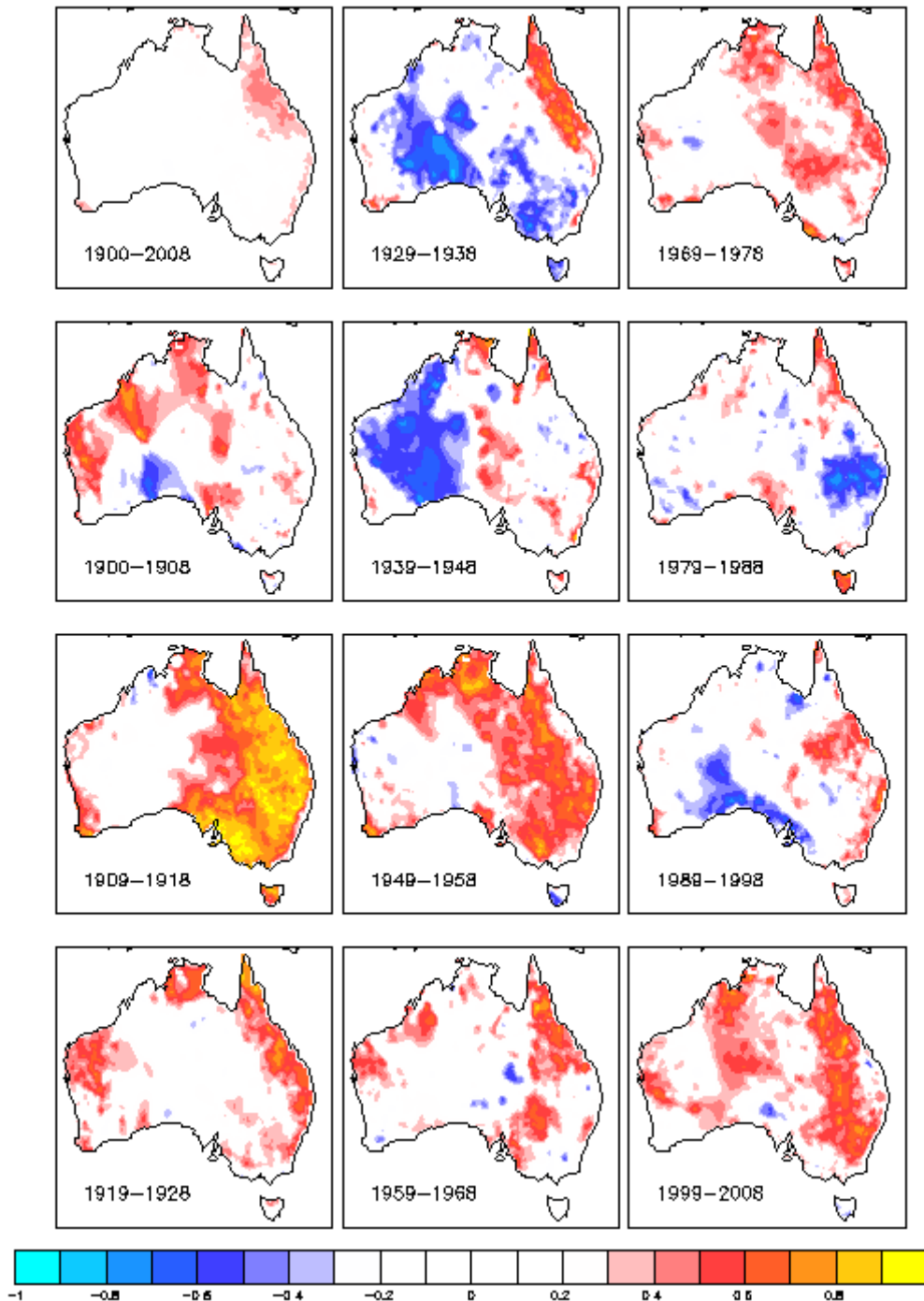


Figure 4.24: Correlation of Australian summer (DJF) rainfall and the WWV_W index 1900 – 2008.

4.2.4 Summary of Niño Spectral Type Results

The analysis for the three indices are summarised in Table 4.2. WHWP pattern is very similar to the northern Hemisphere NAO pattern for the first three decades and in terms of pure correlation range scores very favourably. Although having a small correlation range (0.48) Niño3.4 has the best temporal stability.

Table 4.2: Performance (correlation) results of Niño type indices for the whole period. The last four columns show the ranking of the index in terms of; strength, area coverage, temporal stability and overall performance of their major attribute between decades.

Index	Population Variance		Decadal Variance		Correlation Area		Temporal Stability		Final Score	
	Global	Score	Global	Score	Global	Score	Global	Score	Total	Rank
NAO	0.0115	1	2	3	38	2	50	2	8	6
Niño3.4	0.0187	2	1.83	2	38	10	45	1	15	4
WHWP	0.0221	3	2	3	23	5	50	2	13	5
WWV	0.0214	3	2.75	6	24	6	55	3	18	3
WWV_E	0.0130	1	2.2	4	39	10	64	5	20	2
WWV_W	0.0216	3	2.2	4	29	7	82	10	24	1

4.2.5 Mixture Types

4.2.5.1 Pacific Decadal Oscillation (PDO)

PDO (Figure 4.25) exhibits a mean correlation range of -0.154 and achieves -0.445 in the 1910s. Mean significant regional coverage was 29% and temporal stability of the most significant pattern was at 45%. From an annual perspective (not shown) the correlation patterns are similar but weaker.

4.2.5.2 Inter Decadal Pacific Oscillation (IPO)

IPO as shown in Figure 4.26 exhibiting a mean correlation range of -0.23 achieving a maximum of 0.47 in the 1940s. Mean area coverage was 35% and temporal stability of a significant pattern occurred on 55% of occasions. Annually IPO correlation (not shown) is similar but weaker and shows a reversed pattern in the 1960s and 1990s. Overall the IPO pattern is very similar to the PDO except in the 1980s. The BESTindex shows a similar pattern to the IPO.

4.2.6 Summary of Mixture Spectral Types

PDO and IPO have been regarded as to all intents and purposes regarded as very similar to each other (Cai & van Rensch 2012) for they represent equivalent description of the same

event even though PDO is a meridional oscillation and IPO is zonal oscillation. This tends to be borne out by the results comparison in Table 4.3.

Table 4.3: Performance (correlation) results of mixture type indices. The last four columns show the ranking of the index in terms of; strength, area coverage, temporal stability and overall performance of their major attribute between decades.

Index	Population Variance		Decadal Variance		Correlation Area		Temporal Stability		Final Score	
	Global	Score	Global	Score	Global	Score	Global	Score	Total	Rank
IPO	0.0265	4	1.83	2	35	9	55	3	18	1
PDO	0.0143	1	2.2	4	29	7	45	1	13	2

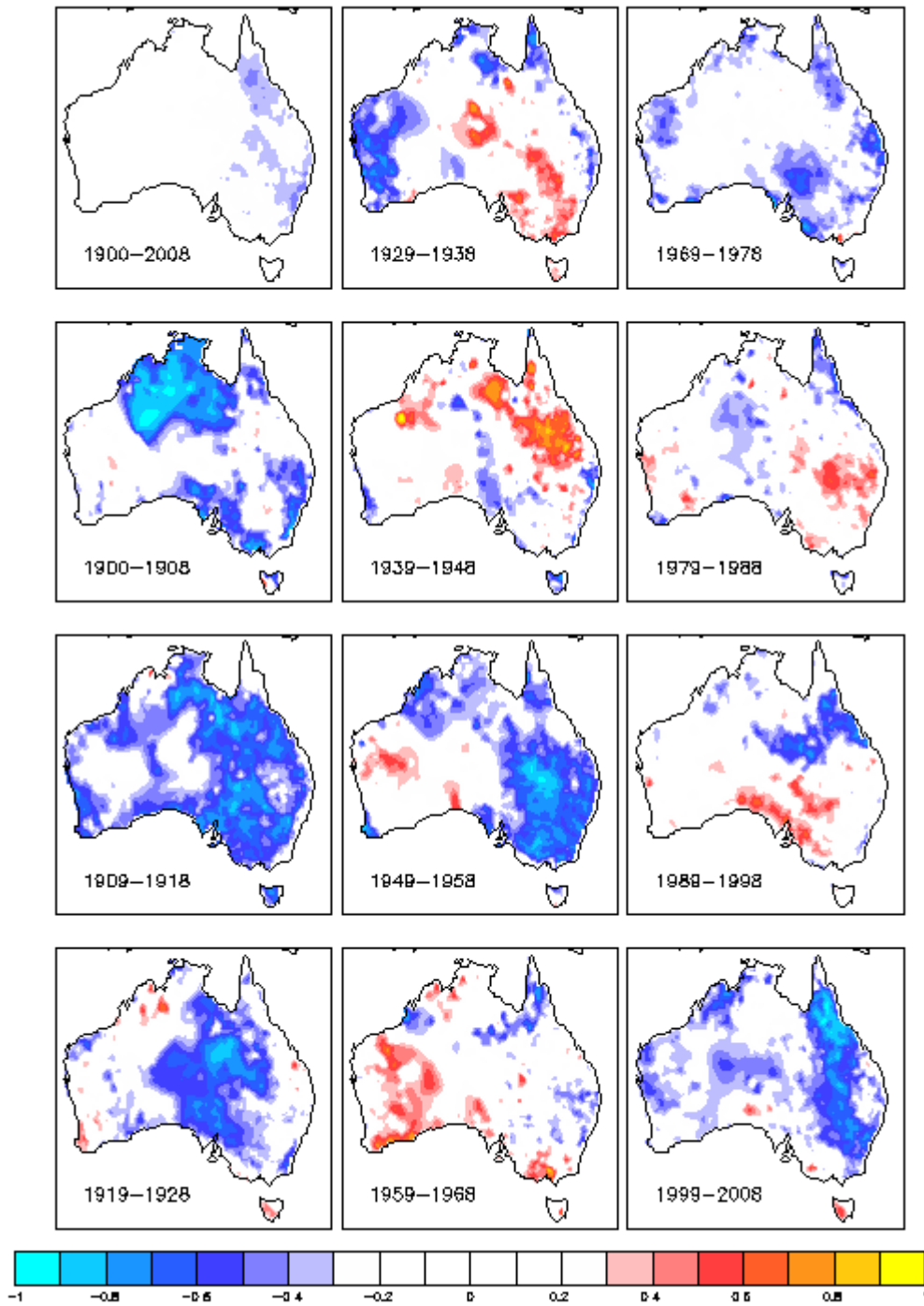


Figure 4.25: Correlation of DJF rainfall and the PDO index.

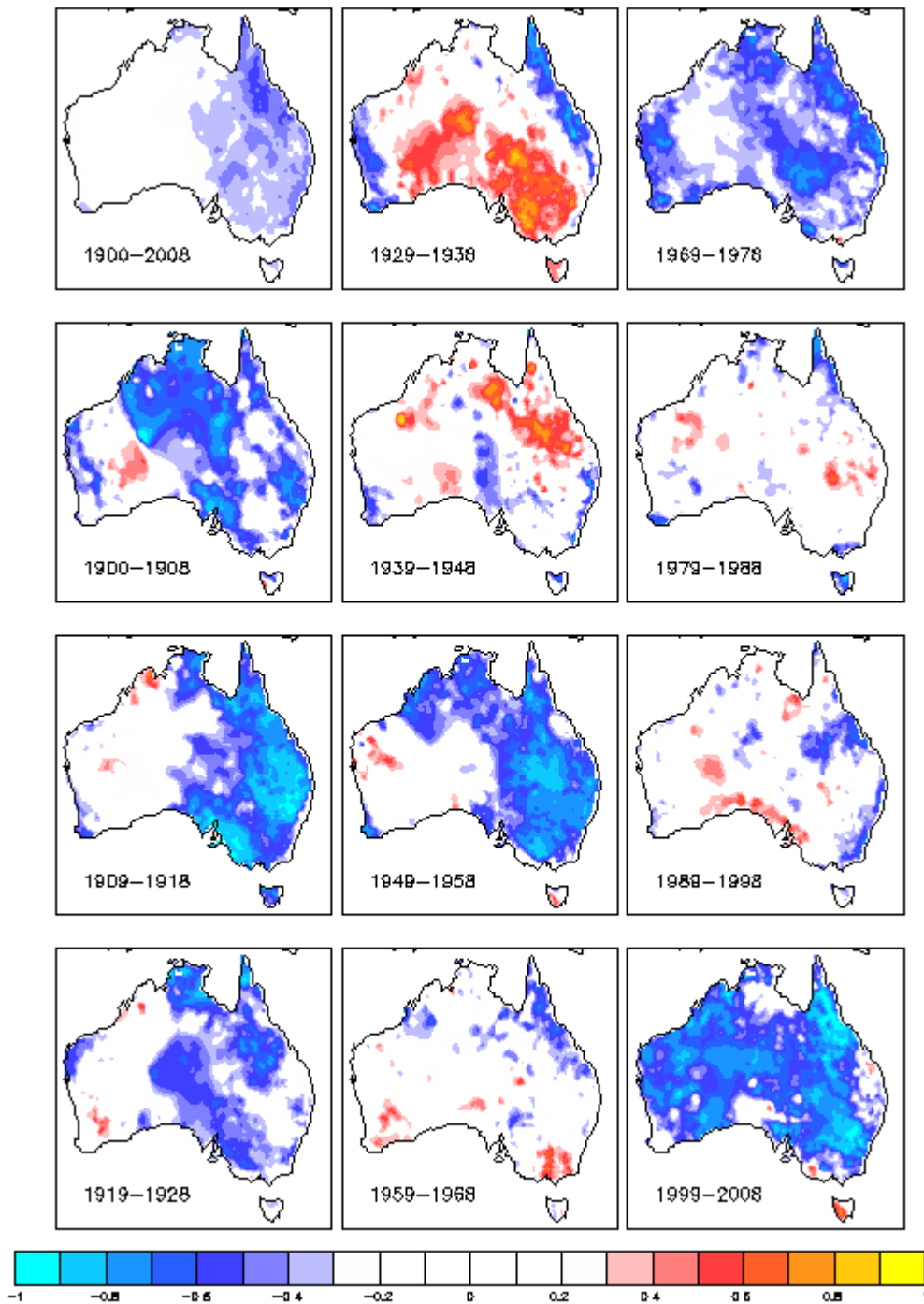


Figure 4.26: Correlation of DJF rainfall and the IPO index.

4.2.7 Meridional Types

4.2.7.1 Northern Oscillation Index (NOI)

The NOI (Figure 4.27) has a mean correlation range of 0.15 increasing to 0.7 in the 1960s and decreasing to 0.4 for the 1980s and 2000s. There is evidence of an isoline of zero

correlation running E – W in the southern part of the continent with positive correlation on the equatorial side for most decades. This configuration reverses for the 1980s and 1990s resulting in a temporal stability of 67%. NOI has a similar pattern for the whole year (not shown) as it does for DJF. The correlation pattern for MEI was found to be similar in the 1960s and 1990s.

4.2.7.2 Southern Annular Mode (SAM)

The correlation pattern of the SAM index otherwise known as the Antarctic Oscillation (Figure 4.28) is unique compared to all other indices considered and has a mean correlation 0.217 which has its highest value (0.32) in the 1970s. Mean area coverage was found to be 35% and temporal stability at 60%. Other attributes were not noteworthy. The configuration for annual resolution (not shown) was found to be similar.

4.2.7.3 Arctic Oscillation Index (AOI)

The AOI (Figure 4.29) was found to have a mean correlation 0.11 attaining a maximum of 0.29 during the 1970s. Mean area coverage was 36% and temporal stability had the same predominant pattern on 67% of occasions. At whole year resolution AOI correlation (not shown) was similar but slightly weaker than DJF. The SAM the Southern Hemisphere counterpart of AOI has a very similar configuration for the 1980s and 1990s. The NAO which is also basically the same index also bears a resemblance throughout the range.

4.2.7.4 Indo Pacific Warm Pool (IPWP)

The IPWP (Figure 4.30) has the highest mean correlation range of any index tested achieving 0.087 an attribute that also remained moderately stable. Mean area coverage was 21% and temporal stability of the most significant correlation pattern was 64%.

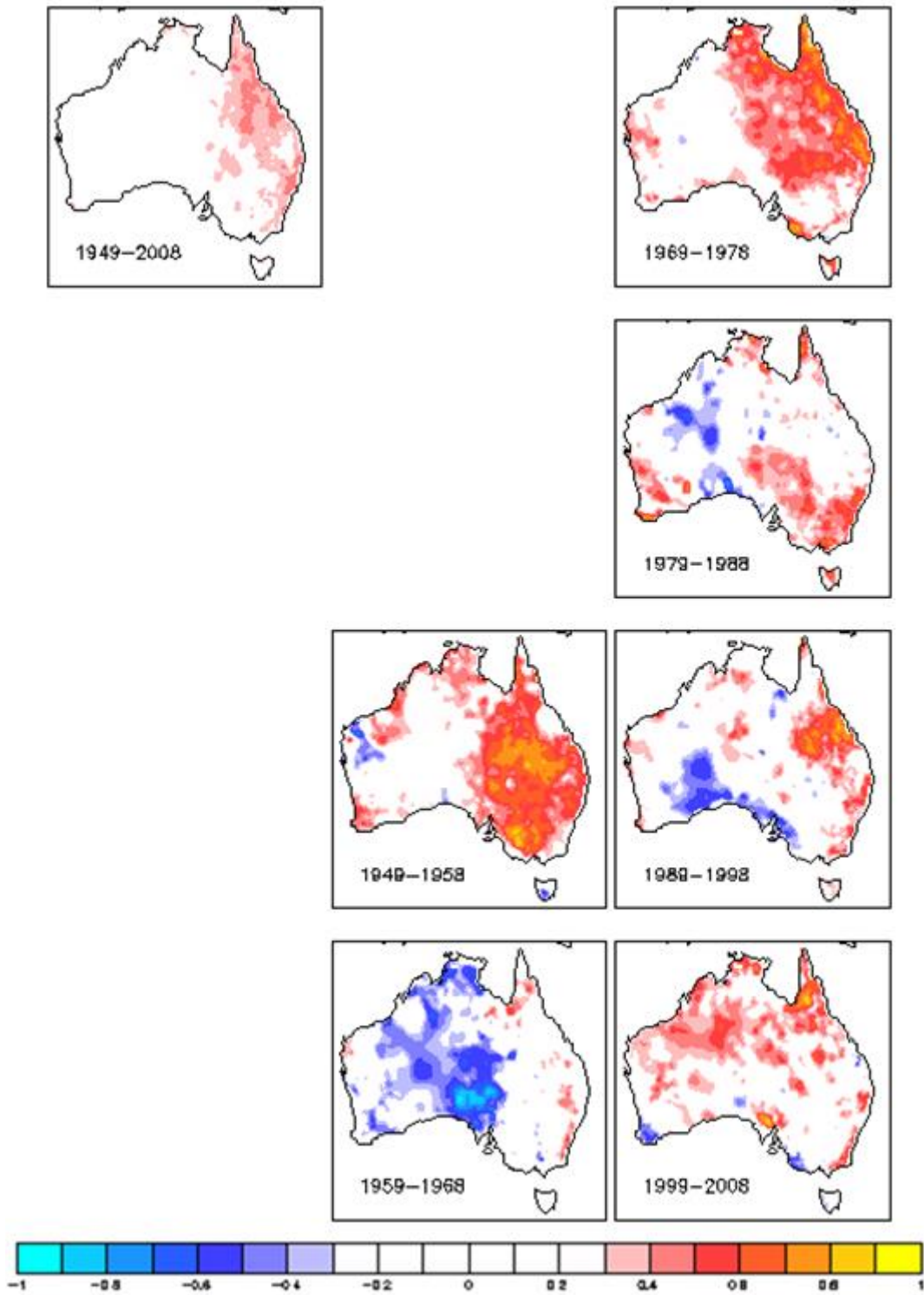


Figure 4.27: Correlation of DJF rainfall and the NOI.

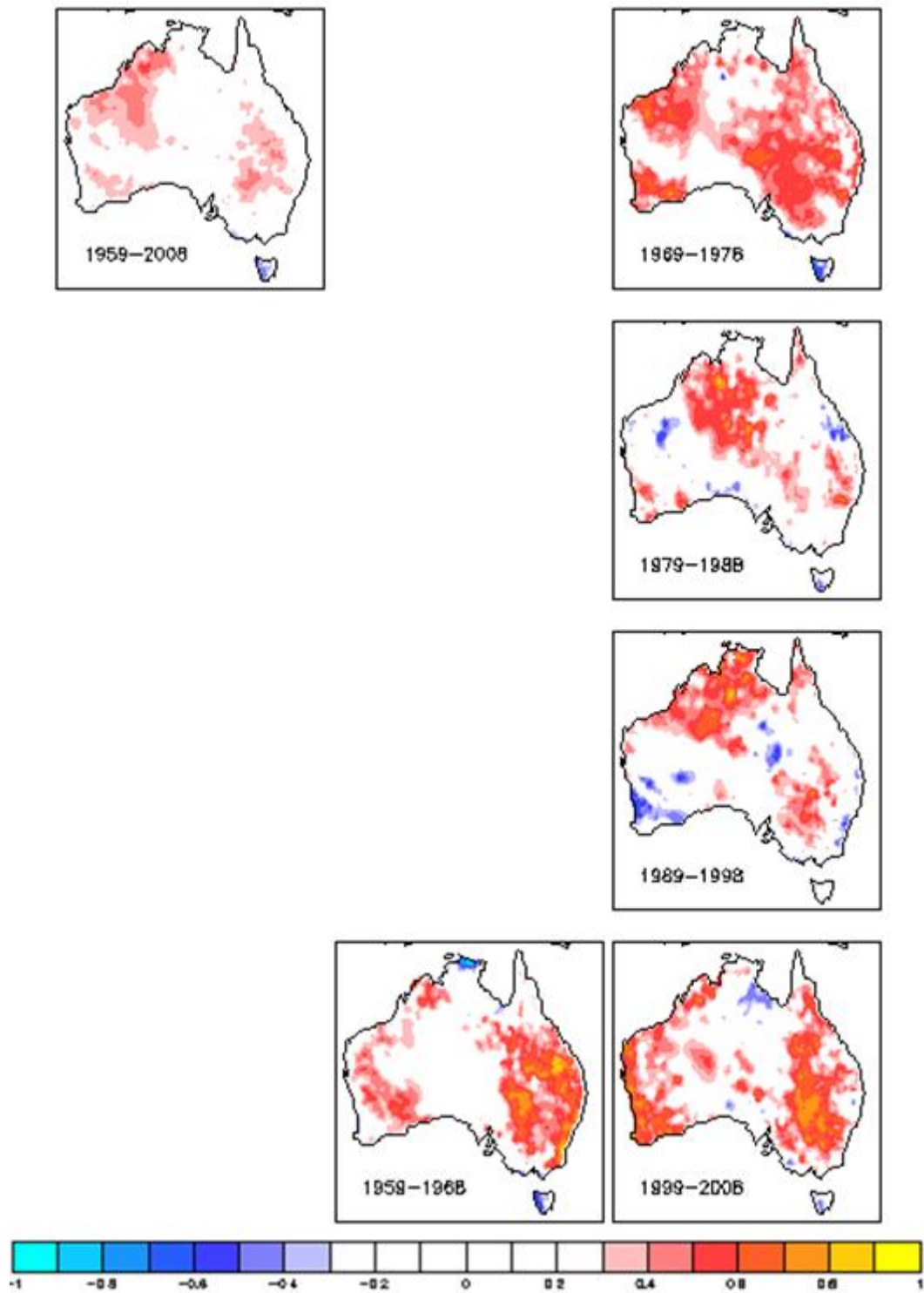


Figure 4.28: Correlation of DJF rainfall and the SAM index.

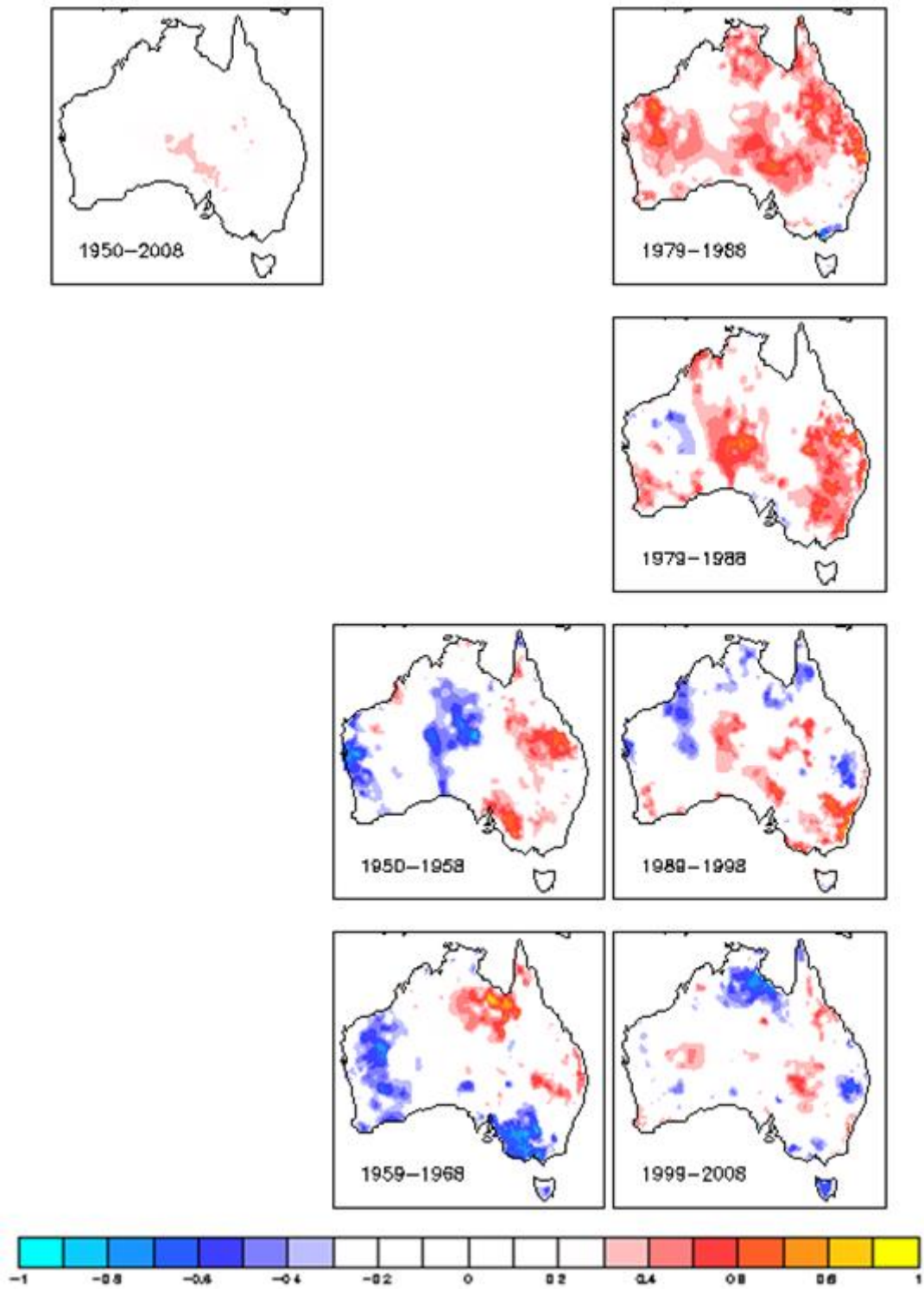


Figure 4.29: Correlation of DJF rainfall and the AOI.

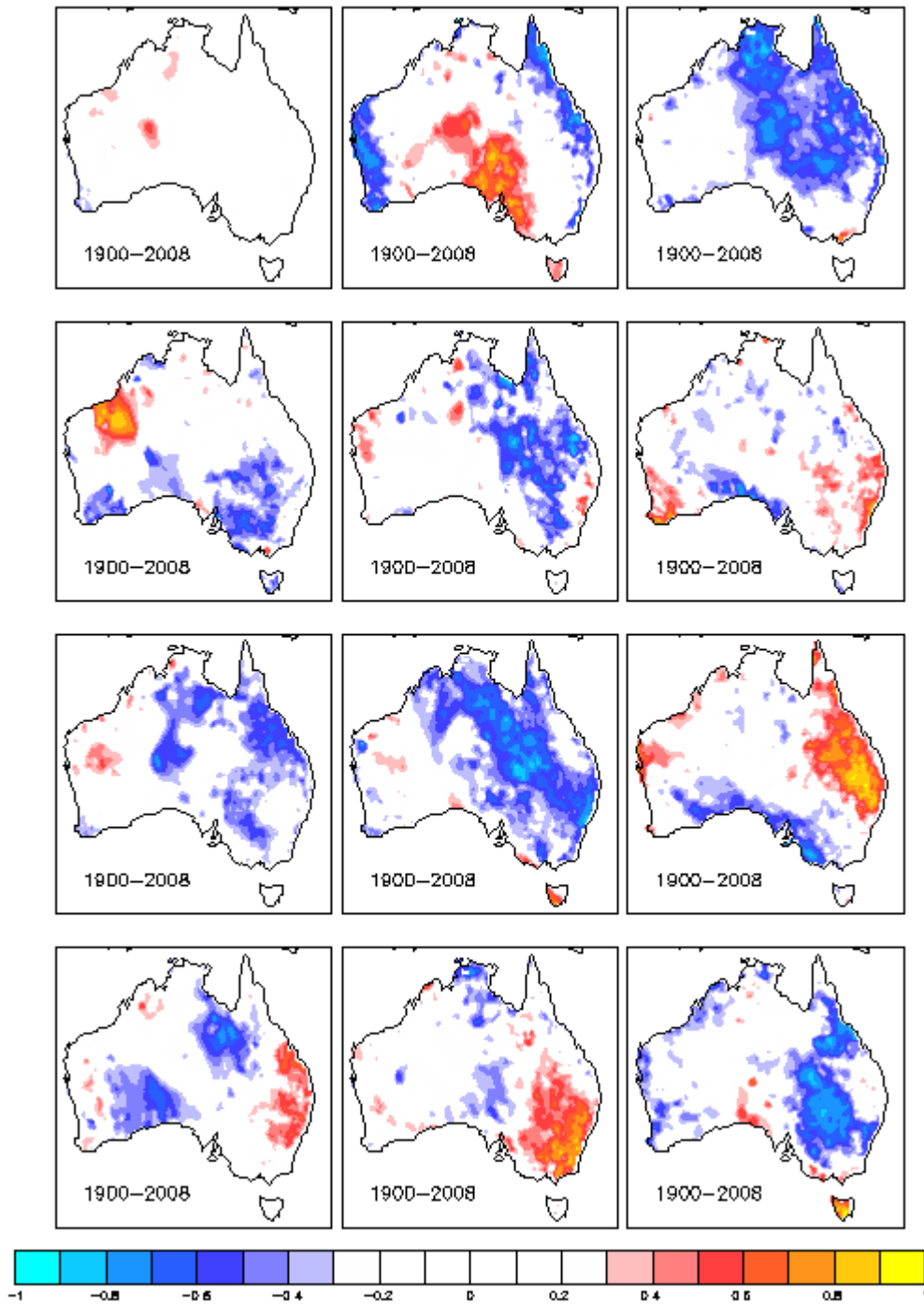


Figure 4.30: Correlation of DJF rainfall and the IPWP index.

The IPWP has a very similar correlation pattern to the PWP except for the 1980s and 1990s.

4.2.8 Summary of Meridional Spectral Type Results

Table 4.4 shows the rankings of the meridional spectral types where it can be seen that the IPWP had the highest ranking due to a significantly higher correlation range when compared to the other indices combined with a greater temporal stability. The high population variance of SAM (third decile) compared to its Northern Hemisphere counterpart the AOI (decile 1) should be noted. In terms of absolute score however the AOI delivers a very similar result to SAM.

Table 4.4: Performance (correlation) results of mixture type indices. The last four columns show the ranking of the index in terms of; strength, area coverage, temporal stability and overall performance of their major attribute between decades.

Index	Population Variance		Decadal Variance		Correlation Area		Temporal Stability		Final Score	
	Global	Score	Global	Score	Global	Score	Global	Score	Final	Score
AOI	0.0108	1	1.5	1	36	9	67	6	17	3
IPWP	0.0201	3	2.75	6	21	5	64	6	20	1
NOI	0.0258	4	2	3	25	6	50	2	15	4
SAM	0.0210	3	1.67	1	35	9	60	5	18	2

4.2.9 Unique Type

4.2.9.1 Quasi Biennial Oscillation (QBO)

Not particularly strong the QBO correlation with Australian rainfall (Figure 4.31) has a mean correlation of -0.0214 which rises to -0.245. Area coverage was found to be 8% and temporal stability of 50%. QBO correlation is quite similar to that other strongly quasi-periodic index covered the IOD for the 1970s, 1990s and the 2000s. The literature once suggested that the QBO and IOD were significantly related (Indeje & Semazzi 2000). QBO details are below (Table 4.5).

Table 4.5: Performance (correlation) results of the QBO.

Index	Population Variance		Decadal Variance		Correlation Area		Temporal Stability		Final Score	
	Global	Score	Global	Score	Global	Score	Global	Score	Total	
QBO	0.0115	1	2	3	8	1	50	2	7	

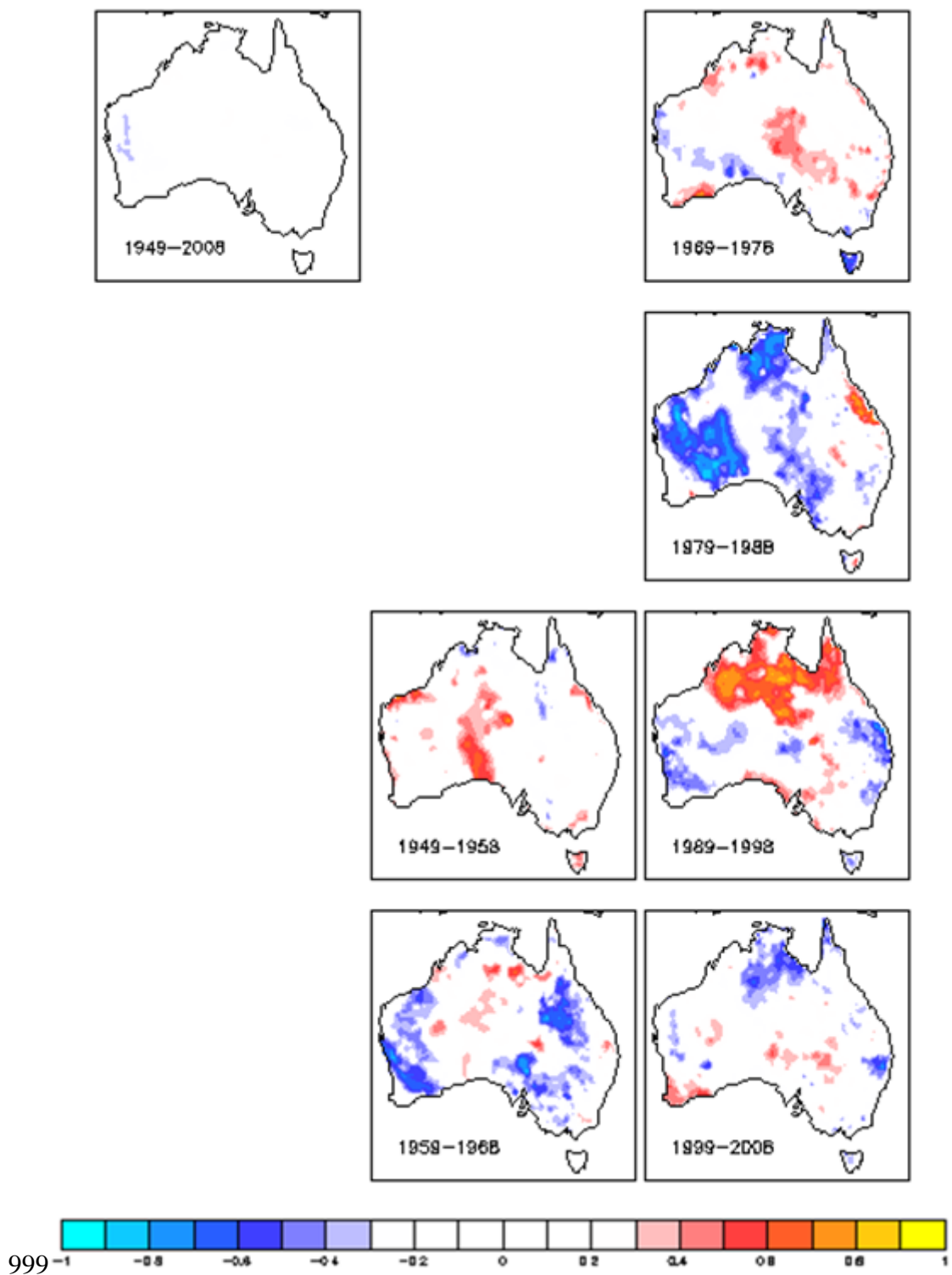


Figure 4.31: Correlation of DJF rainfall and the QBO index.

4.3 Summary of Australian Results

In this section the performance of indices for the whole of Australia are shown in précis format (Table 4.6) and a pictorial summary of the better performing indices is also shown (Figure 4.32). A key result is the outstanding performance of indices based on the characteristics of the oceanic warm pools (WPs).

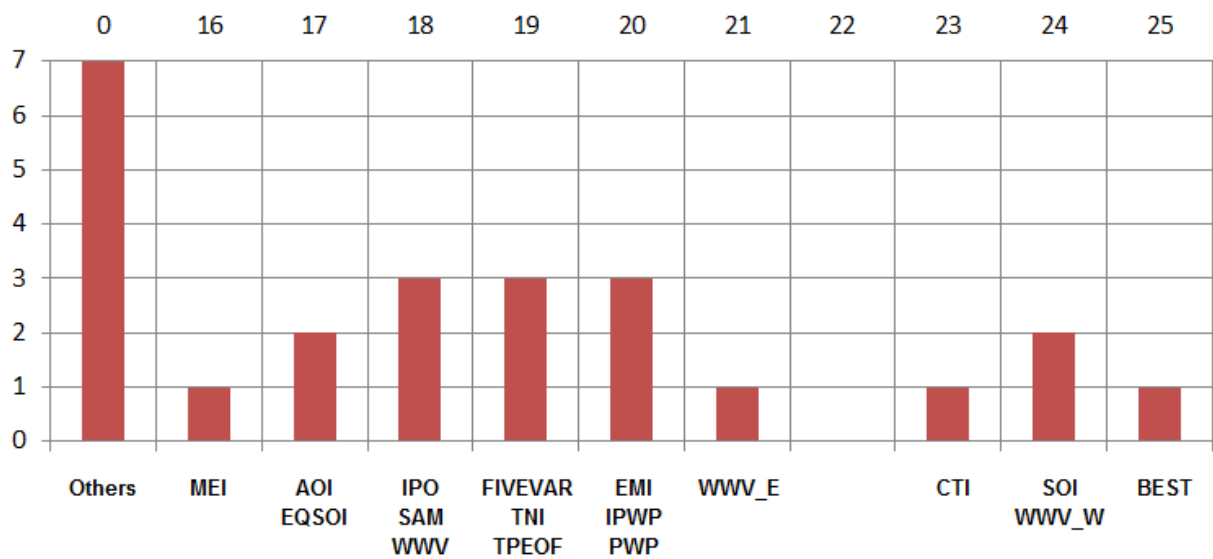


Figure 4.32: Pictorial summary of Australian results. Abscissae shows the number of indices in each of the score bins and ordinate shows the index name.

Table 4.6: Summary of Index Performance with DJF rainfall

Index	Population Variance		Decadal Variance		Correlation Area		Temporal Stability		Final Score	
	Global	Score	Global	Score	Global	Score	Global	Score	Total	Rank
AOI	0.0108	1	1.5	1	36	9	67	6	17	15
BEST	0.0238	4	1.5	1	37	10	80	10	25	1
CTI	0.0132	1	2.2	4	38	10	73	8	23	4
EMI	0.0137	1	2.75	6	39	10	55	3	20	6
EQSOI	0.0151	2	2	3	39	10	50	2	17	15
FIVEVAR	0.0241	4	2	3	37	10	50	2	19	9
IOD	0.0196	3	1.67	1	13	2	60	5	11	22
IPO	0.0265	4	1.83	2	35	9	55	3	18	12
IPWP	0.0201	3	2.75	6	21	5	64	6	20	6
MEI	0.0242	4	1.5	1	34	9	50	2	16	17
NAO	0.0115	1	2	3	38	2	50	2	8	23
Niño3.4	0.0187	2	1.83	2	38	10	45	1	15	18
NOI	0.0258	4	2	3	25	6	50	2	15	18
PDO	0.0143	1	2.2	4	29	7	45	1	13	20
PWP	0.0517	10	1.5	1	28	7	50	2	20	6
QBO	0.0115	1	2	3	8	1	50	2	7	24
SAM	0.0210	3	1.67	1	35	9	60	5	18	12
SOI	0.0177	2	2.75	6	38	10	64	6	24	2
TNI	0.0112	1	3.67	10	29	7	45	1	19	9
TPEOF	0.0252	4	1.5	1	31	8	67	6	19	9
WHWP	0.0221	3	2	3	23	5	50	2	13	20
WWV	0.0214	3	2.75	6	24	6	55	3	18	12
WWV_E	0.0130	1	2.2	4	39	10	64	6	21	5
WWV_W	0.0216	3	2.2	4	29	7	82	10	24	2

This result is not entirely unexpected as the WP regions are comparatively near to Australia and are shown to be centres of global scale climate activity in controlling significant climate modes. The top performing index was WWV_W which has an exceptionally high temporal stability score. SOI performed well due to its sound medium scores in most categories and exhibited similarity to WWV_W in its low frequency signal. Performance of some indices more traditionally used for the purpose, for example Niño3.4 is very poor at summer resolution mainly due to poor temporal stability whereas some of the derived indices based on it: BEST and FIVEVAR fared much better. Surprisingly the northern and southern hemisphere meridional indices; AOI, SAM and NAO is captured in this study as outperforming MEI and TNI. The IPO appears not to be suitable due to the 20 to 30 year signal.

4.4 South East Queensland Correlations of Significance

The treatment for SEQ is the same as the Australian analysis (Section 3.2.4). The only difference is that the correlation maps of the previous section were scrutinised for significant correlation results for the SEQ region. Indices that have been targeted in the literature for South East Queensland (SEQ) were also analysed: SOI, Niño3.4 and IPO/PDO (Cai 2011; Murphy & Ribbe 2004). In addition due to their robust correlations Warm Pool (WP) indices for example; PWP and WWV have also been included. The regional definition of SEQ was determined as the land areas contained within 20.5 – 30.5°S and 150.5 – 154.5°E (Cai & van Rensch 2012) as opposed to 27.5 – 28.5°S and 151.5 – 153.5°S (BoM, A. 2010) in Baum et al. (2010) or the land area within 147°E, the Australian E coast and lat 29 – 22.5°S (Murphy & Ribbe 2004) so as to make the results more similar to the latest significant work conducted for the region.

Standardised, area averaged rainfall anomaly for SEQ is shown in Figure 4.33.a) Decadal, annual and b) decadal DJF rainfall to enable the reader to assess how well correlation and index tracks rainfall. All other graphics in this section, indices and correlations have been subjected to the filtering technique as described in Section 3.2.3.1. Additionally some area averaged correlation graphics have been included to assist the reader's understanding. The approximate 50 year downward trend in rainfall from the end of the 1960s also coincides with the decrease of the SOI. Over the same 50 year period the WPWP SST has increased.

IPO has decreased for the last 3 decades but it is difficult to determine the 20 year decrease in tropical Pacific Meridional Overturning Circulation (MOC).

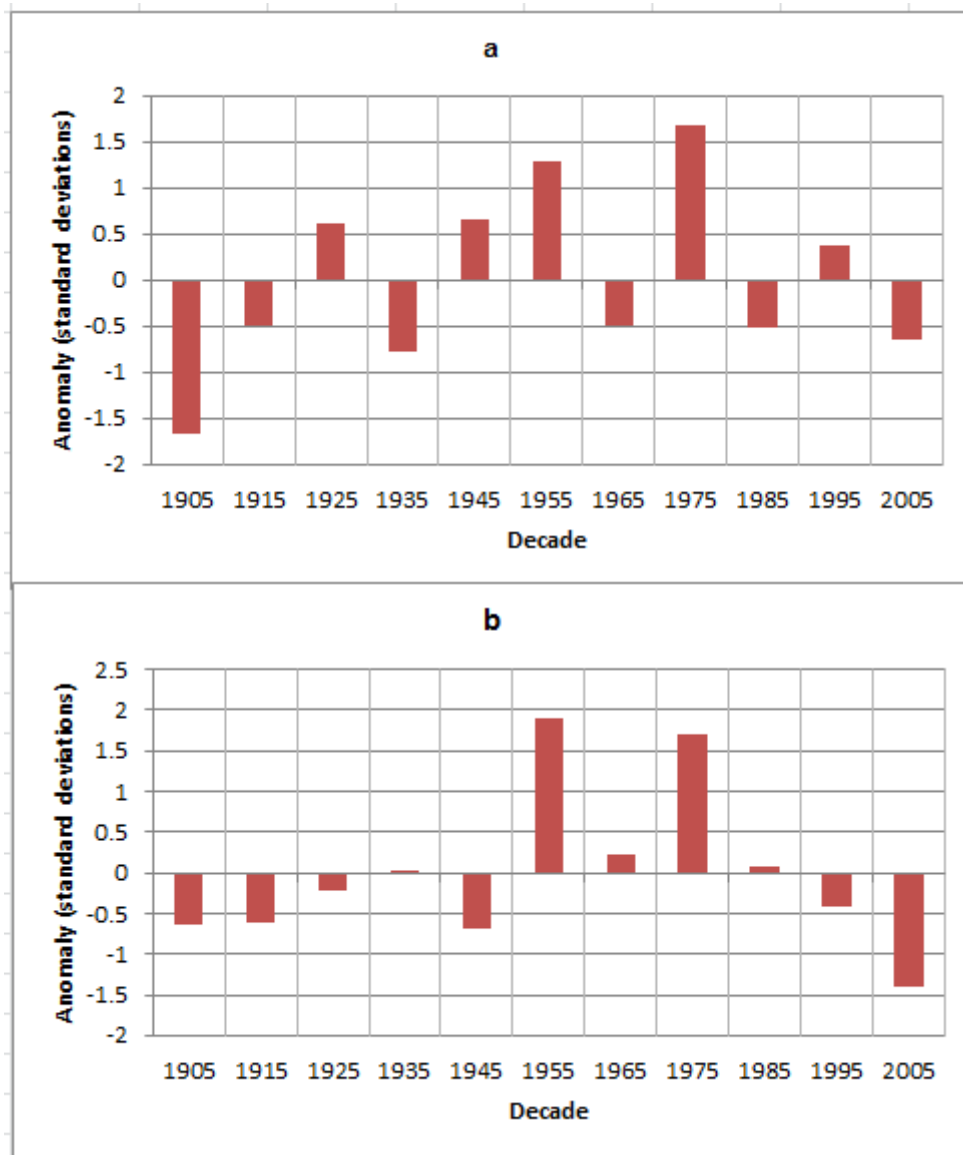


Figure 4.33: Standardised area averaged South East Queensland rainfall anomalies 1900 – 2008 by decade. a) annual rainfall and b) summer (DJF) rainfall.

4.4.1 Southern Oscillation Index (SOI)

The SEQ correlation for the DJF SOI (Figure 4.34) shows a mean correlation of 0.42 for the 1900 – 2008 period showing a very low population variance of 0.0016 and moderately low decadal variance pattern (4th rank). With respect to significant area of correlation for SEQ

SOI occupies the top position with many other indices whilst also having a moderately good temporal stability.

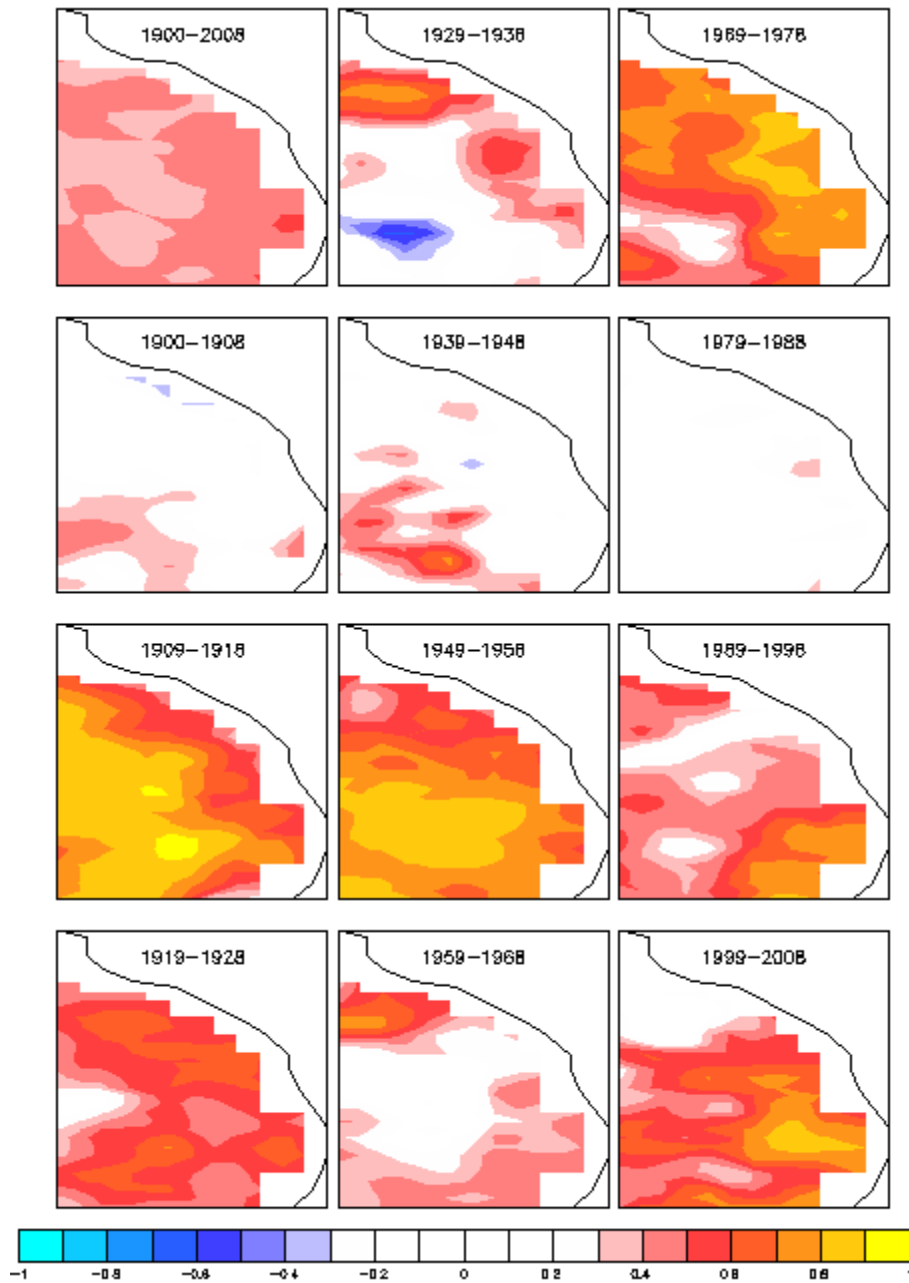


Figure 4.34: Decadal correlation of SEQ DJF rainfall and SOI.

A possible significance is that correlation tracks the decadal DJF SOI in a weak to moderate fashion (Figure 4.35) whereas no such relationship between rainfall and correlation is apparent.

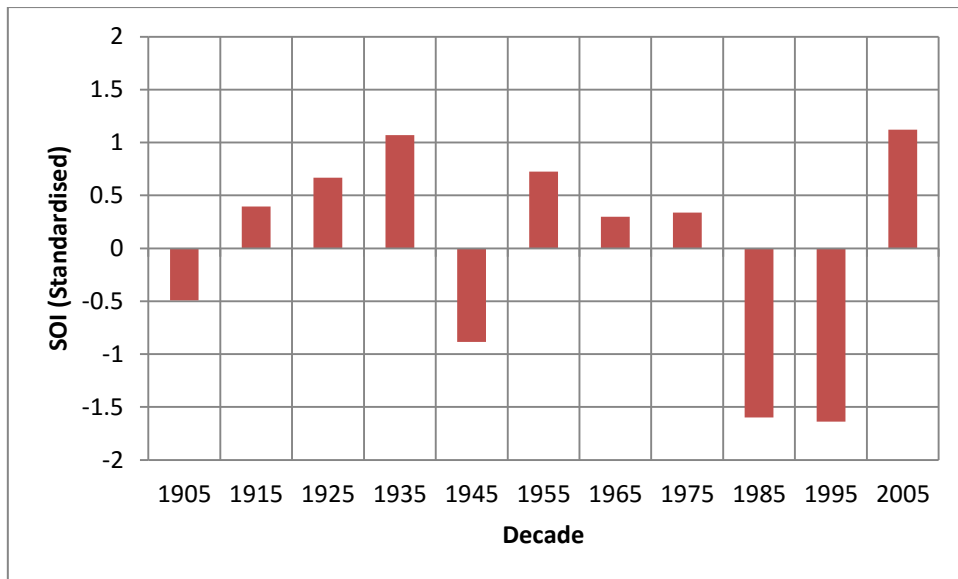


Figure 4.35: Decadal mean summer (DJF) SOI.

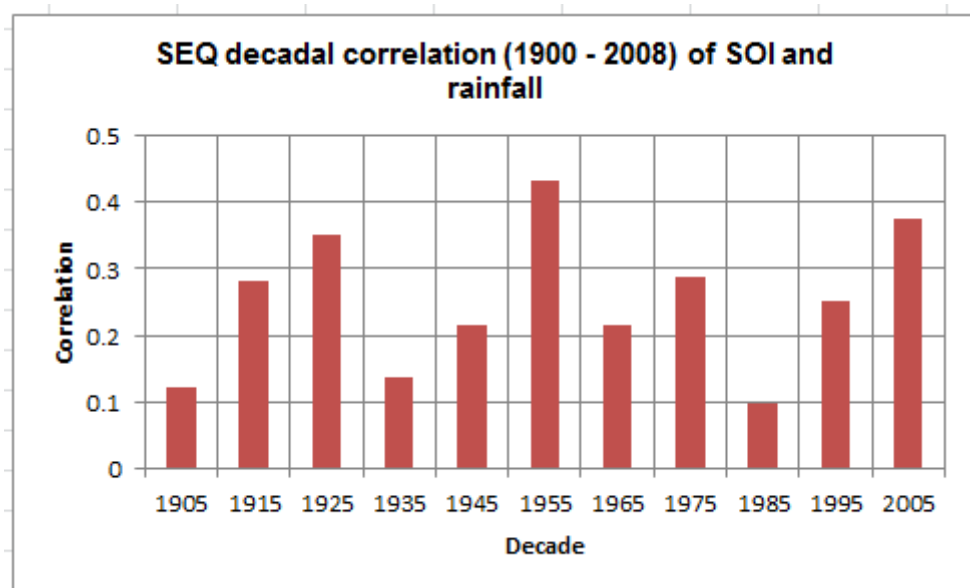


Figure 4.36: Decadal area averaged correlation of SEQ rainfall and SOI.

4.4.2 Niño3.4

The DJF Niño3.4 index correlation with SEQ rainfall is shown (Figure 4.37).

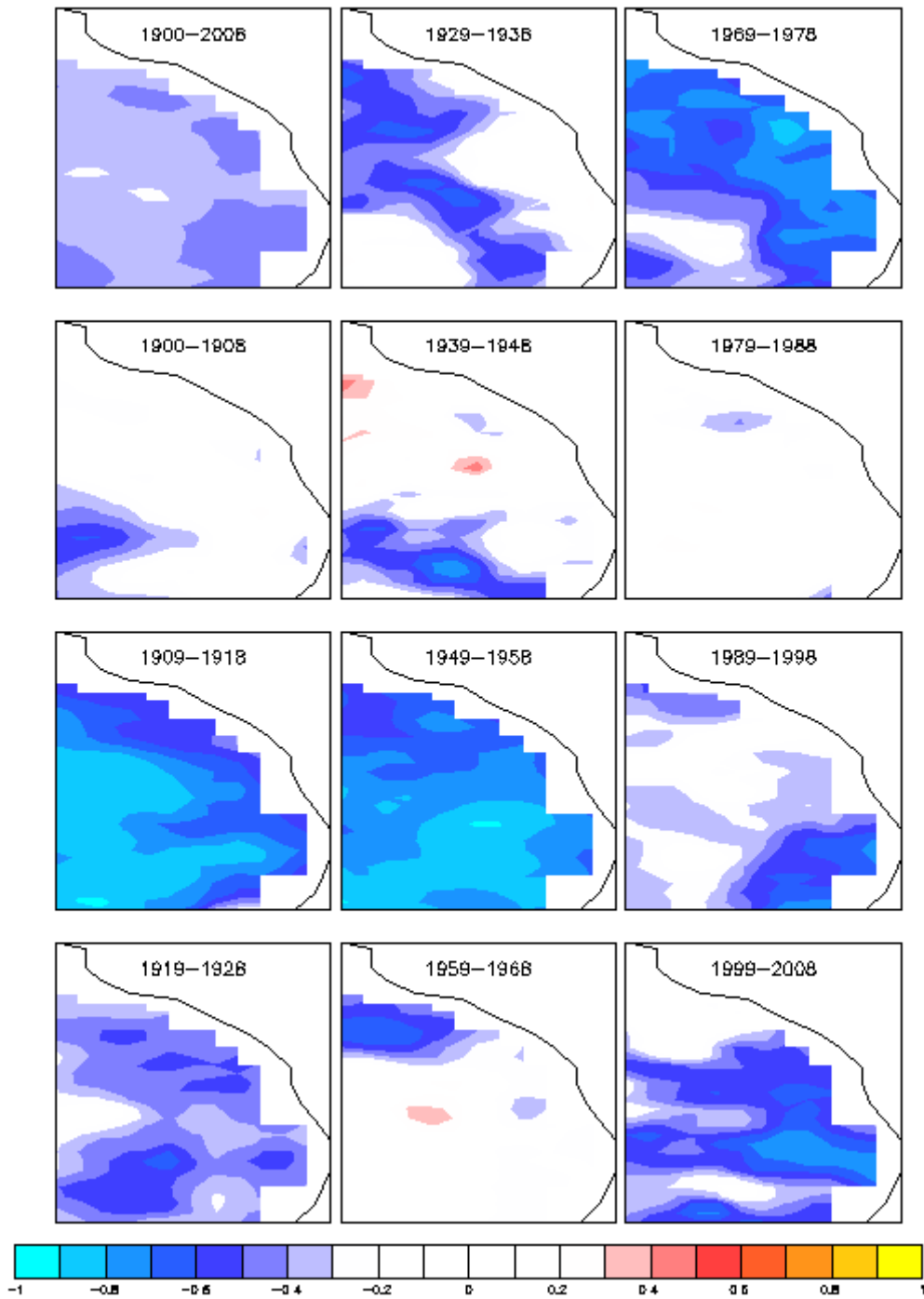


Figure 4.37: Decadal correlation of SEQ DJF rainfall and Niño3.4 index.

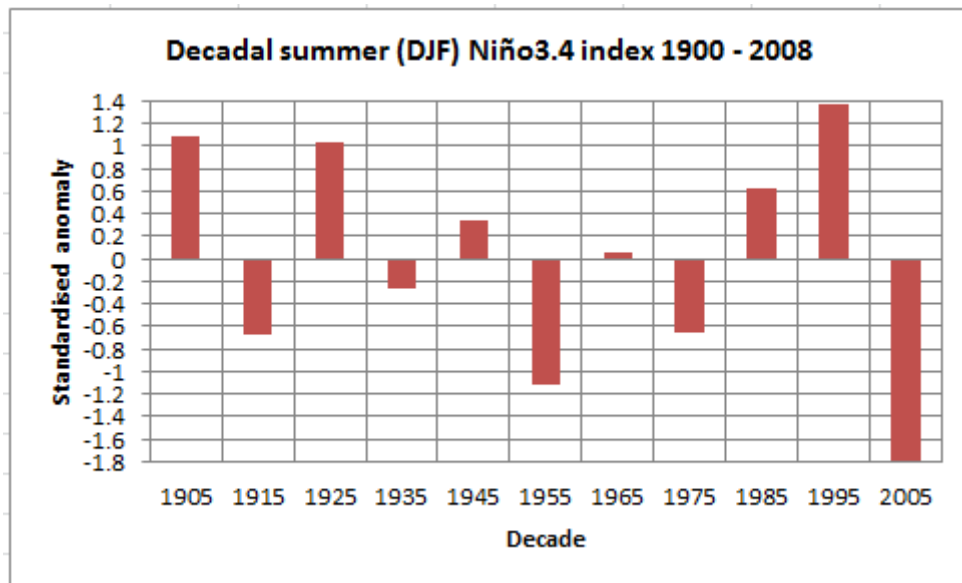


Figure 4.38: Decadal mean summer (DJF) Niño3.4 index 1900 – 2008.

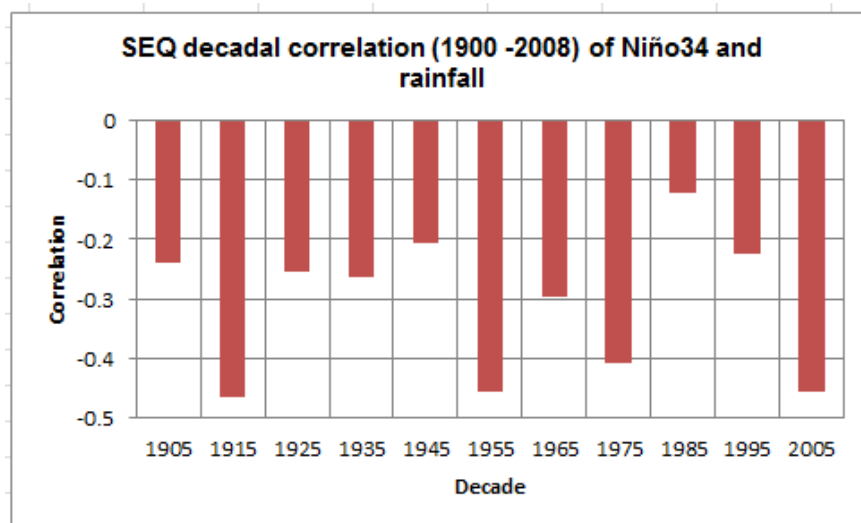


Figure 4.39: Decadal area averaged correlation of SEQ rainfall and Niño3.4 index.

Unlike the results for the Australia wide situation SEQ whole year Niño3.4 correlation (Figure 4.39), still wholly negative, is generally weaker. Overall the whole year correlations are more regular. Niño3.4 correlation pattern was found to be the inverse of the SOI. Other traits it shared were a large area of correlation and moderately high temporal stability.

4.4.3 Inter Decadal Pacific Oscillation (IPO)

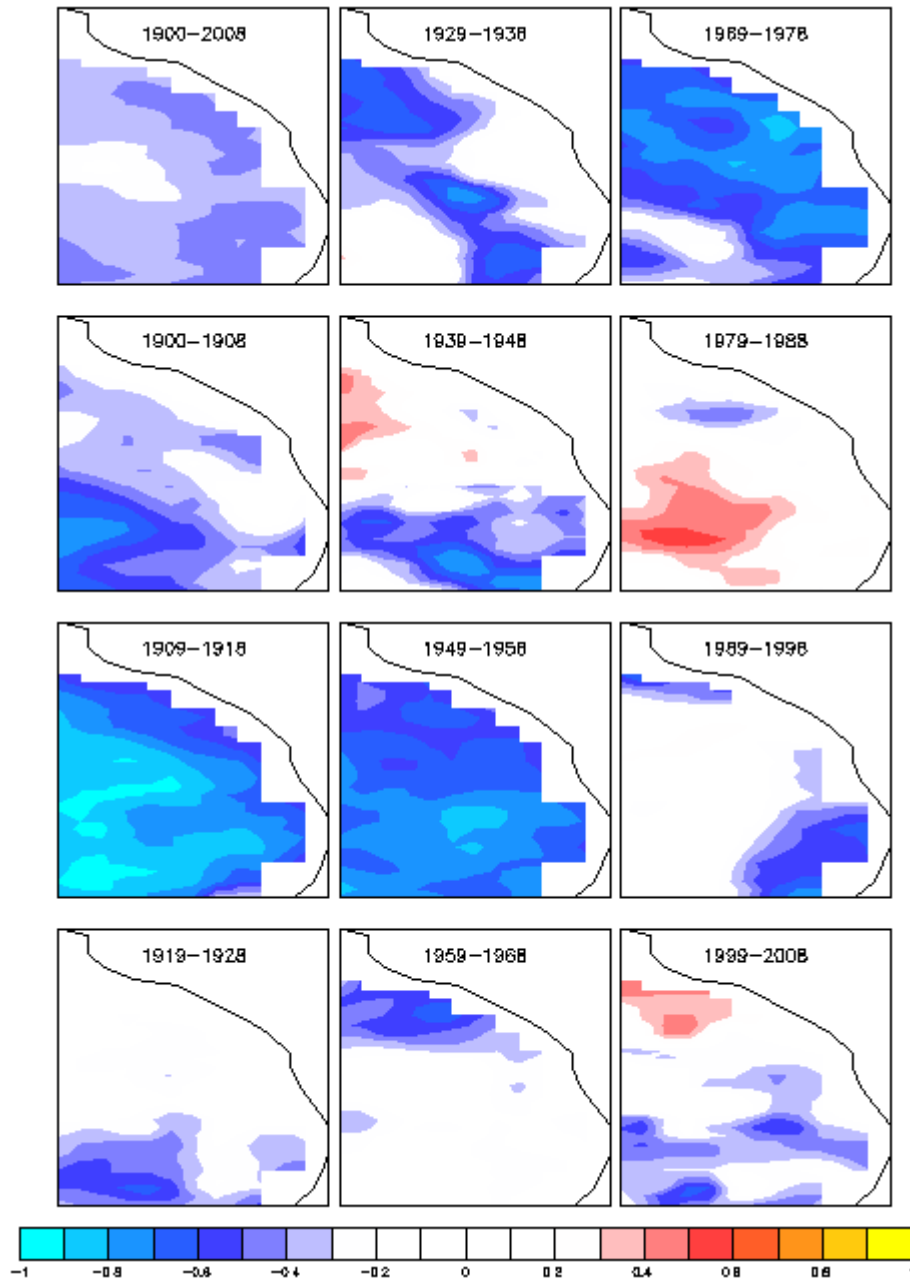


Figure 4.40: Decadal correlation of SEQ DJF rainfall and IPO.

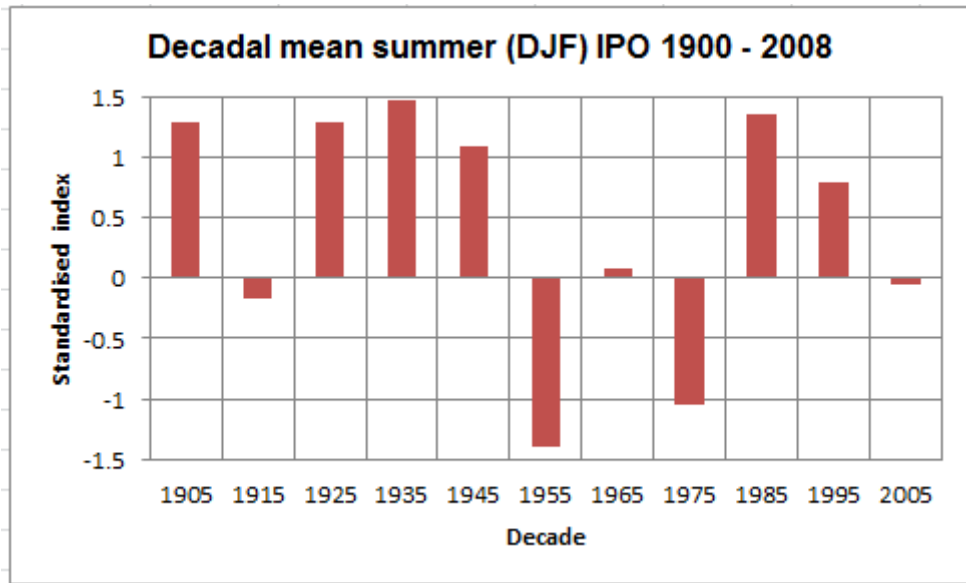


Figure 4.41: Decadal mean DJF IPO index.

The IPO correlation with SEQ rainfall is shown (Figure 4.40) and appears more dynamic at the decadal DJF resolution than for the whole year (not shown). In terms of the analysis criteria score was identical to the SOI and its DJF index is shown (Figure 4.41).

4.4.4 Pacific Warm Pool (PWP)

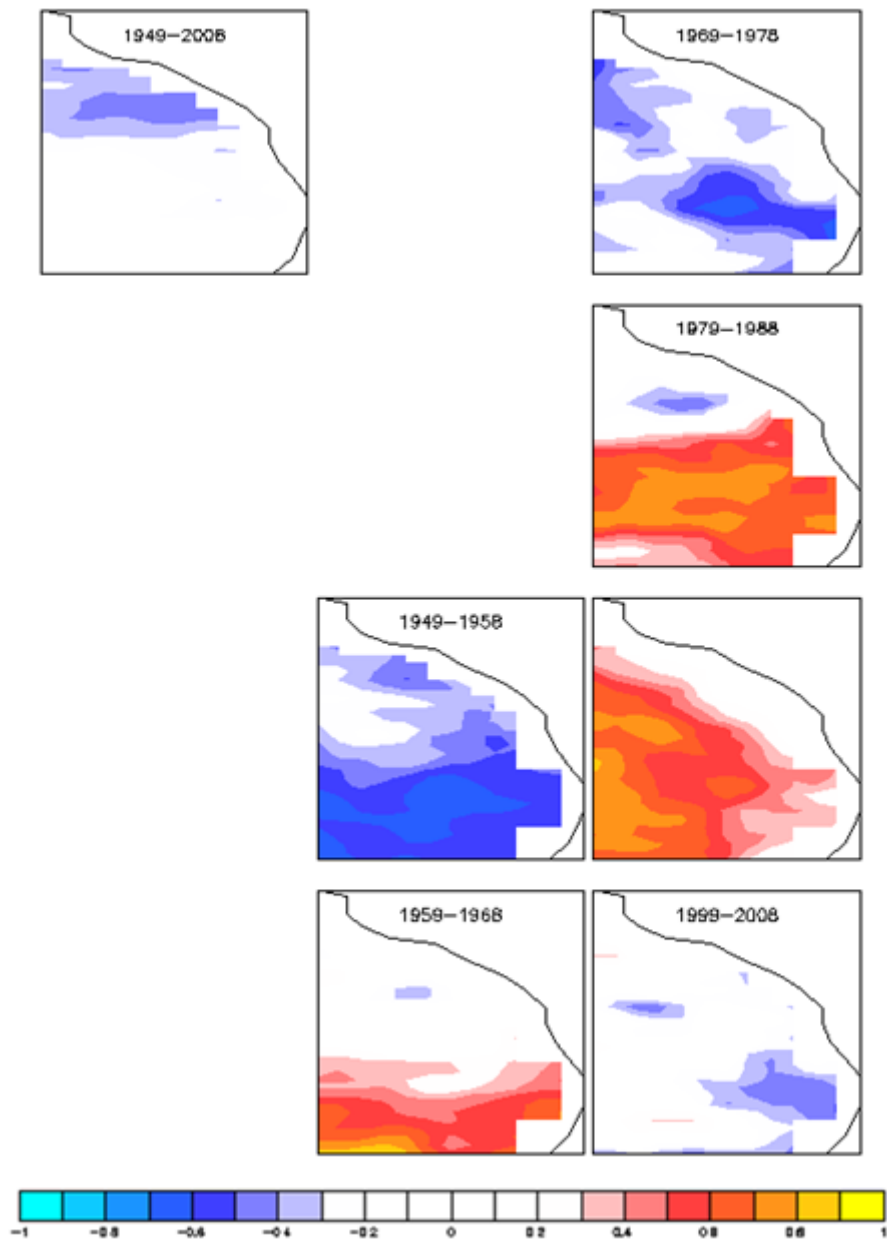


Figure 4.42: Decadal correlation of SEQ DJF rainfall and PWP.

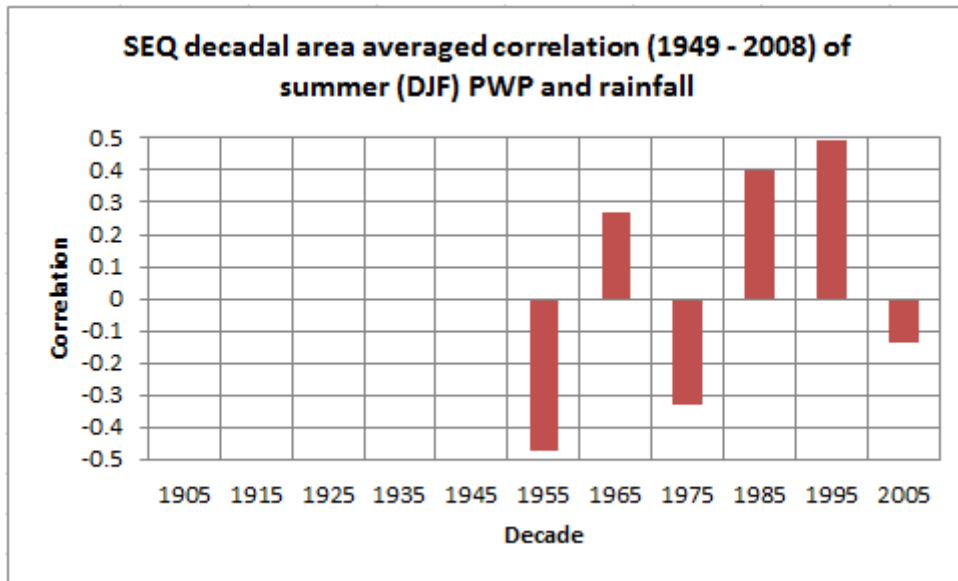


Figure 4.43: Decadal area averaged correlation of SEQ DJF rainfall and PWP.

The correlation of PWP and SEQ rainfall in DJF (Figures 4.42 and 4.43) does not track the 50 year increase in PWP index (Figure 4.44), a proxy for SST in the region as reflected in its poor temporal stability. Instead a multi-decadal pattern, reminiscent of the IPO is apparent between the 1950s and 1980s. IPO has the highest population variance value of any index in respect to SEQ rainfall, but its decadal variability of variance is the worst.

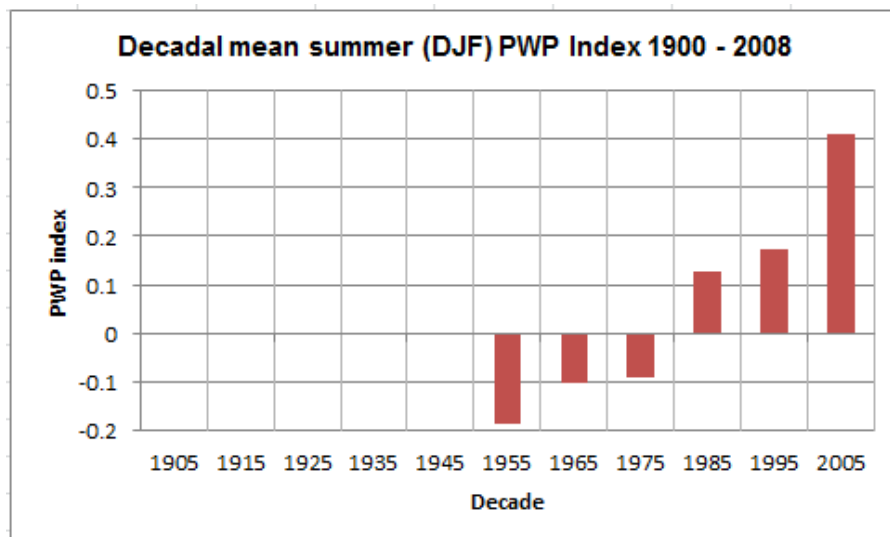


Figure 4.44: Decadal mean DJF PWP index.

DJF PWP index correlation exhibits summer dynamism compared to the whole year (not shown).

4.4.5 Warm Water Volume (WWV)

DJF WWV index (shown in Figure 4.46) shows a moderate positive correlation with SEQ rainfall for the majority of the time (Figure 4.45) turning negative from the 1980s and for the first decade of the 21st century. Area coverage of significant correlation was poor at 18% and whilst having the highest decadal variance stability for SEQ temporal stability was poor. Correlation for the whole year has a similar relationship but is only negative in the 1980s (Figure 4.47).

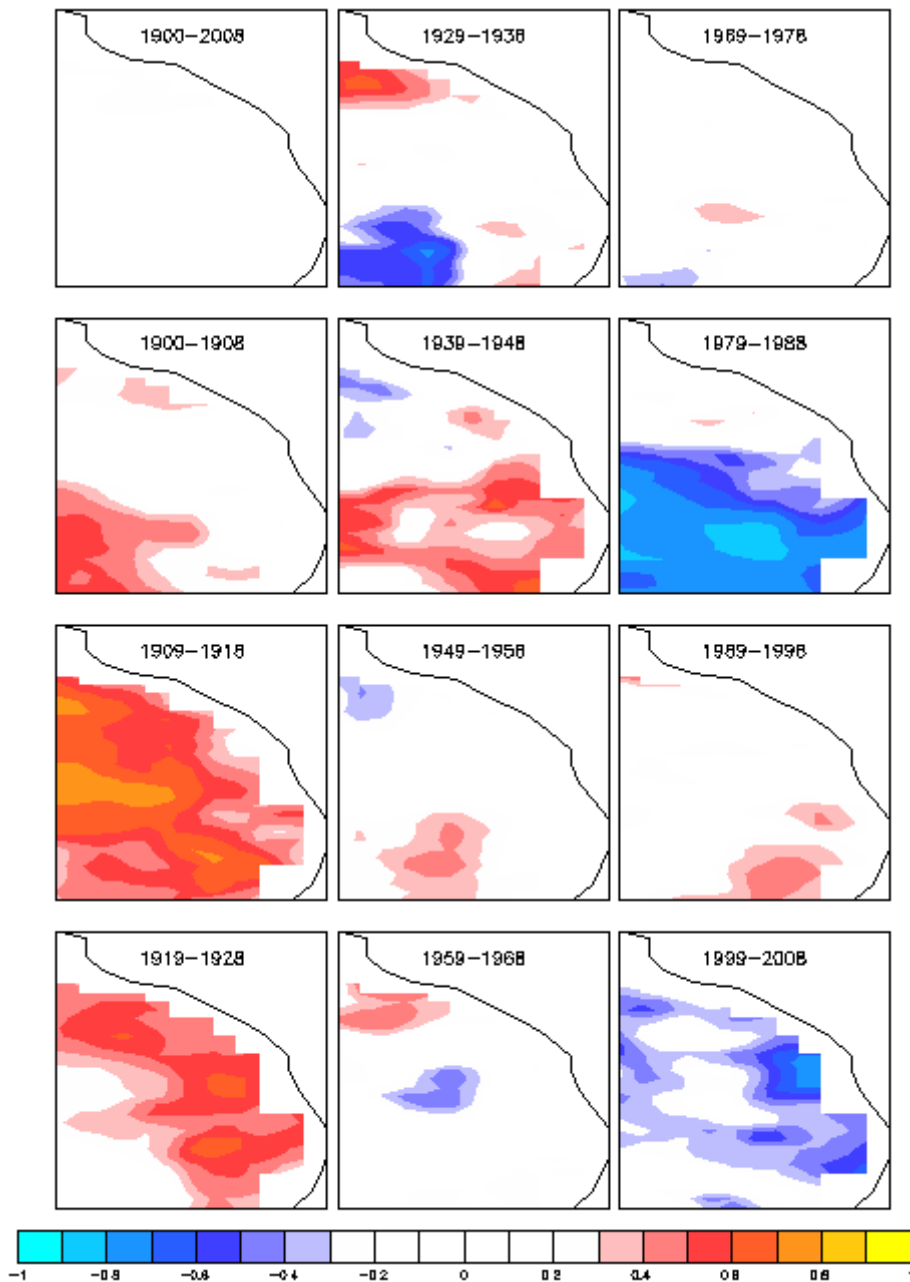


Figure 4.45: Decadal correlation of SEQ DJF rainfall and WWV index.

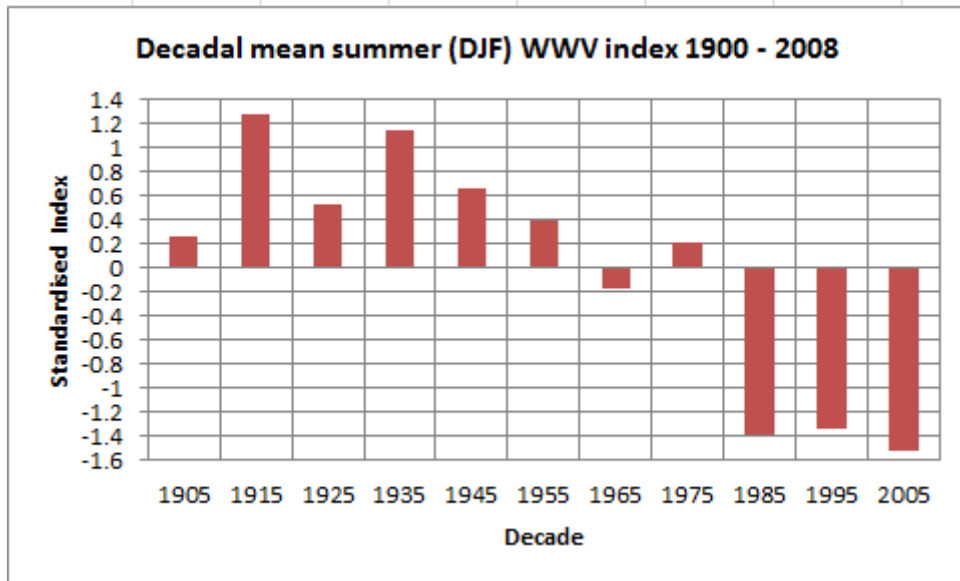


Figure 4.46: Decadal mean DJF WWV index.

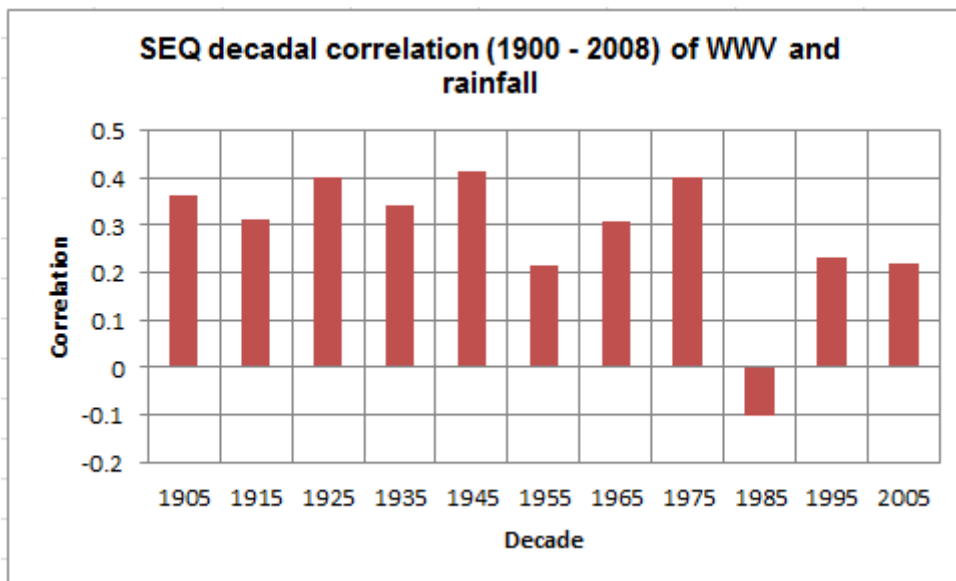


Figure 4.47: Decadal area averaged correlation of SEQ rainfall and WWV index.

4.4.6 Warm Water Volume West (WWV_W)

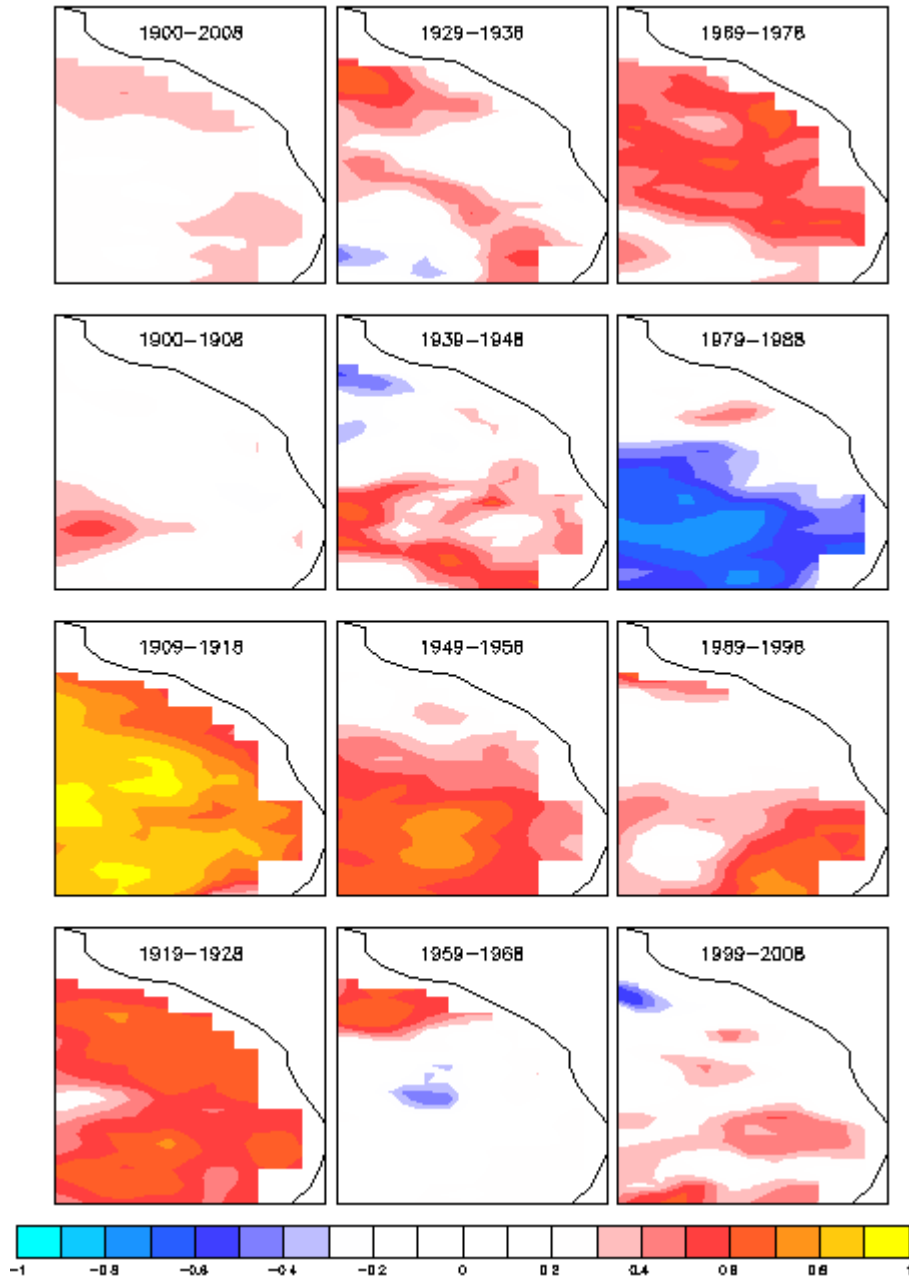


Figure 4.48: Decadal correlation of SEQ DJF rainfall and WWV_W index.

WWV_W correlated with DJF (Figure 4.48) tracks the index (Figure 4.49) very well and was the lowest ranked index for SEQ. WWV_W had a similar correlation to that of the SOI except for the 1940s and 1980s. For whole year correlation (Figure 4.50) similarity was less apparent, but still exhibited slight evidence of a three decadal ramp pattern.

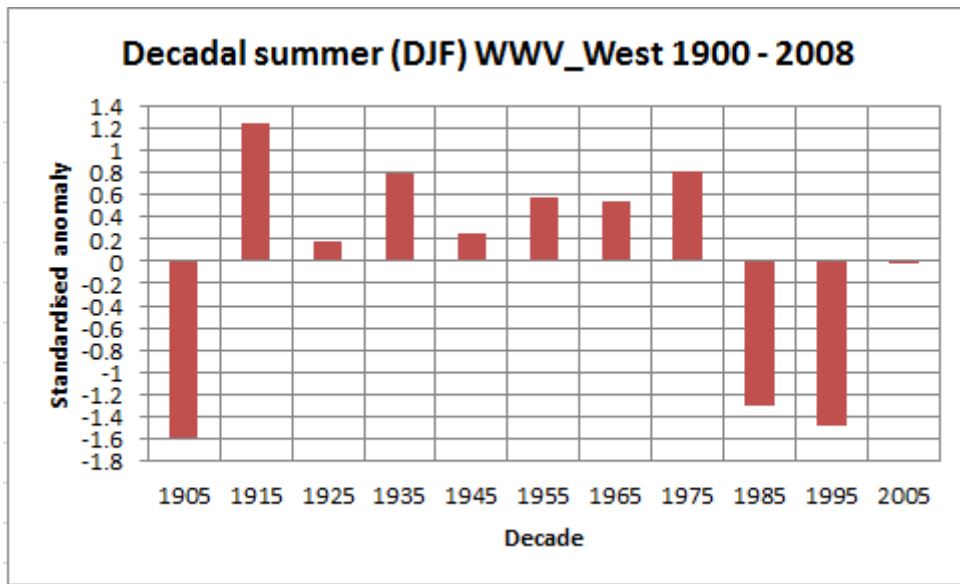


Figure 4.49: Decadal mean DJF WWV_W index.

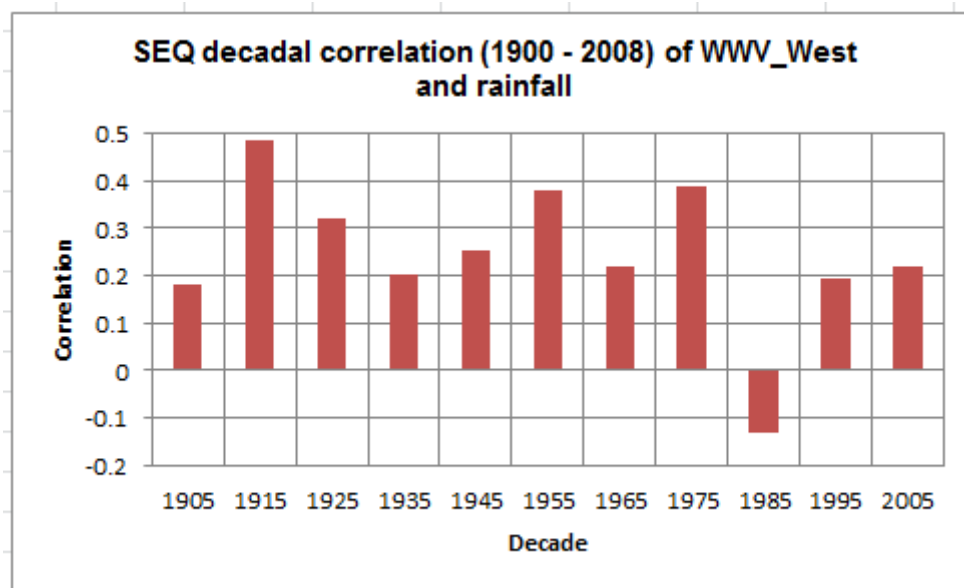


Figure 4.50: Decadal area averaged correlation of SEQ rainfall and WWV_ West index.

4.4.7 Warm Water Volume East (WWV_E)

Decadal DJF WWV_E index (shown in Figure 4.53), the most remote of the WWV regions to Australia, had the most impressive correlation with DJF rainfall (Figure 4.51) of the WWV indices. In terms of the criteria WWV_E performed the best of all indices for SEQ, occupying the highest decile for decadal variance, area of significant correlation and temporal stability.

The whole year correlation (Figure 4.52) shows lesser evidence of this oscillation and bears little relationship to the index (not shown).

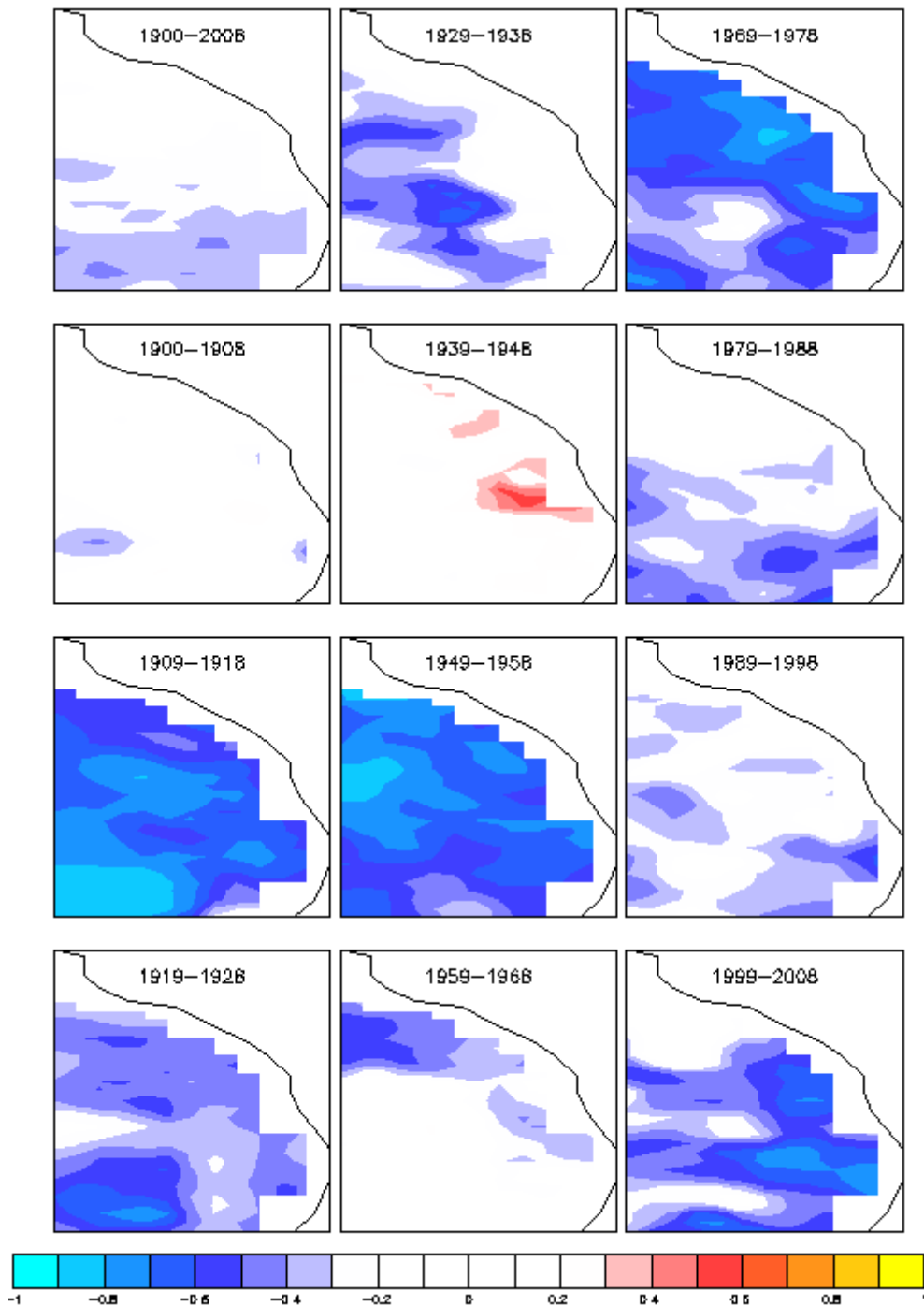


Figure 4.51: Decadal correlation of SEQ DJF rainfall and WWV_E index.

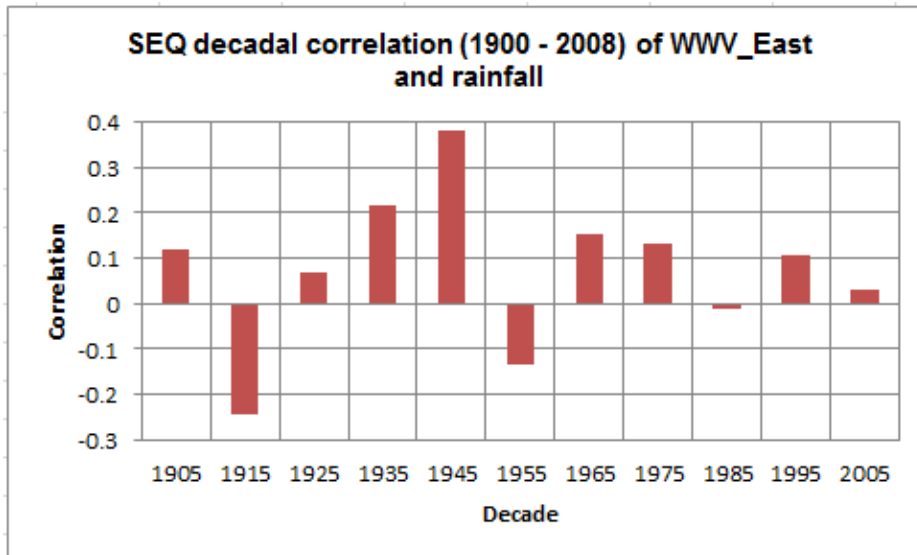


Figure 4.52: Decadal area averaged correlation of SEQ rainfall and WWV_East index.

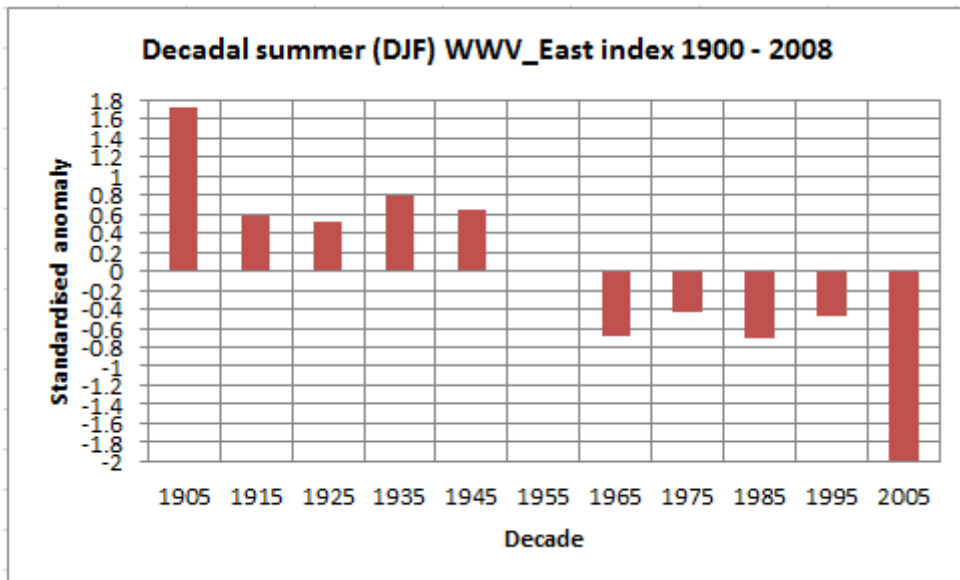


Figure 4.53: Decadal mean DJF WWV_E index.

4.4.8 Indo Pacific Warm Pool (IPWP)

The DJF IPWP index (Figure 4.55) tracks the 50 year increase in temperature in the PWP region and the commensurate increase in heat content/temperature of the IPWP region. Correlation between IPWP (SODA) and rainfall varied in a multi-decadal pattern (Figure 4.54). Correlation between the reanalysis material, IPWP SODA was very similar to the observational material of the PWP except for the first decade of the 21st century and shared its high population variance.

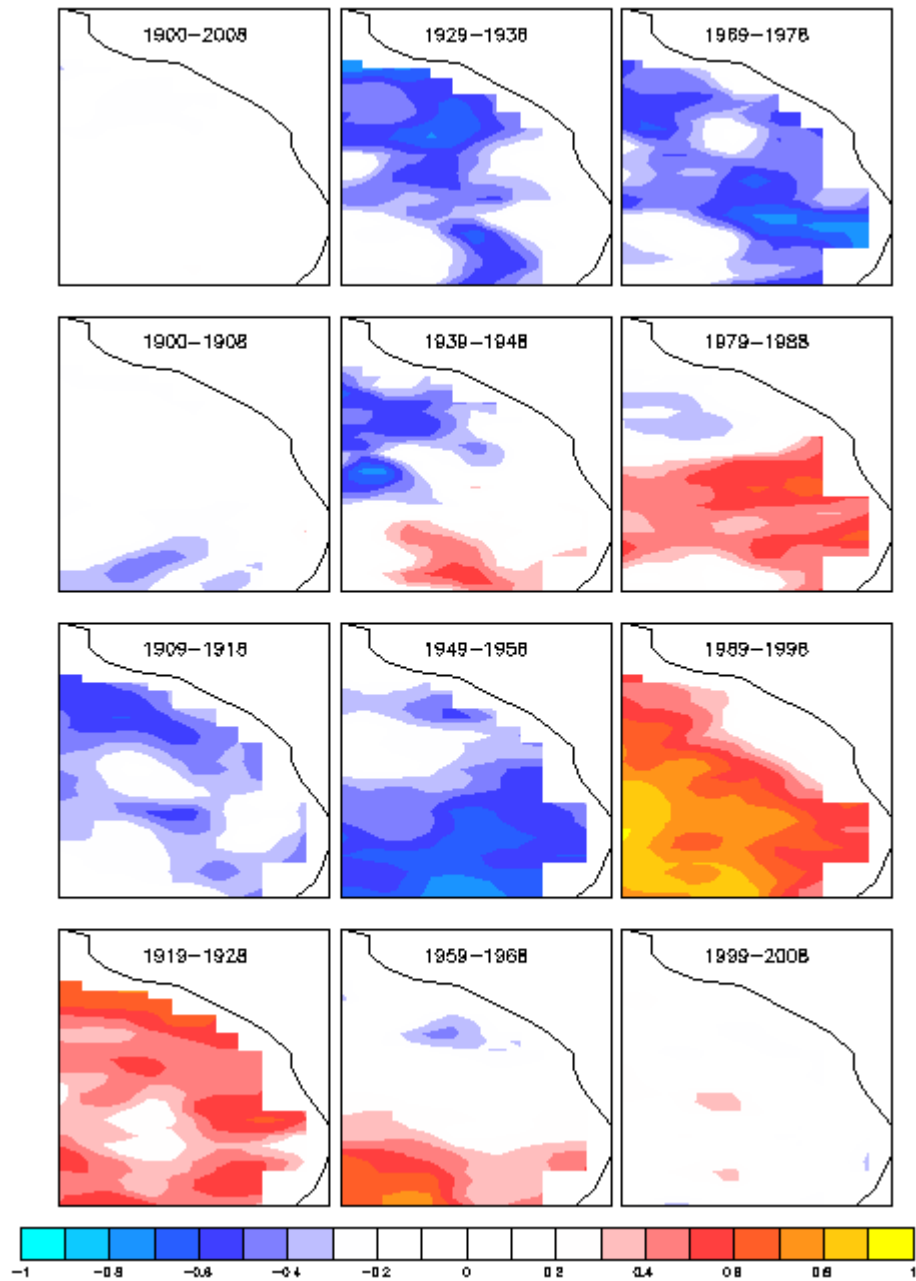


Figure 4.54: SEQ decadal correlation of DJF rainfall and IPWP index.

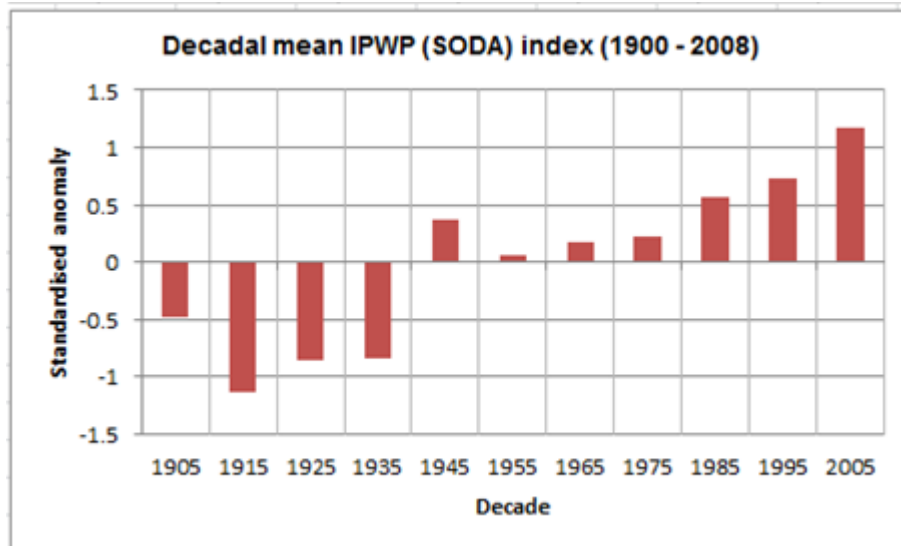


Figure 4.55: Decadal mean DJF IPWP index.

4.4.9 The BEST index

The BEST index was ranked second for SEQ indices in terms of correlation (Figure 4.56) exhibited a moderate negative mean correlation of -0.438. Population variance was low (0.0073) whilst decadal variance appeared good for only six decades of material. High scores in both area and temporal variability helped elevate BEST to the second highest rank. MEI correlation pattern was very similar and CTI, EQSOI, FIVEVAR, Niño3.4 and SOI all bore a resemblance. The IPO pattern looked similar between the 1950s and 1970s.

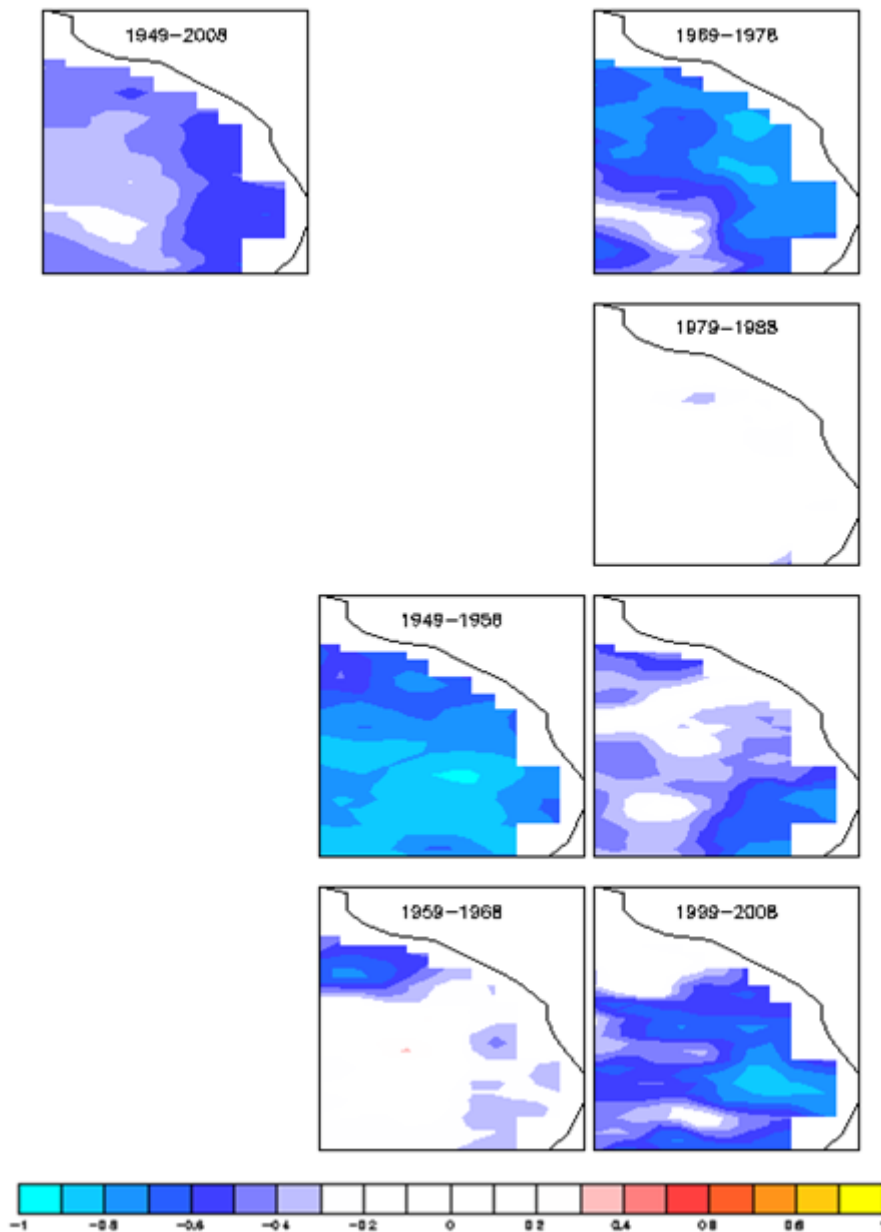


Figure 4.56: SEQ decadal correlation of DJF rainfall and BEST index.

4.4.10 The Cold Tongue Index (CTI)

Four indices enjoyed equal fourth ranking, CTI, EQSOI, NOI and TPEOF. CTI (Figure 4.57) exhibited a mean negative correlation of -0.337 and only turned weakly positive in the 1980s. Population variance was low (0.0022) as was decadal variance stability which was contra to the high temporal stability and area of significant correlation.

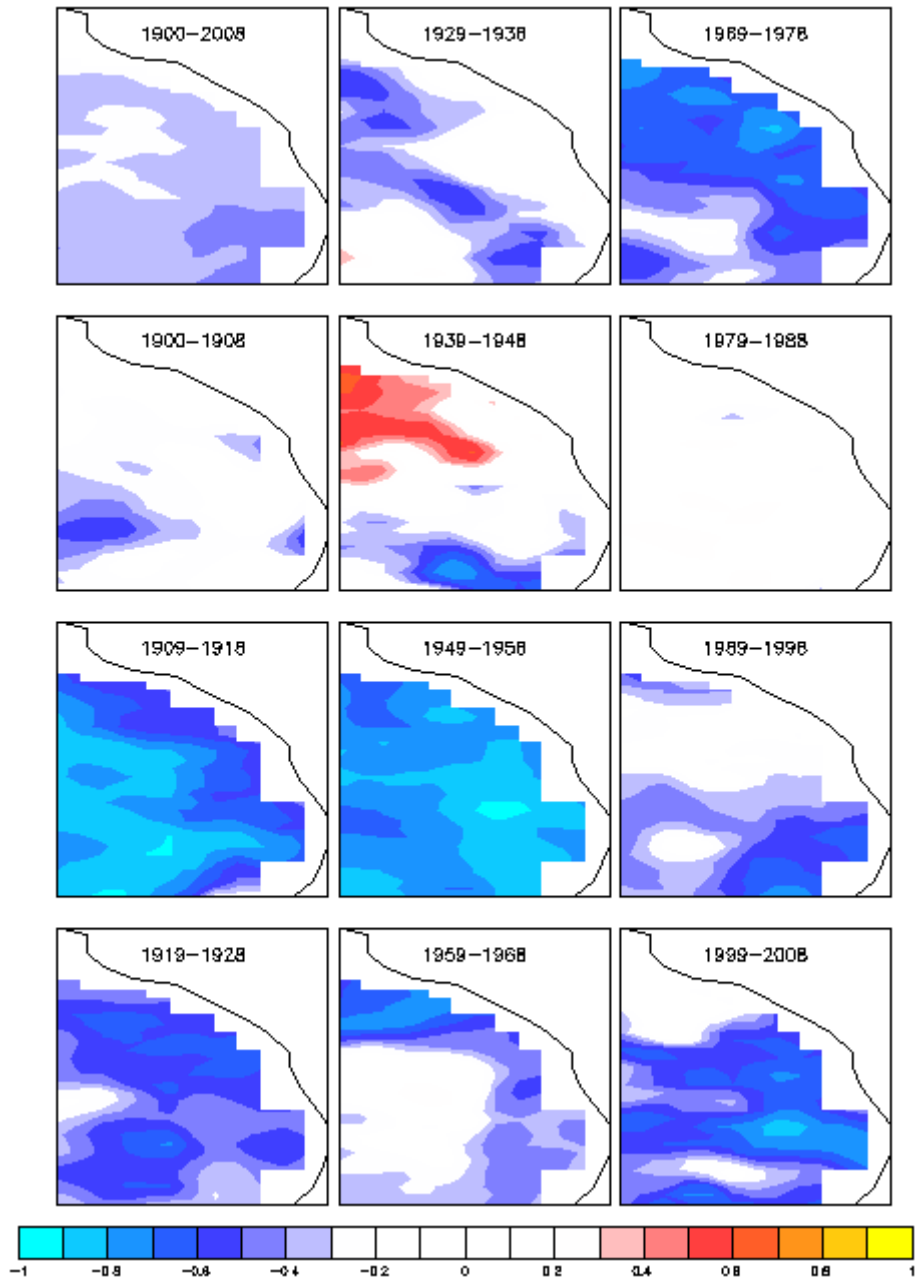


Figure 4.57: SEQ decadal correlation of DJF rainfall and CTI index.

4.4.11 El Niño Modoki (EMI) index

The two best attributes of EMI were a high area of significant correlation and a moderately high temporal stability. EMI (Figure 4.58) bore a remarkable similarity to the TNI (not shown) from the 1930s to the end of the record.

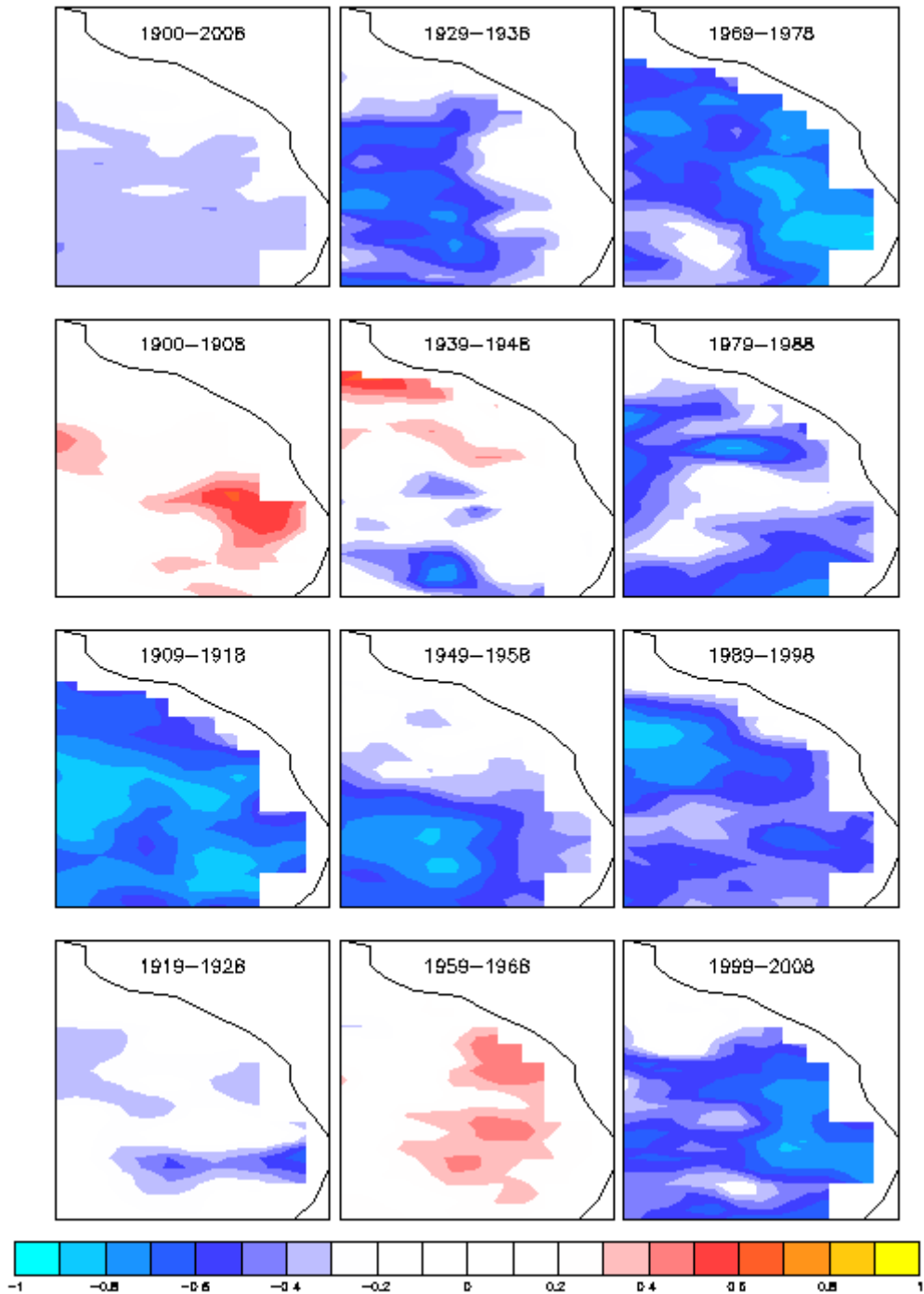


Figure 4.58: SEQ decadal correlation of DJF rainfall and EMI index.

4.4.12 Equatorial SOI (EQSOI)

As previously mentioned EQSOI (Figure 4.59) is very similar in characteristics to CTI.

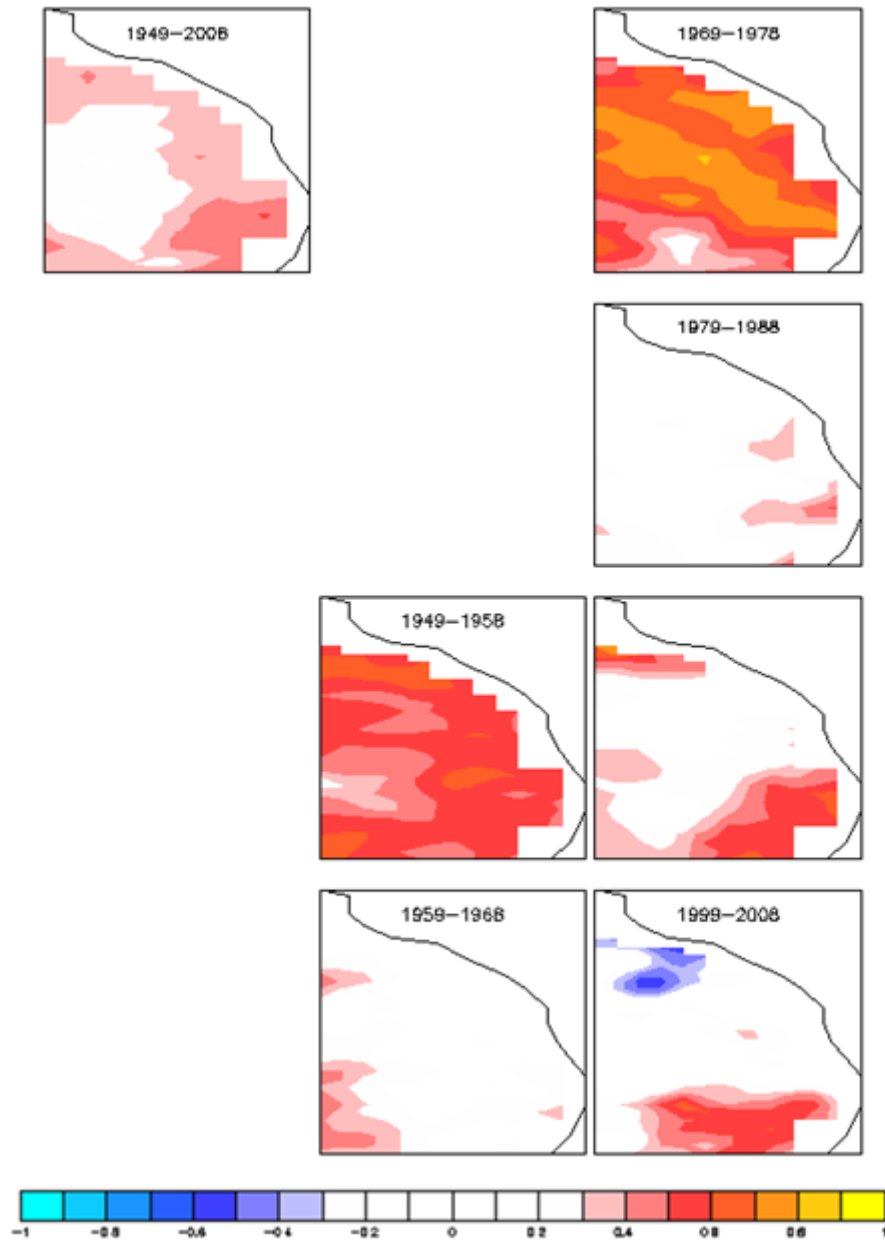


Figure 4.59: SEQ decadal correlation of DJF rainfall and EQSOI index.

4.4.13 FIVEVAR index

Fivevar attributes (Figure 4.60) were almost identical to the BEST index except for a lower population variance indicating a smaller range of correlation value.

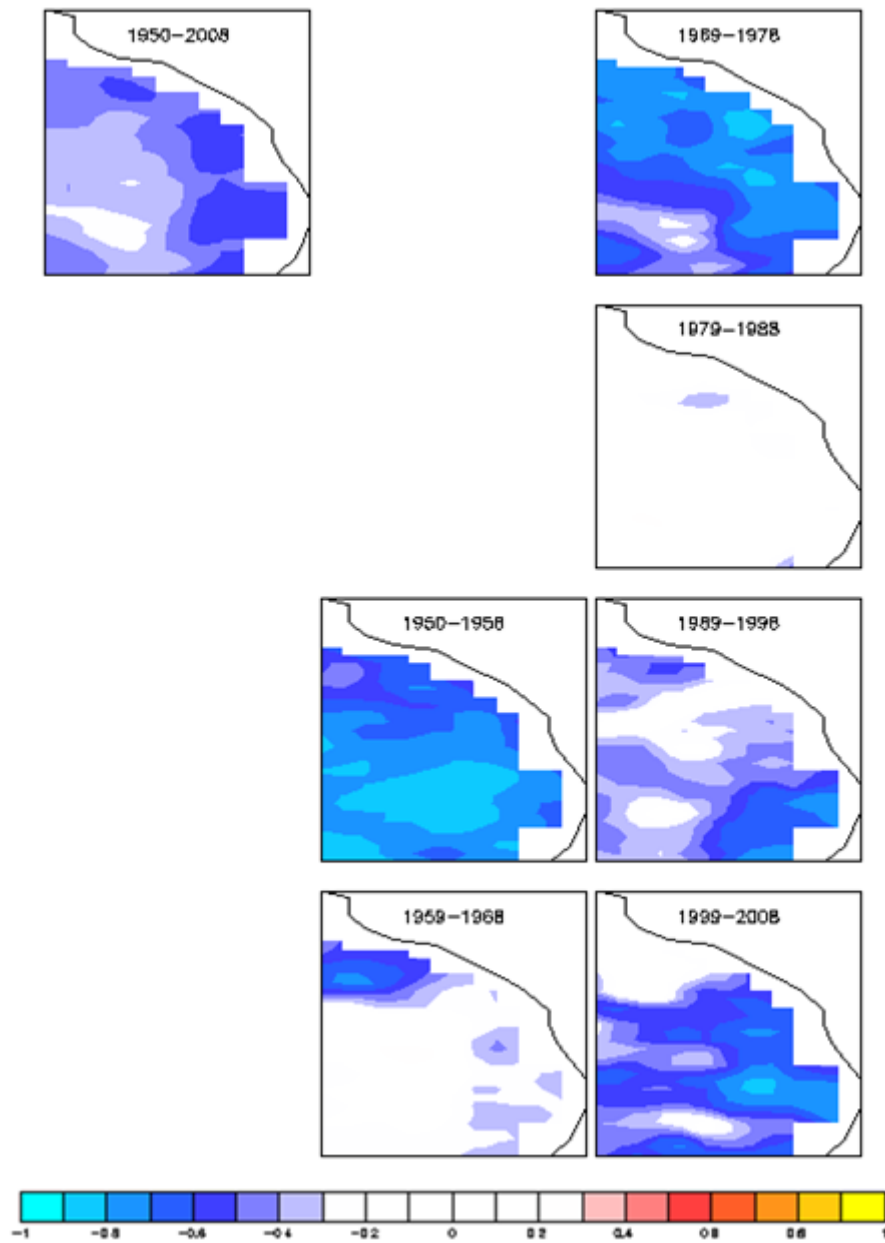


Figure 4.60: SEQ decadal correlation of DJF rainfall and FIVEVAR index.

4.4.14 Multivariate El Niño Index (MEI)

A mid ranking index the MEI (Figure 4.61) performed only slightly better than Niño3.4 and the SOI due in part to its high population variance. Had a longer time series been available the position might have improved with better decadal variance stability.

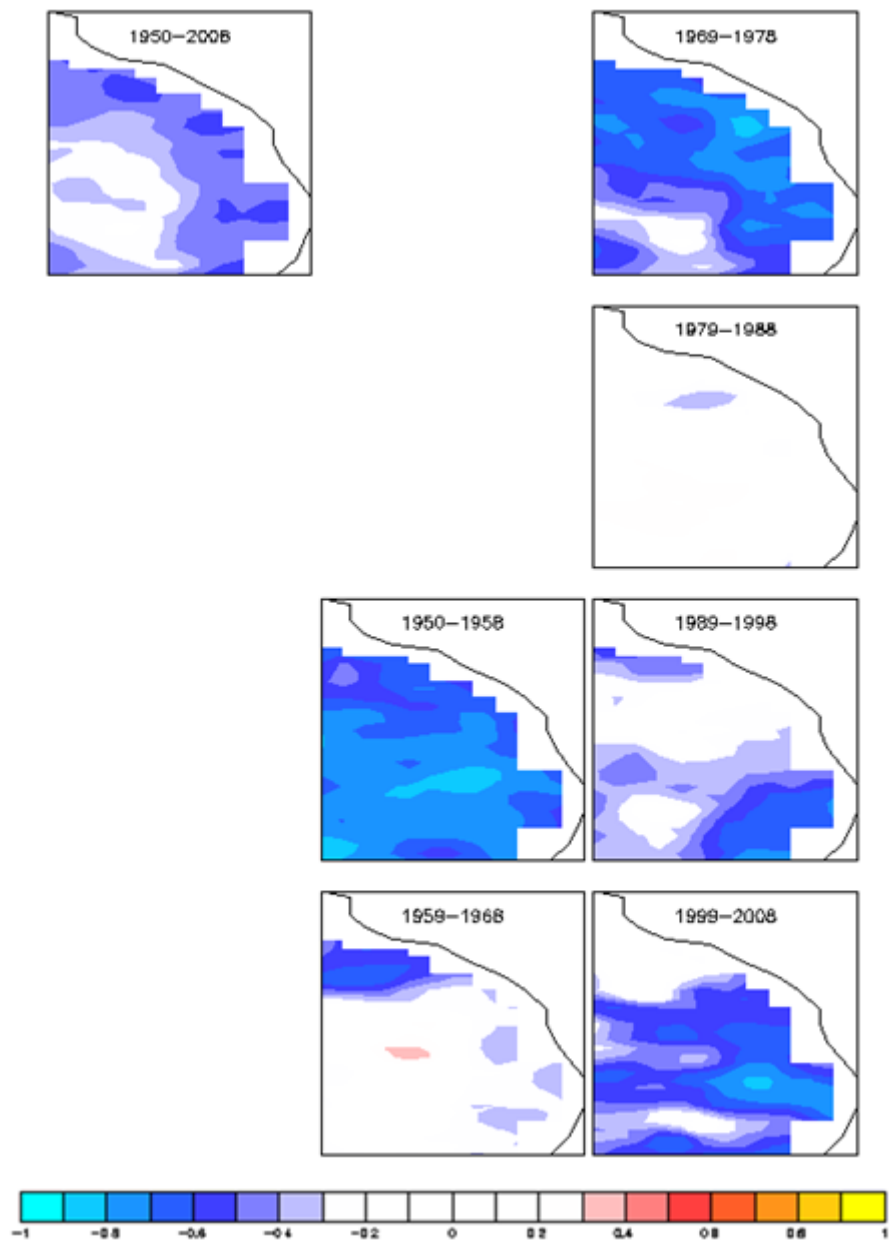


Figure 4.61: SEQ decadal correlation of DJF rainfall and MEI index.

4.4.15 Northern Oscillation Index (NOI)

As previously mentioned this index (Figure 4.62) is similar to and fits into the group of indices led by the BEST index.

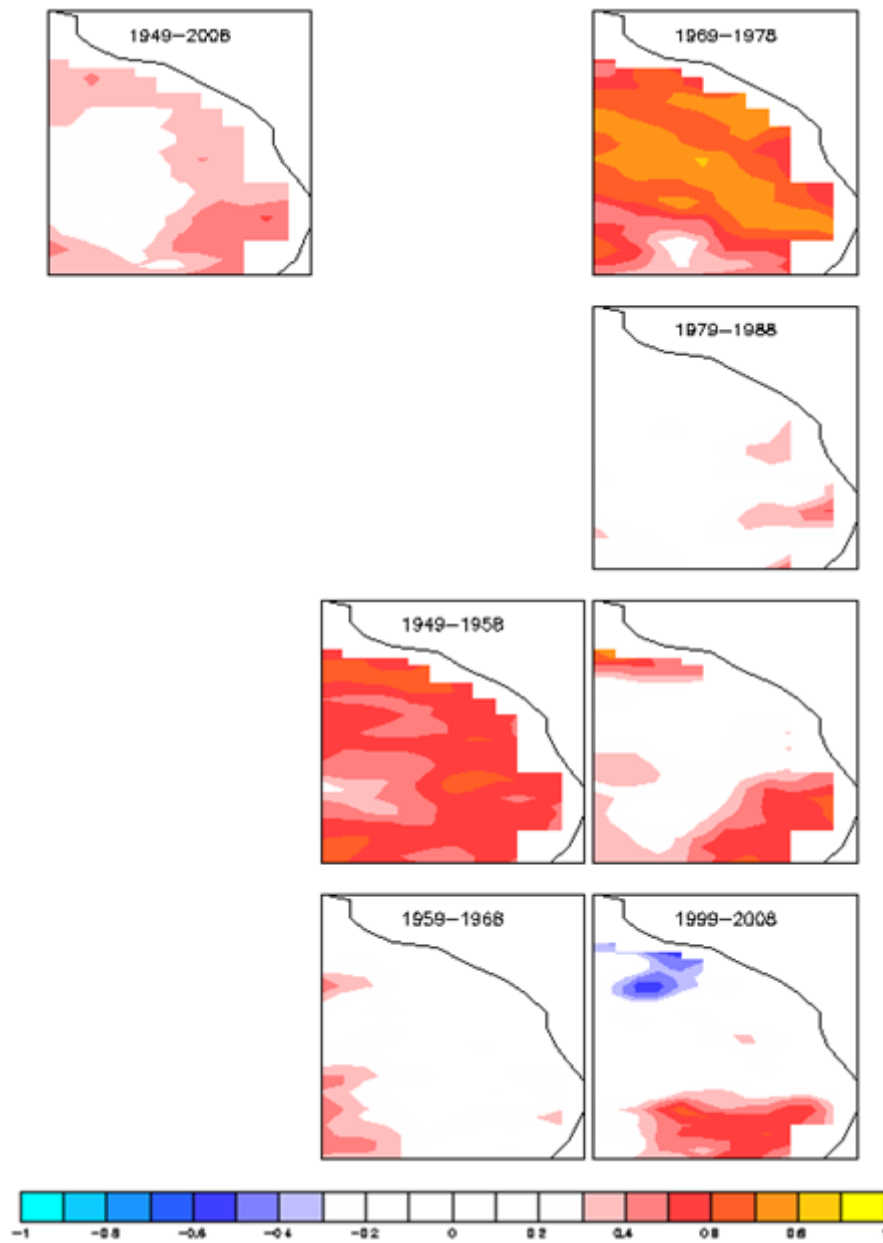


Figure 4.62: SEQ decadal correlation of DJF rainfall and NOI.

4.4.16 Tropical Pacific Empirical Orthogonal Function (TPEOF)

The same observation applies to the TPEOF (Figure 4.63) as to the NOI and others.

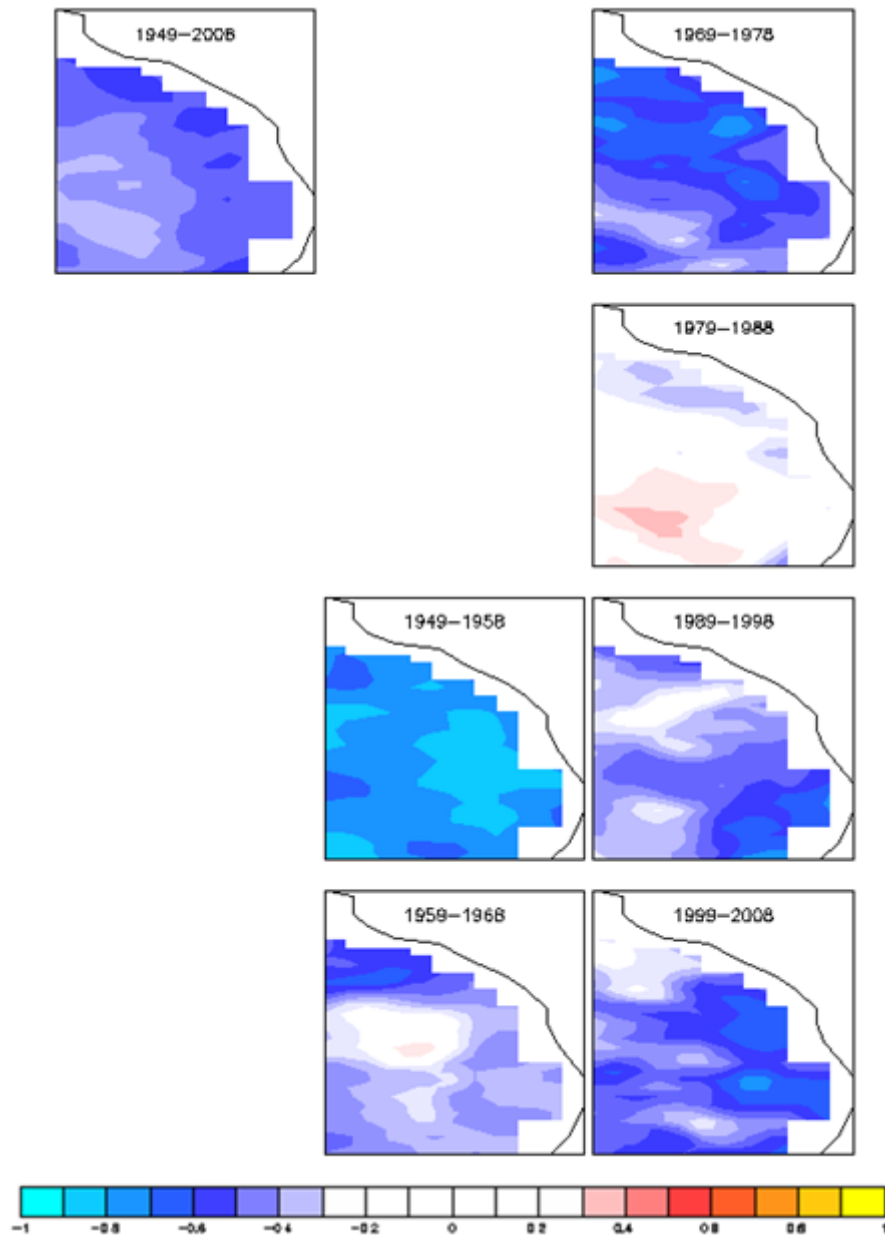


Figure 4.63: SEQ decadal correlation of DJF rainfall and TPEOF Index.

4.4.17 The Western Hemisphere Warm Pool (WHWP)

The two main attributes of the WHWP (Figure 4.64) were a high population variance (0.0139), area of significant correlation (44%) and temporal variance (same pattern for 67% of occasions).

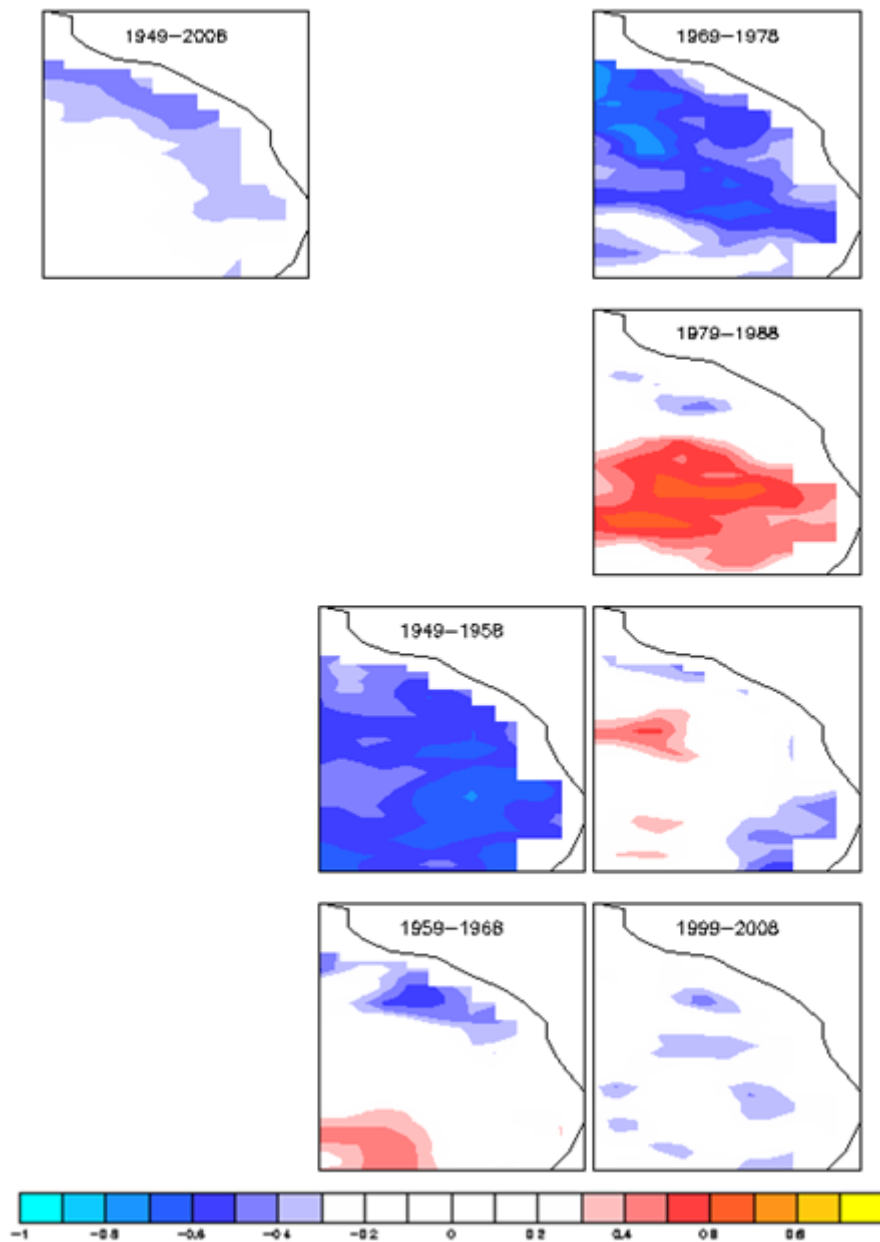


Figure 4.64: SEQ decadal correlation of DJF rainfall and WHWP Index.

4.5 Summary of South East Queensland Results

Table 4.7 and Figure 4.65 summarises the results of South East Queensland (SEQ) correlation of climate indices and decadal summer (December, January and February) rainfall. The traditionally used indices; Niño3.4 and SOI have performed quite differently in SEQ than in the Australian correlations achieving a lower middle order ranking. Possible reasons for this are discussed in Chapter 5 Discussion. Highest scoring index for SEQ was WWV_E by a considerable margin (Figure 4.65), but the other warm pool indices although generally having high population variance achieved lowest overall rank. Meridional indices AOI, its proxy NAO and SAM do not perform well for SEQ and together with the TNI have not been included in the analysis.

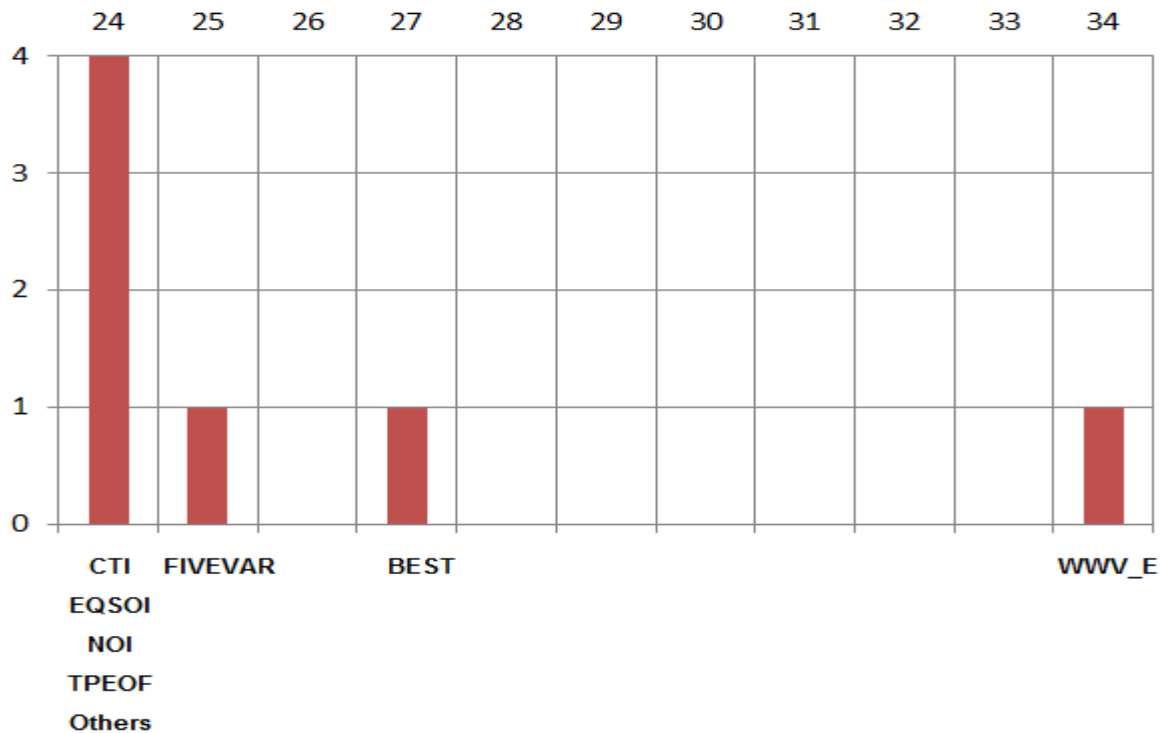


Figure 4.65: Pictorial representation of top SEQ indices

Table 4.7: South East Queensland decadal correlation results of climate indices and summer monthly rainfall.

Index	Population Variance		Decadal Variance		Correlation Area		Temporal Stability		Final score	
	Global	Score	Global	Score	Global	Score	Global	Score	Total	Rank
WWV_E	0.0083	4	5.5	10	58	10	91	10	34	1
BEST	0.0073	3	3	5	60	10	83	9	27	2
FIVEVAR	0.0027	1	3	5	61	10	83	9	25	3
CTI	0.0022	1	2.75	4	61	10	82	9	24	4
EQSOI	0.0067	3	2	2	59	10	83	9	24	4
NOI	0.0058	3	2	2	61	10	83	9	24	4
TPEOF	0.0072	3	2	2	61	10	83	9	24	4
MEI	0.0095	5	2	2	61	10	67	6	23	8
IPO	0.0033	1	2.75	4	61	10	73	7	22	9
SOI	0.0016	1	2.75	4	61	10	73	7	22	9
Niño3.4	0.0017	1	2.75	4	61	10	64	6	21	11
WHWP	0.0139	7	1.5	1	44	7	67	6	21	11
EMI	0.0043	2	2.75	4	61	10	73	4	20	13
PWP	0.0207	10	1.2	1	35	6	50	3	20	13
WWV	0.0116	6	5.5	10	18	3	36	1	20	13
IPWP	0.0172	9	2.2	3	28	5	45	2	19	16
WWV_W	0.0034	1	1.83	2	61	10	55	4	17	17

Chapter 5 Discussion, Conclusions and Future Directions

5.1 Overview

Several results from this study are found to be significant, expanding on the existing knowledge of the relationship between climate indices and rainfall. In particular the following key features of this thesis are:

- The BEST was the highest performing index within the criteria specified
- SOI having been in use for a long time is the best known and the simplest index which performs exceptionally well
- Many Equatorial warm pool (WP) indices adjacent to the Australian continent give strong correlation with Australian rainfall at decadal resolution.
- Without exception all available indices of climate irrespective of their Global source region provided a correlation with Australian rainfall at a decadal resolution.
- Derived ENSO indices, for example the BEST index highlight the relatively poor performance of the more empirically based Niño3.4 index.
- Changes in the atmospheric-oceanic circulations of the Pacific Ocean region have left a signature in many of the correlation results between climate indices and decadal DJF Australian rainfall.

This chapter discusses findings of this thesis and the extant literature. In Section 5.2, the performance of climate indices and Australian decadal rainfall is discussed. Section 5.3 is a discussion on how climate indices correlate to South East Queensland (SEQ) rainfall. Section 5.4 highlights geophysical considerations that effect decadal correlation and Section 5.5 investigates the factors such as bias, statistical significance and scientific rigor that have a significant impact on the study results.

5.2 Australia-wide Index Performance

This section focuses on the summary of the findings as shown in Table 5.1 which ranks climate indices on their performance in correlation with Australian summer rainfall at decadal

resolution. It is hoped that this might change the focus to inferences to help close the knowledge gap.

Columns two to five represent the comparative performance of the indices expressed as a mark out of 10 in terms of their performance (see Chapter 3, Data and Methods, Section 3.2.4) in terms of different assessment criteria. Column two uses population variance as a non-biased indicator of correlation range for whole time series. Similarly column three is a non-biased indicator of the stability of the variance of the correlation between decades. Column four represents the total area of the Australian continent for which significant correlation values was achieved. Temporal stability in column five represents the temporal persistence of the most significant patterns of correlation; column six is the total score achieved for all the criteria and column seven the overall ranking.

Table 5.1: Summary of the performance of 24 climate indices and their correlation with DJF Australian rainfall in respect to: population variance, decadal stability of variance, total area coverage of significant correlation, temporal stability, total score and overall ranking. Table is a précis of the summary in Chapter 4.

	Population Variance	Decadal Variance	Area Coverage	Temporal Stability	Score	Result
Index	Score	Score	Score	Score	Total	Rank
BEST	4	1	10	10	25	1
SOI	2	6	10	6	24	2
WWV_W	3	4	7	10	24	2
CTI	1	4	10	8	23	4
WWV_E	1	4	10	6	21	5
EMI	1	6	10	3	20	6
IPWP	3	6	5	6	20	6
PWP	10	1	7	2	20	6
FIVEVAR	4	3	10	2	19	9
TNI	1	10	7	1	19	9
TPEOF	4	1	8	6	19	9
IPO	4	2	9	3	18	12
SAM	3	1	9	5	18	12
WWV	3	6	6	3	18	12
AOI	1	1	9	6	17	15
EQSOI	2	3	10	2	17	15
MEI	4	1	9	2	16	17
Niño3.4	2	2	10	1	15	18
NOI	4	3	6	2	15	18
PDO	1	4	7	1	13	20
WHWP	3	3	5	2	13	20
IOD	3	1	2	5	11	22
NAO	1	3	2	2	8	23
QBO	1	3	1	2	7	24

In this study the BEST index gave the best overall performance when all the criteria were considered outperforming the other ENSO indices SOI, Niño3.4, CTI and EMI as well as the multivariate FIVEVAR, MEI and TNI. This is a surprising result as this index has usually been associated with US and North American climate and there are few significant studies linking it to Australian climate. Population variance for the BEST index occupies the fourth decile and if the result for PWP is excluded makes it a top performer. In terms of decadal variance stability the index sits in the lowest decile however.

SOI did remarkably well, ranking joint second in the study, its high performance in decadal stability both for variance and temporal stability perhaps explaining its longevity as a climate predictor for Australian rainfall. The meridionally orientated NOI (Schwing, Murphree & Green 2002) although having a high correlation to the SOI (0.77) perhaps indicative of a teleconnection with ENSO ranked only at 18th. Other meridionally orientated indices generally scored poorly with SAM at 12th rank and AOI 15th.

Near Australia warm pool (WP) indices (Figure 2.12) scored very highly in this study with four of them occupying the top six rankings. The WWV_W index whose region is shown in the left hand black rectangle, shared second rank with the SOI. WWV_W correlation maps were remarkably similar to the SOI pattern for many decades. IPWP region (within the blue square) and PWP region (brown square) were both ranked sixth. A little further away the WWV_E (right hand black rectangle) was ranked fifth. Even further away the WHWP (red dashed rectangle) achieved 20th rank. The high performance of the near WP regions is supported generally and to a partial extent by Schepen, Wang and Robertson (2011) who showed that micro regions within both the PWP and IPWP areas correlated well with rainfall in various parts of the Australian continent at a 29 year resolution. According to the literature the PWP has never been correlated to decadal Australian climate also making the study unique.

A very recent work does support the assertion of a strong relationship between near WP SST with Australian climate, Li, Yu and Li (2013) were able to show that increased SST in the tropical West Pacific accounts for 50% of the rainfall increase in North Australia over the past 33 years. Again, but to a lesser extent this assertion is backed up by the work of van der Ent and Savenije (2013) who found that the strongest source areas for continental precipitation are located adjacent to the continent in question. van der Ent and Savenije (2013) also found that with respect to Australia local SST had the biggest effect, but noted that ENSO related SST variations also played a role.

The PWP has a coincident Rain Pool (RP). PWP and RP are portrayed as being situated at the heart of the global climate system and described as its ventricle and atrium respectively (Chen et al. 2004). Considering the PWP region's intimate position relative to Australia it is remarkable that it has not been previously used for correlation with Australian climate.

Other authors have used IPWP data for correlation of climate in other regions, for example Wang and Mehta (2008) showed that the IPWP controlled; shallow tropical atmospheric circulation and the dynamics of both the Hadley and Walker circulation to affect DJF rainfall in the southern United States. This current study is unique in correlating IPWP and Australian decadal rainfall. There would seem to be a compelling reason to investigate parochial phenomenon such as WP SST that effect conditions at a remote situation on other continents but also demonstrate a profound local effect in respect to Australian summer climate.

Some indices that exhibited a long wave spectral signature, PDO and NAO did not fare well in the study and yet the IPO obtained the 12th rank. Close examination of the IPO periodogram shows that it has a spectral peak at ≈ 55 months which is coincident with the SOI (Figure 5.11) which may have influenced its performance.

5.3 South East Queensland Index Performance

The discussion in this section focuses on the summary of the findings as shown in Table 5.2, a listing of how climate indices perform in their correlation with SEQ summer rainfall at decadal resolution. It is hoped that this might change the focus to inferences to help close the knowledge gap. The highest performing index for this region was WWV_E one the furthest away WP regions from SEQ.

Local WP indices figure less prominently for SEQ than for the whole of Australia although IPWP, PWP and WWV achieved a greater maximum strength than WWV_E (Table 5.2). No work was found in the literature that links IPWP to SEQ rainfall. A signal of strongly increasing SST can be seen in the IPWP index (Figure 4.55) which explains its poorer decadal variance. In the case of PWP this is far more marked with a huge increase in SST during the period (Figure 4.44).

For the SEQ region the Niño3.4 index was outperformed by the derived Niño indices BEST, FIVEVAR, MEI and by the SOI. According to Murphy and Ribbe (2004) SEQ region is the land area within 147°E, the Australian east coast and lat 29 – 22.5°S (Figure 5.1) which

differs to that already stated (Cai & van Rensch 2012). This is quite an important observation because the east–west rainfall gradient is quite significant. Rainfall results vary depending on the definition or the region used thus providing a potential for bias in the correlation results. Klingaman, Woolnough and Syktus (2013) supports the observation of an east–west rainfall gradient more indirectly by stating that Queensland generally is under the influence of ENSO during the summer but in SEQ summer climate is driven more by on-shore winds and coastal tropical cyclones. It is therefore evident that dependent on the shape of the region chosen to represent SEQ; a different rainfall pattern might result which would help to explain the discrepancy between results. Murphy and Ribbe (2004) found for example that; Niño4 and Niño3 indices performed generally better than the SOI in the periods 1891 – 2000 and 1891 – 1945.

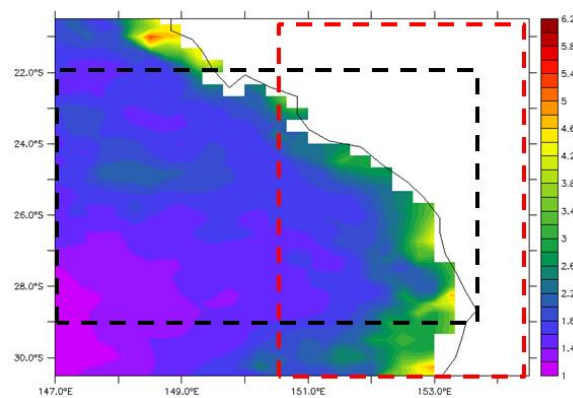


Figure 5.1: Typical SEQ decadal rainfall anomaly (2000 – 2010) in $\text{mm}\cdot\text{day}^{-1}$ emphasising the east–west rainfall gradient. The dashed red outline approximates the region of Cai and van Rensch (2012) and the dashed black rectangle to that of Murphy and Ribbe (2004).

Table 5.2: Summer (DJF) index performance for South East Queensland (land area within 20.5 –30.5°S, 150.5 –154.5°E after Cai and van Rensch (2012), the red dashed rectangle in Figure 5.1) with respect to: population variance, decadal stability of variance, total area coverage of significant correlation, temporal stability, total score and overall ranking. Table is a précis of the material in Chapter 4.

	Population Variance	Decadal Variance	Area Coverage	Temporal Stability	Score	Result
Index	Score	Score	Score	Score	Total	Rank
WWV_E	4	10	10	10	34	1
BEST	3	5	10	9	27	2
FIVEVAR	1	5	10	9	25	3
CTI	1	4	10	9	24	4
EQSOI	3	2	10	9	24	4
NOI	3	2	10	9	24	4
TPEOF	3	2	10	9	24	4
MEI	5	2	10	6	23	8
IPO	1	4	10	7	22	9
SOI	1	4	10	7	22	9
Niño3.4	1	4	10	6	21	11
WHWP	7	1	7	6	21	11
EMI	2	4	10	4	20	13
PWP	10	1	6	3	20	13
WWV	6	10	3	1	20	13
IPWP	9	3	5	2	19	16
WWV_W	1	2	10	4	17	17

5.4 Atmospheric-Ocean effects on Decadal Correlation

Several authors listed on the time line (Figure 2.19) document observed changes in the Pacific environment both tropical and extra tropical that could have an effect on Australian climate occurring in the latter half of the 20th century. These changes which are summarised symbolically in Figure 2.20 include the PDO, Meridional Overturning Circulation, SST increase in the West Pacific Warm Pool, change in the SOI and changes in Australian

rainfall. In correlation between climate index and precipitation these multi-decadal changes are sometimes evident in the results.

5.4.1 Meridional Overturning Circulation

A factor that affects the wind driven shallow Meridional Overturning Circulation (MOC) in the tropical Pacific Ocean is known to be the PDO (McPhaden & Zhang 2004). MOC is composed of the sub-surface Equatorial transport of water which takes approximately 10 years (McPhaden & Zhang 2002) with upwelling near the Equator and consequent upper divergent flow. During the latter part of the 1970s MOC underwent a regime shift (McPhaden & Zhang 2002) being subjected to a marked reduction causing the Cold Tongue SST to rise in temperature by approximately 1°C. The CTI time series in Section 3.2.2, Climate Indices CTI seems to show this. At the end of the 1990s the normal state with respect to MOC was restored but with an associated increase in the speed of tradewinds. Unfortunately the IPCC AR5 WG2 does not have anything specific to relate to Pacific MOC confining its comments to Atlantic MOC (IPCC 2014). How or why this change occurred is still subject to conjecture. Modelling appears to show that it might just be the residual of decadal modulation in the statistics of ENSO variation (Kirtman & Schopf 1998).

In this study it was found that the majority of indices correlation with Australian rainfall underwent a change in the last two decades of the 20th Century. This was evident by a significant reduction or even reversal of sign of the correlation pattern. Indices so affected were SOI, BEST, CTI, EQSOI, IPO, IPWP, MEI, Niño3.4, FIVEVAR, TPEOF, NOI, PWP, WHWP, and WWV_W. It is impossible to draw a link between the change in sign of these correlations and the MOC regime shift, but merely point out that it may possibly be a causal factor.

5.4.2 Sea Surface Temperature Increase

The PWP and IPWP indices are both based on SST/ocean heat content and both show an increase in SST over the last four decades of the 20th Century (Cravatte et al. 2009). It is possible that this represents a global warming signature via greenhouse gas increase although there is extreme doubt that a signature could be extracted from the data given how quickly the trends can reverse due to natural variation (McPhaden & Zhang 2004). However, changes in

IPWP SST have a profound effect on atmospheric deep convection and both the Hadley and Walker Circulations (Wang & Mehta 2008).

5.4.3 Change in Southern Oscillation Index

A long term negative trend in the SOI was noted to begin in 1976 (Trenberth & Hoar 1996), whilst Suppiah (2004) showed SOI had decreased strongly since the 1970s year period due to a 20 year cumulative pressure increase in Darwin whilst Tahiti pressure had remained relatively stable in the same period. Later this was also shown by Power and Smith (2007) and Nicholls (2008). To see what effect, if any, such variation had on the correlation of SOI and rainfall SOI data were modified by the removal of its decreasing linear trend as described by Trenberth and Hoar (1996). These data were then correlated to Australian rainfall and the results compared with the unmodified data series correlation are shown in Figure 5.2. The difference between the two cases is almost indistinguishable. It could therefore be argued that this change in the SOI has not materially affected correlation with Australian decadal rainfall using the windowing technique described at 3.2.3.1. Furthermore a topical study (L'Heureux, Lee & Lyon 2013) back up this assertion by showing that when a 10 year moving window was used there is no significant change in MSLP either for Indonesia or for the east tropical Pacific in respect of the SOI in the last 110 years. L'Heureux, Lee and Lyon (2013) used outputs of 10 reanalyses of west (Indonesian) and east (east Pacific tropical Ocean) MSLPs which are loosely analogous to the situation in Darwin and Tahiti (Figure 5.3). However when moving windows of greater than 10 years were used, a declining trend in the Indonesian MSLP and an increasing trend in the east Pacific MSLP emerged. This would indicate a tendency towards a stronger Walker Circulation tending towards a greater instance of La Niña situations.

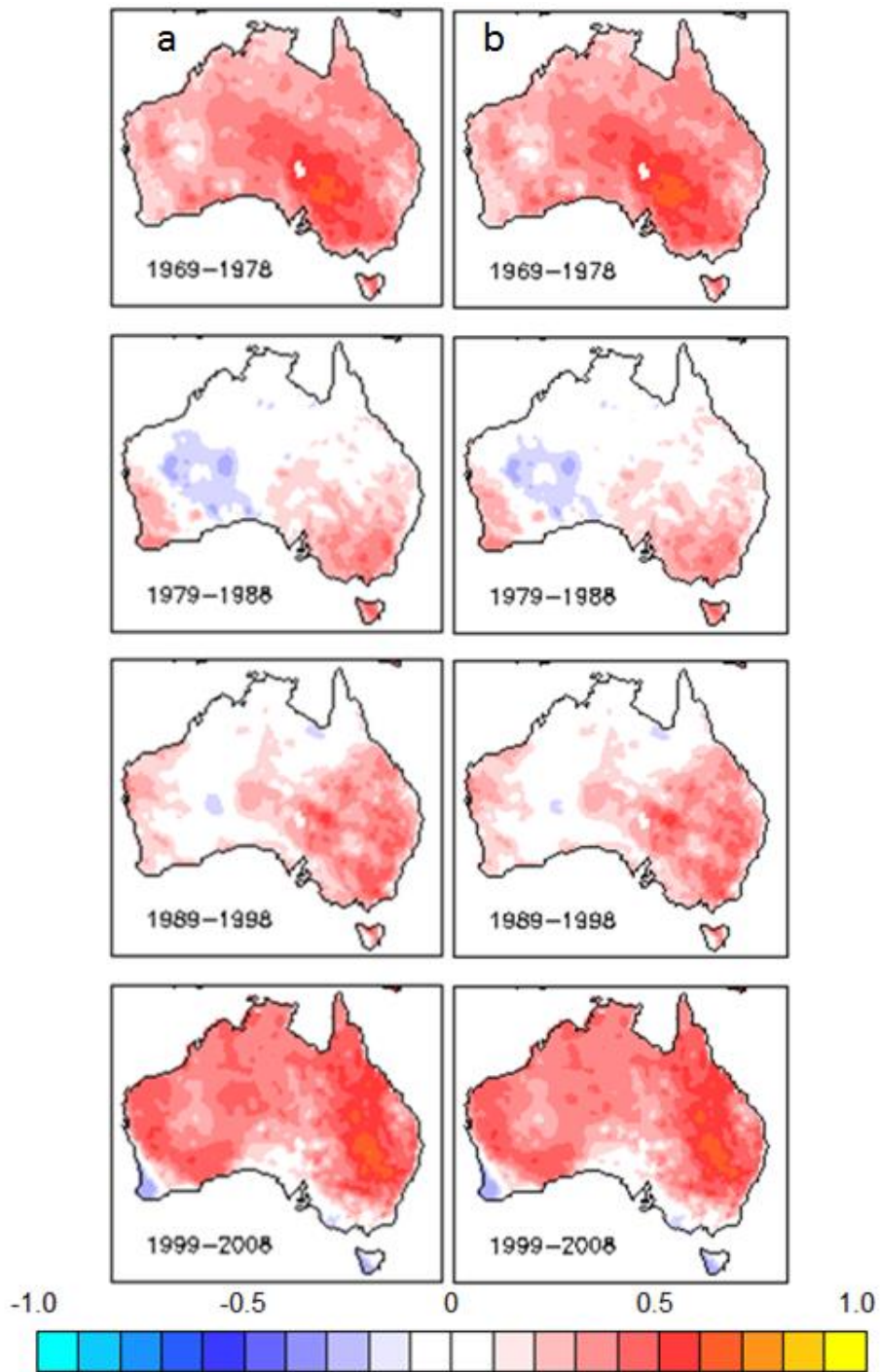
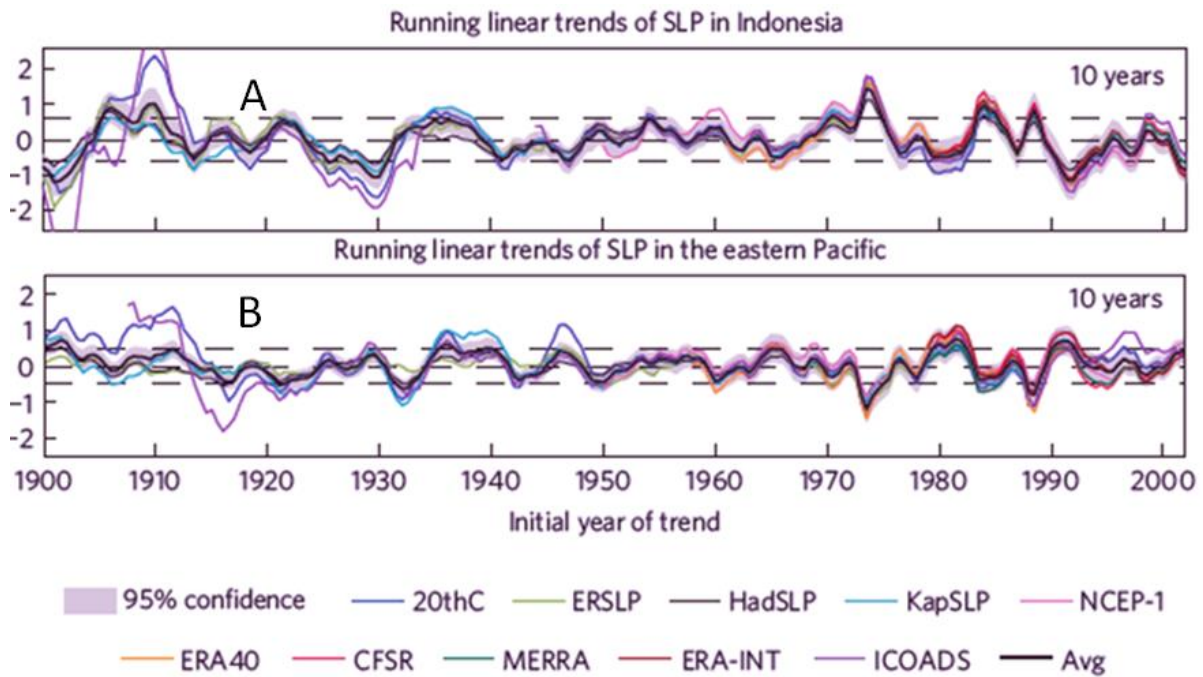


Figure 5.2: Correlation of SOI with Australian decadal rainfall 1969 – 2008. a) Basic bandpassed SOI data. b) Fully detrended, bandpassed (both SOI and rainfall matrix) data for the period discussed by Trenberth and Hoar (1996)



SLP linear trends for 10 and 40-year moving windows from January 1900 to December 2011.

A : trends for the region over Indonesia (110–160 °E, 10 S–10 °N)

and B: for the region over the eastern Pacific Ocean (130–80 °W, 10 S–10 °N).

SLP is expressed as the change (hPa) over the window length. Grey shading represents the 95% confidence level based on a two-tailed Student's *t*-test. The dashed, horizontal lines represent the 95% range of trends based on 1,000 synthetic AR(1) time series. The x axis shows the initial year of the trend (for 10-year windows, 1950 denotes the 1950–1959 trend).

Figure 5.3: Ten year linear trends of Indonesian and east tropical Pacific Ocean MSLP using ten sets of independent reanalysis data; L'Heureux, Lee and Lyon (2013).

5.4.4 Change in Rainfall

A decreasing SOI associated with increasing Darwin MSLP which from first principles alludes to decreasing rainfall for north east Australia (Figure 2.5). Certainly there appears to be some evidence for this in the SEQ decadal rainfall anomaly (Figure 4.33a) from the 1980s onwards and a slight decrease is evident in the Australia DJF case (Figure 4.2).

With respect to Queensland this assertion is backed up by Klingaman, Woolnough and Syktus (2013) who could not find any linear rainfall trend between 1900 – 2010 and who instead state that it is subject to shorter term variability and not a long term evolving trend.

5.4.5 Short Summary of Phenomena Effecting Decadal Correlation

The mid 1970s was singled out by many authors as a time for dramatic shift with the synchronisation of major climate modes (Figure 2.21). In the previous sections some observations have been made as to the likely effect of these climate modes acting through their indices on Australian decadal rainfall correlation. It is however very difficult to ascribe a particular change in conditions to any one particular event in such a complex and inter-related system (Solomon & Newman 2012) and it falls beyond the remit of this study to investigate the geophysical effect on Australian rainfall variability to any greater depth beyond that already discussed.

5.5 Factors Affecting the Study Metrics

In this section factors which might affect the validity of the results are discussed in terms of whether the decadal viewpoint is the best aperture through which to view climate variability or if indeed a more natural interval with respect to climate mode might be better. An example of a more natural window and its effect on results is given. The effect of a different gridding arrangement is also considered as is the validity of the statistical significance. It is also noted that spectral windowing can profoundly alter the representation of data time series.

5.5.1 The Observational Framework

Within the research period (1900 – 2008) the time period over which the variables of interest are viewed is sensitive to resolution. Australian precipitation anomaly at a decadal resolution is very feint.

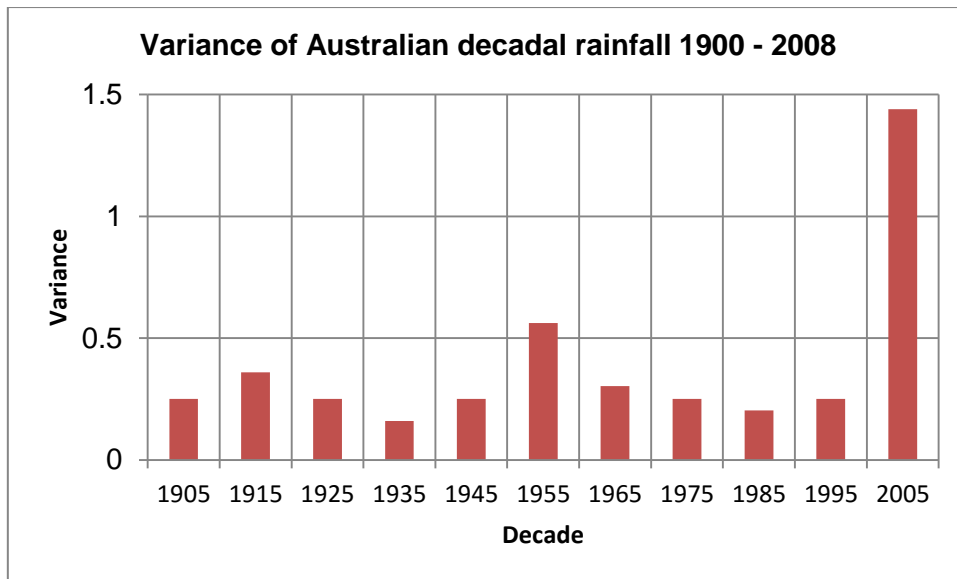


Figure 5.4: Variance of Australian area averaged decadal rainfall anomaly 1900 – 2008

Figure 5.4 shows the variance of the decadal rainfall anomaly. Here it is apparent that for six of the 11 decades the variance was at or below 0.25 and in only two decades variance exceeds 0.5 (1950s and the 2000s).

The term decade in the human reference frame is an artificial construct usually representing, for example the years between 2010 and 2020. Information might be better collated in a reference frame that includes a cycle of significant climate modes (Tsonis, Swanson & Kravtsov 2007). One might use the IPO or even a complete ENSO cycle to obtain a more balanced view of the situation. To investigate this point consider ENSO variability, Table 5.3 lists two similar decades; yellow on the left 1905 – 1914 and green on the right 1909 – 1918 where nominal Niño 3.4 indices are shown (Giese & Ray 2011). As can be seen 1905 – 1914 is more ENSO neutral whilst 1909 – 1918 is more influenced by La Niña (negative residual). This situation affects the decadal correlation quite considerably (Figure 5.5) a four year difference can influence correlations and variances over a whole decade. One can see that on the right at b) a La Niña decade in east Australia is depicted whereas at a) a more ENSO neutral situation is shown. More information might be mined from the situation by using a period based on low frequency climate modes rather than a decadal resolution.

Overall the rainfall data used in this study (Jones, D. A., Wang, W. & Fawcett, R. 2009) were excellent but had a minor shortcoming with respect to gridding. Figure 5.6 shows an on the whole acceptable representation of the Australian land area by using the ETOPO bathymetry data matrix (Smith & Sandwell 1997) as a mask to suppress output from ocean regions. The

whole of Australia correlation in this study therefore used this but a white margin is noticeable over eastern coastal aspects of Australia especially in Tasmania. This problem with the ETOPO data gridding made the method unsuitable for some applications (Smith 1993) where closer examination reveals the white margin on all eastern facing coastal regions becomes significant.

Table 5.3: A comparison of two decades of ENSO observations grouped by colour. Green cells group a decade according to ENSO prominence; yellow cells represent an arbitrary defined decade using indices obtained from Table 1 in Giese and Ray (2011). The blank cells represent absence of data.

	1905 - 1914	1909 - 1918
1905	1.4	
1906	0.4	
1907	-1.5	
1908	-1.5	
1909	-1.5	-1.5
1910	-1.5	-1.5
1911	0.3	0.3
1912	1.8	1.8
1913	1.2	1.2
1914	1.2	1.2
1915		1.2
1916		-2.1
1917		-2.1
1918		-0.4
Residual	0.3	-1.9
Tendency	ENSO neutral	La Niña

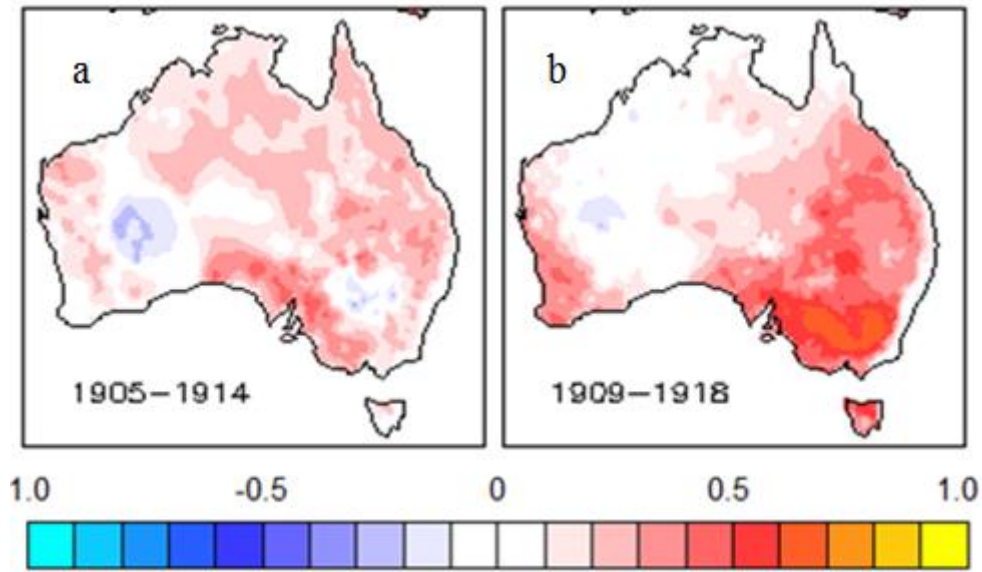


Figure 5.5: Effect on SOI of a natural reference frame as opposed to a human one. a) 1905 – 1914 containing a more natural ENSO cycle. b) 1909 – 1918 artificial reference frame capturing La Niña dominance.

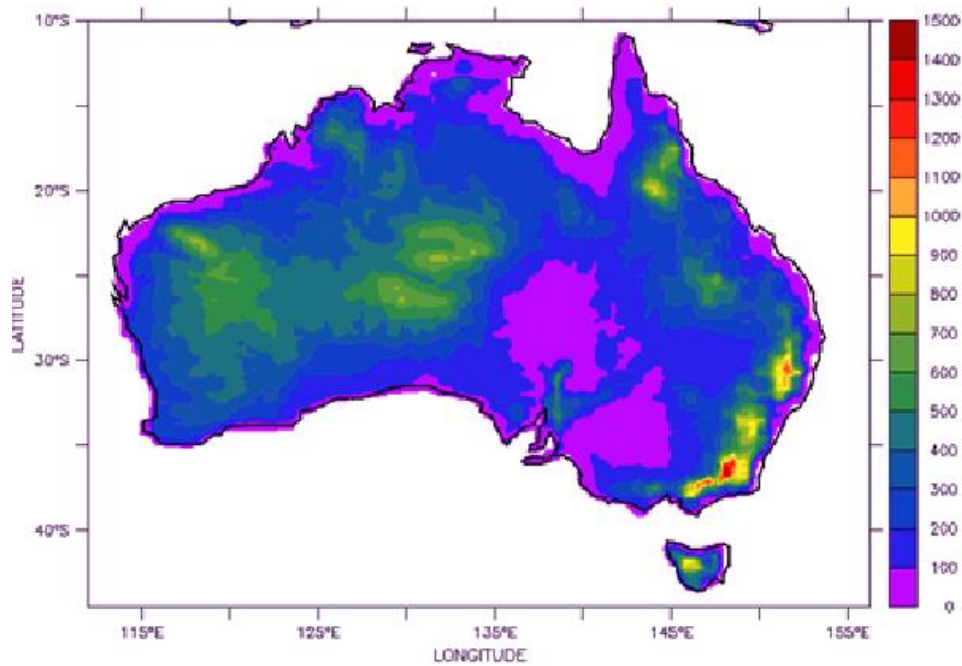


Figure 5.6: Current Australia relief map (terrain altitude m) using the latitude and longitude register produced from the Australian weather and rainfall data set (Jones, D. A., Wang, W. & Fawcett, R. 2009).

Consider the South East Queensland (SEQ) region as used by Cai and van Rensch (2012) encompassing 20.5 – 30.5°S, 150.5 – 154.5°E (Figure 5.7). The use of the mask for

calculating mean correlations in the region could be in error as $\approx 7\%$ of the land is missing. This immediate coastal area has the highest rainfall amounts; often three times that of more inland regions (Figure 5.1). An opposite problem is shown (Figure 5.8) in Western Australia where too much land is represented effecting output significantly. A final spatially-resolved aggregated index will have to deal with these inconsistencies to be a true indicator of rainfall for a particular geographical region.

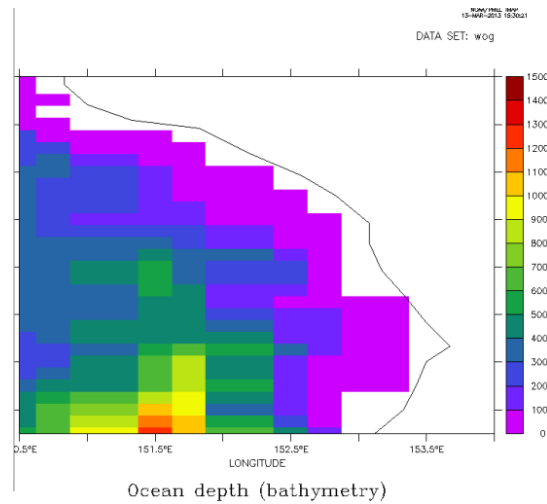


Figure 5.7: The region of South East Queensland; after Cai and van Rensch (2012).

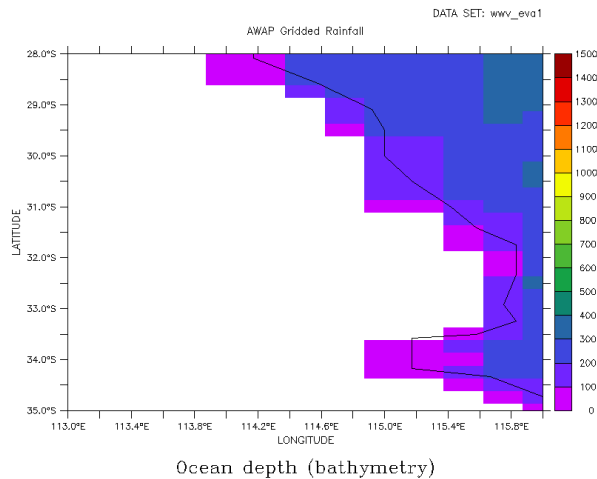


Figure 5.8: Region of Western Australia

Initially to achieve a higher skill for this study bathymetric masking of the sea adjacent to the SEQ coast was dispensed with and a mask matrix constructed in MATLAB was used. In

practical terms the difference in correlation was found to be insignificant so the bathymetry method was retained.

5.5.2 Statistical Significance

The literature is quite disparate on the statistical significance of climate fields and smoothed Pearson's 'r' tests. Some like Bretherton et al. (1999) reason that the effective degrees of freedom (EDoF) are reduced whilst others; Fraedrich, Ziehm and Sielmann (1995) assert that they are increased and are further enhanced when bandpassed data are used. Wallace, Cheng and Sun (1991) used a Monte Carlo technique to add validity to their results.

In this study validation of the method was performed using synthetically generated data. The raw time series were designed to have a monthly temporal resolution and normal distribution. The raw time series were generated and then filtered using the method outlined in chapter 3. These data were compared with the filtered area averaged monthly rainfall over Australia for each decade. This represents a test of random data against extremely low spatially resolved gridded rainfall data. The random synthetic indices were correlated using Pearson's r method with the rainfall in the same manner as shown in chapter 3. Figure 5.9 shows the distribution of Pearson's r for each decade using an aggregate of 10^6 data sets each 120 years long. Overlaid is the fitted distribution of Pearson's r for filtered data and the equivalent of 2σ for a pseudo-Gaussian fit of the correlations. This shows a significant feature of consequence to this thesis; correlations of the filtered data at the decadal level need to be high to be a "true" correlated index. In this case, correlation of approximately $|r| > 0.60$ is required to reach the equivalent of 2σ for whole year data. For DJF month rainfall this cut-off increases to $|r| > 0.68$.

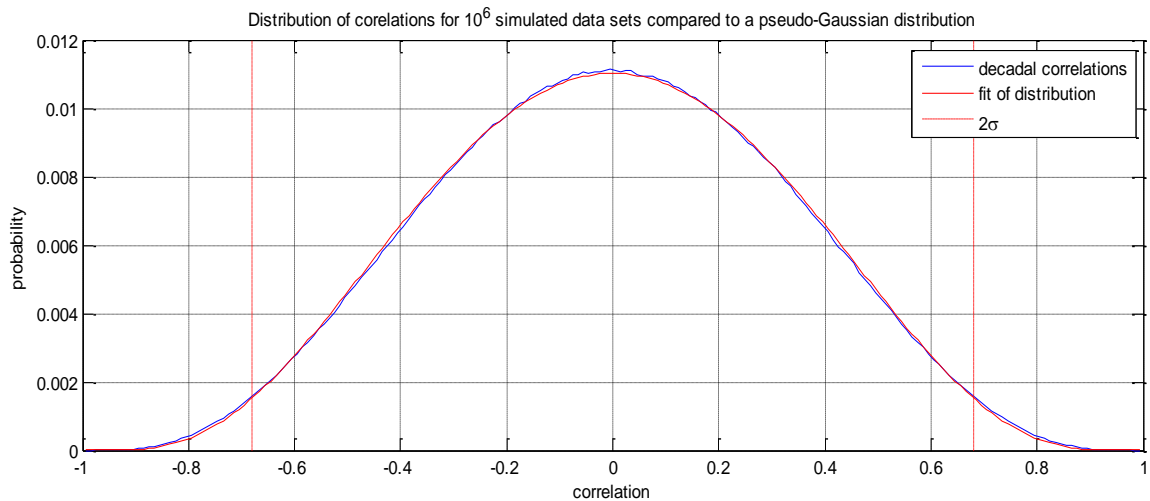


Figure 5.9: Blue line shows distribution of Pearson’s r for each decade using an aggregate of 10^6 data sets each 120 years long. Red line shows the fit distribution of Pearson’s r for filtered data and in red dashes the equivalent of 2σ for a pseudo-Gaussian fit of the correlations.

Consider a continuous sequence of randomly generated (but filtered) decades over the observation period. The correlations need to be robust not just over geospatial Australia but also geo-temporal (a time series at a spatial grid point in) Australia. A continuous index should be in robust correlation with rainfall if it is significantly correlated over a 120 year period. Figure 5.10 shows the distribution of the average correlation of the simulated and filtered decadal data over a continuous 120 year periods and a fit of the distribution using a Gaussian function. Overlaid is a demarcation at 2σ of the Gaussian fit. Using a two-tailed selection criteria an index is likely not a random sequence if the mean of the sequence of 11 decadal correlations (of DJF month data) is $|r| > 0.20$. Using the same criteria for sequence of 6 decadal correlations: $|r| > 0.25$. Thus for a single spatial grid point over the entire observation period in Australia an average of correlation magnitude over ~ 0.23 will in general relate to observable behaviour on timescales longer than a year (due to the filtering).

Two sets of criteria have been found for DJF correlated data sets: (1) Magnitude of correlation between a simulated random index and DJF rainfall for isolated decades of greater than 0.68. (2) An aggregate magnitude of correlation over 6 and 11 consecutive decades of 0.25 and 0.2, respectively. As a note for completeness, over the same 6 and 11 decade periods correlations of 0.22 and 0.18 were needed for whole year data.

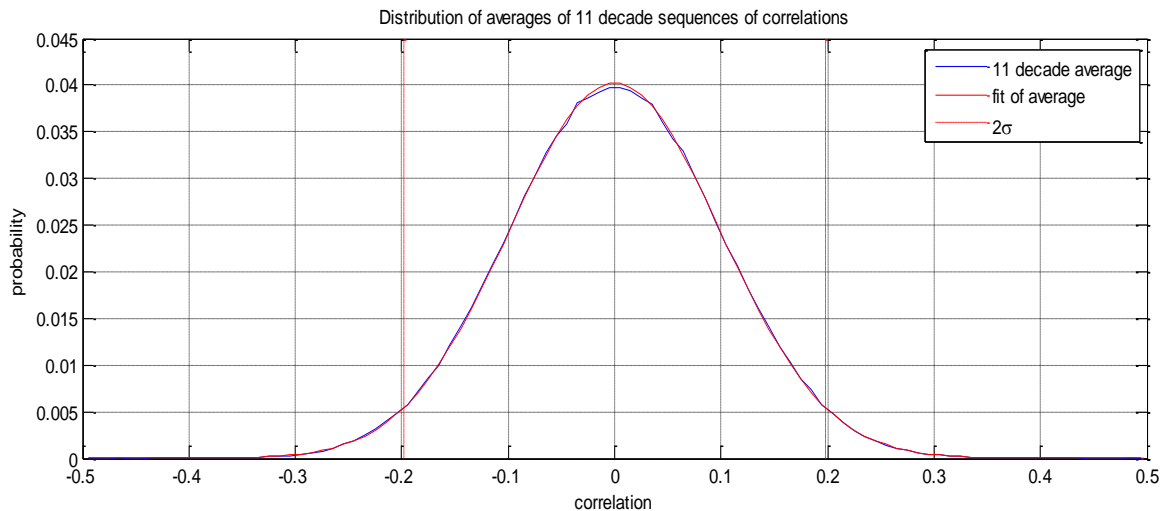


Figure 5.10: Blue line shows the distribution of the average correlation of the simulated and filtered decadal data over a continuous 120 year period and in red the fit of the distribution using a Gaussian function. Overlaid (red dashes) is a demarcation at 2σ of the Gaussian fit.

The conclusion from this study of significance is that results meeting these criteria should not have been realised purely by chance and the 28 DoF used in the study is prudent.

5.5.3 Spectral Significance

Fast Fourier Transform periodograms showed that both the SOI and IPO had a strong spectral signature at 55 months. When one compares the two indices using this signature it reveals how very closely they compare with each other (Figure 5.11).

In addition the SOI and IPO relationship brings up another point of interest where it should be noted that statistical methods exist whereby the truncation at the ends of interdecadally varying time series can be minimised (Kennedy 2008). Kennedy (2008) demonstrated such a technique at the UK Met Office by extending the series end values out in time to beyond half the spectral width of the window used. A similar method is shown in the Wavelet Toolbox users guide (MathWorks 2007) where the ends of time series can be padded with zeroes. This might prove to be of great benefit to other researchers to make maximum use of the available data.

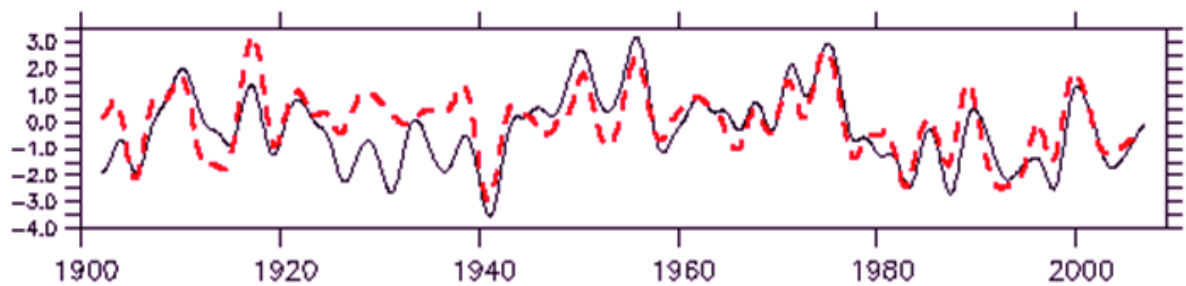


Figure 5.11: 55 month smoothed time series of SOI (black) and inverted IPO (red).

5.5.4 Performance Criteria

The criteria used to assess the performance of the indices were chosen to give the best overall picture and wherever possible unbiased indicators were used. It should be appreciated however that these criteria are a compromise when dealing with a large variety of indices and a diversity of regions.

Consider population variance for example, a large region like the continent of Australia is divided into six different climate regimes (Figure 2.2) so a large population variance is more able to capture the associated different correlations that might occur in them. This might prove to be a disadvantage in a smaller region such as SEQ where a significantly similar correlation value might provide more information.

Area of significant correlation results is irrefutably a most important criterion providing useful information to certain sections of society to assist in decision making. Decadal variance stability is a property that emphasises the robustness of the correlation results over time so is again an important criterion.

Interpretation of temporal stability is somewhat two edged as it could be argued that correlation is robust under a changing climate regime. Alternative it may be argued that correlation pattern is reacting to the changing climate regime.

Outside the framework of this study clearly there are many other criteria which might prove more important than those used.

5.6 Concluding Remarks

The premise, methods, results and conclusions of this thesis are outlined in the following points:

1. This research is premised on the fact that climate indices can have high correlations with observables such as SST and rainfall. It follows that climate indices can correlate to Australian rainfall to a great degree. However, not all indices will correlate with rainfall to high degree. This study was designed to determine which climate indices have robust correlations to Australian rainfall and especially SEQ rainfall.
2. In this study 24 climate indices and Australian rainfall were subjected to bandpass filtering to remove interannual and intraannual variability and correlated using a Pearson's "r" procedure. Climate indices and Australian rainfall were analysed using this procedure on a decadal basis from 1900–2008 for whole year and DJF rainfall. A subset of these indices included those utilised previously by other authors and those that by inspection showed suitable potential were then correlated with SEQ rainfall. Correlation range is not a non-biased indicator. Data performance was assessed by the rank of: population variance, decadal variance, area of coverage, and temporal stability before obtaining a final ranking.
3. The results show that in addition to SOI and Niño3.4 scoring only two for population variance, one of the near Australia oceanic warm pool indices the PWP achieved a 10 and the derived ENSO indices, BEST, FIVEVAR and MEI scored four. With respect to SEQ WWV_E was ranked first being the best all round index by a considerable margin whereas SOI and Niño3.4 could only achieve ninth and 11th ranking respectively.
4. The significant results show that more indices than have been currently demonstrated in the literature can have an equivalent or better correlation with Australian and SEQ DJF rainfall than the more frequently utilised indices for example, SOI and Niño3.4. SOI possibly the oldest and simplest of climate indices did remarkably well for the whole of Australia no doubt due to its reflection of the state of the Walker Circulation.
5. Based on the results shown there is scope to more fully investigate the relationship of Australian rainfall and global climate indices.

5.6.1 Possible Future Work

Cross correlation between different pairs of climate indices can vary. An example of high cross correlation would be that between the SOI and the Niño3.4 index (Figure 3.9) and both are frequently used for correlation with Australian regional rainfall. The combination of these indices, the BEST index was the highest performing index in this study. Paired with another index the SOI with the PWP for example has a significantly poorer cross correlation but both demonstrate strong correlation with SEQ rainfall. This unique observation indicates a potential for using such poorer correlating pairs for better overall performance for rainfall prediction.

In the same vein the use of spectral analysis to quantify climate indices shows potential. Consider the SOI and IPO where a common spectral peak is shown to be 55 months. If the two time series are given a minimum of manipulation IE the IPO signal inverted and both subjected to a 55 month Lanczos filter and compared (Figure 5.11) it is found that two completely different indices have several points of commonality over the time series range. This may throw some light on the suspected modulation of SOI correlation with SEQ rainfall as modified by the IPO as alluded to by previous authors (Cai & van Rensch 2012). It also opens up the intriguing possibility of constructing artificial climate indices by the use of Wavelet Analysis (Webster & Hoyos 2004).

The research performed here shows that many diverse indices can have high correlation with rainfall to statistically significant levels. The mechanism behind these correlations still needs investigation in many cases.

Decadal scale analysis should continue but with the introduction of lagged correlation to investigate predictive ability.

The use of WP indices need to be investigated in terms of their short term predictive ability in terms of Australian rainfall rather in the fashion demonstrated in the prediction of Indian Summer Monsoon onset (Rajeevan & McPhaden 2004) where WWV performed excellently. These indices have never previously been used for the purpose.

Appendix I

One possible treatment of climate indices and rainfall is by using the normal computational recipe (CR) (von Storch & Zwiers 2001) where monthly climatologies are removed from the data series to leave an anomaly compared to a 30 year base period. Anomalies can also be calculated by removing long term cyclic signals. A filter, provided that the cut-out frequencies include the cyclic signal, can simulate much of the same effect of calculating an anomaly. Figure A.1 shows average Australian rainfall during the target period of this study; one plot depicts the yearly cyclic rainfall and the other is reduced to rainfall anomaly through subtraction of the monthly climatology.

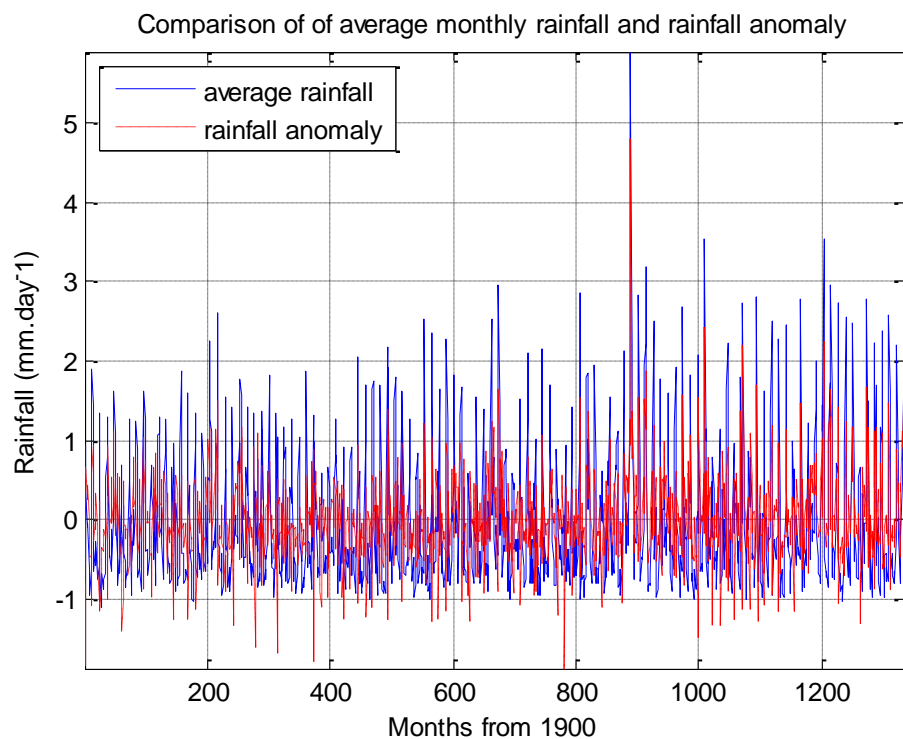


Figure A.1: AWAP monthly rainfall and anomaly

Over the course of a year the average rainfall has large deviations due to ordinary seasonal variation. The anomaly does not. Figure A.2 shows the comparison between the normalised FFTs of the unfiltered and filtered rainfall and anomaly. Figure A.3 shows the signal power (and phase which is not shown as it appears as a mess of 'random' phases) of the FFTs, it is apparent that almost all the content of the unfiltered signals is unchanged by the subtraction of the anomaly. Thus one can be confident that by filtering out this frequency component by using a Fourier window a similar result will be obtained from both the raw rainfall and anomaly data.

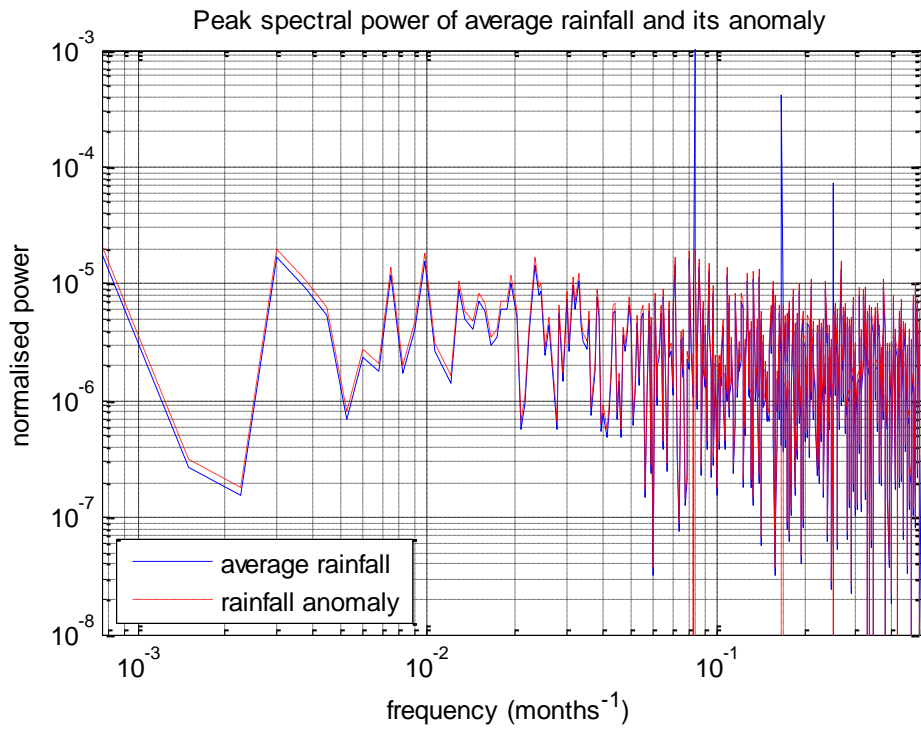


Figure A.2: Comparison of spectral power of rainfall and its anomaly.

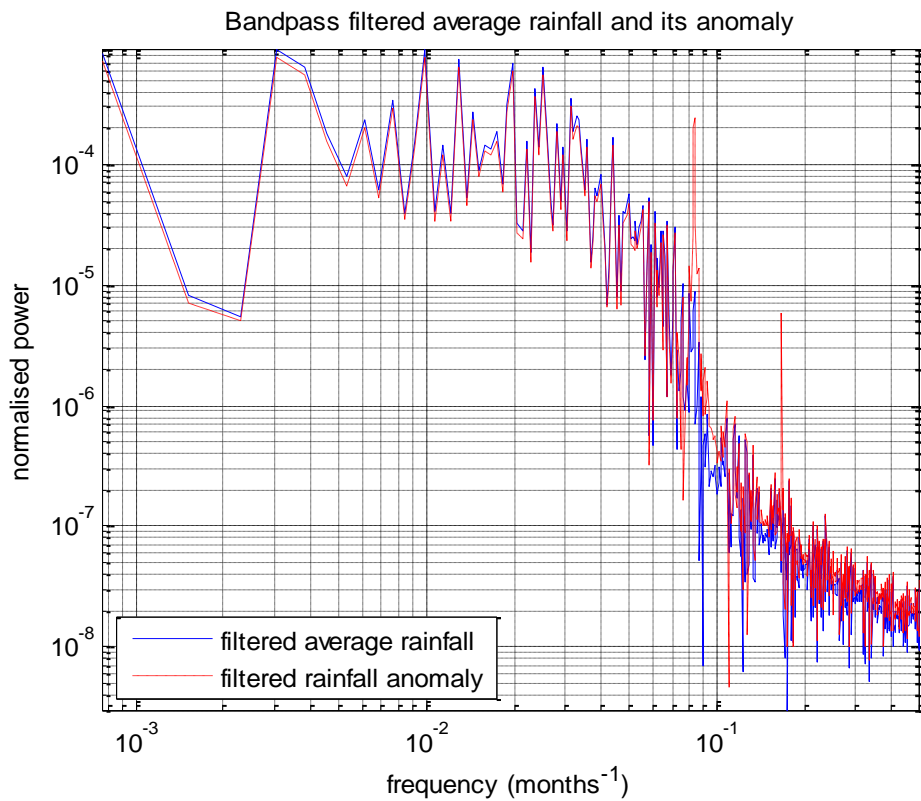


Figure A.3: Bandpass filtered average rainfall and its anomaly.

In Figure A.3 this is demonstrated. Instead of having large and regular peaks at the year time scale the filtering has reduced the contribution of power to significantly within the average of low frequency power contribution. Further, somewhat predictably, Pearson's r correlation between the average and anomaly is improved after filtering changing from 0.65 to 0.97. Given this is applied to each data set considered one does not conceive of any particular difficulty of analysis in presence of the interannual variation.

A practical example of this follows:

A simplistic approach was adopted for data handling in this study. Due to the nature of the bandpass filter used gratuitous manipulation of data was not required as demonstrated by example. Consequently the computational recipe (CR) approach where data values are subtracted from a monthly climatology of the 30 year climatological base period was redundant. Instead data was prepared by standardisation using the population mean and standard deviation. This latter technique also has the advantage of producing a smaller condition number than would raw data in subsequent matrix manipulation.

The correlation of the Niño3.4 index with the Australian DJF monthly gridded rainfall data series (1/1900 – 12/2009) was produced by two methods:

1. Using a CR approach where a monthly climatology for the 1961 – 1990 base period was subtracted from the monthly SST data to provide an anomaly. This series is termed Niño3.4 CR.
2. The monthly SST was standardised using the population mean to give a mean of 0 and $\sigma = 1$. This series is termed Niño3.4 Std.

Table A.1 compares the statistics obtained by each method, the only difference is a very slight skewness due to the difference of the base periods.

Table A.1: Statistics of Niño3.4 data series compared, in column 2 by CR and column 3, standardisation.

Statistic	Niño3.4 CR	Niño3.4 Std
Minimum	-0.61064	-0.60809
Maximum	0.15353	0.15295
Mean	-0.24785	-0.24737
Standard deviation	0.13694	0.13689
Pop variance	0.01875	0.01874
Significant map area	38%	38%

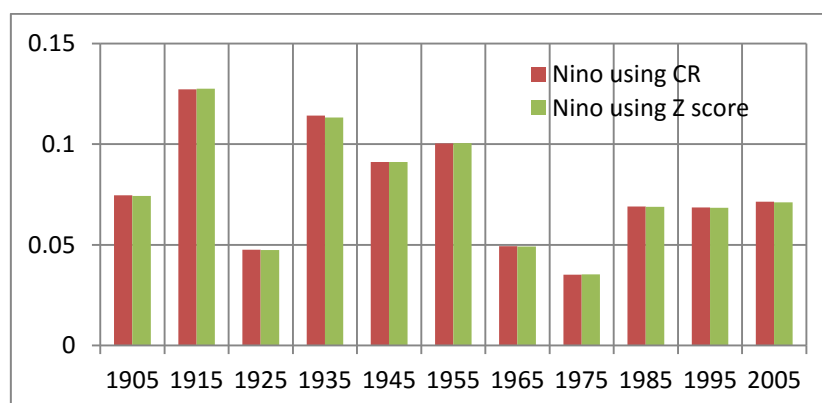


Figure A.4: Decadal variance of Niño3.4 CR compared to Niño3.4 Std.

Additionally if the decadal variances are compared (Figure A.4) no significant difference is apparent there either.

Finally if the correlation for the whole of Australia is compared using the two methods (Figures A5 and A6) absolutely no difference is apparent between the two results.

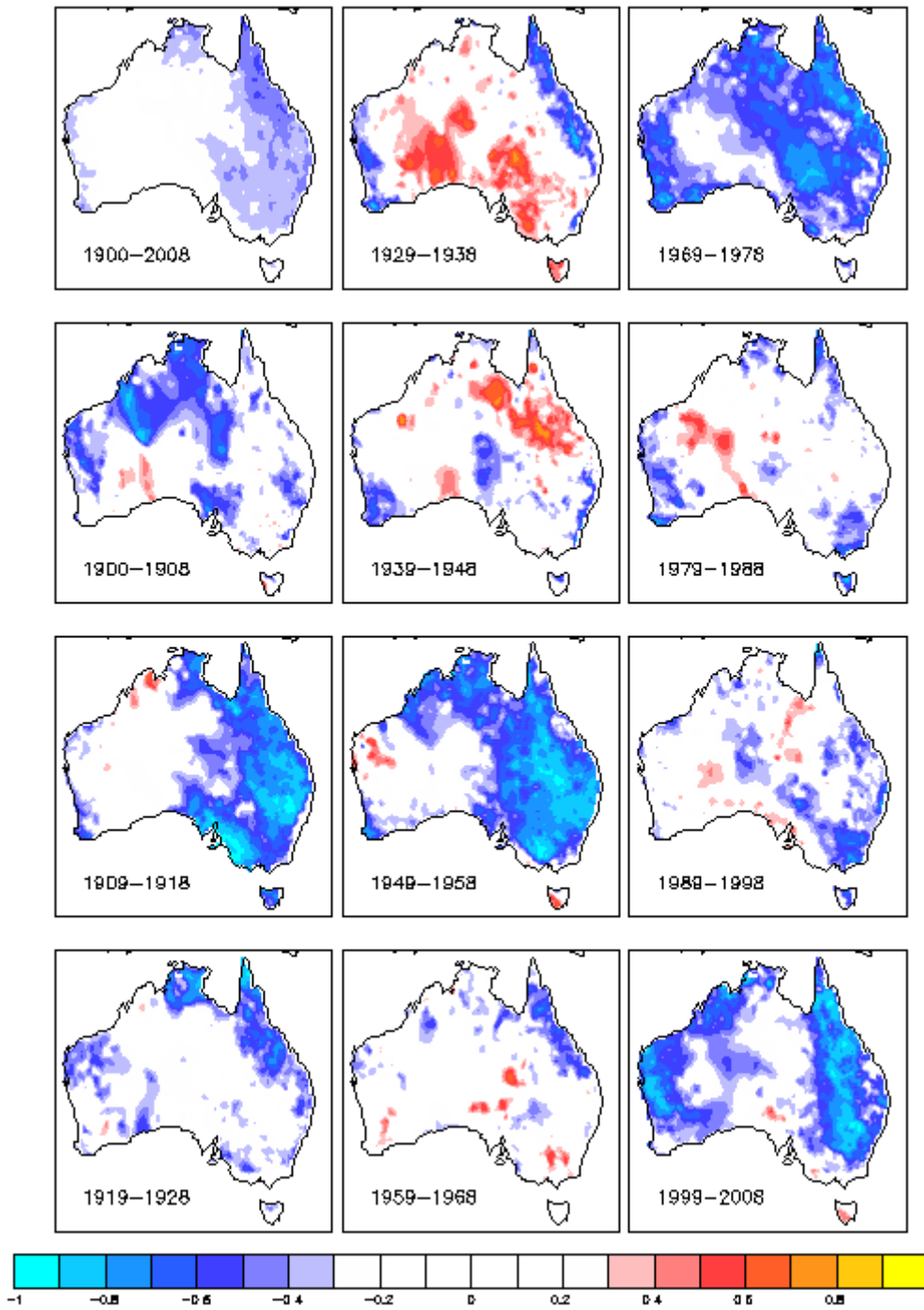


Figure A.5: Decadal DJF correlation of Niño3.4 CR with rainfall

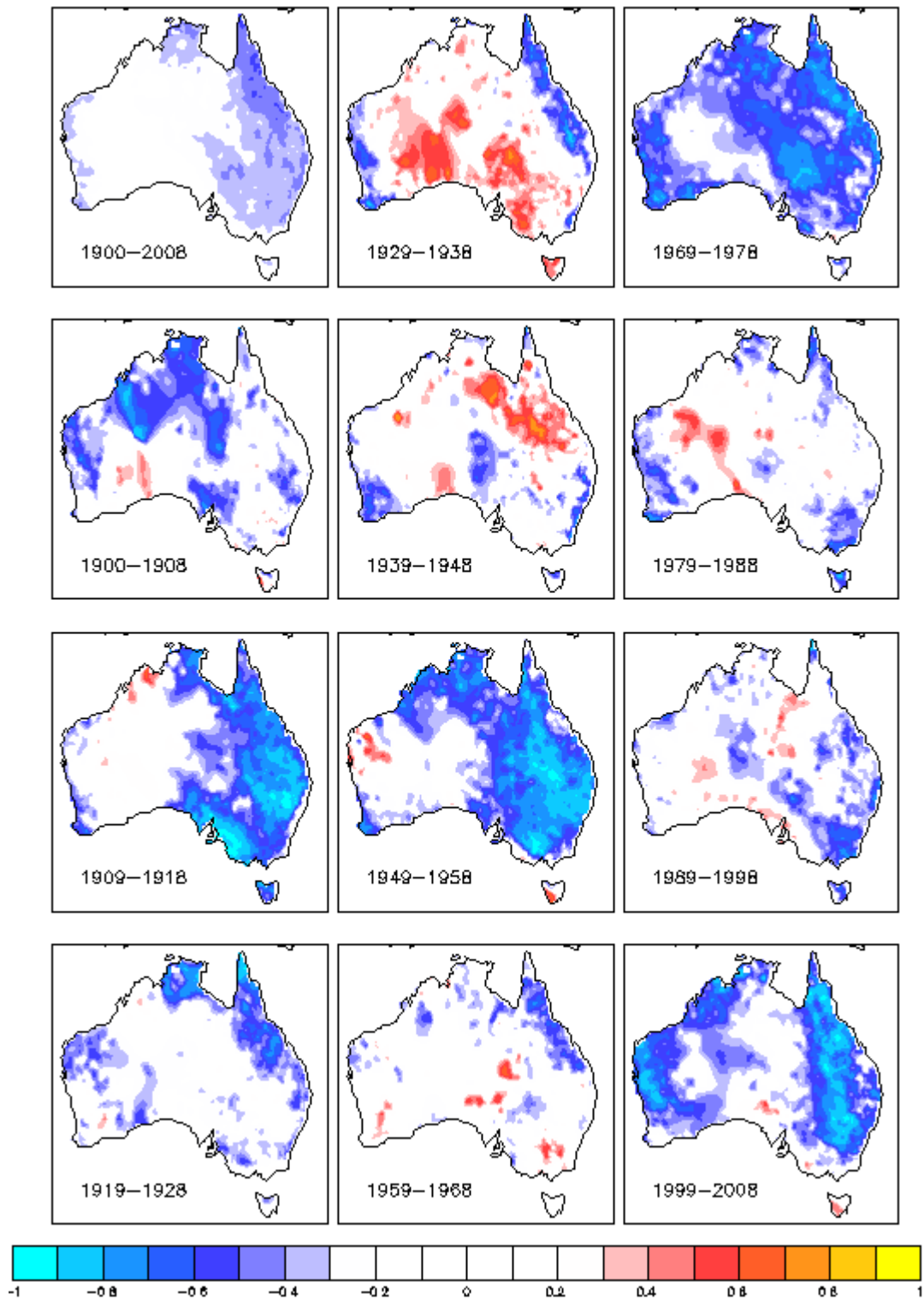


Figure A.6: Decadal DJF correlation of Niño3.4 Std with rainfall

References:

Allen, R 2006, '*Gilbert Walker: A pioneer of modern day climatology*', HM Government, access date 8/01/2012, <http://www.walker-institute.ac.uk/about/sir_gilbert.htm>.

Ansell, TJ, Reason, CJC, Smith, IN & Keay, K 2000, 'Evidence for decadal variability in southern Australian rainfall and relationships with regional pressure and sea surface temperature', *International Journal of Climatology*, vol. 20, no. 10, pp. 1113-29, <[http://dx.doi.org/10.1002/1097-0088\(200008\)20:10<1113::AID-JOC531>3.0.CO;2-N](http://dx.doi.org/10.1002/1097-0088(200008)20:10<1113::AID-JOC531>3.0.CO;2-N)>.

APDRC 2014, *soda_pop2.2.4 SODA v2.2.4 monthly means*, University of Hawaii, viewed 12/1/2014, <http://apdrc.soest.hawaii.edu/dods/public_data/SODA>.

Ashok, K 2013, *Time series of El Niño Modoki*, Personal communication from author 14/02/013.

Ashok, K & Yamagata, T 2009, 'Climate change: The El Nino with a difference', *Nature*, vol. 461, no. 7263, pp. 481-4, <<http://dx.doi.org/10.1038/461481a>>.

Ashok, K, Behera, SK, Rao, SA, Weng, H & Yamagata, T 2007, 'El Niño Modoki and its possible teleconnection', *J. Geophys. Res.*, vol. 112, no. C11, p. C11007, <<http://dx.doi.org/10.1029/2006JC003798>>.

Baird, G, Chandler, E, Watkins, AB & Jones, D 2011, 'How does the 2010-11 La Nina compare with past La Nina events?', *Bulltin of the Australian Meteorological and Oceanographic Society*, vol. 24, p. 17.

Baldwin, M, Gray, L, Dunkerton, T, Hamilton, K, Haynes, P, Randel, W, Holton, J, Alexander, M, Hirota, I & Horinouchi, T 2001, 'The quasi-biennial oscillation', *Reviews of Geophysics*, vol. 39, no. 2, pp. 179-229.

Baldwin, MP, Cheng, X & Dunkerton, TJ 1994, 'Observed correlations between winter-mean tropospheric and stratospheric circulation anomalies', *Geophysical Research Letters*, vol. 21, no. 12, pp. 1141-4.

Baldwin, MP, Gray, LJ, Dunkerton, TJ, Hamilton, K, Haynes, PH, Randel, WJ, Holton, JR, Alexander, MJ, Hirota, I, Horinouchi, T, Jones, DBA, Kinnnersley, JS, Marquardt, C, Sato, K

& Takahashi, M 2001, 'The quasi-biennial oscillation', *Reviews of Geophysics*, vol. 39, no. 2, pp. 179-229, <<http://dx.doi.org/10.1029/1999RG000073>>.

Bamston, AG, Chelliah, M & Goldenberg, SB 1997, 'Documentation of a highly ENSO-related sst region in the equatorial pacific: Research note', *Atmosphere-Ocean*, vol. 35, no. 3, pp. 367-83.

Basnett, T & Parker, D 1997, '*Development of the global mean sea level pressure data set GMSLP version 2*', UK Meteorological Office, Brackley UK.

Battisti, DS & Hirst, AC 1989, 'Interannual variability in a tropical atmosphere-ocean model: Influence of the basic state, ocean geometry and nonlinearity', *Journal of the Atmospheric Sciences*, vol. 46, no. 12, pp. 1687-712.

Baum, S, Crick, F, Czarnecki, J, Field, G, Choy, DL, McDonald, J, Mustelin, J, Sanò, M & Serrao-Neumann, S 2010, 'Climate change adaptation in South East Queensland human settlements: Issues and context'.

Berlage, H 1966, 'The Southern oscillation and world weather', *Mededelingen en verhandelingen/Koninklijk Nederlands meteorologisch instituut*, no. 88.

Bjerknes, J 1961, "'El Niño" study based on analysis of ocean surface temperatures 1935-57', *Inter-American Tropical Tuna Commission Bulletin*, vol. 5, no. 3, pp. 217-303.

Bjerknes, J 1966, 'A possible response of the atmospheric Hadley circulation to equatorial anomalies of ocean temperature', *Tellus*, vol. 18, no. 4, pp. 820-9, <<http://dx.doi.org/10.1111/j.2153-3490.1966.tb00303.x>>.

Bjerknes, J 1969, 'Atmospheric teleconnections from the equatorial Pacific 1', *Monthly Weather Review*, vol. 97, no. 3, pp. 163-72, <[http://dx.doi.org/10.1175/1520-0493\(1969\)097<0163:ATFTEP>2.3.CO;2](http://dx.doi.org/10.1175/1520-0493(1969)097<0163:ATFTEP>2.3.CO;2)>.

Bjornsson, HaVS 1997, *A Manual for EOF and SVD Analyses of Climatic Data*, , McGill University, , Montreal, Canada.,<

BoM 2005, *Australian climate zones - major classification groups*, viewed 14/02/13, <http://www.bom.gov.au/climate/environ/other/kpn_group.shtml>.

BoM 2010a, *Changeover to a new computer forecasting model*, viewed 1/11/13, <<http://www.bom.gov.au/weather-services/about/service-changes/modelchangeover.shtml>>.

BoM 2010b, *Australian climate influences*, viewed 15/12/2013, <<http://www.bom.gov.au/watl/about-weather-and-climate/australian-climate-influences.shtml#page-top>>.

BoM 2010c, *Past Weather & Climate Data*, viewed 23/09/2010, <<http://www.bom.gov.au/climate/data/?ref=ftr>>.

BoM 2011, *Winter brings no relief to long-term rainfall deficiencies in southwest WA*, viewed 8/09/2012, <<http://www.bom.gov.au/climate/drought/drought.shtml>>.

BoM 2013a, *Australian trend in annual total rainfall (mm 10yr-1) during 1970 – 2012* viewed 16/12/2013, <<http://www.bom.gov.au/cgi-bin/climate/change/trendmaps.cgi?map=rain&area=aus&season=0112&period=1970>>.

BoM 2013b, *About El Nino and La Nina*, viewed 22/11/2013, <<http://www.bom.gov.au/climate/enso/about-el-nino-la-nina.shtml#impacts>>.

BoM, A 2010, viewed 21/11/2014, <http://www.bom.gov.au/cgi-bin/climate/change/timeseries_graphs_of_Qld_seasonal_mean_temperatures>.

Box, GE, Jenkins, GM & Reinsel, GC 2013, *Time series analysis: forecasting and control*, John Wiley & Sons, Hoboken, New Jersey, USA.

Bretherton, CS, Widmann, M, Dymnikov, VP, Wallace, JM & Blade, I 1999, 'The effective number of spatial degrees of freedom of a time-varying field', *Journal of Climate*, vol. 12, no. 7, pp. 1990-2009.

Cai, Whetton & Pittock 2001, 'Fluctuations of the relationship between ENSO and northeast Australian rainfall', *Climate Dynamics*, vol. 17, no. 5, pp. 421-32, <<http://dx.doi.org/10.1007/PL00013738>>.

Cai, W 2011, 'How the three-headed dog (the SAM, the IOD, and ENSO) of Australian climate influences its tail (the STR) ', in *South Eastern Australian Climate Initiative 16/09/2011: proceedings of the South Eastern Australian Climate Initiative 16/09/2011 SEACI*, viewed <<http://www.seaci.org/events/2011workshop/presentations/>>.

Cai, W & van Rensch, P 2012, 'The 2011 southeast Queensland extreme summer rainfall: A confirmation of a negative Pacific Decadal Oscillation phase?', *Geophys. Res. Lett.*, vol. 39, no. 8, p. L08702, <<http://dx.doi.org/10.1029/2011GL050820>>.

Cai, W, Sullivan, A & Cowan, T 2010, 'Interactions of ENSO, the IOD, and the SAM in CMIP3 Models', *Journal of Climate*, vol. 24, no. 6, pp. 1688-704, <<http://dx.doi.org/10.1175/2010JCLI3744.1>>.

Cai, W, van Rensch, P, Cowan, T & Sullivan, A 2010, 'Asymmetry in ENSO Teleconnection with Regional Rainfall, Its Multidecadal Variability, and Impact', *Journal of Climate*, vol. 23, no. 18, pp. 4944-55, <<http://dx.doi.org/10.1175/2010JCLI3501.1>>.

Cai, W, van Rensch, P, Cowan, T & Hendon, HH 2011, 'Teleconnection Pathways of ENSO and the IOD and the Mechanisms for Impacts on Australian Rainfall', *Journal of Climate*, vol. 24, no. 15, pp. 3910-23, <<http://dx.doi.org/10.1175/2011JCLI4129.1>>.

Cai, W, Purich, A, Cowan, T, van Rensch, P & Weller, E 2014, 'Did Climate Change–Induced Rainfall Trends Contribute to the Australian Millennium Drought?', *Journal of Climate*, vol. 27, no. 9, pp. 3145-68, viewed 2014/04/24, <<http://dx.doi.org/10.1175/JCLI-D-13-00322.1>>

<http://journals.ametsoc.org/doi/pdf/10.1175/JCLI-D-13-00322.1>>.

Cai, WJ, Sullivan, A & Cowan, T 2009, 'Rainfall Teleconnections with Indo-Pacific Variability in the WCRP CMIP3 Models', *Journal of Climate*, vol. 22, no. 19, pp. 5046-71, <<Go to ISI>://WOS:000270423300006>.

Carton, JA & Giese, BS 2008, 'A reanalysis of ocean climate using Simple Ocean Data Assimilation (SODA)', *Monthly Weather Review*, vol. 136, no. 8, pp. 2999-3017.

Carton, JA, Chepurin, G, Cao, X & Giese, B 2000, 'A Simple Ocean Data Assimilation Analysis of the Global Upper Ocean 1950–95. Part I: Methodology', *Journal of Physical Oceanography*, vol. 30, no. 2, pp. 294-309, <[http://dx.doi.org/10.1175/1520-0485\(2000\)030<0294:ASODAA>2.0.CO;2](http://dx.doi.org/10.1175/1520-0485(2000)030<0294:ASODAA>2.0.CO;2)>.

Cattiaux, J & Cassou, C 2013, 'Opposite CMIP3/CMIP5 trends in the wintertime Northern Annular Mode explained by combined local sea ice and remote tropical influences', *Geophysical Research Letters*, vol. 40, no. 14, pp. 3682-7.

Catto, JL, Jakob, C & Nicholls, N 2012, 'The influence of changes in synoptic regimes on north Australian wet season rainfall trends', *J. Geophys. Res.*, vol. 117, no. D10, p. D10102, <<http://dx.doi.org/10.1029/2012JD017472>>.

Chen, G, Fang, C, Zhang, C & Chen, Y 2004, 'Observing the coupling effect between warm pool and “rain pool” in the Pacific Ocean', *Remote sensing of environment*, vol. 91, no. 2, pp. 153-9.

Cleugh, H, Smith, MS, Battaglia, M & Graham, P 2011, *Climate change: science and solutions for Australia*, CSIRO, Collingwood, VIC, Australia.

Climate Prediction Centre, Internet TEAM 2005, *Arctic Oscillation (AO)*, Climate Prediction Centre (CPC) National Centre for Environmental predictions (NCEP) National Oceanographic and Atmospheric Administration (NOAA), Maryland, 12/12/2005, <http://www.cpc.ncep.noaa.gov/products/precip/CWlink/daily_ao_index/ao.shtml>.

Cokelet, ED 1999, *lsl_lowpass filter*, viewed 9/04/2013, <<http://ferret.pmel.noaa.gov>>.

Connor, J, Schwabe, K, King, D, Kaczan, D & Kirby, M 2009, 'Impacts of climate change on lower Murray irrigation*', *Australian Journal of Agricultural and Resource Economics*, vol. 53, no. 3, pp. 437-56, <<http://dx.doi.org/10.1111/j.1467-8489.2009.00460.x>>.

Cravatte, S, Delcroix, T, Zhang, D, McPhaden, M & Leloup, J 2009, 'Observed freshening and warming of the western Pacific warm pool', *Climate Dynamics*, vol. 33, no. 4, pp. 565-89.

Crutzen, PJ & Ramanathan, V 2000, 'The ascent of atmospheric sciences', *Science*, vol. 290, no. 5490, p. 299.

De Deckker, P, Tapper, N & Van Der Kaars, S 2003, 'The status of the Indo-Pacific Warm Pool and adjacent land at the Last Glacial Maximum', *Global and Planetary Change*, vol. 35, no. 1, pp. 25-35.

de Viron, O, Dickey, JO & Ghil, M 2013, 'Global modes of climate variability', *Geophysical Research Letters*, pp. n/a-n/a, <<http://dx.doi.org/10.1002/grl.50386>>.

de Viron, O, Dickey, J & Ghil, M 2013, 'Global modes of climate variability', *Geophysical Research Letters*, vol. 40, no. 9, pp. 1832-7.

DeCarlo, LT 1997, 'On the meaning and use of kurtosis', *Psychological methods*, vol. 2, no. 3, p. 292.

Derman, E 2011, *Models. Behaving. Badly.: Why Confusing Illusion with Reality Can Lead to Disaster, on Wall Street and in Life*, Google.com.au, viewed 13/6/2013, <<https://books.google.com.au/>>.

Dessai, S, Hulme, M, Lempert, R & Pielke Jr, R 2009, 'Climate prediction: a limit to adaptation', *Adapting to climate change: thresholds, values, governance*, pp. 64-78.

Drosowsky, W & Chambers, LE 2001, 'Near-Global Sea Surface Temperature Anomalies as Predictors of Australian Seasonal Rainfall', *Journal of Climate*, vol. 14, no. 7, pp. 1677-87, viewed 2013/10/14, <[http://dx.doi.org/10.1175/1520-0442\(2001\)014<1677:NACNGS>2.0.CO;2](http://dx.doi.org/10.1175/1520-0442(2001)014<1677:NACNGS>2.0.CO;2)>.

Duchon, CE 1979, 'Lanczos filtering in one and two dimensions', *Journal of Applied Meteorology*, vol. 18, pp. 1016-22.

Emanuel, B 2009, *Climate indices*, University of Columbia, viewed 02/01/2014, <<http://iridl.ldeo.columbia.edu/dochelp/StatTutorial/Indices/>>.

ERSL 2011, *Pacific Warm Pool (PWP)*, National Oceanographic and Atmospheric Administration, viewed 14/06/2013, <<http://www.esrl.noaa.gov/psd/data/correlation/pacwarm.data>>.

Fawcett, R 2014, *FIVEVAR time series*, personal communication 21/11/2013, BoM, Melbourne.

Feldstein, SB & Franzke, C 2006, 'Are the North Atlantic Oscillation and the northern annular mode distinguishable?', *Journal of the Atmospheric Sciences*, vol. 63, no. 11, pp. 2915-30.

Fogt, RL, Bromwich, DH & Hines, KM 2011, 'Understanding the SAM influence on the South Pacific ENSO teleconnection', *Climate Dynamics*, vol. 36, no. 7-8, pp. 1555-76.

Folland, C, Parker, D, Colman, A & Washington, R 1999, *Large scale modes of ocean surface temperature since the late nineteenth century*, Hadley Centre UK MO, Exeter UK.

Fraedrich, K, Ziehm, C & Sielmann, F 1995, 'Estimates of spatial degrees of freedom', *Journal of Climate*, vol. 8, no. 2, pp. 361-70.

Fu, Q 2013, 'Ocean-atmosphere interactions: Bottom up in the tropics', *Nature Clim. Change*, vol. 3, no. 11, <<http://dx.doi.org/10.1038/nclimate2039>>.

Gallant, AJE, Reeder, MJ, Risbey, JS & Hennessy, KJ 2013, 'The characteristics of seasonal-scale droughts in Australia, 1911–2009', *International Journal of Climatology*, vol. 33, no. 7, pp. 1658-72, <<http://dx.doi.org/10.1002/joc.3540>>.

Gandin, L 1960, 'On optimal interpolation and extrapolation of meteorological fields', *Trudy GGO*, vol. 114, pp. 75-89.

Garfinkel, CI, Waugh, DW, Oman, LD, Wang, L & Hurwitz, MM 2013, 'Temperature trends in the tropical upper troposphere and lower stratosphere: Connections with sea surface temperatures and implications for water vapor and ozone', *Journal of Geophysical Research: Atmospheres*, vol. 118, no. 17, pp. 9658-72, <<http://dx.doi.org/10.1002/jgrd.50772>>.

Giese, BS & Ray, S 2011, 'El Niño variability in simple ocean data assimilation (SODA), 1871 to 2008', *J. Geophys. Res.*, vol. 116, no. C2, p. C02024, <<http://dx.doi.org/10.1029/2010JC006695>>.

Glantz, MH 2000, *Currents of change: impacts of El Niño and La Niña on climate and society*, Cambridge University Press, Cambridge UK.

Goni, G, Roemmich, D, Molinari, R, Meyers, G, Rossby, T, Sun, C, Boyer, T, Baringer, M, Garzoli, S & Vissa, G 2010, 'The ship of opportunity program', *Proceedings of the OceanObs*, vol. 9.

Gottschalck, J, KOUSKY, V, HIGGINS, W & HEUREUX, L 2010, 'Madden-Julian Oscillation (MJO)', *US Nat'l Weather Service*.

Graham, N 1994, 'Decadal-scale climate variability in the tropical and North Pacific during the 1970s and 1980s: Observations and model results', *Climate Dynamics*, vol. 10, no. 3, pp. 135-62.

Hammer, G, Holzworth, D & Stone, R 1996, 'The value of skill in seasonal climate forecasting to wheat crop management in a region with high climatic variability', *Crop and Pasture Science*, vol. 47, no. 5, pp. 717-37.

Hansard, HoRO 2011, 'Wednesday, 9 February 2011 HOUSE OF REPRESENTATIVES 173', *House of Representatives Official Hansard*, p. 173.

Hennessy, KJ, Suppiah, R & Page, CM 1999, 'Australian rainfall changes, 1910-1995', *Australian Meteorological Magazine*, vol. 48, no. 1, pp. 1-13, <<Go to ISI>://WOS:000079688000001>.

Higgins, RW, Shi, W, Yarosh, E & Joyce, R 2000, *Improved United States Precipitation Quality Control System and Analysis. NCEP/Climate Prediction Center Atlas No. 7*, U. S. Department of Commerce., viewed 5/11/14.

Hirsch, MW, Smale, S & Devaney, RL 2012, *Differential equations, dynamical systems, and an introduction to chaos*, Academic Press, Waltham, Maryland, USA.

Hoerling, MP 2009, *The Pacific Warmpool*, viewed 11/02/2012, <<http://www.esrl.noaa.gov/psd/data/climateindices/list/#Pacificwarm>>.

Hoerling, MP, Kumar, A & Xu, T 2001, 'Robustness of the Nonlinear Climate Response to ENSO's Extreme Phases', *Journal of Climate*, vol. 14, no. 6, pp. 1277-93, viewed 2011/11/07, <[http://dx.doi.org/10.1175/1520-0442\(2001\)014<1277:ROTNCR>2.0.CO;2](http://dx.doi.org/10.1175/1520-0442(2001)014<1277:ROTNCR>2.0.CO;2)>.

Hong, L, Zhang, L, Chen, Z & Wu, L 2014, 'Linkage between the Pacific Decadal Oscillation and the low frequency variability of the Pacific Subtropical Cell', *Journal of Geophysical Research: Oceans*, vol. 119, no. 6, pp. 3464-77, <<http://dx.doi.org/10.1002/2013JC009650>>.

Hope, P, Timbal, B & Fawcett, R 2010, 'Associations between rainfall variability in the southwest and southeast of Australia and their evolution through time', *International Journal of Climatology*, vol. 30, no. 9, pp. 1360-71, <<http://dx.doi.org/10.1002/joc.1964>>.

Hopkins, KD & Weeks, DL 1990, 'Tests for normality and measures of skewness and kurtosis: Their place in research reporting', *Educational and Psychological Measurement*, vol. 50, no. 4, pp. 717-29.

Hurrell, JW 1995, 'Decadal trends in the North Atlantic Oscillation: regional temperatures and precipitation', *Science-AAAS-Weekly Paper Edition*, vol. 269, no. 5224, pp. 676-8.

Hurrell, JW & Van Loon, H 1997, 'Decadal variations in climate associated with the North Atlantic Oscillation', *Climatic Change*, vol. 36, no. 3, pp. 301-26, <<http://dx.doi.org/10.1023/A:1005314315270>>.

Ihaka, R & Gentleman, R 1996, 'R: A language for data analysis and graphics', *Journal of computational and graphical statistics*, vol. 5, no. 3, pp. 299-314.

Indeje, M & Semazzi, F 2000, 'Relationships between QBO in the lower equatorial stratospheric zonal winds and East African seasonal rainfall', *Meteorology and Atmospheric Physics*, vol. 73, no. 3-4, pp. 227-44.

IPCC 2014, *Climate Change 2014: Impacts, Adaptation, and Vulnerability. Part B: Regional Aspects. Contribution of Working Group II to the Fifth Assessment Report of the Intergovernmental Panel on Climate Change* Cambridge University Press, Cambridge, United Kingdom and New York, NY, USA.

Jin, FF 2001, 'Low-Frequency Modes of Tropical Ocean Dynamics*', *Journal of Climate*, vol. 14, no. 18, pp. 3874-81.

Jones, Wang & Fawcett 2009, 'High-quality spatial climate data-sets for Australia', *Australian Meteorological and Oceanographic Journal*, vol. 58, pp. 233-48.

Jones, DA & Beard, G 1998, 'Verification of Australian monthly district rainfall totals using high resolution gridded analyses', *Australian Meteorological Magazine*, vol. 47, no. 1, pp. 41-54.

Jones, DA, Wang, W & Fawcett, R 2009, 'High-quality spatial climate data-sets for Australia', *Australian Meteorological and Oceanographic Journal*, vol. 58, no. 4, p. 233.

Jones, P & Salmon, M 2010, *Southern Oscillation Index time series*, viewed 6/6/2013, <<http://www.cru.uea.ac.uk/cru/data/soi/>>.

Kaplan, A, Cane, MA, Kushnir, Y, Clement, AC, Blumenthal, MB & Rajagopalan, B 1998, 'Analyses of global sea surface temperature 1856 to 1991', *J. Geophys. Res.*, vol. 103, no. C9, pp. 18567-89, <<http://dx.doi.org/10.1029/97JC01736>>.

Keenlyside, NS & Ba, J 2010, 'Prospects for decadal climate prediction', *Wiley Interdisciplinary Reviews: Climate Change*, vol. 1, no. 5, pp. 627-35, <<http://dx.doi.org/10.1002/wcc.69>>.

Kennedy, J 2008, *Met Office Hadley Centre observations datasets*, UK Met Office, viewed 3/01/2012, <<http://www.metoffice.gov.uk/hadobs/hadcrut3/smoothing.html>>.

Kirtman, BP & Schopf, PS 1998, 'Decadal Variability in ENSO Predictability and Prediction', *Journal of Climate*, vol. 11, no. 11, pp. 2804-22, <[http://dx.doi.org/10.1175/1520-0442\(1998\)011<2804:DVIEPA>2.0.CO;2](http://dx.doi.org/10.1175/1520-0442(1998)011<2804:DVIEPA>2.0.CO;2)>.

Kistler, R, Kalnay, E, Collins, W, Saha, S, White, G, Woollen, J, Chelliah, M, Ebisuzaki, W, Kanamitsu, M & Kousky, V 2001, 'The NCEP-NCAR 50-year reanalysis: Monthly means CD-ROM and documentation', *Bulletin-American Meteorological Society*, vol. 82, no. 2, pp. 247-68.

Klingaman, NP, Woolnough, S & Syktus, J 2012, 'On the drivers of inter-annual and decadal rainfall variability in Queensland, Australia', *International Journal of Climatology*.

Klingaman, NP, Woolnough, SJ & Syktus, J 2013, 'On the drivers of inter-annual and decadal rainfall variability in Queensland, Australia', *International Journal of Climatology*, vol. 33, no. 10, pp. 2413-30, <<http://dx.doi.org/10.1002/joc.3593>>.

Kovats, RS, Bouma, MJ, Hajat, S, Worrall, E & Haines, A 2003, 'El Niño and health', *The Lancet*, vol. 362, no. 9394, pp. 1481-9.

Kreyszig, E 2006 *Advanced engineering mathematics* 9edn, John Wiley, Hoboken, NJ.

Kug, J-S, Sooraj, KP, Li, T & Jin, F-F 2010, 'Precursors of the El Niño/La Niña onset and their interrelationship', *J. Geophys. Res.*, vol. 115, no. D5, p. D05106, <<http://dx.doi.org/10.1029/2009JD012861>>.

Kuleshov, Y, Qi, L, Fawcett, R & Jones, D 2008, 'On tropical cyclone activity in the Southern Hemisphere: Trends and the ENSO connection', *Geophys. Res. Lett.*, vol. 35, no. 14, p. L14S08, <<http://dx.doi.org/10.1029/2007GL032983>>.

Kumar, A, Chen, M & Wang, W 2013, 'Understanding Prediction Skill of Seasonal Mean Precipitation over the Tropics', *Journal of Climate*, vol. 26, no. 15, pp. 5674-81, <<http://dx.doi.org/10.1175/JCLI-D-12-00731.1>>.

Kumar, KK, Rajagopalan, B, Hoerling, M, Bates, G & Cane, M 2006, 'Unraveling the mystery of Indian monsoon failure during El Niño', *Science*, vol. 314, no. 5796, pp. 115-9.

Kumar, P & Foufoula-Georgiou, E 1997, 'Wavelet analysis for geophysical applications', *Rev. Geophys.*, vol. 35, no. 4, pp. 385-412, <<http://dx.doi.org/10.1029/97RG00427>>.

L'Heureux, ML, Lee, S & Lyon, B 2013, 'Recent multidecadal strengthening of the Walker circulation across the tropical Pacific', *Nature Climate Change*.

Labitzke, K 2004, 'On the signal of the 11-year sunspot cycle in the stratosphere over the Antarctic and its modulation by the Quasi-Biennial Oscillation (QBO)', *Meteorologische Zeitschrift*, vol. 13, no. 4, pp. 263-70.

Lau, N-C 1997, 'Interactions between Global SST Anomalies and the Midlatitude Atmospheric Circulation', *Bulletin of the American Meteorological Society*, vol. 78, no. 1, pp. 21-33, viewed 2015/02/22, <[http://dx.doi.org/10.1175/1520-0477\(1997\)078<0021:IBGSAA>2.0.CO;2](http://dx.doi.org/10.1175/1520-0477(1997)078<0021:IBGSAA>2.0.CO;2)>.

Lavery, B, Joung, G & Nicholls, N 1997, 'An extended high-quality historical rainfall dataset for Australia', *Australian Meteorological Magazine*, vol. 46, no. 1, pp. 27-38.

Legendre, P & Legendre, LF 2012, *Numerical ecology*, 3 edn, vol. 24, Elsevier, Oxford England.

Levitus, S & Boyer, T 1994, 'World Ocean Atlas 1994, vol. 4, Temperature, NOAA Atlas NESDIS 4', *US Department of Commerce, Washington, DC, 117pp*.

Li, X-F, Yu, J & Li, Y 2013, 'Recent Summer Rainfall Increase and Surface Cooling over Northern Australia since the Late 1970s: A Response to Warming in the Tropical Western Pacific', *Journal of Climate*, vol. 26, no. 18, pp. 7221-39, <<http://dx.doi.org/10.1175/JCLI-D-12-00786.1>>.

Limpasuvan, V & Hartmann, DL 1999, 'Eddies and the annular modes of climate variability', *Geophysical Research Letters*, vol. 26, no. 20, pp. 3133-6.

Lorenz, EN 1963, 'Deterministic Nonperiodic Flow', *Journal of the Atmospheric Sciences*, vol. 20, no. 2, pp. 130-41, <[http://dx.doi.org/10.1175/1520-0469\(1963\)020<0130:DNF>2.0.CO;2](http://dx.doi.org/10.1175/1520-0469(1963)020<0130:DNF>2.0.CO;2)>.

Mackellar, D 1908, 'Core of my heart (poem)', *The Spectator*.

Madden, RA & Julian, PR 1972, 'Description of global-scale circulation cells in the tropics with a 40-50 day period', *Journal of the Atmospheric Sciences*, vol. 29, no. 6, pp. 1109-23.

Mantua, NJ, Hare, SR, Zhang, Y, Wallace, JM & Francis, RC 1997, 'A Pacific interdecadal climate oscillation with impacts on salmon production', *Bulletin of the American Meteorological Society*, vol. 78, no. 6, pp. 1069-79.

Marshall, GJ 2003, 'Trends in the Southern Annular Mode from observations and reanalyses', *Journal of Climate*, vol. 16, no. 24, pp. 4134-43.

Mason, SJ & Lindesay, JA 1993, 'A note on the modulation of Southern Oscillation-Southern African rainfall associations with the quasi-biennial oscillation', *Journal of Geophysical Research: Atmospheres*, vol. 98, no. D5, pp. 8847-50, <<http://dx.doi.org/10.1029/92JD01496>>.

MathWorks, T 2007, *MATLAB, 7.5*, The MathWorks, 12/12/2010, <<http://www.mathworks.com/products/matlab/demos.html?file=/products/demos/shipping/matlab/fftdemo.html>>.

Matsuno, T 1966, 'Quasi-geostrophic motions in the equatorial area(Quasi-geostrophic wave motions of inertia-gravity wave type and Rossby wave type in equatorial area)', *Meteorological Society of Japan*, vol. 44, pp. 25-43.

McPhaden, MJ 2004, 'Evolution of the 2002/03 El Niño', *Bulletin of the American Meteorological Society*, vol. 85, no. 5, pp. 677-95,
<<http://ezproxy.usq.edu.au/login?url=http://search.ebscohost.com/login.aspx?direct=true&db=aph&AN=13228213&site=ehost-live>>.

McPhaden, MJ & Zhang, D 2002, 'Slowdown of the meridional overturning circulation in the upper Pacific Ocean', *Nature*, vol. 415, no. 6872, pp. 603-8.

McPhaden, MJ & Zhang, D 2004, 'Pacific Ocean circulation rebounds', *Geophys. Res. Lett.*, vol. 31, no. 18, p. L18301, <<http://dx.doi.org/10.1029/2004GL020727>>.

McPhaden, MJ, Zebiak, SE & Glantz, MH 2006, 'ENSO as an Integrating Concept in Earth Science', *Science*, vol. 314, no. 5806, pp. 1740-5,
<<http://www.sciencemag.org/content/314/5806/1740.abstract>>.

McPhaden, MJ, Zhang, XB, Hendon, HH & Wheeler, MC 2006, 'Large scale dynamics and MJO forcing of ENSO variability', *Geophysical Research Letters*, vol. 33, no. 16, <<Go to ISI>://WOS:000239991700003>.

McPhaden, MJ, Busalacchi, AJ, Cheney, R, Donguy, J-R, Gage, KS, Halpern, D, Ji, M, Julian, P, Meyers, G, Mitchum, GT, Niiler, PP, Picaut, J, Reynolds, RW, Smith, N & Takeuchi, K 1998, 'The Tropical Ocean-Global Atmosphere observing system: A decade of progress', *J. Geophys. Res.*, vol. 103, no. C7, pp. 14169-240,
<<http://dx.doi.org/10.1029/97JC02906>>.

Meehl, GA, Hu, A & Santer, BD 2009, 'The mid-1970s climate shift in the Pacific and the relative roles of forced versus inherent decadal variability', *Journal of Climate*, vol. 22, no. 3, pp. 780-92.

Meehl, GA, Goddard, L, Boer, G, Burgman, R, Branstator, G, Cassou, C, Corti, S, Danabasoglu, G, Doblas-Reyes, F & Hawkins, E 2014, 'Decadal climate prediction: an update from the trenches', *Bulletin of the American Meteorological Society*, vol. 95, no. 2, pp. 243-67.

Mehta, V & Dubey, V 1995, 'Decadal-multidecadal variability of the tropical sea surface temperatures', *WORLD METEOROLOGICAL ORGANIZATION-PUBLICATIONS-WMO TD*, pp. 67-8.

Meinen, CS & McPhaden, MJ 2000, 'Observations of warm water volume changes in the equatorial Pacific and their relationship to El Niño and La Niña', *Journal of Climate*, vol. 13, no. 20, pp. 3551-9.

Meinen, CS & McPhaden, MJ 2001, 'Interannual Variability in Warm Water Volume Transports in the Equatorial Pacific during 1993-99*', *Journal of Physical Oceanography*, vol. 31, no. 5, pp. 1324-45.

Meinke, H, deVoil, P, Hammer, GL, Power, S, Allan, R, Stone, RC, Folland, C & Potgieter, A 2005, 'Rainfall Variability at Decadal and Longer Time Scales: Signal or Noise?', *Journal of Climate*, vol. 18, no. 1, pp. 89-96, viewed 2014/11/03, <<http://dx.doi.org/10.1175/JCLI-3263.1>>.

Mitchell, T 1999, *The "cold tongue index" (CTI)* Joint Institute for the Study of Atmosphere and Ocean (JISAO), viewed 06 02 2012, <http://jisao.washington.edu/data_sets/cti/>.

Mitchell, T 2012, *Pacific Decadal Oscillation Index time series*, viewed 9/09/2013, <<http://margaret.atmos.washington.edu/pdo/PDO.latest>>.

Mitchell, TP & Wallace, JM 2004, 'Recent trends in the Southern Oscillation', in *15th Symposium on Global Change and Climate Variations: proceedings of the 15th Symposium on Global Change and Climate Variations*.

Murphy, BF & Ribbe, J 2004, 'Variability of southeastern Queensland rainfall and climate indices', *International Journal of Climatology*, vol. 24, no. 6, pp. 703-21, <<Go to ISI>://WOS:000221485600003>.

Naito, Y & Hirota, I 1997, 'Interannual variability of the northern winter stratospheric circulation related to the QBO and the solar cycle', *Journal of the Meteorological Society of Japan*, vol. 75, no. 4, pp. 925-37.

Nelson, R, Kokic, P, Crimp, S, Meinke, H & Howden, S 2010, 'The vulnerability of Australian rural communities to climate variability and change: Part I—Conceptualising and measuring vulnerability', *Environmental Science & Policy*, vol. 13, no. 1, pp. 8-17.

Nicholls, N 2008, 'Recent trends in the seasonal and temporal behaviour of the El Niño–Southern Oscillation', *Geophysical Research Letters*, vol. 35, no. 19, p. L19703, <<http://dx.doi.org/10.1029/2008GL034499>>.

Nicholls, N & Lavery, B 1992, 'Australian rainfall trends during the twentieth century', *International Journal of Climatology*, vol. 12, no. 2, pp. 153-63, <<http://dx.doi.org/10.1002/joc.3370120204>>.

Nicholls, N, Drosowsky, W & Lavery, B 1997, 'Australian rainfall variability and change', *Weather*, vol. 52, no. 3, pp. 66-72.

Pagès, F, González, HE, Ramón, M, Sobarzo, M & Gili, J-M 2001, 'Gelatinous zooplankton assemblages associated with water masses in the Humboldt Current System, and potential predatory impact by *Bassia bassensis* (Siphonophora: Calycophorae)', *Marine Ecology Progress Series*, vol. 210, pp. 13-24, <<http://www.int-res.com/abstracts/meps/v210/p13-24/>>.

Palmer, T, Alessandri, A, Andersen, U, Cantelaube, P, Davey, M, Délecluse, P & Déqué, M 2004, 'Development of a European Multimodel Ensemble System for Seasonal-To Prediction (Demeter)', *Bulletin of the American Meteorological Society*, vol. 85, pp. 853-72.

Palutikof, J 2010, 'The view from the front line: adapting Australia to climate change'.

Park, JY, Yeh, SW & Kug, JS 2012, 'Revisited relationship between tropical and North Pacific sea surface temperature variations', *Geophysical Research Letters*, vol. 39, no. 2, p. L02703.

Parker, DE, Jones, PD, Folland, CK & Bevan, A 1994, 'Interdecadal changes of surface temperature since the late nineteenth century', *J. Geophys. Res.*, vol. 99, no. D7, pp. 14373-99, <<http://dx.doi.org/10.1029/94JD00548>>.

Philander, SG 1990, *El Niño, La Niña, and the southern oscillation*, vol. 46, Academic Pr.

PMEL 2008, *El Nino Theme Page*, Department of Commerce / National Oceanic and Atmospheric Administration

Pacific Marine Environmental Laboratory / Tropical Atmosphere Ocean Project, viewed 11/11/2013, <<http://www.pmel.noaa.gov/tao/elnino/nino-home.html>>.

PMEL, NPFTD 2011, *Ferret version 6.72*, viewed 10/12/2011, <Website <http://ferret.pmel.noaa.gov>>.

Pontecorvo, G 2001, 'Supply side uncertainty and the management of commercial fisheries: - Peruvian Anchovetta, an illustration', *Marine Policy*, vol. 25, no. 2, pp. 169-72, <<http://www.ingentaconnect.com/content/els/0308597x/2001/00000025/00000002/art00039>> [http://dx.doi.org/10.1016/S0308-597X\(00\)00039-7](http://dx.doi.org/10.1016/S0308-597X(00)00039-7)>.

Potgieter, AB, Hammer, GL & Butler, D 2002, 'Spatial and temporal patterns in Australian wheat yield and their relationship with ENSO', *Australian Journal of Agricultural Research*, vol. 53, no. 1, pp. 77-89, <<http://www.publish.csiro.au/paper/AR01002>>.

Power, Tseitkin, Mehta, Lavery, Torok & Holbrook 1999, 'Decadal climate variability in Australia during the twentieth century', *International Journal of Climatology*, vol. 19, no. 2, pp. 169-84, <[http://dx.doi.org/10.1002/\(SICI\)1097-0088\(199902\)19:2<169::AID-JOC356>3.0.CO;2-Y](http://dx.doi.org/10.1002/(SICI)1097-0088(199902)19:2<169::AID-JOC356>3.0.CO;2-Y)>.

Power, S, Haylock, M, Colman, R & Wang, X 2006, 'The predictability of interdecadal changes in ENSO activity and ENSO teleconnections', *Journal of Climate*, vol. 19, no. 19.

Power, S, Tseitkin, F, Mehta, V, Lavery, B, Torok, S & Holbrook, N 1999, 'Decadal climate variability in Australia during the twentieth century', *International Journal of Climatology (United Kingdom)*.

Power, SB & Smith, IN 2007, 'Weakening of the Walker Circulation and apparent dominance of El Niño both reach record levels, but has ENSO really changed?', *Geophysical Research Letters*, vol. 34, no. 18, p. L18702, <<http://dx.doi.org/10.1029/2007GL030854>>.

Power., Casey, T, Folland, C, Colman, A & Mehta, V 1999, 'Inter-decadal modulation of the impact of ENSO on Australia', *Climate Dynamics*, vol. 15, no. 5, pp. 319-24.

Przborski, P 1972, *The Blue Marble*, Goddard Space Flight Center, viewed 6/01/2012, <<http://visibleearth.nasa.gov/view.php?id=57723>>.

Rahmstorf, S 2006, *Thermohaline Ocean Circulation*, Newnes Newmarket, UK.

Rajeevan, M & McPhaden, MJ 2004, 'Tropical Pacific upper ocean heat content variations and Indian summer monsoon rainfall', *Geophysical Research Letters*, vol. 31, no. 18, p. L18203.

Rao, B, V., do Carmo, AMC & Franchito, SH 2003, 'Interannual variations of storm tracks in the Southern Hemisphere and their connections with the Antarctic oscillation', *International Journal of Climatology*, vol. 23, no. 12, pp. 1537-45, <<http://dx.doi.org/10.1002/joc.948>>.

Rasmusson, EM & Carpenter, TH 1982, 'Variations in tropical sea surface temperature and surface wind fields associated with the Southern Oscillation/El Niño', *Monthly Weather Review*, vol. 110, no. 5, pp. 354-84.

Rasmusson, EM & Wallace, JM 1983, 'Meteorological aspects of the El Nino/southern oscillation', *Science*, vol. 222, no. 4629, pp. 1195-202.

Raupach, MR, Briggs, P, Haverd, V, King, E, Paget, M & Trudinger, C 2009, *Australian water availability project (AWAP): CSIRO marine and atmospheric research component: final report for phase 3*, Bureau of Meteorology and CSIRO.

Rayner, NA, Parker, DE, Horton, EB, Folland, CK, Alexander, LV, Rowell, DP, Kent, EC & Kaplan, A 2003, 'Global analyses of sea surface temperature, sea ice, and night marine air temperature since the late nineteenth century', *J. Geophys. Res.*, vol. 108, no. D14, p. 4407, <<http://dx.doi.org/10.1029/2002JD002670>>.

Reynolds, RW & Smith, TM 1994, 'Improved global sea surface temperature analyses using optimum interpolation', *Journal of Climate*, vol. 7, no. 6, pp. 929-48.

Risbey, JS, Pook, MJ, McIntosh, PC, Wheeler, MC & Hendon, HH 2009, 'On the Remote Drivers of Rainfall Variability in Australia', *Monthly Weather Review*, vol. 137, no. 10, pp. 3233-53, viewed 2014/09/28, <<http://dx.doi.org/10.1175/2009MWR2861.1>>.

Ropelewski, CF & Jones, PD 1987, 'An extension of the Tahiti–Darwin Southern Oscillation Index', *Monthly Weather Review*, vol. 115, no. 9, pp. 2161-5, <[http://dx.doi.org/10.1175/1520-0493\(1987\)115<2161:AEOTTS>2.0.CO;2](http://dx.doi.org/10.1175/1520-0493(1987)115<2161:AEOTTS>2.0.CO;2)>.

Saji, N, Goswami, BN, Vinayachandran, P & Yamagata, T 1999, 'A dipole mode in the tropical Indian Ocean', *Nature*, vol. 401, no. 6751, pp. 360-3.

Sarewitz, D & Pielke Jr, R 1999, 'Prediction in science and policy', *Technology in Society*, vol. 21, no. 2, pp. 121-33, <<http://www.sciencedirect.com/science/article/pii/S0160791X99000020>>.

Schepen, A, Wang, QJ & Robertson, D 2011, 'Evidence for Using Lagged Climate Indices to Forecast Australian Seasonal Rainfall', *Journal of Climate*, vol. 25, no. 4, pp. 1230-46, <<http://dx.doi.org/10.1175/JCLI-D-11-00156.1>>.

Schwing, F, Murphree, T & Green, P 2002, 'The Northern Oscillation Index (NOI): a new climate index for the northeast Pacific', *Progress in Oceanography*, vol. 53, no. 2-4, pp. 115-39.

Shi, G, Ribbe, J, Cai, W & Cowan, T 2008, 'An interpretation of Australian rainfall projections', *Geophysical Research Letters*, vol. 35, no. 2, p. L2072.

Singh, A, Kulkarni, MA, Mohanty, UC, Kar, SC, Robertson, AW & Mishra, G 2012, 'Prediction of Indian summer monsoon rainfall (ISMR) using canonical correlation analysis of global circulation model products', *Meteorological Applications*, vol. 19, no. 2, pp. 179-88, <<http://dx.doi.org/10.1002/met.1333>>.

Singh, O 2001, 'Multivariate ENSO index and Indian monsoon rainfall: relationships on monthly and subdivisional scales', *Meteorology and Atmospheric Physics*, vol. 78, no. 1, pp. 1-9.

Smith, CA & Sardeshmukh, PD 2000, 'The effect of ENSO on the intraseasonal variance of surface temperatures in winter', *International Journal of Climatology*, vol. 20, no. 13, pp. 1543-57.

Smith, IN & Timbal, B 2012, 'Links between tropical indices and southern Australian rainfall', *International Journal of Climatology*, vol. 32, no. 1, pp. 33-40, <<http://dx.doi.org/10.1002/joc.2251>>.

Smith, TM, Reynolds, RW, Livezey, RE & Stokes, DC 1996, 'Reconstruction of Historical Sea Surface Temperatures Using Empirical Orthogonal Functions', *Journal of Climate*, vol. 9, no. 6, pp. 1403-20, viewed 2012/11/27, <[http://dx.doi.org/10.1175/1520-0442\(1996\)009<1403:ROHSST>2.0.CO;2](http://dx.doi.org/10.1175/1520-0442(1996)009<1403:ROHSST>2.0.CO;2)>.

Smith, WHF 1993, 'On the accuracy of digital bathymetric data', *Journal of Geophysical Research: Solid Earth*, vol. 98, no. B6, pp. 9591-603, <<http://dx.doi.org/10.1029/93JB00716>>.

Smith, WHF & Sandwell, DT 1997, 'Global Sea Floor Topography from Satellite Altimetry and Ship Depth Soundings', *Science*, vol. 277, no. 5334, pp. 1956-62, <<http://www.sciencemag.org/content/277/5334/1956.abstract>>.

Snedecor, G & Cochran, W 1967, *statistical methods, ed 6, Ames, Iowa, 1967*, Iowa State University Press.

Solomon, A & Newman, M 2012, 'Reconciling disparate twentieth-century Indo-Pacific ocean temperature trends in the instrumental record', *Nature Climate Change*, vol. 2, no. 9, pp. 691-9.

Steinbach, M, Tan, P-N, Boriah, S, Kumar, V, Klooster, S & Potter, C 2006, 'The Application of Clustering to Earth Science Data: Progress and Challenges', in *Proceedings of the 2nd NASA Data Mining Workshop: proceedings of the Proceedings of the 2nd NASA Data Mining Workshop*.

Stephens, GL 1984, 'The Parameterization of Radiation for Numerical Weather Prediction and Climate Models', *Monthly Weather Review*, vol. 112, no. 4, pp. 826-67, <[http://dx.doi.org/10.1175/1520-0493\(1984\)112<0826:TPORFN>2.0.CO;2](http://dx.doi.org/10.1175/1520-0493(1984)112<0826:TPORFN>2.0.CO;2)>.

Stone, R & Auliciems, A 1992, 'SOI phase relationships with rainfall in eastern Australia', *International Journal of Climatology*, vol. 12, no. 6, pp. 625-36, <<http://dx.doi.org/10.1002/joc.3370120608>>.

Stone, RC, Hammer, GL & Marcussen, T 1996, 'Prediction of global rainfall probabilities using phases of the Southern Oscillation Index', *Nature*, vol. 384, no. 6606, pp. 252-5, <<http://dx.doi.org/10.1038/384252a0>>.

Stone, RC, Best, P & Sosenko, O 2008, 'Prospects for and value of long-time series data using global reanalysis data sets in the development of global climate derivatives', in *Proceedings of the 2008 International Conference on Reanalyses Data, Historical Reanalyses and Climate Applications 23 - 25 June: proceedings of the Proceedings of the 2008 International Conference on Reanalyses Data, Historical Reanalyses and Climate Applications 23 - 25 June Atmospheric Circulation Reconstructions over the Earth (ACRE)*, Zurich Switzerland, viewed <<http://eprints.usq.edu.au/7573/>>.

Sturman, AP & Tapper, NJ 1996, *The weather and climate of Australia and New Zealand*, Oxford University Press Melbourne.

Sun, C, Li, J, Feng, J & Xie, F 2014, 'A Decadal-Scale Teleconnection between the North Atlantic Oscillation and Subtropical Eastern Australian Rainfall', *Journal of Climate*, vol. 28, no. 3, pp. 1074-92, viewed 2015/02/05, <<http://dx.doi.org/10.1175/JCLI-D-14-00372.1>>
<<http://journals.ametsoc.org/doi/abs/10.1175/JCLI-D-14-00372.1>>.

Suppiah, R 2004, 'Trends in the southern oscillation phenomenon and Australian rainfall and changes in their relationship', *International Journal of Climatology*, vol. 24, no. 3, pp. 269-90, <<Go to ISI>://WOS:000220278200001>.

Suppiah, R & Hennessy, KJ 1996, 'Trends in the intensity and frequency of heavy rainfall in tropical Australia and links with the Southern Oscillation', *Australian Meteorological Magazine*, vol. 45, no. 1, pp. 1-17, <<Go to ISI>://WOS:A1996UH41600001>.

TAO, Project., Office 2011, *Indices of Equatorial Pacific Heat Content*, Seattle, WA 98115, <<http://www.pmel.noaa.gov/tao/elnino/www/>>.

Taschetto, AS, Sen Gupta, A, Hendon, HH, Ummenhofer, CC & England, MH 2011, 'The Contribution of Indian Ocean Sea Surface Temperature Anomalies on Australian Summer

Rainfall during El Niño Events', *Journal of Climate*, vol. 24, no. 14, pp. 3734-47, viewed 2011/07/23, <<http://dx.doi.org/10.1175/2011JCLI3885.1>>.

Taschetto, AS, Haarsma, RJ, Gupta, AS, Ummenhofer, CC, Hill, KJ & England, MH 2010, 'Australian Monsoon Variability Driven by a Gill–Matsuno-Type Response to Central West Pacific Warming', *Journal of Climate*, vol. 23, no. 18, pp. 4717-36, <<http://journals.ametsoc.org/doi/abs/10.1175/2010JCLI3474.1>>.

Taylor, GI 1962, 'Gilbert, Thomas Walker. 1868-1958', *Biographical Memoirs of Fellows of the Royal Society*, vol. 8, pp. 167-74.

Thorade 1909, 'Die Kalifornischen Meeresströmungen.', *Annalen der Hydrographie und Meteorologie*, vol. 37, pp. 17-34,63-76.

Tierney, JE, Oppo, DW, Rosenthal, Y, Russell, JM & Linsley, BK 2010, 'Coordinated hydrological regimes in the Indo-Pacific region during the past two millennia', *Paleoceanography*, vol. 25, no. 1.

Torok, SJ & Nicholls, N 1996, 'A historical annual temperature dataset for Australia', *Australian Meteorological Magazine*, vol. 45, no. 4, pp. 251-60.

Torrence, C & Compo, GP 1998, 'A Practical Guide to Wavelet Analysis', *Bulletin of the American Meteorological Society*, vol. 79, no. 1, p. 61, <<http://ezproxy.usq.edu.au/login?url=http://search.ebscohost.com/login.aspx?direct=true&db=a9h&AN=216314&site=ehost-live>>.

Torrence, C & Webster, PJ 1998, 'The annual cycle of persistence in the El Niño/Southern Oscillation', *Quarterly Journal of the Royal Meteorological Society*, vol. 124, no. 550, pp. 1985-2004, <<http://dx.doi.org/10.1002/qj.49712455010>>.

Trenberth, KE 1997, 'The definition of El Niño', *Bulletin of the American Meteorological Society*, vol. 78, no. 12, pp. 2771-8.

Trenberth, KE & Hoar, TJ 1996, 'Longest on record', *Geophysical Research Letters*, vol. 23, no. 1, pp. 57-60.

Trenberth, KE & Stepaniak, DP 2001, 'Indices of El Niño Evolution', *Journal of Climate*, vol. 14, no. 8, pp. 1697-701, <<http://journals.ametsoc.org/doi/abs/10.1175/1520-0442%282001%29014%3C1697%3ALIOENO%3E2.0.CO%3B2>>.

Troup, AJ 1965, 'The 'southern oscillation'', *Quarterly Journal of the Royal Meteorological Society*, vol. 91, no. 390, pp. 490-506, <<http://dx.doi.org/10.1002/qj.49709139009>>.

Tsonis, AA, Swanson, K & Kravtsov, S 2007, 'A new dynamical mechanism for major climate shifts', *Geophys. Res. Lett.*, vol. 34, no. 13, p. L13705, <<http://dx.doi.org/10.1029/2007GL030288>>.

Ummenhofer, CC, Sen Gupta, A, Taschetto, AS & England, MH 2009, 'Modulation of Australian Precipitation by Meridional Gradients in East Indian Ocean Sea Surface Temperature', *Journal of Climate*, vol. 22, no. 21, pp. 5597-610, <<http://ezproxy.usq.edu.au/login?url=http://search.ebscohost.com/login.aspx?direct=true&db=a9h&AN=44786594&site=ehost-live>>.

Ummenhofer, CC, Sen Gupta, A, Briggs, PR, England, MH, McIntosh, PC, Meyers, GA, Pook, MJ, Raupach, MR & Risbey, JS 2011, 'Indian and Pacific Ocean Influences on Southeast Australian Drought and Soil Moisture', *Journal of Climate*, vol. 24, no. 5, pp. 1313-36, <<http://ezproxy.usq.edu.au/login?url=http://search.ebscohost.com/login.aspx?direct=true&db=a9h&AN=59761506&site=ehost-live>>.

University Hamburg 2012, *Climate Indices*, viewed 7/12/2013, <http://icdc.zmaw.de/climate_indices.html?L=1>.

van der Ent, RJ & Savenije, HHG 2013, 'Oceanic sources of continental precipitation and the correlation with sea surface temperature', *Water Resources Research*, pp. n/a-n/a, <<http://dx.doi.org/10.1002/wrcr.20296>>.

Van Loon, H & Labitzke, K 1987, 'The Southern Oscillation. Part V: The anomalies in the lower stratosphere of the Northern Hemisphere in winter and a comparison with the Quasi-Biennial Oscillation', *Monthly Weather Review*, vol. 115, no. 2, pp. 357-69.

von Helmholtz, H 1977, *Epistemological Writings: The Paul Hertz/Moritz Schlick centenary edition of 1921, with notes and commentary by the editors*, vol. 37, Springer Science & Business Media.

von Storch, H & Zwiers, FW 2001, *Statistical analysis in climate research*, Cambridge university press, Cambridge UK.

von Storch, H, Bürger, G, Schnur, R & von Storch, J-S 1995, 'Principal Oscillation Patterns: A Review', *Journal of Climate*, vol. 8, no. 3, pp. 377-400, <[http://dx.doi.org/10.1175/1520-0442\(1995\)008<0377:POPAR>2.0.CO;2](http://dx.doi.org/10.1175/1520-0442(1995)008<0377:POPAR>2.0.CO;2)>.

- Wackerly, DD, Mendenhall, W & Scheaffer, RL 2008, *Mathematical statistics with applications*, Brooks/Cole, Pacific Grove CA USA.
- Wackerly, DD, Mendenhall, W & Scheaffer, RL 2002, *Mathematical statistics with applications*, 6 edn, Duxbury., Pacific Grove, CA:.
- Walck, C 2007, *Hand-book on STATISTICAL DISTRIBUTIONS for experimentalists*, University of Stockholm.
- Walford, N 2011, *Practical statistics for geographers and earth scientists*, Wiley, Chichester W Sussex.
- Walker & Bliss 1937, 'World weather VI ', *Memoirs of the Royal Meteorological Society* vol. 4 no. 39, pp. 119–39.
- Walker, G 1928, 'World weather', *Quarterly Journal of the Royal Meteorological Society*, vol. 54, no. 226, pp. 79-87.
- Walker, J 1997, 'Pen portraits of presidents—Sir Gilbert Walker, CSI, ScD, MA, FRS', *Weather*, vol. 52, no. 7, pp. 217-20.
- Wallace, JM, Cheng, X & Sun, D 1991, 'Does low-frequency atmospheric variability exhibit regime-like behavior?', *Tellus B*, vol. 43, no. 4, pp. 16-26, <<http://dx.doi.org/10.1034/j.1600-0889.1991.t01-3-00004.x>>.
- Wallace, JM, Rasmusson, EM, Mitchell, TP, Kousky, VE, Sarachik, ES & von Storch, H 1998, 'On the structure and evolution of ENSO-related climate variability in the tropical Pacific: Lessons from TOGA', *J. Geophys. Res.*, vol. 103, no. C7, pp. 14241-59, <<http://dx.doi.org/10.1029/97JC02905>>.
- Wang, B & Wang, Y 1996, 'Temporal Structure of the Southern Oscillation as Revealed by Waveform and Wavelet Analysis', *Journal of Climate*, vol. 9, no. 7, pp. 1586-98, viewed 2014/09/28, <[http://dx.doi.org/10.1175/1520-0442\(1996\)009<1586:TSOTSO>2.0.CO;2](http://dx.doi.org/10.1175/1520-0442(1996)009<1586:TSOTSO>2.0.CO;2)>.
- Wang, C & Enfield, DB 2001, 'The tropical Western Hemisphere warm pool', *Geophysical Research Letters*, vol. 28, no. 8, pp. 1635-8.
- Wang, C & Enfield, DB 2003, 'A Further Study of the Tropical Western Hemisphere Warm Pool', *Journal of Climate*, vol. 16, no. 10, pp. 1476-93,

<<http://journals.ametsoc.org/doi/abs/10.1175/1520-0442%282003%29016%3C1476%3AAFSOTT%3E2.0.CO%3B2>>.

Wang, G & Hendon, HH 2007, 'Sensitivity of Australian Rainfall to Inter–El Niño Variations', *Journal of Climate*, vol. 20, no. 16, pp. 4211- 26.

Wang, G, Hudson, D, Yin, Y, Alves, O, Hendon, H, Langford, S, Liu, G & Tseitkin, F 2011, 'POAMA-2 SST skill assessment and beyond', *CAWCR Research Letters*, no. 6, pp. 40-6.

Wang, G, Alves, O, Zhong, A, Smith, N, Schiller, A, Meyers, G, Tseitkin, F, Godfrey, S & Power, S 2004, 'POAMA: AN AUSTRALIAN OCEAN-ATMOSPHERE MODEL FOR CLIMATE PREDICTION', in *Extended Abstracts, 15th Symp. on Global Change and Climate Variations: proceedings of the Extended Abstracts, 15th Symp. on Global Change and Climate Variations* Melbourne Australia 15/01/2004.

Wang, H & Mehta, VM 2008, 'Decadal Variability of the Indo-Pacific Warm Pool and Its Association with Atmospheric and Oceanic Variability in the NCEP-NCAR and SODA Reanalyses', *Journal of Climate*, vol. 21, no. 21, pp. 5545-65.

Watterson, IG 2001, 'Wind-Induced Rainfall and Surface Temperature Anomalies in the Australian Region', *Journal of Climate*, vol. 14, no. 9, pp. 1901-22, viewed 2014/09/21, <[http://dx.doi.org/10.1175/1520-0442\(2001\)014<1901:WIRAST>2.0.CO;2](http://dx.doi.org/10.1175/1520-0442(2001)014<1901:WIRAST>2.0.CO;2)>.

Watterson, IG 2010, 'Relationships between southeastern Australian rainfall and sea surface temperatures examined using a climate model', *Journal of Geophysical Research: Atmospheres*, vol. 115, no. D10, p. D10108, <<http://dx.doi.org/10.1029/2009JD012120>>.

Weare, BC, Navato, AR & Newell, RE 1976, 'Empirical Orthogonal Analysis of Pacific Sea Surface Temperatures', *Journal of Physical Oceanography*, vol. 6, no. 5, pp. 671-8, <[http://dx.doi.org/10.1175/1520-0485\(1976\)006<0671:EOAOPS>2.0.CO;2](http://dx.doi.org/10.1175/1520-0485(1976)006<0671:EOAOPS>2.0.CO;2)>.

Webster, PJ & Hoyos, C 2004, 'Prediction of monsoon rainfall and river discharge on 15-30-day time scales', *Bulletin of the American Meteorological Society*, vol. 85, no. 11, pp. 1745-+, <<Go to ISI>://WOS:000225557200015>.

Weickmann, KM & Sardeshmukh, PD 1994, 'THE ATMOSPHERIC ANGULAR-MOMENTUM CYCLE-ASSOCIATED WITH A MADDEN-JULIAN OSCILLATION', *Journal of the Atmospheric Sciences*, vol. 51, no. 21, pp. 3194-208, <<Go to ISI>://WOS:A1994PQ83700007>.

Weisheimer, A, Doblas-Reyes, FJ, Palmer, TN, Alessandri, A, Arribas, A, Déqué, M, Keenlyside, N, MacVean, M, Navarra, A & Rogel, P 2009, 'ENSEMBLES: A new multi-model ensemble for seasonal-to-annual predictions'; Skill and progress beyond DEMETER in forecasting tropical Pacific SSTs', *Geophys. Res. Lett.*, vol. 36, no. 21, p. L21711, <<http://dx.doi.org/10.1029/2009GL040896>>.

Wells, LE 1990, 'Holocene history of the El Niño phenomenon as recorded in flood sediments of northern coastal Peru', *Journal Name: Geology; (USA); Journal Volume: 18:11*, pp. Medium: X; Size: Pages: 1134-7.

Williams, AAJ & Stone, RC 2009, 'An assessment of relationships between the Australian subtropical ridge, rainfall variability, and high-latitude circulation patterns', *International Journal of Climatology*, vol. 29, no. 5, pp. 691-709, <<http://dx.doi.org/10.1002/joc.1732>>.

Wolter, K 2009, 'A new and improved Multivariate ENSO Index (MEI)', in *21st Conference on Climate Variability and Change: proceedings of the 21st Conference on Climate Variability and Change*.

Wolter, K & Timlin, M 1998, 'Measuring the strength of ENSO events - how does 1997/98 rank?', *Weather*, vol. 53, pp. 315-24.

Wolter, K & Timlin, MS 2011, 'El Niño/Southern Oscillation behaviour since 1871 as diagnosed in an extended multivariate ENSO index (MEI.ext)', *International Journal of Climatology*, vol. 31, no. 7, pp. 1074-87, <<http://dx.doi.org/10.1002/joc.2336>>.

Woodruff, SD, Slutz, RJ, Jenne, RL & Steurer, PM 1987, 'A Comprehensive Ocean-Atmosphere Data Set', *Bulletin of the American Meteorological Society*, vol. 68, no. 10, pp. 1239-50, <[http://dx.doi.org/10.1175/1520-0477\(1987\)068<1239:ACOADS>2.0.CO;2](http://dx.doi.org/10.1175/1520-0477(1987)068<1239:ACOADS>2.0.CO;2)>.

Wright, PB, Wallace, JM, Mitchell, TP & Deser, C 1988, 'Correlation Structure of the El Niño/Southern Oscillation Phenomenon', *Journal of Climate*, vol. 1, no. 6, pp. 609-25, <[http://dx.doi.org/10.1175/1520-0442\(1988\)001<0609:CSOTEN>2.0.CO;2](http://dx.doi.org/10.1175/1520-0442(1988)001<0609:CSOTEN>2.0.CO;2)>.

Wu, Z, Huang, NE, Long, SR & Peng, CK 2007, 'On the trend, detrending, and variability of nonlinear and nonstationary time series', *Proceedings of the National Academy of Sciences*, vol. 104, no. 38, p. 14889.

Wyrtki, K 1975, 'El Niño—The Dynamic Response of the Equatorial Pacific Ocean to Atmospheric Forcing', *Journal of Physical Oceanography*, vol. 5, no. 4, pp. 572-84, <[http://dx.doi.org/10.1175/1520-0485\(1975\)005<0572:ENTDRO>2.0.CO;2](http://dx.doi.org/10.1175/1520-0485(1975)005<0572:ENTDRO>2.0.CO;2)>.

Yan, X-H, Ho, C-R, Zheng, Q & Klemas, V 1992, 'Temperature and size variabilities of the Western Pacific Warm Pool', *Science*, vol. 258, no. 5088, pp. 1643-5.

Yang, X & DelSole, T 2011, 'Systematic Comparison of ENSO Teleconnection Patterns between Models and Observations', *Journal of Climate*, vol. 25, no. 2, pp. 425-46, <<http://dx.doi.org/10.1175/JCLI-D-11-00175.1>>.

Yu, J-Y 2013, *Indian Ocean Dipole Data series*, JAMSTEC, viewed 16/03/2013, <http://www.jamstec.go.jp/frsgc/research/d1/iod/e/iod/about_iod.html>.

Zhao, Y & Nigam, S 2015, 'The Indian Ocean Dipole: A Monopole in SST', *Journal of Climate*, vol. 28, no. 1, pp. 3-19, viewed 2016/02/09, <<http://dx.doi.org/10.1175/JCLI-D-14-00047.1>>.

Zhou, Y, Higgins, RW, Kim, H & Center, CP 2001, *Relationships between El Niño-Southern Oscillation and the Arctic Oscillation: a climate-weather link*, NOAA, National Weather Service, National Centers for Environmental Prediction, Climate Prediction Center, <http://www.cpc.ncep.noaa.gov/> 15/11/2012>.